

XXXVI Pan-Hellenic conference on Solid-State Physics and Materials Science
Heraklion, 26-28 September 2022



Book of Abstracts

*XXXVI Panhellenic Conference on
Solid State Physics & Materials Science*

26-28 September 2022
Heraklion, Crete, Greece

Organizing Committee

George Kioseoglou (chair)

Maria Chatzinikolaidou

Kiriaki Chrissopoulou

George Kopidakis

Ioannis N. Remediakis

Dimitra Vernardou



ΠΑΝΕΠΙΣΤΗΜΙΟ ΚΡΗΤΗΣ
UNIVERSITY OF CRETE



Department of Materials Science
and Technology



FORTH

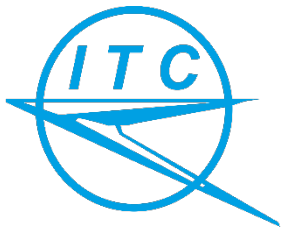
INSTITUTE OF ELECTRONIC STRUCTURE AND LASER



Sponsors



Ελληνική Εταιρεία Επιστήμης
και Τεχνολογίας της Συμπυκνωμένης Ύλης



International Technology Corporation



36^ο Πανελλήνιο Συνέδριο Φυσικής Στερεάς Κατάστασης και Επιστήμης Υλικών

36th Panhellenic Conference on Solid State Physics and Materials Science

Program

Monday, 26/09/2022

08:00 Registration

08:45 Opening remarks: G. Kioseoglou, Conference Chair

Department of Materials Science and Technology, University of Crete and FORTH/IESL

Welcome, S.H. Anastasiadis, Director

Institute of Electronic Structure and Laser, Foundation for Research and Technology - Hellas

Session: 2D Materials

Chair: G. Kioseoglou

09:00 **Xavier Marie (Keynote)**

Exciton Complexes and Spin/valley Pumping in 2D semiconductors

S. Doukas, A.C. Tasolamprou, A.D. Koulouklidis, S. Tzortzakis, I. Goykhman, A.C. Ferrari,

09:40 *E. Lidorikis*

A self-consistent framework for modeling graphene-based optoelectronic devices

S. Psilodimitrakopoulos, L. Mouchliadis, G.M. Maragkakis, G. Kourmoulakis, I. Demeridou,

09:55 *A. Lemonis, G. Kioseoglou, E. Stratakis*

Polarization-Resolved Second Harmonic Generation Imaging in 2D Materials

M. Stavrou, A. Stathis, D. Theodoropoulou, N. Chazapis, S. Couris

10:10 *Nonlinear optical properties of 2D materials: from graphene to silicene and to other 2D materials*

I. Paradisanos, G. Wang, E.M. Alexeev, A.R. Cadore, A.C. Ferrari, X. Marie, B. Urbaszek,

10:25 *M.M. Glazov*

Efficient phonon cascades in an atomically thin semiconductor

10:40 *S. Katsiaounis, Nikos Delikoukos, J. Parthenios, K. Papagelis*

Time-Resolved Raman scattering in exfoliated and CVD graphene crystals

I.K. Sideri, G. Charalambidis, A.G. Coutsolelos, R. Arenal, N. Tagmatarchis

10:55 *Pyridine vs imidazole axial ligation on cobaloxime grafted graphene: Hydrogen evolution reaction insights*

11:10

Coffee break

Session: Photonics - Optoelectronics I

Chair: M. Kafesaki

11:40 M. Kandyla (Invited)

Laser micro/nano processing for photonics, optoelectronics, and smart surfaces

A. Laskarakis (Invited)

12:05 *Optimizing large area fabrication of printed nanolayers for Organic Electronics by In-Line Metrology*

K. Kosma, K. Konstantinos, E. Kaselouris, M. Kaniolakis-Kaloudis, M. Bakarezos, M. Tatarakis, V. Dimitriou, N.A. Papadogiannis

12:30 *Pump-probe Reflectivity Studies of Ultrashort Laser-induced Acoustic Strains in Layered Materials*

G. Antoniou, P. Yuan, L. Koutsokeras, P.E. Keivanidis

12:45 *Triplet-excited State Fusion as a Tool to Photostimulate Vertically-configured Organic Photodetectors*

A. Bardakas, A. Segkos, G. Katsikis, G. Vekinis, C. Tsamis

13:00 *Performance of SiC-doped 3D printed PLA for triboelectric energy harvesting*

A.D. Koulouklidis, A.C. Tasolamprou, S. Doukas, E. Kyriakou, C. Daskalaki, M. Said Ergoktas,

13:15 E.N. Economou, E. Lidorikis, M. Kafesaki, C. Kocabas, S. Tzortzakis
THz Self-induced Actions on a Graphene Based Thin Film Absorber

M. Gioti, D. Tselekidou, K. Papadopoulos, V. Kyriazopoulos, K.C. Andrikopoulos,

13:30 A.K. Andreopoulou, J.K. Kallitsis
Single-layer white OLEDs: blended polymers and copolymers as emitting films

13:45 **Lunch break**

Session: Nanomaterials I

Chair: M. Katsikini

S. Gardelis (Invited)

14:45 *Silver-decorated silicon nanostructures for plasmon-induced enhancement of Raman scattering and fluorescence*

P.E. Stamatopoulou, S. Fiedler, C. Wolff, N.A. Mortensen, C. Tserkezis, A. Assadillayev,

15:10 S. Raza, H. Sugimoto, M. Fujii
Transition radiation in cathodoluminescence spectra of silicon nanoparticles

15:25 N. Sorogas, K. Papagelis, A.N. Anagnostopoulos, J. Arvanitidis, D. Christofilos
Comparative Study of Sn_{Sx}Se_{2-x} alloys by High Pressure Raman Spectroscopy

15:40 I. Konidakis, E. Stratakis
Post-melting encapsulation for the development of advanced composite glasses

M.P. Minadakis, R. Canton-Vitoria, C. Stangel, N. Tagmatarchis, R. Arenal

15:55 *Exfoliated WS₂ interfacing Ni-porphyrin with (photo)electrocatalytic activity for the oxygen evolution reaction*

16:10 M.-A. Apostolaki, S. Gardelis, V. Likodimos, E. Sakellis, P. Tsipas, N. Boukos, A. Dimoulas
Co-assembly of Heterojunction WO₃/TiO₂ Inverse Opal Films for Photoinduced Applications

16:25

Coffee break

Session: Polymers

Chair: E. Pavlopoulou

16:45 **T. Krasia-Christoforou (Invited)**
Polymer-based electrospun fibrous nanocomposites

17:10 **M. Chatzichristidi (Invited)**
Fluoropolymer surfaces modification via lithographic techniques

17:35 A. Rissanou, A.F. Behbahani, V. Harmandaris
Study of Polybutadiene/Silica Nanocomposites through Molecular Dynamics Simulations

17:50 A.A. Barmdaki, E.E. Zavvou, M.A. Botzakaki, N.J. Xanthopoulos, A. Giannakas, C.E Salmas,
P.K. Karahaliou, P. Svarnas, A. Ladavos, C.A. Krontiras
Influence of filler and/or ZnO-coating on the physical properties of Poly(lactic acid)/TiO₂ bionanocomposites

18:05 Th.-M. Chatzaki, F. Krasanakis, K. Chrissopoulou, S.H. Anastasiadis
Utilizing Polymer Coatings for the Development of Superhydrophobic and Water Repellent Surfaces

18:20 S.X. Drakopoulos, J. Cui, M. Asandulesa, S. Bronnikov, A. Nogales, K. Asadi
Charge Transport and Interfacial Dipolar Effects in Conjugated Polymers

Session: Posters I

18:45 Posters and discussion

Tuesday, 27/09/2022

Session: Biomaterials

Chair: S. H. Anastasiadis

- 09:00 G. Malliaras (Keynote)**
New Materials and Devices for Bioelectronic Medicine
- 09:40 A.A. Bakopoulou (Invited)**
Applications of Advance Therapy Medicinal Products in Oral Medicine
- 10:05 Ch.E. Lekka, (Invited)**
Anti-bacteria Ti- based alloys for bone implants
- 10:30 K. Loukelis, G.-I. Kontogianni, D. Vlassopoulos, M. Chatzinikolaidou**
3D bioprinted constructs for bone tissue regeneration
- 10:45 G.K. Pouroutzidou, E. Kontonasaki, D. Bikiaris**
Incorporation of Moxifloxacin-Loaded Silica-Based Mesoporous Nanocarriers in Electrospun PLGA Fibers for Periodontal Regeneration
- 11:00 A. Kordas, P. Manganas, A. Ranella, M. Farsari**
3D scaffolds via Multi-Photon Polymerization for the directed neurite development in co-culture systems
- 11:15 Coffee break**

Session: Energy

Chair: E. Kymakis

- 11:45 F. Farmakis (Invited)**
Micro and nano-engineered silicon for high energy density lithium-ion cells
- 12:10 P.S. Ioannou, E. Kyriakides, O. Schneegans, J. Giapintzakis**
Lithionic two-terminal resistive switching devices with analog memory and a nanobattery architecture based on $Li_{1-x}CoO_2$ cathode, SiO_x electrolyte and $Li_{4+3x}Ti_5O_{12}$ anode
- 12:25 E. Glynos, G. Nikolakakou, D. Kritsiotakis, C. Pantazidis, G. Sakellariou**
High Performance Single-ion Polymer Electrolytes via Macromolecular Engineering
- 12:40 D.K. Manousou, S.B. Atata, M. Calamiotou, S. Gardelis, Y.J. Sohna, K. Friese**
Phase evolution of $V_{1-x}Fe_xO_2$, ($x=0, 0.5, 0.75, 1.0$ %) system as a function of temperature
- 12:55 A. Kostopoulou, K. Brintakisa, D. Vernardou, E. Stratakis**
Advanced photonic processes for low-cost and safe perovskite-based energy storage devices
- 13:10 L. Zouridi, E. Gagaoudakis, E. Mantsiou, A. Vourros, J. Garagounis, G.E. Marnellos, V. Binas**
Mechanochemical synthesis, processing and printability of $La_{1-x}Sr_xTi_{1-y}Mn_yO_{3+\delta}$ perovskites as mixed ion-electron conducting (MIEC) materials
- 13:25 G. Viskadouros, K. Rogdakis, I. Kalogerakis, E. Spiliarotis, E. Kymakis**
Integration of two-dimensional materials-based perovskite solar panels into a stand-alone solar farm
- 13:40 Lunch break**

Session: Strongly Correlated Systems

Chair: C. Stoumpos

- 14:45** R. Frantzeskakis, J. Van Dyke, S. Economou, E. Barnes
Time-crystalline behavior in central-spin models with Heisenberg interactions
- Z. Viskadourakis, G. Kenanakis, J. Giapintzakis
- 15:00** *Magnetic field effect on the thermoelectric properties of semiconducting $\text{LaNi}_{0.2}\text{Co}_{0.8}\text{O}_3$ and metallic $\text{LaNi}_{0.7}\text{Co}_{0.3}\text{O}_3$*
- 15:15** S. Komineas, N. Papanicolaou
Skyrmions in antiferromagnets
- M. Kaitatzi, A. Deltsidis, A. Missiul, E.S. Bozin, A. Lappas
- 15:30** *Hybrid networks based on the interplay of Au nano-particles and CuPcSu ligands-electronic transport in mesoscopic scale*
- 15:45** O. Manos, A. Sigalos, D. Niarchos
COMSOL simulations of assemblies of sub-millimeter NdFeB -based magnets
- 16:00** **Coffee break**

Session: Photonics - Optoelectronics II

Chair: J. Parthenios

L.C. Palilis (**Invited**)

- 16:20** *Metal oxides and organic molecules for interface engineering in high performance polymer solar cells*
- M. Maniadi, B. Cucco, X. Wang, S. Li, A. Pantousas, M. Kepenekian, P. Guo, G. Volonakis,
- 16:45** C.C. Stoumpos
'Breathing' 2D Hybrid Double Halide Perovskites consisting of non-toxic elements
- A.E. Mavropoulis, N. Vasileiadis, T. Tsiamis, C. Theodorou, L. Sygelloud, P. Normand,
- 17:00** G.Ch. Sirakoulis, P. Dimitrakis
On the effect of SOI substrate in silicon nitride resistance switching MIS structures
- 17:15** P. Pascariu, L. Georgescu, E. Koudoumas, M.P. Suchea
Electrospinning of TiO_2 based semiconductor nanofibers with enhanced photocatalytic properties
- N. Mouti, A. Kaidatzis, K. Giannakopoulos
- 17:30** *Superhydrophilic low temperature TiO_2 ultra thin films deposited on CSP mirrors by magnetron Sputtering*

Session: Posters II

18:00 Posters and discussion

21:00

Conference dinner

Wednesday, 28/09/2022

Session: Theory and Simulations

Chair: P. Kelires

- 09:00** G.M. Kavoulakis
Quantum droplets in mixtures of cold atomic gases
- 09:15** E.G. Karvelas, Christos Liosis, I. Sarris, T.E. Karakasidis
Evaluation of the Tesla valve as a micromixer for Fe₃O₄ nanoparticles and contaminated water
- 09:30** O. Tsilipakos, M. Kafesaki, E.N. Economou, C.M. Soukoulis, T. Koschny
Artificial multiresonant sheet materials for broadband wave manipulations
- 09:45** A. Theodosi, O. Tsilipakos, C.M. Soukoulis, E.N. Economou, M. Kafesaki
Hybrid Graphene – Gold Metasurfaces for Enhanced Third Harmonic Generation Efficiency
- G.D. Tsibidis, P. Lingos, E. Stratakis
- 10:00** *The synergy of electromagnetic effects and thermophysical properties of metals in the formation of laser induced periodic surface structures*
- M. Arnittali, A.N. Rissanou, V. Harmandaris
- 10:15** *Nanostructured Systems of Diphenylalanine Peptides and Graphene Sheets: an Atomistic Simulation Study*
- E. Pervolarakis, D. Katerinopoulou, G. Kiriakidis, Z. Łodziana, E. Iliopoulos, G.A. Tritsarlis, P. Rosakis, I.N. Remediakis
- 10:30** *Case-Studies for Computer-aided Materials Design: alloyed Hausmanites and Gold Nanoparticles*
- R.M. Giappa, A. Pantousas, G. Kopidakis, I.N. Remediakis, C.C. Stoumpos
- 10:45** *Modelling catalyst materials for CO₂ reduction: from metal nanoparticles to halide perovskites*
- 11:00** **Coffee break**

Session: Nanomaterials II

Chair: E. Lidorikis

- 11:30** D. Mantione, E. Istif, L. Vallan, G. Dufil, D. Parker, E. Stavrinidou, E. Pavlopoulou
Novel Conducting Trimers for In Vivo Electronic Functionalization of Tissues
- 11:45** G.G. Gkikas, V. Spanou, C.C. Stoumpos, A. Lappas
Phase transitions and electric dipole moments in hybrid halide perovskite single crystals
- G. Zyla, S. Gorb, A. Ostendorf
- 12:00** *Nature as an inspiration for printing angle-insensitive structural colors using two-photon polymerization*
- 12:15** K. Papadopoulos, K. Manousakis, G.K. Angeli, C. Tsangarakis, E. Loukopoulos, P.N. Trikalitis
Design and Development of Functionalized PillarLayered MOFs
- I. Vamvasakis, E.K. Andreou, G.S. Armatas
- 12:30** *Co-catalyst assisted mesoporous II-VI metal sulfide nanocrystal assemblies for highly efficient photochemical water-splitting and hydrogen production*

C. Floraki, K. Brintakis, A. Kostopoulou, E.Stratakis, D. Vernardou

12:45 *Spray Deposition of LiFePO₄ on Al foil as cathode for Li-ion batteries*

Industrial Session & Closing

13:00 *Industrial session*

13:30

Closing Remarks

14:00

Light Lunch

Posters I - Monday

Surfaces, nanomaterials, and low-dimensional systems

- E.K. Andreou, I. Vamvasakis, G.S. Armatas
P1.1 *Mesoporous Architectures of Spinel Chalcogenide Nanoparticles Coupled with Transition Metal Phosphides for Photochemical Water Splitting and Hydrogen Production*
- G.K. Angeli, C. Tsangarakis, P.N. Trikalitis
P1.2 *Novel Metal Organic Frameworks for Desulfurization of Oil based Fuels*
- S.B. Atata, I. Lelidis
P1.3 *Phase diagram and Freedericks transition in nanocomposites of a liquid crystal and quantum dots*
- N. Balakeras, K. Filintoglou, A. Michail, K. Stergiou, I. Parthenios, K. Papagelis
P1.4 *Scaling up the synthesis of single layer MoS₂ crystals*
- K. Brintakis, A. Kostopoulou, E. Stratakis,
P1.5 *Laser-assisted processes on metal halide perovskite nanocrystals: Shape/dimensionality transformations and conjugation with 2D materials*
- M. Charalampakis, E. Loukopoulos, E. Skliri, G. Kyriakidis, P.N. Trikalitis, V. Bina
P1.6 *Formation of Black Titania by Ammonolysis for Photocatalytic Hydrogen Production*
- N. Dimogerontaki, K. Turlouki, E. Svinterikos, N. Kehagias
P1.7 *Development of novel Nanostructured surfaces using Residual Layer Free Nanoimprint Lithography and Metal Assisted Chemical Etching*
- A. Douloumis, C.C. Stoumpos, G. Kopidakis, I.N. Remediakis
P1.8 *Electronic structure of photocatalytic materials: doped ZnO and gold-perovskite interfaces.*
- K.G. Froudas, G.K. Angeli, P.N. Trikalitis
P1.9 *Implementation of Hard-Soft Chemistry for one-Pot Synthesis of Bimetallic MOFs Suitable for Xe/Kr Separation*
- K. Giannaris, S. Stefa, V. Binas, M.M. Stylianakis, K. Chrissopoulou, S.H. Anastasiadis
P1.10 *Dispersibility Determination of Stable g-C₃N₄ Colloidal Suspensions in Common Solvents*
- F. Gojda, L. Papoutsakis, M. Loulakis, S. Tzortzakis, K. Chrissopoulou, S.H. Anastasiadis
P1.11 *Development of Functional Materials Surfaces*
- I. Karnis, F. Krasanakis, A.N. Rissanou, K. Karatasos, K. Chrissopoulou
P1.12 *Polymer / Graphene Oxide Nanocomposites: Investigating the Effect of the Interfacial Interactions on Structure and Properties*
- D. Katrisioti, E. Katsipoulaki, E. Stratakis, G. Kioseoglou
P1.13 *Photochemically doped MoSe₂ monolayers*
- E. Katsipoulaki, I. Demeridou, E. Stratakis, G. Kioseoglou
P1.14 *Control of electron density in WSe₂ monolayers via photochlorination*
- I. Kochylas, M.A. Apostolaki, V. Likodimos, S. Gardelis, A. Dimitriou, L. Patsiouras,
P1.15 *M.C. Skoulikidou, N. Papanikolaou, G.Geka, A. Kanioura, P.Petrou*
SiNWs/Ag nanostructures fabricated by a single step MACE process for the detection of biological substances
- G. Kourmoulakis, S. Psilodimitrakopoulos, G.M. Maragkakakis, L. Mouchliadis, A. Michail,
P1.16

- J.A. Christodoulides, J. Parthenios, K. Papagelis, E. Stratakis, G. Kioseoglou
Identification of non-uniform strain in WS₂ monolayers using P-SHG
C.G. Livas, G.E. Froudakis, E. Tyliaakis
- P1.17** *Enhancing of CO uptake in Metal-Organic Frameworks by linker functionalization; A Multi-scale theoretical study*
E. Loukopoulos, M. Charalampakis, K. Papadopoulos, E. Skliri, V. Binas, P.N. Trikalitis
- P1.18** *Development of TiO₂/MOF Nanostructured Composites Towards Photocatalytic Hydrogen Conversion*
S. Loukopoulos, S. Gardelis, V. Iikodimos, Z. Sideratou, F. Katsaros, E. Sakelis, A.G. Kontos
- P1.19** *Heterostructured Au/Ag-MoS₂-TiO₂ inverse opal photocatalysts*
E. Gagaoudakis, E. Mantsiou, L. Zouridi, X. Maragaki, E. Aperathitis, G. Kiriakidis, V. Binas
- P1.20** *Study of the thermochromic performance of hydrothermally synthesized Vanadium dioxide powder for energy efficient buildings*
G.M. Maragkakis, S. Psilodimitrakopoulos, L. Mouchliadis, A.S. Sarkar, A. Lemonis,
- P1.21** *Nonlinear Optical Imaging of In-Plane Anisotropy in Two-Dimensional SnS*
G. Kioseoglou, E. Stratakis
- P1.22** *Ferromagnetic Resonance in Ru/Co/MoPt multilayers*
P. Ntetsika, R. Gupta, R. Brucas, P. Svedlindh, G. Mitrikas, I. Panagiotopoulos
- P1.23** *Surface modification of Mo-BiVO₄ photonic crystal photocatalysts by Au and Ag plasmonic nanoparticles*
M. Pylarinou, S. Gardelis, V. Iikodimos, E. Sakellis, P. Tsipas, N. Boukos, A. Dimoulas
- P1.24** *Can accurate machine learning models pinpoint the best materials efficiently?*
A.P. Sarikas, G.S. Fanourgakis, G.E. Froudakis
- P1.25** *Chemically modified carbon nanostructures as carriers of enhanced qualities for fabrics performing under critical operational conditions*
I.K. Sideri, A. Kagkoura, C. Stangel, S. Vasilakos, D. Siamidis, S. Pavlidou, P. Perimenis, N.S. Heliopoulos, N. Tagmatarchis
- P1.26** *Highly active catalysts (Ni, Pt) supported on strontium titanate (SrTiO₃) for hydrogen evolution*
A.P. Souri, E. Skliri, I. Vamvasakis, G.S. Armatas, V. Binas
- P1.27** *Room temperature synthesis of hydrophilic, highly-fluorescent metal halide perovskite nanocrystals for biomedical applications*
M. Splinaki, A. Kostopoulou, K. Brintakis, E. Stratakis
- P1.28** *From Order to Disorder of Alkanethiol SAMs on Complex Au (211), (221) and (311) Surfaces: Impact of the Substrate*
D. Stefanakis, V. Harmandaris, G. Kopidakis, I. Remediakis
- P1.29** *Thermoelectric properties of n-type PbS nanocrystals doped with two-dimensional lead bromide perovskites*
M.E. Trantafyllou-Rundell, C. Fiedler, C.C. Stoumpos, M. Ibáñez
- P1.30** *Performance and stability improvement of inverted perovskite solar cells by interface modification of charge transport layers using an Azulene-pyridine molecule.*
N. Tzoganakis, B. Feng, M. Loizos, K. Chatzimanolis, M. Krassas, D. Tsikritzis, X. Zhuang, E. Kymakis
- P1.31** *Performance and stability improvement of inverted perovskite solar cells by interface modification of charge transport layers using an Azulene-pyridine molecule.*
D. Tsikritzis, N. Tzoganakis, B. Feng, M. Loizos, M. Krassas, X. Zhuang, and E. Kymakis

Surface engineering of charge transport in inverted perovskite solar cells with azulene derivatives

G. Vailakis, G. Kopidakis

P1.32 *Electronic band structure of Gr/MS_2 ($M=Mo, W$) and WX_2/MoX_2 ($X=S, Se$) van der Waals heterostructures*

M. Vlachos, E. Tylianakis, E. Klontzas, M. Severi, G. Turtù, F. Zerbetto, G. Froudakis

P1.33 *Multiscale Computational study of 5- Fluorouracil delivery by Zeolite Imidazole Frameworks (ZIFs)*

N.R. Vrithias, M. Sevastaki, G. Kenanakis

P1.34 *3D printed photocatalysts against liquid laundry detergents*

Structural, dynamical and mechanical properties of condensed matter

D. Fylaktopoulou, K. Kamarakis, A. Tsanios, P.S. Selinof, A. Kassas, D. Delali, P.M. Kiritsi,

P1.35 S. Rentzis, Y. Fortouna, A. Balerba, Ch. E. Lekka

Structural and electronic properties of β Ti-based alloys by density functional theory

K. Mavridou, F. Pinakidou, M. Katsikini, J. Arvanitidis, E.C. Paloura, M. Brzhezinskaya,

P1.36 M. Zervos

Raman and NEXAFS study of the oxidation of Cu_3N thin films during their growth procedure

P1.37 K. Manousakis, K. Papadopoulos, G.K. Angeli, E. Loukopoulos, C. Tsangarakis, P.N. Trikalitis

A Highly Stable, Flexible Metal Organic Framework for Selective Sorption Applications

P1.38 A. Michail, K. Filintoglou, N. Balakeras, N.N. Lathiotakis, J. Parthenios, K. Papagelis

Strain induced frequency shifts of the second order Raman modes of monolayer WS_2

M.E. Nousia, S. Papadoniou Chatzis, B. Liontos, A. Mosxou, Ch. Kourti, A.X. Galani,

P1.39 A. Delaporta, A. Balerba, Ch. E. Lekka

Ab initio calculations on β Ti-based implant surfaces

C. Papamichail, C.C. Stoumpos

P1.40 *Thermochemical properties of hybrid two-dimensional lead halide perovskites based on bulky aromatic spacer cations*

Ceramics, composites, minerals and metals

M. Apostolopoulou, C. Floraki, K. Anagnostou, A. Kostopoulou, K. Brintakis, E. Stratakis,

P1.41 E. Kymakis, D. Vernardou

Si-Graphene Oxide Heterostructures as Anode Material in Li-air Energy Storage Devices: Effect of the Si Loading

A. Bouranta, I.V. Tudose, L. Georgescu, N.R. Vrithias, G. Kenanakis, E. Sfakaki, N. Mitrizakis,

P1.42 G. Strakantounas, N. Papandroulakis, C. Romanitan, C. Pachiou, O. Tutunaru, L. Barbu -Tudoran,

M.P. Sucheai, E. Koudoumas

3D printed composite materials with antifouling properties for aquaculture applications

C. Gioti, I. Villis, A. Karakassides, S. Gkiouzel, G. Asimakopoulos, Maria Baikous, C.E. Salmas,

P1.43 Z. Viskadourakis, G. Kenanakis, M.A. Karakassides

Carbon-red mud foam/paraffin hybrid materials for thermal energy storage and electromagnetic interference shielding applications

P1.44 S. Gkiouzel, K.C. Vasilopoulos, I. Kitsou, E. Roussi, E. Kagiara, A. Tsetsekou, S. Agathopoulos,

M.A. Karakassides

MgO-C refractories containing nanoadditives: the effect of graphite content and of use modified graphite with Fe and Si.

- P1.45** D. Katerinopoulou, E. Pervolarakis, Z. Łodziana, I.N. Remediakis, E. Iliopoulos
Study of the electronic transport mechanism in MnZn-Ni spinel oxides
- P1.46** M. Moschogiannaki, E. Gagaoudakis, G. Kiriakidis, V. Binas
Ultra-stable CoV₂O₆ hydrogen gas sensor, operating at room temperature
- P1.47** A.C. Patsidis, S. Gioti, A. Sanida, G.C. Manika, G.C. Psarras, G.N. Mathioudakis, Th. Speliotis
Probing the Multi-Functional Performance of Magnetic Nanoparticles/Epoxy Resin Hybrid Nanocomposites
- P1.48** S. Gioti, A. Sanida, G.C. Manika, A.C. Patsidis, G.C. Psarras, G.N. Mathioudakis, Th. Speliotis
Ceramic Inclusions/Epoxy Resin Hybrid Nanodielectrics: Development, Characterization and Multi-Functional Performance
- P1.49** A. Symvoulidou, G. Vekinis
Mechanical and thermal properties of spinel refractories mixed with blast furnace waste slag

Posters II – Tuesday

Photonics and optoelectronics

- P2.1** Ch. Aivalioti, E. Manidakis, Z. Viskadourakis, N.T. Pelekanos, C.C. Stoumpos, M. Modreanu, E. Aperathitis
Cation and Anion co-doping of NiO for enhancing the UV-PV performance of NiO/TiO₂ heterostructures
- P2.2** N.G. Chatzarakis, A. Kostopoulos, G. Konstantinidis, G. Deligeorgis, G. Raino, M. Bodnarchuk, M.V. Kovalenko, N.T. Pelekanos
Reduced Stark effect in CsPbBr₃ Perovskite Nanocrystals
- P2.3** A. Dagkli, A. Chatzilari, S. Doukas, E. Lidorikis
Electro-optic free-space ultrafast pulse-shaping in a graphene-loaded Bragg resonator
- P2.4** E.M. Darivianaki, M. Androulidaki, K. Tsagaraki, M. Kayambaki, G. Stavrinidis, G. Konstantinidis, E. Dimakis, N.T. Pelekanos, C.C. Stoumpos
Hybrid GaAs nanowire/halide perovskite optoelectronic devices
- P2.5** I. Demeridou, M. Mavrotsoupakis, L. Mouchliadis, P.G. Savvidis, E. Stratakis, G. Kioseoglou
High room temperature valley polarization in WS₂/Graphite
- P2.6** K. Faka, M.G. Manidakis, G. Gkikas, C.C. Stoumpos
Volatile Hybrid Organic/Inorganic Copper (I) Iodides/Polyiodides for Efficient Thin-Film Deposition of CuI
- P2.7** T. Giannakis, M. Kandyla
Measuring optical forces using single beam optical tweezers
- P2.8** A. Anastasopoulos, A. Kaltzoglou, A. Sinani, A. Bogris C. Riziotis, M. Kandyla
Formamidinium lead bromide perovskite as visible-light detector
- P2.9** I. Katsantonis, M. Kafesaki
Enhanced chiral sensing using gain metamaterials
- P2.10** D. Ladika, V. Melissinaki, G.D. Barmparis, M. Farsari
Micro-optical elements fabricated onto an optical fiber adaptor for beam guidance
- P2.11** E. Lampadariou, K. Kaklamanis, D. Goustouridis, I. Raptis, E. Lidorikis
Nonlocal effective medium (NLEM) for quantitative modelling of nanoroughness in spectroscopic reflectance
- P2.12** K. Rogdakis, M. Loizos, G. Viskadourous, E. Kymakis
Memristive perovskite solar cells for self-powered IoT edge computing
- P2.13** E.C. Macropulos, M.E. Triantafyllou Rundell, L. Li, J. Bennett, P. Guo, M. Kepenekian, C.C. Stoumpos
Electrochemically active supramolecular entities in layered hybrid halide perovskites
- P2.14** Y. Liu, S. Geng, Y.-P. Gong, M.-L. Feng, D. Manidaki, C.C. Stoumpos, W.-X. Zhang, Z. Xiao, L. Mao
Hybrid Germanium Bromine Perovskites with Tunable Second Harmonic Generation
- P2.15** E.G. Manidakis, N.G. Chatzarakis, K. Tsagaraki, D. Tsikritzis, C.C. Stoumpos, N.T. Pelekanos
Strong passivation effect at the MAPbI₃/GaAs heterointerface
- P2.16** E.G. Manidakis, I. Syngelakis, Ch. Aivalioti, M. Androulidaki, K. Tsagaraki, C.C. Stoumpos,

- N.T. Pelekanos, G. Kenanakis, A. Klini, M. Farsari, E. Aperathitis
The effect of different architectures of TiO₂ as electron transport layer in perovskite solar cells
- P2.17** M. Mavrotsoupakis, M. Triantafillou, M. Chairetis, G. Paschos, C.C. Stoumpos, P.G. Savvidis
Polariton lasing in 2D Perovskite Microcavities
- P2.18** D. Ladika, G. Zyla, G. Maconi, V. Melissinaki, I. Kassamakov, M. Farsari
Photonic nanojets fabricated by multiphoton polymerization technique
- P2.19** A. Pantousas, C.C. Stoumpos, P. Guo, R.M. Giappa
(CH₃(CH₂)₅NH₃)₂(CH₃NH₃)_{n-1} Pb_nBr_{3n+1}: A homologous series of 2D halide perovskites with tuneable energy gap in the blue and green visible spectrum
- P2.20** K. Papadopoulos, D. Tselekidou, S. Kassavetis, M. Gioti, V. Kyriazopoulos, A.K. Andreopoulou, K. Andrikopoulos, J.K. Kallitsis
A comparative study of Carbazole based polymer and Polyfluorene derivatives as emissive layer for blue emitting flexible PLED devices
- P2.21** S. Papamakarios, M. Farsari
Fabrication and analysis of 3D-printed metamaterials
- P2.22** A. Polymerakis, I. Vaggelidis, E. Lidorikis
Photocurrent generation mechanisms for the description of Metal-Graphene-Metal photodetectors' responsivity.
- P2.23** C. Saitanidou, N.G. Chatzarakis, G. Kourmoulakis, G. Stavrinidis, G. Konstantinidis, G. Raino, M. Bodnarchuk, M.V. Kovalenko, N.T. Pelekanos
Triboelectric generators based on plasma-etched flexible surfaces
- P2. 24** A. Segkos, A. Bardakas, A. Zeniou, E. Gogolides, and C. Tsamis
Performance of SiC-doped 3D printed PLA for triboelectric energy harvesting
- P2.25** A.C. Tasolamprou, E. Skoulas, G. Perrakis, M. Vlahou, Z. Viskadourakis, E.N. Economou, M. Kafesaki, G. Kenanakis, E. Stratakis
Optical metasurfaces implemented by highlyordered Laser Induced Periodic Surface Structures
- P2.26** P.E. Stamatopoulou, N.A. Mortensen, C. Tserkezis
Exciton polaritons for reconfigurable chirality
- P2.27** A. Verykios, A. Soultati, V.P. Vidali, G. Pistolis, M. Vasilopoulou, P. Argitis
Tuning the emitting color of organic light-emitting diodes by dispersing the red dye DANS in the green emitter for biosensing applications

Polymers, organic materials, biomaterials

- P2.28** P. Bousboura, G. Vekinis
Low temperature tensile strength of Polylactic acid filled with ceramic nanopowders and glass bubbles
- P2.29** E. Christofi, V. Harmandaris, W. Li, A. Chazirakis, M. Doxastakis, M.A. Nicolaou, C. Chrysostomou
Generative Networks for Re-inserting Atomic detail in Coarse-grained Multi-component Macromolecules
- P2.30** E. Giannakaki, K. Giannaris, M.M. Stylianakis, A. Fidelli, P. Krassa, K. Chrissopoulou, S. H. Anastasiadis
Development of Polyurethane/r-GO Nanocomposites with Reinforced Self-healing Properties

- E. Kanakousaki, P. Kavatzikidou, A. Manousaki, E. Stratakis, A. Ranella
P2.31 *Effect of topography and statin loaded micropatterned polymeric replicas on osteogenic differentiation*
- C. Katsodridakis, E. Svinterikos, K. Turlouki, N. Kehagias, P. Argitis
P2.32 *Novel polymer resins for ultraviolet light assisted nanoimprint lithography applications*
- G.-I. Kontogianni, A.F. Bonatti, C. De Maria, R. Naseem, C. Coelho, G. Vozzi, K. Dalgarno,
P2.33 P. Quadros, M. Chatzinikolaidou
Co-culture of osteoblasts and osteoclasts in composite scaffolds support osteogenesis in vitro
- K. Kordos, M. Andrea, D.G. Papageorgiou
P2.34 *PCDTBT: Accurate Force Field Derivation and Molecular Dynamics Simulation*
- M.I. Kotzabasaki, C. Maraveas, T. Bartzanas
P2.35 *Agricultural Plastics: Recent Developments in Waste management and Recycling*
- I. Marinakis, E. Kapetanakis, V. Saltas, C. Katsogridakis, P. Argitis, P. Normand
P2.36 *Bias stress effect in organic thin film transistors operating in irradiation-activated electrolyte*
- A. Parlanis, E. Kanakousaki, P. Kavatzikidou, A. Manousaki, E. Stratakis, A. Ranella,
P2.37 A. Tsouknidas
Effect of topography and cellulose nanocrystals on micropatterned polymeric replicas
- V. Platania, K. Loukelis, N. Koutsomarkos, D. Vlassopoulos, M. Chatzinikolaidou
P2.38 *3D bioprinted polysaccharide-based constructs for endothelial tissue engineering*
- S. Skrepetos, G. Flamourakis, L. Papadimitriou, A. Ranela, M. Farsari
P2.39 *Metamaterials as immunoengineering scaffolds*
- V.M.V. Stavropoulou, A.A. Barmdaki, E.E. Zavvou, P.K. Karahaliou, C.A. Krontiras,
P2.40 A. Giannakas, A. Ladavos
Morphological, Structural, Thermal and Dielectric Properties of PLA/PCL based nanocomposites
- I. Tanis, V. Harmandaris
P2.41 *Structural and dynamic properties of poly(ethylene oxide)/silica nanocomposites as studied by molecular dynamics simulations: Effects of temperature and silica concentration*

Strongly correlated electronic systems, magnetism and superconductivity

- A. Deltsidis, M. Kaitatzi, L. Simonelli, A. Lappas
P2.42 *Hyper expanded molecule intercalated iron selenides with robust superconducting response*
- G. Kastrinakis
P2.43 *Order parameters in underdoped copper oxides: charge and pair density waves*
- D. Kechrakos, R. Tomasello, F. Gemenetzi, G. Finocchio
P2.44 *Skyrmion dynamics in ring-shaped synthetic antiferromagnetic racetracks*
- A. Kaidatzis, N. Mouti, K. Giannakopoulos, D. Niarchos
P2.45 *C-doped $L1_0$ -MnAl ferromagnetic thin films*

Interdisciplinary applications

- P2.46** A. Argyrou, K. Brintakis, E. Gagaoudakis, V. Binas, A. Kostopoulou, E. Stratakis,
Unravelling the ozone sensing mechanism of allinorganic metal halide perovskites
- P2.47** S.X. Drakopoulos, T. Cowell, E. Kendrick
Graphite-SiO_x electrodes with a biopolymeric binder for Li-ion batteries
- P2.48** M.A. Karageorgou, P. Bouziotis, D. Stamopoulos
⁶⁸Ga-DPD-Fe₃O₄ as a dual-modality contrast agent: magnetic resonance imaging on mice
- P2.49** M.A. Karageorgou, P. Bouziotis, D. Stamopoulos
⁶⁸Ga-DPD-Fe₃O₄ as a dual-modality contrast agent: biodistribution study on mice and biocompatibility with peripheral human blood cells
- P2.50** N.D. Dinas, A.X. Krestou, A.Z. Stimoniaris, G. Ch. Kalogeropoulos
Design and development of detachable water PLA filters using 3D printing
- P2.51** A. Michail, J.A. Young, K.J. Thompson, C.A. Nattoo, C.S. Bailey, A. Daus, E. Pop, J. Parthenios, K. Papagelis
Flexible 2D material transistors under controlled biaxial deformation
- P2.52** A. Michailidis-Barakat, E. Pervolarakis, C.C. Stoumpos, I.N. Remediakis
Band gap prediction & data analysis of inorganic halide perovskites using machine learning
- P2.53** K. Mouratis, I.V. Tudose, C. Romanitan, M. Popescu, G. Simistiras, S. Couris, M.P. Sucheas, E. Koudoumas
Fabrication and performance of electrochromic devices based on V₂O₅ and WO₃ thin films
- P2.54** E. Nanou, P. Kourelis, D. Stefan, S. Couris, V. Kokkinos, C. Bouras, E. Konstantinou, E. Manolopoulou, E. Tsakalidou
A laser-based technique for the classification of milk samples based on their animal origin
- P2.55** D. Polygenis, D. Stefan, N.C. Mavrikakis, K. Siderakis, K. Mouratis, E. Koudoumas, S. Couris
Mechanical and thermal properties of spinel refractories mixed with blast furnace waste slag
- P2.56** F. Sofos, T.E. Karakasidis, M. Valasaki, C.G. Papakonstantinou
Mechanical and structural properties of FRP concrete: data-driven, machine learning approaches
- P2.57** I.V. Tudose, C. Romanitan, C. Pachiou, I. Rosca, K. Petrotos, S. Zaoutsos, G.A. Fragkiadakis, A. Bouranta, M.P. Sucheas, E. Koudoumas
PLA nanocomposites with antimicrobial action, based on encapsulated natural extracts for food packaging applications

LAST NAME	FIRST NAME	AFFILIATION
AIVALIOTI	CH.	IESL/FORTH & KAUST
ANASTASIADIS	SPIROS	IESL/FORTH
ANDREOU	EVANGELOS	UNIVERSITY OF CRETE
ANGELI	GIASEMI	NATIONAL HELLENIC RESEARCH FOUNDATION
ANTONOPOULOU	SOFIA	UNIVERSITY OF CRETE
APERATHITIS	ELIAS	IESL/FORTH
APOSTOLAKI	MARIA ATHINA	NATIONAL AND KAPODISTRIAN UNIVERSITY OF ATHENS
APOSTOLOPOULOU	MARIA	HELLENIC MEDITERRANEAN UNIVERSITY
ARGYROU	AIKATERINI	UNIVERSITY OF CRETE
ARNITTALI	M.	IACM/FORTH & UNIVERSITY OF CRETE
ATATA	STEFANOS	NATIONAL AND KAPODISTRIAN UNIVERSITY OF ATHENS
BAKOPOULOU	ATHINA	ARISTOTLE UNIVERSITY OF THESSALONIKI
BALAKERAS	NIKOLAOS	ARISTOTLE UNIVERSITY OF THESSALONIKI
BAMPAITI	ANASTASIA	SUNLIGHT GROUP ENERGY STORAGE SYSTEMS
BARMPAKI	AIMILIA	UNIVERSITY OF PATRAS
BOURANTA	ANDRIANNA	HELLENIC MEDITERRANEAN UNIVERSITY
BOUSBOURA	PANAYIOTA	UNIVERSITY OF IOANNINA
BRINTAKIS	KONSTANTINOS	IESL/FORTH
CHARALAMPAKIS	MICHALIS	IESL/FORTH
CHATZAKI	THALEIA MICHAELA	IESL/FORTH
CHATZARAKIS	NIKOLAOS	UNIVERSITY OF CRETE
CHATZICHRISTIDI	MARGARITA	NATIONAL AND KAPODISTRIAN UNIVERSITY OF ATHENS
CHATZINIKOLAIDOU	MARIA	UNIVERSITY OF CRETE
CHERETIS	MINOAS	UNIVERSITY OF CRETE
CHOUCHOUMI	NIKOLETA	NATIONAL TECHNICAL UNIVERSITY OF ATHENS
CHRISPOPOULOU	KIRIAKI	IESL/FORTH
CHRISTOFI	ELEFTHERIOS	THE CYPRUS INSTITUTE
DAGKLI	ALVA	UNIVERSITY OF IOANNINA
DARIVIANAKI	ELEFThERIA	UNIVERSITY OF CRETE
DELTSIDIS	ALEXANDROS	IESL/FORTH
DEMERIDOU	I.	IESL/FORTH & UNIVERSITY OF CRETE
DIMITRAKIS	PANAGIOTIS	NCSR DEMOKRITOS
DIMOGERONTAKI	NEFELI	NATIONAL TECHNICAL UNIVERSITY OF ATHENS & NCSR
DOUKAS	SPYROS	UNIVERSITY OF IOANNINA
DOULOUMIS	ANDREAS	UNIVERSITY OF CRETE
DRAKONAKI	CHRYSOVALANTO-MARIA	UNIVERSITY OF CRETE
DRAKOPOULOS	STAVROS X.	UNIVERSITY OF BATH
ERLANO	NIKOLETA	UNIVERSITY OF CRETE
FAKA	KONSTANTINA	UNIVERSITY OF CRETE
FARMAKIS	FILIPPOS	DEMOCRITUS UNIVERSITY OF THRACE
FARSARI	MARIA	FORTH
FLORAKI	CHRISTINA	HELLENIC MEDITERRANEAN UNIVERSITY
FLYTZANIS	NIKOS	UNIVERSITY OF CRETE
FRANTZESKAKIS	RAFAIL	IESL/FORTH & UNIVERSITY OF CRETE
FROUDAS	KONSTANTINOS	UNIVERSITY OF CRETE
FYLAKTOPOULOU	DIMITRA	UNIVERSITY OF IOANNINA
GAGAOUDAKIS	EMMANOUIL	IESL/FORTH
GARDELIS	SPIROS	NATIONAL AND KAPODISTRIAN UNIVERSITY OF ATHENS
GEORGIOS	KOPIDAKIS	UNIVERSITY OF CRETE
GIANNAKAKI	EVANGELIA	IESL/FORTH & UNIVERSITY OF CRETE
GIANNAKIS	THEODOROS	NATIONAL HELLENIC RESEARCH FOUNDATION
GIANNARIS	KOSMAS	IESL/FORTH
GIAPPA	RAFAELA MARIA	UNIVERSITY OF CRETE
GIOTI	CHRISTINA	UNIVERSITY OF IOANNINA
GKIKAS	GIANNIS	FORTH & UNIVERSITY OF CRETE
GKIOUZEL	SEVASTEIA-MARIA	UNIVERSITY OF IOANNINA
GLYNOS	EMMANOUIL	UNIVERSITY OF CRETE
GOJDA	FRANCESKA	IESL/FORTH & UNIVERSITY OF CRETE
IOANNOU	PANAGIOTIS	UNIVERSITY OF CYPRUS
KADIANAKI	KATERINA	IESL/FORTH
KAFESAKI	MARIA	FORTH & UNIVERSITY OF CRETE

KAITATZI	MYRSINI	FORTH
KALOGEROPOULOS	GEORGIOS	WESTERN MACEDONIA UNIVERISTY
KANAKOUSAKI	ELENI	FORTH
KANDYLA	MARIA	NATIONAL HELLENIC RESEARCH FOUNDATION
KARAGEORGOU	MARIA-ARGYRO	NATIONAL AND KAPODISTRIAN UNIVERSITY OF ATHENS
KARNIS	IOANNIS	IESL/FORTH
KARVELAS	EVANGELOS	UNIVERSITY OF THESSALY
KASTRINAKIS	GEORGE	IESL/FORTH
KATERINOPOULOU	D.	IESL/FORTH & UNIVERSITY OF CRETE
KATRISIOTI	DANAI	UNIVERSITY OF CRETE
KATSANTONIS	IOANNIS	FORTH & UNIVERSITY OF CRETE
KATSIDIS	CHARALAMPOS	UNIVERSITY OF CRETE
KATSIKINI	MARIA	ARISTOTLE UNIVERSITY OF THESSALONIKI
KATSIPOULAKI	EIRINI	IESL/FORTH & UNIVERSITY OF CRETE
KATSOGRIDAKIS	C.	NCSR
KAVOULAKIS	GEORGIOS	HELLENIC MEDITERRANEAN UNIVERSITY
KAVOUSANOS	NIKOS	HELLENIC MEDITERRANEAN UNIVERSITY
KECHRAKOS	DIMITRIS	SCHOOL OF PEDAGOGICAL AND TECHNOLOGICAL EDUCATION
KEHAGIAS	NIKOS	INN-NNT
KEIVANIDIS	PANAGIOTIS	CYPRUS UNIVERSITY OF TECHNOLOGY
KELIRIS	PANTELIS	CYPRUS UNIVERSITY OF TECHNOLOGY
KIOSEOGLOU	GEORGE	IESL/FORTH & UNIVERSITY OF CRETE
KOCHYLAS	IOANNIS	NATIONAL AND KAPODISTRIAN UNIVERSITY OF ATHENS
KOMINEAS	STAVROS	UNIVERSITY OF CRETE
KONIDAKIS	I.	IESL/FORTH
KONTOGIANNI	GEORGIA-IOANNA	UNIVERSITY OF CRETE
KOPIDAKIS	GEORGIOS	UNIVERSITY OF CRETE
KORDAS	ANTONIS	IESL/FORTH
KORDOS	KONSTANTINOS	UNIVERSITY OF IOANNINA
KOSMA	KYRIAKI	HELLENIC MEDITERRANEAN UNIVERSITY
KOSMA	ADAMANTIA	NATIONAL AND KAPODISTRIAN UNIVERSITY OF ATHENS
KOSTOPOULOU	ATHANASIA	IESL/FORTH
KOTZAMPASAKI	MARIANNA	AGRICULTURAL UNIVERSITY OF ATHENS
KOULOUKLIDIS	ANASTASIOS	IESL/FORTH
KOURMOULAKIS	GEORGE	IESL/FORTH
KRASANAKIS	FANOURIOS	IESL/FORTH
KRASIA-CHRISTOFOROU	THEODORA	UNIVERSITY OF CYPRUS
KRESTOU	ATHINA	UNIVERSITY OF WESTERN MACEDONIA
KYMAKIS	EMMANUEL	IESL/FORTH
LADIKA	DIMITRA	IESL/FORTH
LAMPADARIOU	ELEFThERIA	UNIVERSITY OF IOANNINA
LASKARAKIS	ARGIRIS	ARISTOTLE UNIVERSITY OF THESSALONIKI
LEKKA	CHRISTINA	UNIVERSITY OF IOANNINA
LIVAS	CHARALAMPOS	UNIVERSITY OF CRETE
LOIZOS	MICHALIS	HELLENIC MEDITERRANEAN UNIVERSITY
LOUKELIS	KONSTANTINOS	UNIVERSITY OF CRETE
LOUKOPOULOS	STYLIANOS	NATIONAL AND KAPODISTRIAN UNIVERSITY OF ATHENS
LOUKOPOULOS	EDOUARDOS	UNIVERSITY OF CRETE
LUSHA	MARGARITA	UNIVERSITY OF CRETE
MACROPULOS	ELENI CONSTANTINA	UNIVERSITY OF CRETE
MALLIARAS	GEORGE	UNIVERSITY OF CAMBRIDGE
MANGOU	VASSO	MEGALAB S.A.
MANIADI	MARIA	UNIVERSITY OF CRETE
MANIDAKI	DESPOINA	UNIVERSITY OF CRETE
MANIDAKIS	EMMANOUIL	UNIVERSITY OF CRETE
MANOS	O.	AMEN NEW TECHNOLOGIES
MANOUSAKIS	KYRIAKOS	UNIVERSITY OF CRETE
MANOUSOU	DIMITRA K.	NATIONAL AND KAPODISTRIAN UNIVERSITY OF ATHENS
MANTSIOU	ELENI	FORTH/IESL
MANTSIOU	ELENI	IESL/FORTH
MARAGKAKIS	GEORGE MILTOS	IESL/FORTH & UNIVERSITY OF CRETE
MARIE	XAVIER	UNIVERSITÉ DE TOULOUSE

MARINAKIS	IOANNIS	HELLENIC MEDITERRANEAN UNIVERSITY
MARKOZANNE	GEORGIA	IESL/FORTH
MAVROPOULIS	ALEXANDROS-ELEFThERIOS	NCSR DEMOKRITOS
MAVROTSOUPAKIS	MANOLIS	UNIVERSITY OF CRETE
MELISSINAKI	VASILEIA	IESL/FORTH
MERGIANNIS	GEORGE	UNIVERSITY OF CRETE
MICHAIL	ANTONIOS	UNIVERSITY OF PATRAS
MICHAILIDIS - BARAKAR	ALAELEDDIN	UNIVERSITY OF CRETE
MINADAKIS	MICHAIL PANAGIOTIS	NATIONAL HELLENIC RESEARCH FOUNDATION
MOSCHOGIANNAKI	MARILENA	FORTH & UNIVERSITY OF CRETE
MOURATIS	KYRIAKOS	HELLENIC MEDITERRANEAN UNIVERSITY
MOURZIDIS	KONSTANTINOS	UNIVERSITY OF CRETE
MOUTI	NAFSICA	NCSR DEMOKRITOS
NANOU	ELENI	UNIVERSITY OF PATRAS
NIARCHOS	DIMITRIOS	AMEN TECHNOLOGIES
NIKOLETA NATALIA	TAVERNARAKI	IESL/FORTH
NOUSIA	M.E.	UNIVERSITY OF IOANNINA
NTETSIKA	PANAGIOTA	UNIVERSITY OF IOANNINA
PALILIS	LEONIDAS	UNIVERSITY OF PATRAS
PANAGOPOULOU	EFI	KRAHN HELLAS S.A.
PANTOUSAS	APOSTOLOS	UNIVERSITY OF CRETE
PAPADOPOULOS	KONSTANTINOS	UNIVERSITY OF CRETE
PAPAMAKARIOS	SAVVAS	IESL/FORTH
PAPAMICHAIL	CHRYSOSTOMOS	UNIVERSITY OF CRETE
PARADISANOS	IOANNIS	INSA/CNRS
PARLANIS	ANDREAS	IESL/FORTH
PARTHENIOS	JOHN	ICE-HT/FORTH
PATSIDIS	A.C.	UNIVERSITY OF PATRAS
PAVLOPOULOU	ELENI	FORTH
PELEKANOS	NIKOLAOS	FORTH & UNIVERSITY OF CRETE
PENNOS	LEONIDAS	I.T.C.
PERVOLARAKIS	EMMANOUIL	UNIVERSITY OF CRETE
PITANIOS	NIKOLAOS	UNIVERSITY OF CRETE
PLATANIA	VARVARA	UNIVERSITY OF CRETE
POLYGENIS	DIMITRIOS	UNIVERSITY OF PATRAS
POLYMERAKIS	ANASTASIOS	UNIVERSITY OF IOANNINA
POUROUTZIDOU	GEORGIA K	ARISTOTLE UNIVERSITY OF THESSALONIKI
PSARRAS	G.C.	UNIVERSITY OF PATRAS
PSILODIMITRAKOPOULOS	SOTIRIS	ULMNP/IESL/FORTH
PYLARINOU	MARTHA	NATIONAL AND KAPODISTRIAN UNIVERSITY OF ATHENS
REMEDIAKIS	IOANNIS	UNIVERSITY OF CRETE
RISSANOU	ANASTASIA	IACM/FORTH & UNIVERSITY OF CRETE
ROGDAKIS	KONSTANTINOS	HELLENIC MEDITERRANEAN UNIVERSITY
SARGENTIS	CHRISTOS	HELIX SQUARED P.C.
SARIKAS	ANTONIOS	MATERIALS MODELING & DESIGN GROUP
SEGKOS	APOSTOLOS	NCSR DEMOKRITOS
SIAITANIDOU	CHRISTINA	UNIVERSITY OF CRETE
SIDERI	IOANNA	NATIONAL HELLENIC RESEARCH FOUNDATION
SKREPETOS	STAVROS	IESL/FORTH
SOFOS	FILIPPOS	UNIVERSITY OF THESSALY
SOROGAS	NIKI	ARISTOTLE UNIVERSITY OF THESSALONIKI
SOURI	ANNA PANAGIOTA	IESL/FORTH
SPLINAKI	MARKELLA	ULMNP/IESL/FORTH
STAMATOPOULOU	ELLI	UNIVERSITY OF SOUTHERN DENMARK
STAMOPOULOS	DIMOSTHENIS	NATIONAL AND KAPODISTRIAN UNIVERSITY OF ATHENS
STAVROPOULOU	VASILIKI-MARIA	UNIVERSITY OF PATRAS
STAVROU	MICHALIS	UNIVERSITY OF PATRAS
STEFANAKIS	DIMITRIOS	UNIVERSITY OF CRETE
STOUMPOS	KONSTANTINOS	UNIVERSITY OF CRETE
STRATAKIS	EMMANUEL	IESL/FORTH
STYLIANAKIS	MINAS	IESL/FORTH
SUCHEA	MIRELA	IMT BUCHAREST & HMU

SYMVOULIDOU	AIKATERINI	UNIVERSITY OF IOANNINA & NCSR
TANIS	I.	THE CYPRUS INSTITUTE
TASOLAMPROU	ANNA	IESL/FORTH
THEODOSI	ANNA	UNIVERSITY OF CRETE
THOMOS	ALEXANDROS	IESL/FORTH
TRIANTAFYLLOU	MARIOS	UNIVERSITY OF CRETE
TSANGARAKIS	CONSTANTINOS	UNIVERSITY OF CRETE
TSERKEZIS	CHRISTOS	UNIVERSITY OF SOUTHERN DENMARK
TSIBIDIS	GEORGE	FORTH
TSIKRITZIS	DIMITRIS	HELLENIC MEDITERRANEAN UNIVERSITY
TSILIPAKOS	ODYSSEAS	IESL/FORTH
TUDOSE	IOAN VALENTIN	HELLENIC MEDITERRANEAN UNIVERSITY
VAILAKIS	GEORGIOS	UNIVERSITY OF CRETE
VAMVASAKIS	IOANNIS	UNIVERSITY OF CRETE
VERNARDOU	DIMITRA	HELLENIC MEDITERRANEAN UNIVERSITY
VERYKIOS	APOSTOLIS	NCSR
VLACHOS	MICHAIL	UNIVERSITY OF CRETE
VRITHIAS	NIKOLAOS RAPHAEL	UNIVERSITY OF CRETE
ZOURIDI	LEILA	IESL/FORTH & MST-UOC
ZYLA	GORDON	IESL/FORTH

Exciton Complexes and Spin/valley Pumping in 2D semiconductors

Xavier MARIE

*Université de Toulouse, INSA-CNRS-UPS,
Laboratoire de Physique et Chimie des Nano-Objets,
135 Avenue de Rangueil, 31077 Toulouse, France
marie@insa-toulouse.fr*

In this talk I will first recall briefly the general properties of 2D excitons in Transition Metal Dichalcogenides (TMD) monolayers: giant binding energy, oscillator strength, exchange interactions, spin/valley...¹.

Encapsulation of TMD monolayers in hexagonal boron nitride (hBN) yields narrow optical transitions approaching the homogeneous exciton linewidth^{2,3}. We demonstrate that the exciton radiative rate in these van der Waals heterostructures can be tailored by a simple change of the hBN encapsulation layer thickness as a consequence of the Purcell effect⁴.

We also measured the exciton fine structure of MoS₂ and MoSe₂ monolayers encapsulated in boron nitride by magneto-photoluminescence spectroscopy in magnetic fields up to 30 T^{5,6}.

Finally, I will present recent experimental results on spin/valley pumping of resident electrons in WSe₂ and WS₂ monolayers^{7,8}. The spin/valley diffusion length of these electrons will also be discussed⁹.

¹ G. Wang *et al*, Rev. Mod. Phys. **90**, 021001 (2018)

² F. Cadiz *et al*, Phys. Rev. X **7**, 021026 (2017)

³ G. Wang *et al*, Phys. Rev. Lett. **119**, 047401 (2017)

⁴ H. Fang *et al*, Phys. Rev. Lett. **123**, 067401 (2019)

⁵ C. Robert *et al*, Phys. Rev. Lett. **126**, 067403 (2021)

⁶ C. Robert *et al*, Nature Com. **11**, 4037 (2020)

⁷ C. Robert *et al*, Nature Com. **12**, 5455 (2021)

⁸ M. Yang *et al*, Phys. Rev. B **105**, 085302 (2022)

⁹ L. Ren *et al*, Arxiv 2202.01050 (2022)

A self-consistent framework for modeling graphene-based optoelectronic devices

S. Doukas^{1*}, A.C. Tasolamprou², A.D. Koulouklidis², S. Tzortzakis²
I. Goykhman³, A.C. Ferrari⁴, E. Lidorikis^{1,5}

¹*Department of Materials Science and Engineering,
University of Ioannina, 45110 Ioannina, Greece*

²*Institute of Electronic Structure and Laser, FORTH,
70013 Heraklion, Crete, Greece*

³*Micro Nanoelectronics Research Center, Technion, 320000 Haifa, Israel*

⁴*Cambridge Graphene Centre, University of Cambridge,
CB3 0FA Cambridge, United Kingdom*

⁵*University Research Center of Ioannina (URCI),
Institute of Materials Science and Computing, 45110 Ioannina, Greece*

Graphene based optoelectronics require an accurate description of the interactions between light and graphene carriers. The interplay between graphene's electrical, optical and thermal properties must be self-consistently treated, to design and optimize devices based on graphene. Here, we present a multi-physics simulation framework, developed in the University of Ioannina, for the versatile and efficient modeling of graphene-based photodetectors, sensors and modulators operating from the mid-IR to the THz spectral regime.

In the mid-IR, we demonstrate a thermionic graphene/Si Schottky photodetector. We show that under proper device optimization, the external responsivity can be pushed to the 1 A/W regime, resulting to detectivity up to 10^7 Jones in an ultrafast photodetection platform [1]. In the far-IR, we exploit plasmonic resonances in graphene nanoribbons forming a series of graphene/Si Schottky junctions, capable to electrically detect graphene plasmons with an external responsivity up to 110 mA/W and noise equivalent power of 190 pW/Hz^{0.5} [2]. Finally, in the THz regime, we present the self-induced ultrafast absorption modulation of a Salisbury screen type of a graphene-based device. Upon strong (up to 654 kV/cm), our calculations show a 30 dB absorption modulation, in excellent agreement with the experimental findings [3]. The presented framework can be used to design different optoelectronic devices reliably and realistically, across a broadband spectral regime, using a plethora of materials alongside graphene.

The research leading to these results has received funding from the European Union's Horizon 2020 research and innovation programme under Grant Agreement No. 881603 Graphene Flagship for Core3.

References

- [1] S. Doukas, Phys. Rev. B **105**, 115417 (2022).
- [2] S. Doukas *et al.*, submitted to Appl. Phys. Lett.
- [3] A. D. Koulouklidis *et al.*, submitted to ACS Photonics.

*s.doukas@uoi.gr

Polarization-Resolved Second Harmonic Generation Imaging in 2D Materials

S. Psilodimitrakopoulos^{*}, L. Mouchliadis, G. M. Maragkakis, G. Kourmoulakis, I. Demeridou, A. Lemonis, G. Kioseoglou, E. Stratakis^{*}
*Institute of Electronic Structure and Laser-Foundation for Research and
Technology-Hellas, GR-711 10, Heraklion, Greece*

The emerging family of two-dimensional (2D) materials has provided researchers with fertile ground for exploring fundamental physical phenomena and developing innovative technological solutions. Lately, nonlinear optical measurements, including second-harmonic generation (SHG) have created new opportunities for improving the image resolution of 2D crystals [1,2] (Fig1a). At the same time, the polarization of the SHG field depends on the 2D crystal symmetry and orientation (Fig1b). Based on such SHG signal dependencies, the crystal quality of TMDs can be evaluated using polarization-resolved SHG (P-SHG) imaging [1,2] (Fig1c). Moreover, 2D TMDs can be assembled in vertical stacks. This creates new physical properties that depend on the relative orientation (twist angle) between the TMD monolayers. P-SHG imaging provides precise and real-time measurement of the twist angle, which is of utmost importance for characterizing a twisted 2D TMD heterostructure [3] (Fig1d). Additionally, degenerate minima in momentum space –valleys– in 2D materials provide an additional degree of freedom that can be used for information transport and storage. P-SHG imaging reveals that the temperature-induced changes of the P-SHG, is a unique fingerprint of valley population imbalance (VPI) [4] (Fig.1e). We envisage the optical P-SHG imaging as a powerful tool for the characterization of 2D TMD heterostructures and the engineering of their physical properties for emerging applications.

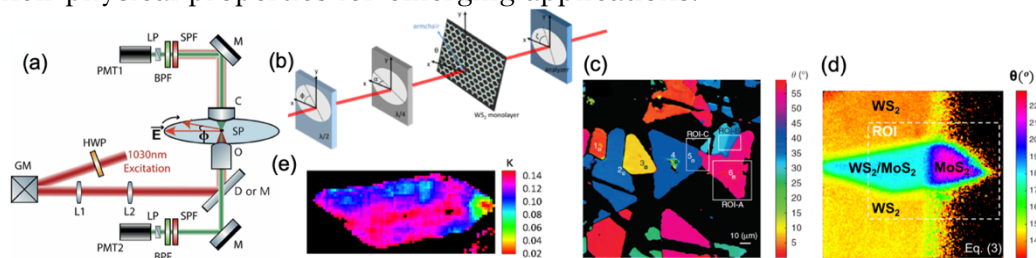


Figure 1: (a) Experimental setup for P-SHG imaging microscopy, (b) coordinates system for the theoretical model describing the P-SHG from 2D TMDs. (c) P-SHG imaging of crystal imperfections (d) Real-time imaging of twist-angle, (e) P-SHG imaging of VPI.

References

- [1] S. Psilodimitrakopoulos, L. Mouchliadis, I. Paradisanos, et al. Ultrahigh-resolution nonlinear optical imaging the armchair orientation in 2D transition metal dichalcogenides. *Light Sci Appl* 7, doi: 18005 10.1038/lsa.2018.5 (2018).
- [2] G. M. Maragkakis, S. Psilodimitrakopoulos, L. Mouchliadis, et al. "Imaging the crystal orientation of 2D transition metal dichalcogenides using polarization-resolved second-harmonic generation," *Opto-Electron. Adv.* **2**, 190026, (2019).
- [3] S. Psilodimitrakopoulos, L. Mouchliadis, G. M. Maragkakis, et al. "Real-time spatially resolved determination of twist angle in transition metal dichalcogenide heterobilayers," *2D Materials*, **8**, 015015, (2021).
- [4] L. Mouchliadis, S. Psilodimitrakopoulos, G.M. Maragkakis, et al. "Probing valley population imbalance in transition metal dichalcogenides via temperature-dependent second harmonic generation imaging," *npj 2D Mater. Appl* **5**, 6, (2021).

* stratak@iesl.forth.gr

* sopsilo@iesl.forth.gr

Nonlinear optical properties of 2D materials: from graphene to silicene and to other 2D materials

M. Stavrou^{1,2*}, A. Stathis^{1,2}, D. Theodoropoulou^{1,2}, N. Chazapis^{1,2} and S. Couris^{1,2}

¹*Department of Physics, University of Patras, 26504 Patras, Greece*

²*Institute of Chemical Engineering Sciences (ICE-HT), Foundation for Research and Technology-Hellas (FORTH), P.O. Box 1414, Patras 26504, Greece*

Nonlinear optical (NLO) materials are the basis for several photonic and optoelectronic devices and applications. Among them, the 2D materials have attracted enormous interest due to their outstanding optoelectronic properties which endow them with great possibilities for a plethora of applications, as e.g. in ultrafast lasers, optical information processing and storage, telecommunications, sensors, etc.

The pioneer of 2D materials, graphene, being characterized by chemical inertness, zero bandgap and exhibiting dispersibility problems, is of limited use in photonics and optoelectronics. However, some graphene derivatives, such as: graphene oxides (GOs), graphene acid, fluorographene, nitrogen- and/or boron-doped graphenes and others, being readily dispersible in aqueous and/or other common organic solvents and exhibiting non-zero energy bandgap, seem to have great future and have gained increasing interest as they allow the efficient tailoring of their NLO response towards NLO materials with custom-made properties.

The popularity of graphene has triggered the interest for other graphene-like 2D materials based on other IVA group elements (Si, Ge, Sn, Pb), which share some of the outstanding properties envisaged for graphene. Recently, silicon nanosheets (SiNSs) have revealed comparable and even larger NLO response than graphenes, emphasizing their potential for 2D-material-based photonics and optoelectronic applications and devices.

During last years, 2D materials of the type MX_2 , with M a transition-metal atom (Mo, W, etc.) and X a chalcogen atom (S, Se, or Te), also known as transition metal dichalcogenides (TMDCs), have also triggered the research interest, for their potential for micro-electronics and nano-photonics applications. Layered TMDCs, depending on their structural phases (trigonal prismatic-2H or octahedral-1T) exhibit semiconducting or metallic properties. The diversity of crystalline structure and structural phase of the d electrons, as well as the number and type of layer stacking sequences of TMDCs, result in a broad range of opto-electronic properties of these van der Waals nanostructures. Consequently, it is reasonably expected that the engineering of crystalline structure of TMDCs can modify their NLO response as well.

Another class of 2D materials, with very interesting optoelectronic properties are some atomically thin non-van-der Waals (vdW)-layered nanostructures. Among them, hematene and magnetene, the two archetypical 2D iron-ore magnetic materials presenting thicknesses down to the atomically thin sheets have very recently attracted the research interest.

In this presentation, we will review some recent experimental findings of our group pertaining to the nonlinear optical properties of these 2D nanostructures, including graphene derivatives, silicon nanosheets, some vdW-layered TMDCs and some non-vdW-layered iron oxides. The NLO response of these nanostructures was investigated in time scales from ns to fs, using Z-scan and pump-probe Optical Kerr effect (OKE) techniques. In addition, the dynamics and the operating physical mechanisms responsible for the NLO response will be discussed. Additionally, the critical role of defect-engineering, chemical functionalization, size-effects, and crystalline phase on the NLO response of these 2D materials will be highlighted.

* m.stavrou@iceht.forth.gr

Efficient phonon cascades in an atomically thin semiconductor

I. Paradisanos*, G. Wang, E. M. Alexeev, A. R. Cadore, A. C. Ferrari
*Cambridge Graphene Centre, University of Cambridge, Cambridge CB3 0FA,
 U.K.*

X. Marie, B. Urbaszek
*Universite de Toulouse, INSA-CNRS-UPS, LPCNO, 135 Avenue Rangueil, 31077
 Toulouse, France*

M. M. Glazov
Ioffe Institute, 194021, St.-Petersburg, Russia

Energy relaxation of photo-excited charge carriers is of significant fundamental interest and crucial for the performance of layered semiconductors in optoelectronics. The primary stages of carrier relaxation affect a plethora of subsequent physical mechanisms. Here we measure light scattering and emission in tungsten diselenide (WSe_2) monolayers close to the laser excitation energy (down to ~ 0.6 meV). We reveal a series of periodic maxima in the hot photoluminescence intensity, stemming from energy states higher than the A-exciton state. We find a period ~ 15 meV for 7 peaks below (Stokes) and 5 peaks above (anti-Stokes) the laser excitation energy, with a strong temperature dependence. These are assigned to phonon cascades, whereby carriers undergo phonon-induced transitions between real states above the free-carrier gap with a probability of radiative recombination at each step. We infer that intermediate states in the conduction band at the Λ -valley of the Brillouin zone participate in the cascade process of WSe_2 monolayers. This provides a fundamental understanding of the first stages of carrier-phonon interaction, useful for optoelectronic applications of layered semiconductors. [1]

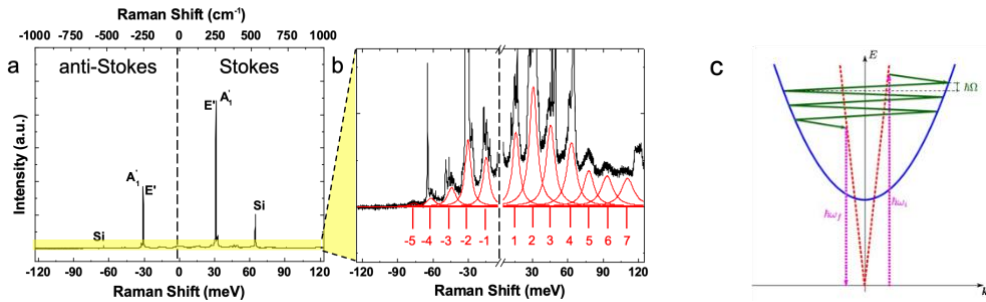


Figure 1: **(a)** Scattering spectrum of 1L- WSe_2 at 295K. The degenerate in-plane (E') and out-of-plane (A_1') Raman mode ~ 250 cm^{-1} , as well as the Si Raman peak ~ 521 cm^{-1} , are prominent in both Stokes (S) and anti-Stokes (AS). **(b)** Magnified portion of the spectrum in yellow in **a**. This reveals 7 periodic S peaks and 5 AS. **(c)** Scheme of phonon-assisted hot PL. Incident and outgoing photons are shown by dotted magenta vertical arrows. The phonons participating in the cascade are indicated by the green arrows. The exciton dispersion curve is the blue parabola.

References

[1] I. Paradisanos, G. Wang., E. M. Alexeev *et al.*, Nat Commun **12**, 538 (2021)

* paradeis@insa-toulouse.fr

Time-Resolved Raman scattering in exfoliated and CVD graphene crystals

S. Katsiaounis^{1,2}, Nikos Delikoukos^{1,2}, J. Parthenios¹, K. Papagelis^{1,3}

¹Foundation of Research and Technology Hellas, Institute of Chemical Engineering Sciences, P.O. Box 1414, GR-26504 Patras, Greece

²Department of Physics, University of Patras, GR-26504 Patras, Greece

³School of Physics, Department of Solid-State Physics, Aristotle University of Thessaloniki, Thessaloniki 54124, Greece

We have developed an experimental set-up to perform Time-Resolved Incoherent Anti-stokes Raman Scattering (TRIARS) experiments in graphene crystals to directly investigate the ultrafast dynamics of G- phonons [1]. In this technique an intense pump beam generates a non-equilibrium population of G phonons which decays to lower energy phonons via anharmonic interactions [2]. This decay process is monitored by the intensity of the anti-Stokes Raman signal, induced by the less intense probe beam, as a function of the delay-time between the pump and probe beams. We performed measurements in HOPG, 1-3L exfoliated graphene samples on Si/SiO₂ as well as CVD polycrystalline monolayers and stacks of monolayers onto Si/SiO₂ and quartz substrates.

We have found that the underlying substrate strongly reduces the G phonon lifetime of exfoliated and CVD monolayer via the provision of additional relaxation channels. In thicker exfoliated samples the G-mode lifetimes are close to that of graphite, implying that anharmonic coupling between phonon modes is insensitive to weak inter-planar interactions. The electron-phonon (*e-ph*) coupling strength of graphite is found to be $\sim 10.6 \text{ cm}^{-1}$ in excellent agreement with first principles calculations [2]. Polycrystalline monolayer and layer decoupled 2L, 3L CVD samples exhibit systematically smaller lifetimes than exfoliated ones. Measurements on stacks of two or three CVD monolayers gave almost similar results. The measured G phonon lifetimes in CVD graphene samples on quartz exhibit systematically higher lifetimes compared to the corresponding ones on Si/SiO₂ [1]. Very recently, we have extended the applicability of TRIARS to investigate the influence of hole doping by means of HNO₃ doped CVD graphene on the ultrafast dynamics of G phonons. A reduction of G phonon lifetime with doping is observed, resulting in an increased *ph-ph* contribution and a concomitant considerable reduction of the *e-ph* contribution to the G band linewidth.

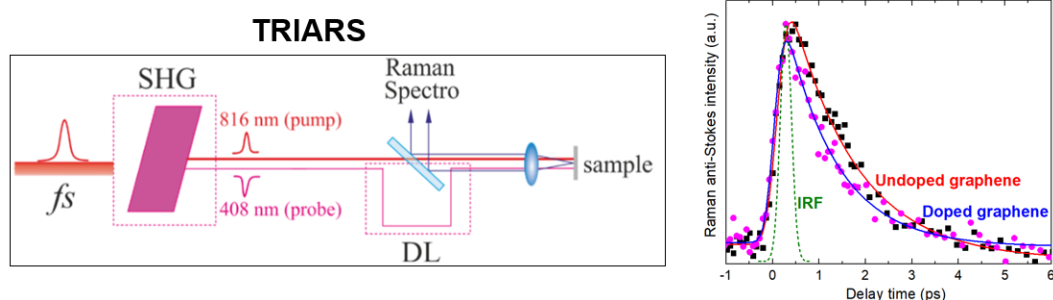


Figure 1: (Left) Simplified schematic representation of TRIARS set-up. fs: femtosecond pulse, SHG: Second Harmonic Generation, DL: Delay Line. (Right) Characteristic normalized anti-Stokes Raman intensity of G phonons as a function of delay-time for graphene, before and after doping. The green dashed curve corresponds to instrument response function (IRF).

References

1. S. Katsiaounis, A. V. Sharkov, E. V. Khoroshilov, G. Paterakis, J. Parthenios and K. Papagelis, *The Journal of Physical Chemistry C*, 2021, **125**, 21003-21010.
2. N. Bonini, M. Lazzeri, N. Marzari and F. Mauri, *Phys Rev Lett*, 2007, **99**.

Pyridine vs imidazole axial ligation on cobaloxime grafted graphene: Hydrogen evolution reaction insights

Ioanna K. Sideri,^{a*} Georgios Charalambidis,^b Athanassios G. Coutsolelos,^b Raul Arenal^{c,d,e} and Nikos Tagmatarchis^a

^a*Theoretical and Physical Chemistry Institute, National Hellenic Research Foundation, 48 Vassileos Constantinou Avenue, Athens 11635, Greece.*

^b*Chemistry Department, Laboratory of BioInorganic Chemistry, University of Crete, PO Box 2208, 710 03 Heraklion, Crete, Greece.*

^c*Laboratorio de Microscopias Avanzadas (LMA), Universidad de Zaragoza, Mariano Esquillor s/n, 50018 Zaragoza, Spain.*

^d*Instituto de Nanociencia y Materiales de Aragon (INMA), CSIC-U. de Zaragoza, Calle Pedro Cerbuna 12, 50009 Zaragoza, Spain.*

^e*ARAID Foundation, 50018 Zaragoza, Spain.*

Cobaloximes have been protagonists in the (photo)electrocatalytic H₂ production research scene for a while now, owing to their redox-active metal center and their closely lying polar oximes coordinated in a square-planar geometry. However, there have been insights that the outer coordination sphere of the cobaloxime catalytic center e.g. the axial and equatorial ligation, drastically affects the hydrogen evolution reaction (HER) performance,[1] being a worth-studying topic appealing to researchers engaged in catalyst design. Aspiring to bring this study in a hydrogen fuel cell realistic set-up, we envisioned a rationally designed heterogeneous electrocatalytic system, compatible with practical aqueous acidic conditions, in order to study the HER performance of two twin electrocatalysts with sole difference their axial ligation to the cobaloxime complex. Covalent functionalization of graphene was selected as an ideal route to ensure the required stability for cobaloxime under such conditions, while pyridine and imidazole functionalities were selected as the axial ligands, based on their versatility, occurrence and different electron-donating ability. Interestingly, while pyridine axial ligation mirrors a drastically superior electrocatalytic performance, imidazole exhibits a remarkable long-term stability.[2]

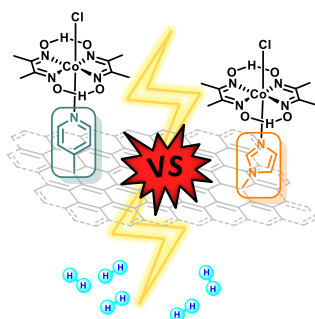


Figure 1: Pyridine vs imidazole axial ligation of a cobaloxime complex covalently grafted on graphene and their effect on hydrogen evolution reaction (HER) performance

References

[1] A. Panagiotopoulos, K. Ladomenou, D. Sun, V. Artero and A. G. Coutsolelos, Dalton Trans. **45**, 6732 (2016).

[2] I. K. Sideri, G. Charalambidis, A. G. Coutsolelos, R. Arenal and N. Tagmatarchis, Submitted (2022).

* isideri@eie.gr

Laser micro/nano processing for photonics, optoelectronics, and smart surfaces

M. Kandyla*

Theoretical and Physical Chemistry Institute, National Hellenic Research Foundation, 48 Vasileos Constantinou Ave., 11635 Athens, Greece

The need for advanced materials and systems with new functionalities has motivated the development of micro/nanostructures on solid surfaces, which are necessary for the fabrication of functional devices for novel applications. In this talk, we will discuss the development of functional micro/nanostructures, based on laser-processed surfaces. Laser micro/nanofabrication presents distinct advantages, such as low cost, simplicity (tabletop apparatuses, maskless processes), large-scale potential, high spatial resolution (localized modifications, order of magnitude optical wavelengths).

Coating micro/nanostructures with thin metallic films results in plasmonic substrates with enhanced electromagnetic response across the entire visible range, which are used for plasmonic optical trapping [1,2] and surface-enhanced Raman spectroscopy (SERS) [3]. Combining silicon micro/nanostructures with thin semiconducting films results in electronic heterojunctions with increased surface area for improved optoelectronic performance [4,5]. “Smart” surfaces of controllable extreme wetting states are obtained by combining thermoresponsive polymers or photoresponsive metal oxides with micro/nanostructured substrates [6]. Also, surfaces with controlled topography, either at the micro- or at the nano-scale, for targeted cell cultures for biomedical applications [7].

References

- [1] D.G. Kotsifaki, M. Kandyla, and P.G. Lagoudakis, Near-field enhanced optical tweezers utilizing femtosecond-laser nanostructured substrates, *Applied Physics Letters* **107**, 211111 (2015).
- [2] D.G. Kotsifaki, M. Kandyla, and P.G. Lagoudakis, Plasmon enhanced optical tweezers with gold-coated black silicon, *Scientific Reports* **6**, 26275 (2016).
- [3] M. Kanidi, A. Dagkli, N. Kelaidis, D. Palles, S. Aministragia-Giamini, J. Marquez-Velasco, A. Colli, A. Dimoulas, E. Lidorikis, M. Kandyla, and E.I. Kamitsos, Surface-enhanced Raman spectroscopy of graphene integrated in plasmonic silicon platforms with a three-dimensional nanotopography, *Journal of Physical Chemistry C* **123**, 3076 (2019).
- [4] G. Chatzigiannakis, A. Jaros, R. Leturcq, J. Jungclaus, T. Voss, S. Gardelis, and M. Kandyla, Laser-microstructured ZnO/p-Si photodetector with enhanced and broadband responsivity across the ultraviolet-visible-near-infrared range, *ACS Applied Electronic Materials* **2**, 2819 (2020).
- [5] G. Chatzigiannakis, A. Jaros, R. Leturcq, J. Jungclaus, T. Voss, S. Gardelis, and M. Kandyla, Broadband wavelength-selective isotype heterojunction n⁺-ZnO/n-Si photodetector with variable polarity, *Journal of Alloys and Compounds* **903**, 163836 (2022).
- [6] M. Kanidi, A. Papagiannopoulos, A. Matei, M. Dinescu, S. Pispas, and M. Kandyla, Functional surfaces of laser-microstructured silicon coated with thermoresponsive PS/PNIPAM polymer blends: switching reversibly between hydrophilicity and hydrophobicity, *Applied Surface Science* **527**, 146841 (2020).
- [7] M. Kanidi, A. Papadimitropoulou, C. Charalampous, Z. Chakim, G. Tsekenis, A. Sinani, C. Riziotis, and M. Kandyla, Regulating MDA-MB-231 breast cancer cell adhesion on laser-patterned surfaces with micro- and nanotopography, *Biointerphases* **17**, 021002 (2022).

* kandyla@eie.gr

Optimizing large area fabrication of printed nanolayers for Organic Electronics by In-Line Metrology

A. Laskarakis

*Nanotechnology Lab LTFN, Department of Physics,
Aristotle University of Thessaloniki, 54124 Thessaloniki, Greece*

The optoelectronic and charge transport properties of printed semiconductor nano-layers for Organic Electronics-OEs (e.g. polymer donors and acceptors, luminescent polymers) is mainly controlled by the structural morphology and crystallization dynamics during their fabrication in functional OE device architectures. Despite the numerous advances reported on the structure-property relationships on these materials by lab-scale solution-based methods, their reliable manufacturing on flexible substrates by large scale roll-to-roll (R2R) printing processes is accompanied by numerous challenges, such as the formation of structural inhomogeneities and defects, and non-reproducible performance over large areas. These challenges can provide significant obstacles for R2R printing to meet the requirements for reliable large-scale manufacturing of high-performance OE devices on flexible substrates for commercial applications.

In this presentation, we will provide an overview of the main factors that affect the optoelectronic performance and the large area homogeneity of printed photoactive nanolayers (such as PBDB-T, BTP-12, PPDT2FBT) in binary and ternary configurations, on flexible substrates. Moreover, we present the valuable contribution of intelligent in-line metrology (optical, electronic, structural) to understand the formation mechanisms, blend morphology and the factors for defect formation. Finally, we report how we can extract from single optical in-line measurements, useful information about the nanolayer quality, structure and morphology. By this approach, we demonstrate an optimized fabrication process of fully printed large scale flexible OE devices with improved charge transport properties and performance and significant device-to-device reproducibility. [1,2]

References

[1] EU H2020 Project RealNano (www.realnano-project.eu)

[1] EU H2020 Project MUSICODE (www.musicode.eu)

[1] Watson and Crick, Nature **171**, 737 (1953).

Pump-probe Reflectivity Studies of Ultrashort Laser-induced Acoustic Strains in Layered Materials

K. Kosma^{1,2}, K. Kaleris^{1,2}, E. Kaselouris^{1,2}, M. Kaniolakis-Kaloudis^{1,2},
M. Bakarezos^{1,2}, M. Tatarakis^{1,3}, V. Dimitriou^{1,2},
and N. A. Papadogiannis^{1,2}

¹ Institute of Plasma Physics & Lasers, Hellenic Mediterranean University
Research Center, Rethymno 74100, Greece

² Department of Music Technology & Acoustics, Faculty of Music and
Optoacoustic Technologies, Hellenic Mediterranean University, Rethymno
74100, Greece

³ Department of Electronic Engineering, School of Engineering, Hellenic
Mediterranean University Chania 73133, Greece

In the present work the implementation of an experimental optical pump-probe set-up, based on ultrasonic acoustic wave generation and detection by laser pulses is demonstrated. The generated acoustic strains are of several tens of femtoseconds duration and are applied to the characterization of nanostructured layered targets and processes of high scientific and technological interest. For the proposed pump-probe experiments the output pulses of a Ti: Sapphire amplifier system at 800 nm, with duration ~ 30 fs, energy per pulse ~ 1 mJ and repetition rate of 1 kHz are used.

Due to the interaction with the target material, the pump beam generates a longitudinal acoustic wave that propagates perpendicular to the target surface. The probe beam focuses on the target after a variable delay relative to the pump beam, which is introduced through a controlled change in the optical path of the probe beam. Part of the probe beam is reflected by the propagating mechanical distortion and therefore changes in the reflectivity signal are observed. These changes in reflectivity are related to the dynamic behavior of the elastic wave propagation, and consequently to the dynamics of the material as it returns to its equilibrium state after experiencing the mechanical deformation. More specifically, with the present method the Brillouin scattering of the probe photons by the acoustic phonons can be detected and conclusions about the physical properties of the materials under study can be drawn.

The materials studied are in the form of thin films of thicknesses of a few tens to hundreds of nanometers. The films are covered with thin metal coatings such as gold (Au) or titanium (Ti) of tens of nanometers thickness (10–30 nm). The metal coatings play the role of the optoacoustic transducer, that is, in the coating the conversion of the optical energy absorbed by the metal, into an acoustic wave takes place. Results are presented for materials of high technological interest for industrial applications, such as solar cells, nanoelectronics, converters and sound absorbers, touch screens, sensors, etc. Such materials like silicon Si, but also complex semiconductors like ZnO, constitute the building blocks of

semiconductor systems. With the method presented, properties of the materials such as: acoustic impedance, velocity of sound, elasticity, etc. can be determined with very high accuracy. The future goal of the project is the development of a standard workstation in IPPL for the rapid and reliable investigation of materials with high technological impact.

The experimental results are validated by numerical results of thermomechanical analysis, using the finite element method. The method simulates the mechanism of acoustic wave generation after absorption of optical energy from the material, taking into account the transfer of energy from non-thermal electrons to thermal electrons and then from the thermal electron cloud to the crystal lattice. Thus, characteristics such as space-time distribution, intensity and speed of propagation of the acoustic wave, as well as displacement and temperature of the crystal lattice can be calculated with extremely high accuracy and can be compared with the experimental findings.

AKNOWLEDGEMENTS: This project is funded by the Hellenic Foundation for Research & Innovation H.F.R.I. in the framework of the action “2nd Call for H.F.R.I. Research Projects to Support Post-Doctoral Researchers”, proposal no: 1336. This work was supported by computational time granted by the Greek Research & Technology Network (GRNET) in the National HPC facility ARIS-under project ID pr011027-LaMPIOS.

References

- [1] E. Tzianaki, M. Bakarezos, G. D. Tsibidis, Y. Orphanos, P. A. Loukakos, C. Kosmidis, P. Patsalas, M. Tatarakis, and N. A. Papadogiannis, *Opt. Express* **23** (13), 17191 (2015).
- [2] M. Bakarezos, E. Tzianaki, S. Petrakis, G. Tsibidis, P. A. Loukakos, V. Dimitriou, C. Kosmidis, M. Tatarakis, and N. A. Papadogiannis, *Ultrasonics* **86**, 14 (2018).
- [3] V. Dimitriou, E. Kaselouris, Y. Orphanos, M. Bakarezos, N. Vainos, M. Tatarakis, and N. A. Papadogiannis, *Applied Physics Letters* **103** (11), 114104 (2013).
- [4] V. Dimitriou, E. Kaselouris, Y. Orphanos, M. Bakarezos, N. Vainos, I. K. Nikolos, M. Tatarakis, and N. A. Papadogiannis, *Applied Physics A* **118** (2), 739 (2015).
- [5] K. Ishioka, A. Beyer, W. Stolz, K. Volz, H. Petek, U. Hofer, and C. J. Stanton, *J. Phys.: Condens. Matter*, **31** (9), 4003 (2018).
- [6] J. D. Aussel, A. Le Brun, and J. C. Baboux, *Ultrasonics* **26** (5), 245 (1988).
- [7] V. V. Temnov, C. Klieber, K. A. Nelson, T. Thomay, V. Knittel, A. Leitenstorfer, D. Makarov, M. Albrecht, and R. Bratschitsch, *Nature Communications* **4**, 1468 (2013).
- [8] N. M. Stanton, R. N. Kini, A. J. Kent, M. Henini, and D. Lehmann, *Physical Review B* **68** (11), 113302 (2003).
- [9] T. Dehoux, M. A. Ghanem, O. F. Zouani, M. Ducouso, N. Chigarev, C. Rossignol, N. Tsapis, M.-C. Durrieu, and B. Audoin, *Ultrasonics* **56**, 160 (2015).

Triplet-excited State Fusion as a Tool to Photostimulate Vertically-configured Organic Photodetectors

G. Antoniou, P. Yuan, L. Koutsokeras, P. E. Keivanidis*

Device Technology and Chemical Physics Laboratory, Department of Mechanical Engineering and Materials Science and Engineering, Cyprus University of Technology, Limassol 3041, Cyprus

Photon energy up-conversion via triplet-triplet annihilation (TTA-UC) is a particularly attractive wavelength-shifting tool to enable photoactuation *i.e.* the sensitization of organic solar cells (OSCs) or the photo-stimulation of optogenetic platforms. Essentially, TTA-UC refers to the photophysical process where the energy level of an emissive excited state is prepared by the synergetic effects of lower energy photons via triplet-triplet annihilation photochemical reactions. The TTA-UC phenomenon occurs in multicomponent systems comprising a triplet-excited sensitizer mixed with a ground state activator. Typical activators include a large set of acene-based aromatic hydrocarbons and π -conjugated polymers, whereas the sensitizers are organic phosphorescent dyes with long-lived triplet excited states, *e.g.* transition-metal-containing complexes. Encouraging results have been presented recently on the photoluminescence quantum yield (PLQY) of the archetypical TTA-UC system of the 9,10 di-phenyl anthracene (DPA) emitter mixed with the (2,3,7,8,12,13,17,18-octaethyl-porphyrinato) platinum^{II} (PtOEP) metallorganic sensitizer; a green-to-blue PLQY_{TTA-UC} as high as 8% was reported for solution-processable solid-state DPA:PtOEP films [1]. Nevertheless, the binary nature of the DPA:PtOEP composite film introduces severe implications in terms of device engineering aspects, and the incorporation of the DPA:PtOEP up-converting interlayers in OSC devices with vertically-stacked geometries is hard to achieve.

Herein we present a simple methodology for incorporating a photon absorbing layer of the PtOEP sensitizer, as a self-TTA annihilator medium in a vertically stacked photodiode device structure. The participation of the fusion process in the mechanism of charge photogeneration manifests in the supralinear dependence of the short-circuit current density on the incoming photoexcitation intensity [2]. At low-power illumination, the PtOEP photodiode exhibits photocurrent generation via the fusion of optically-induced PtOEP excited states and it develops an open-circuit voltage as high as 1.15 V. The structural and spectroscopic characterization of the nanostructured PtOEP photoactive layer in combination with electronic structure calculations identify PtOEP dimer species as the annihilating excited state responsible for the formation of charges. Building on this insight, the PtOEP annihilator is further utilized for stimulating the response of UV-only organic photodetector with visible light. These findings propose that triplet-excited annihilator species are valuable photoactive components to be deployed in smart light-management applications.

References

- [1] S. Raišys, S. Juršenai, K. Kazlauskas, Sol. RRL **6**, 2100873, (2022).
- [2] G. Antoniou, P. Yuan, L. Koutsokeras, S. Athanasopoulos, D. Fazzi, J. Panidi, D. G. Georgiadou, T. Prodromakis, P. E. Keivanidis, J. Mater. Chem. C, **10**, 7575, (2022).

Acknowledgement

This work was co-funded by the European Regional Development Fund and the Republic of Cyprus through project EXCELLENCE/1216/0010 ‘Low Photon-Energy Up-Conversion induced Sensitized Photocurrent Generation in Organic Photodiodes’ of the Research and Innovation Foundation.

*p.keivanidis@cut.ac.cy

Performance of SiC-doped 3D printed PLA for triboelectric energy harvesting

A. Bardakas, A. Segkos, G. Katsikis, G. Vekinis, C. Tsamis*
NCSR “Demokritos”, Institute of Nanoscience and Nanotechnology,
15310 Aghia Paraskevi, Athens, Greece

Based on contact electrification and electrostatic induction between two surfaces that are in relative motion for converting mechanical energy to electrical energy, TENGs are emerging as one of the most promising power sources for autonomous electronics and sensors. Although several technologies have been proposed in the literature for the fabrication of TENGs, 3D printing technologies are expected to promote the rapid development and widespread application for the next-generation portable electronics and Internet-of-Things applications [1]. In this work we investigate the performance of SiC-doped 3D printed PLA in triboelectric applications.

A series of specimens was produced by first extruding filaments of PLA containing 1-3% SiC (average size $15\mu\text{m}$) and then using them to 3D-print discs of diameter 32mm and thicknesses 0.3mm and 9mm. The samples were subsequently polished using grinding papers of various grit sizes, resulting in samples of different surface roughness.

Electrical characterization of the samples was performed in contact-separation mode using Kapton[®] as a reference electrode (Fig. 1a). The output of the triboelectric generator was monitored as a function of time, in conjunction with respective charging of a 0.47 μF capacitor (Fig. 1b).

The results indicate that for the 2% SiC doped PLA the capacitor voltage reaches much higher values compared to the other samples which can be explained if we assume an increase of surface charge density. Simulation studies were also performed using COMSOL showing a good agreement between simulated and experimental results for the undoped PLA and the 2%SiC doped PLA, if we assume that the surface charge for the latter case increases by 50% compared the other samples.

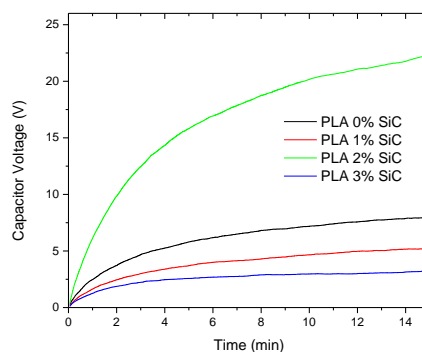
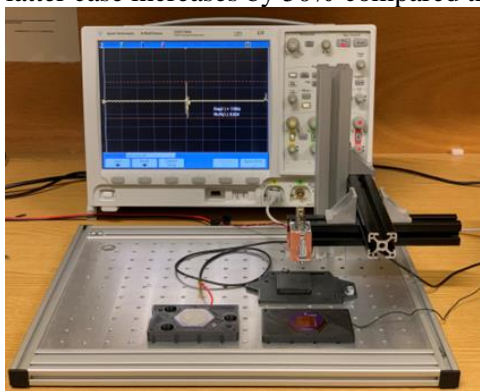


Figure 1 a) Experimental setup for contact-separation mode measurements and b) Capacitor voltage as a function of time for the PLA discs with different concentrations.

References

[1] B. Chen et al, Materials Today, Vol 50 (2021), Pages 224-238

Acknowledgements

This research has been co-financed by the European Union and Greek national funds through the Operational Program Competitiveness, Entrepreneurship and Innovation, under the call RESEARCH – CREATE – INNOVATE (EFOS, project code: T2EAK-00350).

* c.tsamis@inn.demokritos.gr

THz Self-induced Actions on a Graphene Based Thin Film Absorber

Anastasios D. Koulouklidis^{1,*}, Anna C. Tasolamprou¹, Spyros Doukas², Eudokia Kyriakou^{1,3}, Christina Daskalaki¹, M. Said Ergoktas^{4,5}, Eleftherios N. Economou^{1,6}, Eleftherios Lidorikis^{2,7}, Maria Kafesaki^{1,3}, Coskun Kocabas^{4,5,8}, and Stelios Tzortzakis^{1,3,9}

¹*Institute of Electronic Structure and Laser, FORTH, 70013 Heraklion, Crete, Greece*

²*Department of Materials Science and Engineering, University of Ioannina, Ioannina 45110, Greece*

³*Department of Materials Science and Technology, University of Crete, 70013, Heraklion Crete, Greece*

⁴*Department of Materials, University of Manchester, Manchester, M13 9PL, UK*

⁵*National Graphene Institute, University of Manchester, Manchester, M13 9PL, UK*

⁶*Department of Physics, University of Crete, 70013 Heraklion, Crete, Greece*

⁷*Institute of Materials Science and Computing, University Research Center of Ioannina (URCI), 45110 Ioannina, Greece*

⁸*Henry Royce Institute for Advanced Materials, University of Manchester, Manchester M13 9PL, UK*

⁹*Science Program, Texas A&M University at Qatar, P.O. Box 23874 Doha, Qatar*

The era of terahertz (THz) wireless communication opens ahead revealing the high importance of the development of fast modulation devices operating at the THz part of the electromagnetic spectrum. Towards this direction many devices based on graphene have been proposed to modulate radiation at THz frequencies [1,2]. Here, we demonstrate a graphene-based THz perfect absorber based on a cavity of monolayer graphene over a grounded dielectric that can be self-modulated using intense THz fields.

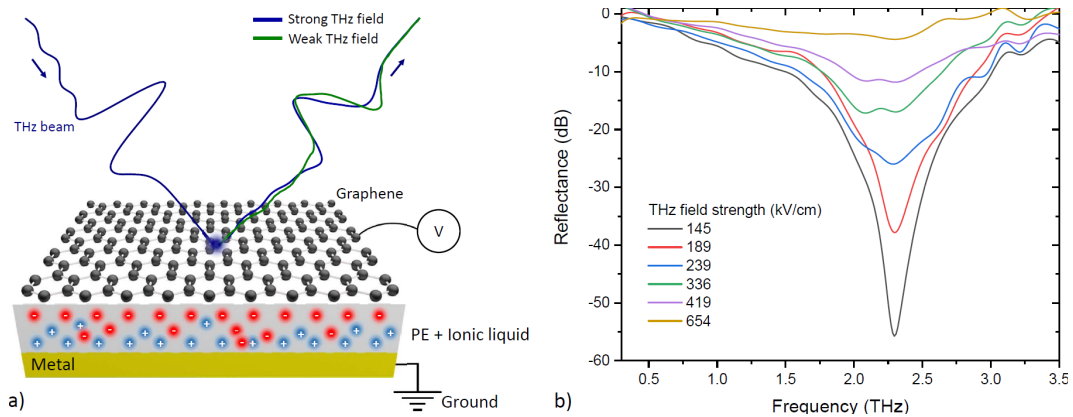


Fig. 1: (a) Schematic representation of the device. (b) Reflection spectra for various incident THz field strengths.

The cavity (Fig. 1a) is formed by a 25 μm thick, porous membrane sandwiched between a monolayer graphene and a gold electrode. The porous membrane was soaked with room-temperature ionic liquid electrolyte that allowed us to fine tune the Fermi energy of graphene with an external gating. For the excitation of the device a high-power THz source based on two-color filamentation was used, providing THz pulses with peak electric field strengths reaching 700 kV/cm. At low THz field strengths, the device achieves an absorption of -56 dB at 2.3 THz that drops to -4 dB for high field strengths (Fig. 1b). Detailed theoretical analysis indicates that the origin of the THz nonlinear response is the THz induced heating of the graphene's carriers, that leads to a reduction of its conductivity, and consequently to reduced absorption of the THz radiation. Our results can find applications in future dynamically controlled flat optics and spatiotemporal shaping of intense THz electric fields.

References

- [1] Kakenov et al., ACS Photonics, **3**, (2016) 1531–1535.
- [2] Tasolamprou et al., ACS Photonics, **6**, (2019) 720–727.

Single-layer white OLEDs: blended polymers and copolymers as emitting films

M. Gioti* , D. Tselekidou, K. Papadopoulos

Nanotechnology Lab LTFN, Department of Physics, Aristotle University of Thessaloniki, GR-54124, Thessaloniki, Greece

V. Kyriazopoulos

Organic Electronic Technologies P.C. (O E T), 20th KM Thessaloniki – Tagarades, 57001 Thermi Greece

K.C. Andrikopoulos, A.K. Andreopoulou, J.K. Kallitsis

Department of Chemistry, University of Patras, Caratheodory 1, University Campus, GR-26504 Patras, Greece

White organic light emitting diodes (WOLEDs), processed from solution, have attracted significant research interest in recent years for lighting applications. WOLEDs with a single emissive layer, either using fluorescent or phosphorescent compounds in blends, or copolymers that bearing different chromophores have been proposed as promising methodologies for the easy fabrication of high-performance devices. However, precise control of the dopant concentration in the guest-host system, for the case of blends, or of the chromophore ratio, for the case of copolymers, are essential for achieving the required color coordinates of the emitting light (Fig. 1). In this work, were utilized commercial blue Poly(9,9-di-n-octylfluorenyl-2,7-diyl) (PFO), green Poly(9,9-dioctylfluorene-alt-benzothiadiazole) (F8BT) and red spiro-copolymer (SPR) light emitting materials to develop blends, and Distyrylanthracene, dis-tyrlylcarbazole and distyrylbenzothiadiazole chromophores as yellow, blue and orange-red emitters, respectively, to synthesize novel copolymers. Single layer solution processed WOLED devices of two- and three-phase blends and copolymers bearing two and three chromophores were fabricated. The comparative optical, photophysical and electrooptical characterization of the produced films and devices demonstrated the predominant emission mechanism for each case.

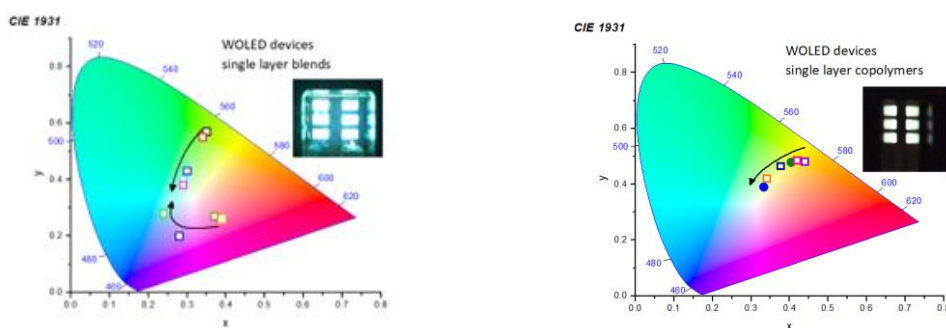


Figure 1: The EL CIE color coordinates of the OLED devices with single layer blends and copolymers

Acknowledgements: This research has been co-funded by the European Regional Development Fund of the European Union and Greek national funds through the Operational Program Competitiveness, Entrepreneurship, and Innovation, under the call RESEARCH-CREATE-INNOVATE (project code: T1EDK-01039).

* mgiot@physics.auth.gr

Silver-decorated silicon nanostructures for plasmon-induced enhancement of Raman scattering and fluorescence

Spiros Gardelis*

Section of Condensed Matter Physics, Department of Physics, National and Kapodistrian University of Athens, Panepistimiopolis Zografou, 15784 Athens, Greece

Three-dimensional metal nanostructures can give rise to considerable plasmon-induced enhancement of Raman scattering and fluorescence, rendering these spectroscopies sensitivities down to single molecule detection. Specifically, excitation of surface plasmons at nanogaps between metallic nanoparticles can greatly enhance local electric fields so that Raman signals of substances at these gaps can be increased considerably in comparison to conventional Raman. This is known as Surface-Enhanced Raman Scattering (SERS). Also, if the absorption or the emission spectrum of a substance overlaps with the excitation spectrum of a metal plasmon in the vicinity of the substance then this coupling can induce considerable fluorescence enhancement. In this study, we present a method to fabricate a Si-based three-dimensional nanostructure decorated with silver nanoparticles and demonstrate its high potential to render significant Raman and fluorescence enhancements [1]. In this method, silicon nanowires (SiNWs) were developed by metal-assisted chemical etching (MACE) and decorated either with silver dendrites or silver aggregates. Silver aggregates show greater uniformity regarding SERS whereas dendritic silver nanostructures show better performance for fluorescence. For the evaluation of the samples prototype analytes such as rhodamine R6G and crystal violet were used. Finally, the performance of the samples in detecting substances of biological interest is going to be presented.

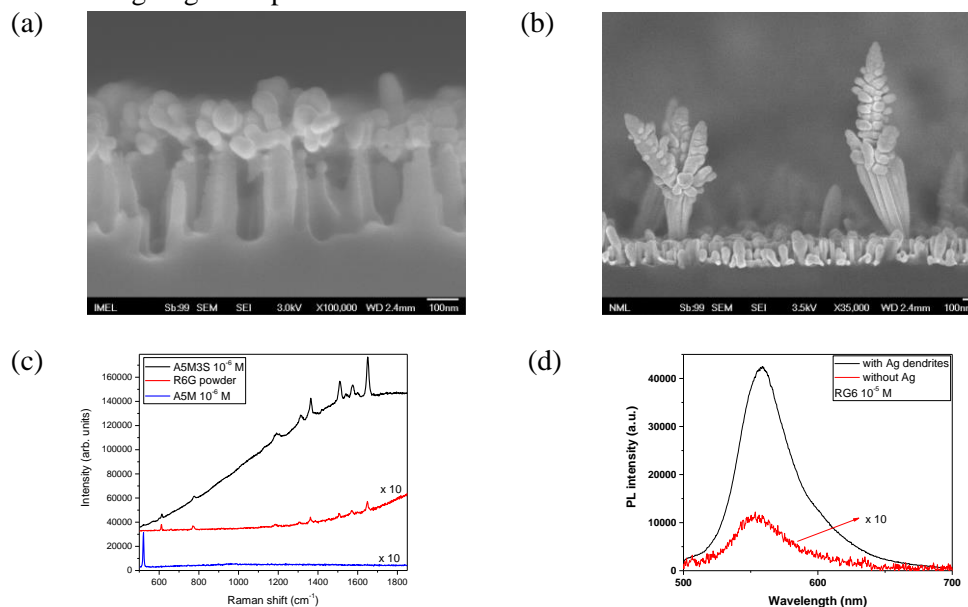


Figure 1: SEM images of the silver decorated SiNWs grown by MACE: a) silver aggregates, b) silver dendrites. Plasmon-induced: c) Raman and d) fluorescence enhancement.

References

[1] I. Kochylas, S. Gardelis, V. Likodimos, K.P. Giannakopoulos, P. Falaras and A. G. Nassiopoulou, *Nanomaterials* **11**, 1760 (2021)

* sgardelis@phys.uoa.gr

Transition radiation in cathodoluminescence spectra of silicon nanoparticles

P.E. Stamatopoulou*, S. Fiedler, C. Wolff, N.A. Mortensen, C. Tserkezis
Center for Nano Optics, University of Southern Denmark, Denmark

A. Assadillayev, S. Raza
Department of Physics, Technical University of Denmark, Denmark

H. Sugimoto, M. Fujii
Department of Electrical and Electronic Engineering, Kobe University, Japan

Cathodoluminescence (CL) spectroscopy, where signals generated from the excitation of a material by a fast electron beam are harnessed, has been extensively employed for analyzing the optical properties of plasmonic and dielectric nanostructures. Despite its undeniable success, particular care must be taken when interpreting the CL measurements, since the recorded signal can originate from the interplay of different excitation mechanisms. Transition radiation (TR) is a prominent source of coherent radiation emission, generated when the electron beam penetrates the nanoparticle [1]. As the electron approaches the surface of the particle, so does its image charge inside the medium, until, at contact, the two charges collapse. Therefore, two electric dipoles are formed—at the entrance and the exit point of the electron beam—that can interfere constructively or destructively [see Fig. 1(a)], depending on the electron time of flight inside the medium [2].

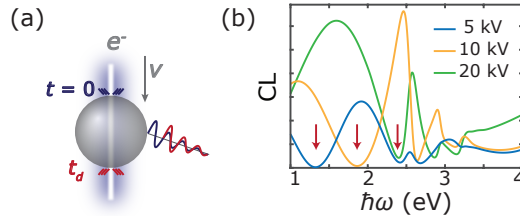


Figure 1: (a) Emergence of TR at the upper and lower surfaces of a nanoparticle crossed by an electron beam through its center. (b) Theoretical CL spectra for a silicon sphere 75 nm in radius, for the different acceleration voltages given in the inset. The arrows indicate the destructive interference minima.

Here we show, experimentally and theoretically, that interfering TR signals can generate distinct spectral features that distort the recorded spectrum and lead to potentially erroneous assignment of modal character to them [see Fig. 1(b)] [3]. We then offer an intuitive analogy that helps distinguish between the particle Mie resonances and the TR contribution.

References

- [1] García de Abajo, F. J., *Rev. Mod. Phys.* **82**, 209 (2010).
- [2] Pogorzelski, R., and Yeh, C., *Phys. Rev. A* **8**, 137 (1973).
- [3] Fiedler, S. et al, *Nano Lett.* **22**, 2320 (2022).

*elli@mci.sdu.dk

Comparative Study of $\text{SnS}_x\text{Se}_{2-x}$ alloys by High Pressure Raman Spectroscopy

N. Sorogas*, K. Papagelis, A. N. Anagnostopoulos, and J. Arvanitidis
Physics Department, Aristotle University of Thessaloniki, 54124, Thessaloniki, Greece

D. Christofilos

School of Chemical Engineering & Laboratory of Physics, Faculty of Engineering, Aristotle University of Thessaloniki, 54124, Thessaloniki, Greece

In this work, the hydrostatic pressure response of the phonon modes of ternary $\text{SnS}_x\text{Se}_{2-x}$ ($x=0.6, 0.8, 1$) alloys has been studied by means of Raman spectroscopy. High pressure (up to 8 GPa) was generated using a gas membrane-type diamond anvil cell. Owing to the two-mode behaviour of the E_g and A_{1g} modes in the ternary dichalcogenide alloys investigated [1], four Raman bands are observed at ambient conditions and the frequency evolution of three of them $\{E_g(\text{SnSe}_2\text{-like}), A_{1g}(\text{SnSe}_2\text{-like})$ and $A_{1g}(\text{SnS}_2\text{-like})\}$ was followed with pressure. Upon pressure application, all Raman peaks monotonically shift to higher frequencies due to the volume reduction and the bond strengthening (Figure 1).

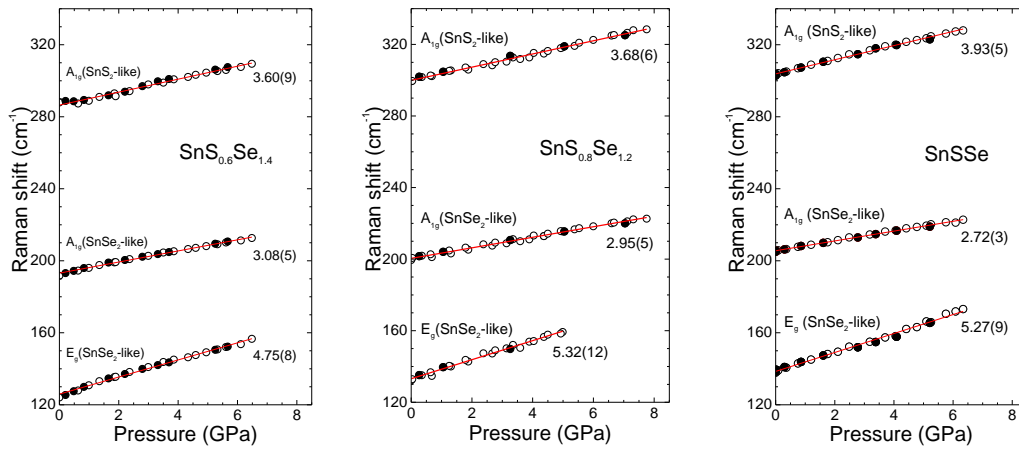


Figure 1: Pressure evolution of the frequencies of the clearly resolved Raman peaks in the $\text{SnS}_x\text{Se}_{2-x}$ alloys. Open (closed) circles correspond to pressure increase (decrease).

The pressure coefficient of the $A_{1g}(\text{SnS}_2\text{-like})$ peak frequency increases gradually from 3.60 to 3.93 $\text{cm}^{-1}\text{GPa}^{-1}$ with increasing S content, x . These values are compatible with those reported in the literature for the binary SnS_2 [2]. At the same time, the pressure coefficient of the $A_{1g}(\text{SnSe}_2\text{-like})$ peak frequency decreases from 3.08 to 2.72 $\text{cm}^{-1}\text{GPa}^{-1}$ with x , being always larger than that observed for the binary SnSe_2 [2]. Furthermore, contrary to the strong covalent bonding along the a -axis compared to the weak van der Waals interactions along the c -axis, the in-plane $E_g(\text{SnSe}_2\text{-like})$ mode exhibits larger pressure coefficient than those of the A_{1g} modes along the c -axis in all the studied alloys. We also extracted the Grüneisen parameters for the $A_{1g}(\text{SnS}_2\text{-like})$: 0.35, 0.34, 0.36 and the $A_{1g}(\text{SnSe}_2\text{-like})$ mode: 0.44, 0.41, 0.37 for $x=0.6, 0.8$ and 1, respectively. These values indicate the stronger Sn-S interaction along the c -axis compared to the Sn-Se one in the ternary alloys, in agreement with the existing X-ray diffraction (XRD) data in the literature [3].

References

- [1] V. G. Hadjiev, D. De, H. B. Peng et al., *Phys. Rev. B* **87**, 104302 (2013).
- [2] S. V. Bhatt, M. Deshpande, V. Sathe et al., *Solid State Commun.* **201**, 54 (2015).
- [3] J. Yu J, C-Y. Xu, Y. Li et al., *Sci. Rep.* **5** 17109 (2015).

* nsorogka@physics.auth.gr

Post-melting encapsulation for the development of advanced composite glasses

I. Konidakis* and E. Stratakis

Institute of Electronic Structure and Laser (IESL), Foundation for Research and Technology-Hellas (FORTH), 70013 Heraklion-Crete, Greece

*Presenting author: ikonid@iesl.forth.gr

Inorganic oxide glasses offer an outstanding platform for the development of transparent materials, architectures, and coatings with unique optoelectronic, optical, and photonic features. A recent approach in this field towards advancing applications potential consists of the incorporation of functional materials like perovskite nanocrystals (PNCs), two-dimensional (2D) materials, and metallic nanoparticles, within various types of glass matrices [1]. However, there are several limitations on the fabrication routes regarding the feasible growth of these materials within inorganic oxide glasses. The main one emerges from the necessity of typical high temperature melting protocols, in some cases exceeding 800 °C, that are required for most glasses [1]. The high temperature melting procedure is cost ineffective for large scale production, while it causes concerns for the stability of the incorporated functional materials. To tackle this scientific challenge, recently in our lab, we have developed a post-glass melting low temperature fabrication procedure that allows the controllable encapsulation of functional materials within glasses, i.e. after the initial glass melting (Figure 1a) [1]. Based on this simplified approach the controllable incorporation of PNCs [2], 2D materials [3], and nanoparticles [4], within transparent phosphate glasses is achieved at the moderate temperature of 160 °C. The perspectives of our fabrication route will be presented towards the realization of stable composite glasses with superior optical and luminescence properties for optoelectronic applications. In particular, the developed perovskite glasses (PV-Glasses) exhibit remarkable photoluminescence (PL) stability since the glass matrix offers great moisture protection to the PNCs, while simple continuous wave laser processing allows the formation of highly luminescent periodic micro-patterns inside the glass (Figure 1b) [2]. In case of 2D materials composite glasses (2D-Glasses), the post-glass melting encapsulation approach allows the enhancement of room temperature PL properties upon inducing B-exciton emission in few-layers of embedded MoS₂ (Figure 1c) [3].

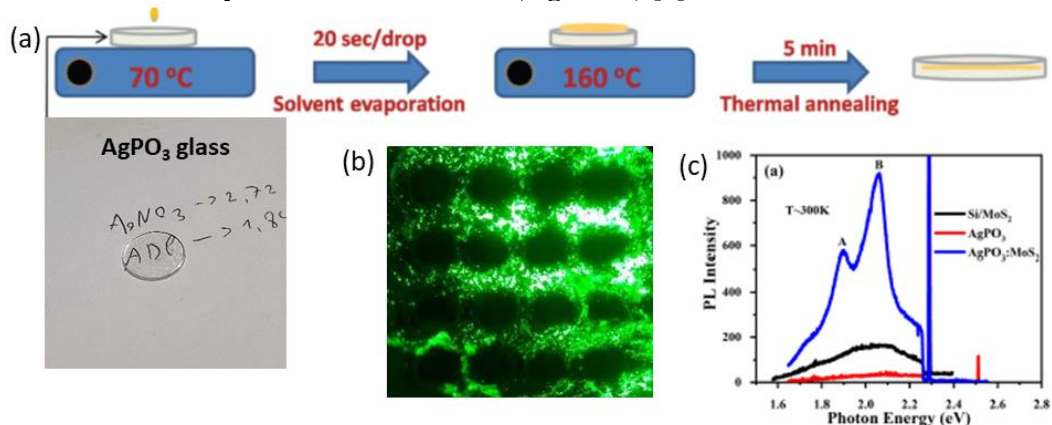


Figure 1: (a) Schematic representation of the post-glass melting encapsulation procedure. (b) Fluorescence photo of an encapsulated PNCs micro-dotted optical pattern. (c) Room temperature photoluminescence (PL) of MoS₂:AgPO₃ nanoheterojunction.

References

- [1] I. Konidakis et al., *Nanoscale* **14**, 2966 (2022). [2] I. Konidakis et al., *Nanoscale* **12**, 13697 (2020). [3] A.S. Sarkar et al., *Sci. Rep.* **10**, 15697 (2020). [4] I. Konidakis et al., *Appl. Phys. A* **124**, 839 (2018).

* ikonid@iesl.forth.gr

Exfoliated WS₂ interfacing Ni-porphyrin with (photo)electrocatalytic activity for the oxygen evolution reaction

Michail P. Minadakis*, Ruben Canton-Vitoria, Christina Stangel and Nikos Tagmatarchis

Theoretical and Physical Chemistry Institute, National Hellenic Research Foundation, 48 Vassileos Constantinou Avenue, 11635 Athens, Greece

Raul Arenal

Laboratorio de Microscopias Avanzadas (LMA), Universidad de Zaragoza, Mariano Esquillor s/n, 50018 Zaragoza, Spain

Instituto de Nanociencia y Materiales de Aragon (INMA), CSIC-U. de Zaragoza Calle Pedro Cerbuna 12, 50009 Zaragoza, Spain

ARAID Foundation, 50018 Zaragoza, Spain

Interfacing exfoliated tungsten disulfide (WS₂) with M-N₄ motifs (M: Ni, Co, Fe etc.) holds a strong potential towards new hybrid nanoelectrocatalysts for the bottleneck of water-splitting procedure, oxygen evolution reaction (OER). WS₂, a well-known member of transition metal dichalcogenides (TMDs) group, is considered ideal substrate for (photo)electrocatalytic applications.[1] Its poor affinity for oxygen species adsorption can be ameliorated by conjugating transition metal carrier systems, where the metal center plays the core part for binding oxygen species. M-N₄ motifs are considered single atom catalyst (SAC) systems and can be found in metal-porphyrins, which apart from being catalytically active at a molecular level, also stand out as excellent photoactive species.[2] In this work, hybrids based on covalently grafted Ni-porphyrin onto WS₂, exhibit comparable activity with the state-of-the-art RuO₂ catalyst for water oxidation. Markedly, this system performs even better under light illumination, in a more realistic photoelectrocatalytic setup (**Figure 1**).[3]

Partial financial support by the Hellenic Foundation for Research and Innovation HFRI under the “2nd Call for HFRI Research Projects to support Faculty Members and Researchers”, Project Number: 2482, is acknowledged.

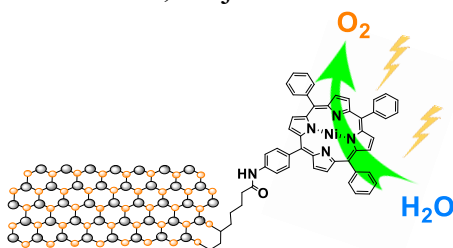


Figure 1. Exfoliated WS₂ interfacing Ni-porphyrin as a hybrid (photo)electrocatalyst for water oxidation.

References

- [1] Z. Ni, H. Wen, S. Zhang, R. Guo, N. Su, X. Liu, C. Liu, *ChemCatChem* 2020, 12 (20), 4962-4999
- [2] X.-F., Yang, A. Wang, B. Quiao, J. Li, J. Liu and T. Zhang, *Acc. Chem. Res.* 2013, 46 (8), 1740–1748
- [3] M. P. Minadakis, R. Canton-Vitoria, C. Stangel, R. Arenal and N. Tagmatarchis, Submitted (2022).

* E-mail: minadakis@eie.gr

Co-assembly of Heterojunction WO₃/TiO₂ Inverse Opal Films for Photoinduced Applications

M.-A. Apostolaki*, S. Gardelis, V. Likodimos
Section of Condensed Matter Physics, Department of Physics, National and Kapodistrian University of Athens, Athens, Greece

E. Sakellis, P. Tsipas, N. Boukos, A. Dimoulas
Institute of Nanoscience and Nanotechnology, National Centre for Scientific Research "Demokritos", Athens, Greece

Photonic crystals (PCs) offer a macroporous periodic structure that activates slow light propagation at spectral regions of weak electronic absorption and enables photochemical enhancement by the synergy of light trapping and material's composition [1]. Mixed WO₃/TiO₂ photonic crystal films in the form of 3D ordered inverse opals were deposited via the co-assembly of monodisperse 211, 261 and 287 nm polymer spheres with Ti(IV) bis(ammonium lactato) dihydroxide [2] and ammonium metatungstate [3] aqueous precursors on FTO substrates at nominal W/Ti molar ratios of 1:0.25, 1:1, 1:2 and 1:5. The structural and optical properties of the heterojunction PC photoelectrodes were investigated as a function of the W/Ti molar ratio and photonic band gap in order to explore synergistic effects between photonic amplification and charge separation in the photochemical performance of the PC films.

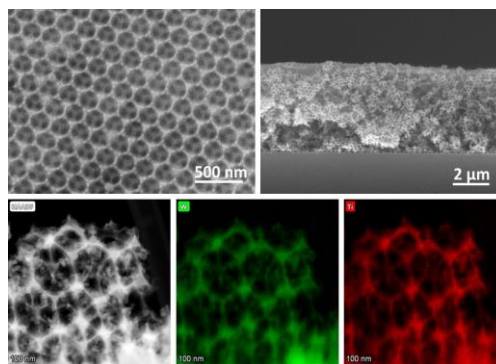


Figure 1: (Upper) SEM images and (Bottom) TEM image and elemental EDX maps of W and Ti for PC261 1:0.25.

SEM and TEM images for the mixed PC films display a 3D network of uniform interconnected void macropores consisting of both metal oxides according to Ti and W EDX elemental maps (Figure 1). The presence of the anatase and monoclinic phases was identified for the single-phase TiO₂ and WO₃ inverse opals, respectively, whereas the relative Raman peaks intensity varied with the TiO₂ content in WO₃/TiO₂ films (Figure 2). Photocurrent generation was evaluated in 0.1 M Na₂SO₄ aqueous electrolyte under UV–visible irradiation, which excites electrons in both semiconductors. Films with high WO₃ content present the highest photocurrent due to the combination of reduced charge carrier recombination and optimal light trapping (Figure 2).

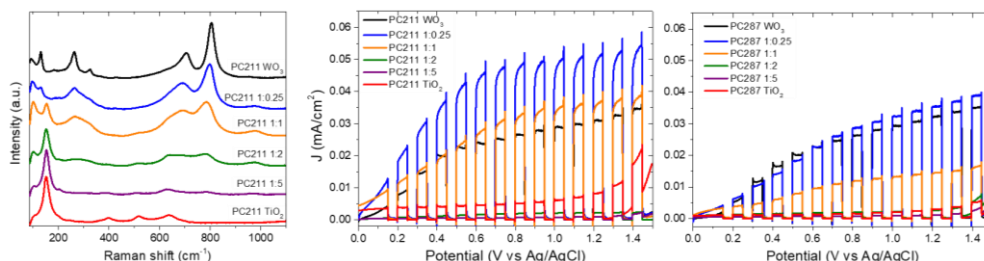


Figure 2: (left) Raman spectra for PC211 films and (right) photocurrent density-potential curves under chopped UV-Vis light illumination for PC211 and PC287 WO₃/TiO₂ films.

Acknowledgements This research has been co-financed by the European Regional Development Fund of the European Union and Greek national funds through the Operational Program Competitiveness, Entrepreneurship and Innovation, under the call RESEARCH—CREATE—INNOVATE (project code: T2EDK-03746).

References

- [1] V. Likodimos, *Appl. Catal. B Environ.* **230**, 269 (2018).
- [2] B. Hatton, L. Mishchenko, S. Davis, K.H. Sandhage, J. Aizenberg, *PNAS* **107**, 10354 (2010).
- [3] M. Sadakane, K. Sasaki, B. Ohtani, R. Abe, W. Ueda, *J. Mater. Chem.* **20**, 1811 (2010).

* marapos@phys.uoa.gr

Polymer-based electrospun fibrous nanocomposites

T. Krasia-Christoforou

*University of Cyprus, Department of Mechanical and Manufacturing Engineering
1 Panepistimiou Avenue, 2109, Aglantzia,
P. O. Box, 20537, Nicosia, CYPRUS*

Electrospinning is considered to be one of the most powerful and versatile fabrication methods used in the production of fibers with diameters in the nano- and micrometer size range. This technique - which has already entered the industrial sector - enables the production of polymer, ceramic and organic-inorganic polymer-based nanocomposite fibers [1]. The latter can be derived through the incorporation of inorganic nanoparticles within polymer fibers during electrospinning or *via* their anchoring onto the fibers' surfaces by following post-modification strategies. Such organic-inorganic fibrous nanocomposites are highly attractive in biomedical, environmental, optoelectronic, sensing, catalytic and energy-related applications, owed to their unique properties including high surface to volume ratios, high porosity, and multifunctionality, deriving from the combination of the organic and inorganic counterparts.

In this presentation electrospinning-derived organic-inorganic fibrous nanocomposites will be presented and discussed, including Fe₃O₄ NP-containing electrospun microfibers and microrods with applicability in biomedicine [2, 3], in water remediation processes [4-6], sensing [7], etc., NP-containing electrospun fibrous mats employed as heterogeneous catalytic supports in organic synthesis [8], and light-emitting materials based on electrospun fibers with embedded upconverting NP and perovskite nanocrystals [9, 10].

References

- [1] Savva and Krasia-Christoforou, "Encroachment of Traditional Electrospinning" in *Electrospinning – Basic Research to Commercialization* (Eds. S. Thomas, K. Ghosal, E. Kny), Royal Society of Chemistry (2018).
- [2] Savva, Odysseos, Evaggelou, Marinica, Vasile, Vekas, Sarigiannis and Krasia-Christoforou *Biomacromolecules* **14**, 4436 (2013).
- [3] Nikolaou, Avraam, Kolokithas-Ntoukas, Bakandritsos, Lizal, Misik, Maly, Jedelsky, Savva, Balanean and Krasia-Christoforou *Materials Science & Engineering C* **126**, 112117 (2021).
- [4] Savva, Marinica, Papatryfonos, Vekas and Krasia-Christoforou *RSC Advances* **5**, 16484 (2015).
- [5] Panteli, Savva, Efstathiou, Vekas, Marinica, Krasia-Christoforou, and Pashalidis *SN Applied Sciences* **1**, 30 (2019).
- [6] Philippou, Christou, Socoliuc, Vekas, Tanasă, Miclau, Pashalidis and Krasia-Christoforou *Journal of Applied Polymer Science* e50212 (2020).
- [7] Petropoulou, Kralj, Karagiorgis, Savva, Loizides, Panagi, Krasia-Christoforou and Riziotis *Scientific Reports* **10**, Article no. 367, 1 (2020).
- [8] Savva, Kalogirou, Chatzinicolaou, Papaphilippou, Pantelidou, Vasile, Vasile, Koutentis, and Krasia-Christoforou, *RSC Advances* **4**, 44911 (2014).
- [9] Antoniadou, Pilch-Wrobel, Riziotis, Bednarkiewicz, Tanasă and Krasia-Christoforou, *Methods and Applications in Fluorescence* **7**, 034002 (2019).
- [10] Papagiorgis, Manoli, Alexiou, Karacosta, Karagiorgis, Papapaskeva, Bernasconi, Bodnarchuk, Kovalenko, Krasia-Christoforou and Itskos, *Frontiers in Chemistry* **7**, 87 (2019).

Fluoropolymer surfaces modification via lithographic techniques

Margarita Chatzichristidi

¹ *Industrial Chemistry Laboratory, Department of Chemistry, National and Kapodistrian University of Athens, Athens, Greece*
e-mail: mchatzi@chem.uoa.gr

The ability to immobilize biomolecules onto a surface with high spatial resolution is crucial for the development of micro- and nanoscale arrays and biosensors. In addition, the chemistry and the topography of a surface can control the size and the structure of cells attached to them, thus affecting their behavior [1].

Patterning techniques using conventional lithography are excellent techniques for high-resolution, precise alignment and thus spatial control of a surface [2]. Those techniques, unfortunately, have the disadvantage of requiring harsh developers and exposure conditions as well as elevated temperatures, which often lead to denaturation of biomolecules. Nevertheless, the use of this technique as a surface modification technique using novel photosensitive materials whose biomolecule adsorption properties change upon exposure to UV light is of high interest.

In the present work, different fluorinated polymers based on two different fluorinated monomers that cleave their fluorinated moieties upon exposure to UV irradiation and subsequent thermal treatment are presented. Those polymers were synthesized and evaluated as potential materials for surface modification through optical lithography. The two monomers have on their side chain either a fluorinated phenyl group or a fluorinated carbon chain which are cleaved from the polymer in the presence of acid and heat. Consequently, by adding a photoacid generator in these materials, it is possible to change the chemistry of the surface in specific areas by UV irradiation through a mask (UV light produce acid only in the exposed areas of the films). In order to improve the film properties (e.g. the film will remain on the surface after immersion in aqueous biomolecule solutions), copolymers containing one of the monomers were synthesized. The characterization of the fluorinated homopolymers and copolymers films in terms of solubility and wettability change before and after exposure to UV radiation were investigated. The novelty of this work is the implementation of optical lithography in combination with novel fluorinated polymers for the creation of well-defined areas on a substrate in order to be used in biological applications requiring site-directed immobilization of biomolecules.

References:

1. R.S. Kane, S. Takayama, E. Ostuni, D.E. Ingber, G.M. Whitesides, *Biomaterials* 20 (1999) 2363-2376.
2. K. M. Midthun et al., *Biomacromolecules* 14 (2013) 993-1002.

Study of Polybutadiene/Silica Nanocomposites through Molecular Dynamics Simulations

Anastassia Rissanou^{1,2,3}, *Alireza F. Behbahani*¹, and *Vagelis Harmandaris*^{1,2,3}

¹*Institute of Applied and Computational Mathematics, Foundation for Research and Technology Hellas, Heraklion GR-71110, Greece*

²*Department of Mathematics and Applied Mathematics, University of Crete, Heraklion GR-71110, Greece*

³*Computation-Based Science and Technology Research Center, The Cyprus Institute, Nicosia 2121, Cyprus*

Presenting author's e-mail: rissanou@iesl.forth.gr

The conformations and the dynamics of poly-(butadiene) chains, of various molecular weights, in PB/silica nanocomposites are studied through long-time atomistic molecular dynamics simulations at $T = 413$ K, well above T_g . The effect of the stereochemistry of PB chains is addressed by simulation of cis-1,4-PB/silica and trans-1,4-PB/silica nanocomposites. The model systems contain 30wt % silica nanoparticles of diameter ≈ 4 nm. The nanocomposites are characterized through analyzing (i) interfacial packing and the dimensions of the PB chains; (ii) statistics of the train, bridge, loop, and tail conformations of adsorbed chains and the coupling between segmental orientational dynamics and chain conformations; and (iii) the orientational and translational dynamics of the polymer chains and the desorption kinetics of chains and segments. The dimensions of PB chains, excluding a small fraction of chains that wrap around the NP, are not affected. The segmental and terminal dynamics of PB chains are slower in the nanocomposites than in the respective bulk melts. Moreover, the dynamics of PB chains in the nanocomposites is very heterogeneous and a coupling between the dynamics and the conformation of PB chains is observed: the adsorbed segments (trains) and the chains that have a higher number of contacts to the NPs are more decelerated. The self-diffusion coefficients, D , of PB chains in the nanocomposites are also reduced compared to the respective bulk systems. A clear crossover from the unentangled (Rouse-like) to the entangled (reptation-like) regime is observed based on the calculation of the segmental mean-square displacement and D as a function of the chain length. The deceleration of dynamics in the nanocomposites, in both Rouse and reptation-like regimes, is discussed in terms of a higher effective monomeric friction coefficient. Finally, the correlation times for the desorption of segments and chains are much larger than the segmental and end-to-end-vector correlation times, respectively.

Keywords: polymer nanocomposites; Atomistic Molecular Simulations

Session 2nd choice: Theory and Multi-scale Modeling of Colloids and Interfaces

Acknowledgements: The work was supported by computational time granted from the Greek Research & Technology Network (GRNET) in the National HPC facility--ARIS under project named POLCOMP-TIRE. This work is supported by the Goodyear Tire and Rubber Company.

References

- [1] A. F. Behbahani, A. Rissanou, G. Kritikos, M. Doxastakis, C. Burkhart, P. Polinska, V. Harmandaris, *Macromolecules*, 2020, 53, 6173
- [2] G. Maurel, F. Goujon, B. Schnell, P. Malfreyt, *J. Phys. Chem. C*, 2015, 119, 4817.

Influence of filler and/or ZnO-coating on the physical properties of Poly(lactic acid)/TiO₂ bionanocomposites

A.A. Barmpaki^{a*}, E.E. Zavvou^a, M.A. Botzakaki^a, N.J. Xanthopoulos^a,
A. Giannakas^b, C.E. Salmas^c, P.K. Karahaliou^a, P. Svarnas^d, A. Ladavos^e and
C.A. Krontiras^a

^a *Department of Physics, University of Patras, 26504 Patras, Greece*

^b *Department of Food Science and Technology, University of Patras, 30100
Agrinio, Greece*

^c *Department of Material Science and Engineering, University of Ioannina, 45110
Ioannina, Greece*

^d *Department of Electrical & Computer Engineering, University of Patras, 26504,
Patras, Greece*

^e *Department of Business Administration of Food and Agricultural Enterprises,
University of Patras, 30100 Agrinio, Greece*

Poly(lactic acid) (PLA) has been extensively employed as an alternative to traditional petroleum-based polymers in a wide range of applications [1-3]. Implementation of bionanocomposites, exploiting PLA as the matrix and a variety of organic or inorganic materials as nanofillers, results in the enhancement of the polymer physical properties [4]. Among the wide family of nanofillers, titanium dioxide (TiO₂), an inert and low-cost inorganic nanoinclusion, is an excellent candidate for the production of such nanocomposite systems [5]. In this work, PLA/TiO₂ bionanocomposites were prepared via twin-screw extrusion, in a wide range of filler content (1, 3, 5, 7 and 10 wt%), and were hot-pressed and quenched in liquid nitrogen, forming amorphous films. Scanning Electron Microscopy studies revealed good dispersion of the nanoparticles within the polymer matrix. Both the glass transition and the melting behavior appear rather independent on the addition of TiO₂ content, while the cold crystallization is strongly affected, as revealed by Differential Scanning Calorimetry. A mild improvement of the thermal stability of nanocomposites upon increasing filler content was obtained through Thermogravimetric Analysis. Water Vapor Transmission studies indicate a small decrease of Water Vapor Transmission Rate (WVTR) with increasing TiO₂ content. Contact angle and surface energy measurements suggest that the wettability of the bionanocomposites remains unaffected. Finally, Zinc oxide (ZnO), a material with antibacterial properties [6], was deposited via Atomic Layer Deposition onto the amorphous samples. The barrier and surface properties of the coated specimens were studied and evaluated in comparison to the uncoated ones.

Acknowledgements

Authors acknowledge Dr. V. Drakopoulos and Dr. E. Mystiridou, Prof. N. Bouropoulos for their assistance in SEM experiments and TGA experiments, respectively. C. Drivas and Prof. S. Kennou are also acknowledged for XPS analysis. The present work was financially supported by the «Andreas Mentzelopoulos Foundation».

References

- [1] Di Lorenzo M.L. & Androsch R., *Advances in Polymer Science*. Springer, Cham, Switzerland, 282, 2018.
- [2] Jamshidian M. et al. *Compr. Rev. Food Sci.* **9**, 552-571 (2010).
- [3] Zavvou E. et al. *J Polym Res* **29**, 284 (2022).
- [4] Rhim J.-W. et al., *Progress in Polymer Science* **38**, 1629– 1652 (2013).
- [5] Kassem M. et al. *Materials* **12**, 3659 (2019).
- [6] Sirelkhatim A. et al. *Nano-Micro Lett.* **7**, 219–242 (2015).

* a.barmpaki@upnet.gr

Utilizing Polymer Coatings for the Development of Superhydrophobic and Water Repellent Surfaces

Th.-M. Chatzaki^{*},^{1,2} F. Krasanakis,¹ K. Chrissopoulou¹ and S. H. Anastasiadis^{1,2}

¹*Institute of Electronic Structure and Laser, Foundation for Research and Technology-Hellas, Heraklion Crete, Greece*

²*Department of Chemistry, University of Crete, Heraklion Crete, Greece*

The development of superhydrophobic and water - repellent coatings has attracted considerable attention due to their wide range of applications. At the same time, polymer materials with optimized properties can be prepared by the incorporation of nano-additives in a polymer matrix, forming a composite material. In this work, we report on the development of superhydrophobic and water - repellent nanohybrid coatings, deposited on flexible Low-Density Polyethylene (LDPE) substrates that have been modified by Corona Treatment. The coatings consisted of a low surface energy polymer matrix into which inorganic nanoparticles of different size were incorporated. The surface properties were evaluated for both the bare and the coated substrates and in the latter case they highly depend on the kind of the polymer matrix (silane/siloxane mixture, fluoropolymer), the thickness of the coating, as well as on the content and size of the added inorganic nanoparticles. Contact angle (CA) and contact angle hysteresis (CAH) measurements revealed that the optimum coating exhibits a superhydrophobic ($CA > 150^\circ$) and water - repellent behaviour ($CAH < 5^\circ$), as shown in Figure 1. Further than their superhydrophobicity, the wetting properties of the coated surfaces against several organic solvents (Glycerol, Ethylene Glycol and Dimethyl Sulfoxide), showed strongly oleophobic behaviour as well. The surface topology and roughness of the coatings were studied by Scanning Electron Microscopy (SEM) providing complementary information towards the interpretation of the results. Furthermore, the optical and thermal properties of the coated LDPE films were evaluated and the transmittance and thermal transitions of the initial LDPE were found unaffected by the presence of the coating. The combination of superhydrophobicity and in certain cases amphiphobicity, low roll off angles and antidust properties make these coatings ideal candidates for greenhouse applications.

Acknowledgements: This research has been co-financed by EU and Greek national funds (INGRECO MIS: 5030174, Action RESEARCH – CREATE - INNOVATE).



Figure 1: Water - repellent behavior of nanostructured coating deposited on LDPE substrate.

* mchatzaki@iesl.forth.gr

Charge Transport and Interfacial Dipolar Effects in Conjugated Polymers

Stavros X. Drakopoulos¹, Jing Cui², Mihai Asandulesa³, Sergei Bronnikov⁴, Aurora Nogales², Kamal Asadi¹

¹Department of Physics, University of Bath, United Kingdom

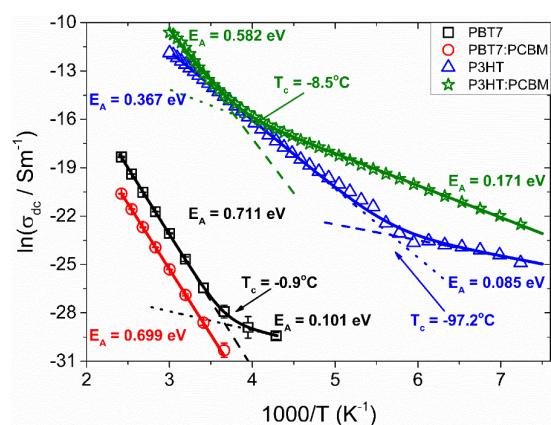
²Instituto de Estructura de la Materia, IEM-CSIC, Spain

³Petru Poni Institute of Macromolecular Chemistry, Romanian Academy, Romania

⁴Institute of Macromolecular Compounds, Russian Academy of Sciences, Russian Federation

Semiconducting conjugated polymers have emerged as a promising cost-effective candidate for realising flexible transistors, solar cells, solid-state batteries and thermoelectric generators. In conjugated polymers, the dielectric constant and dc conductivity dominate power conversion efficiency and performance. Both arise from the chemical structure of the π -conjugated polymers that consist of a conjugated sp^2 hybridized backbone and, typically, an aliphatic side chain. The enhancement of the dielectric constant of the conjugated polymer results in a reduced exciton binding energy which is highly relevant in their application in solar cells, while the enhancement in conductivity of the polymers results in devices with faster response time. The dielectric constant is usually determined under time-varying small electric field conditions at relatively high frequencies. In contrast, the conductivity is usually determined under a steady-state electric field or DC conditions. Consequently, the efforts to tune the dielectric constant or conductivity in conjugated polymers have usually been carried out independent from each other.

The significant difference in electrical conductivity between different phases in heterogeneous materials gives rise to Maxwell-Wagner-Sillars interfacial polarization (IP) effect. The appearance of IP is characterized by a rise in the relative permittivity of the material at low frequencies, accompanied by a relaxation peak in the dielectric loss spectra. The existence of IP and the local build-ups of space-charge can significantly affect the dc conductivity, σ_{dc} , of the material. Therefore, understanding the IP process, its relation between dielectric permittivity and σ_{dc} in conjugated polymers is highly relevant for further improving the performance of their optoelectronic devices. However, the IP process and establishing a direct correlation with σ_{dc} have been overlooked so far in conjugated polymers because identification of the IP in dielectric loss, is usually masked by the conductivity of the samples at low frequencies, even at low temperatures.



New Materials and Devices for Bioelectronic Medicine

George Malliaras

Prince Philip Professor of Technology

University of Cambridge
Department of Engineering
Electrical Engineering Division

Bioelectronic medicine provides a new means of addressing disease via the electrical stimulation of tissues: Deep brain stimulation, for example, has shown exceptional promise in the treatment of neurological and neuropsychiatric disorders, while stimulation of peripheral nerves is being explored to treat autoimmune disorders. To bring these technologies to patients at scale, however, significant challenges remain to be addressed. Key among these is our ability to establish stable and efficient interfaces between electronics and the human body. I will show examples of how this can be achieved using new organic electronic materials and devices engineered to communicate with the body and evolve with it. I will discuss the fundamental materials properties that play a critical role in this endeavor.

Applications of Advanced Therapy Medicinal Products in Oral Medicine

A.A. Bakopoulou*

Department of Prosthodontics, School of Dentistry, Faculty of Health Sciences, Aristotle University of Thessaloniki, Thessaloniki, GR-54124, Greece

Regenerative Medicine/Dentistry offers innovative approaches to restore damaged or lost tissues, based on the principles of tissue engineering (TE). Although research on advanced therapy medicinal products (ATMPs) has been very active in recent years, the number of licensed products remains surprisingly low and restricted to treatment of lethal or highly debilitating incurable diseases. Competent authorities worldwide have focused in developing regulatory pathways to accelerate treatments of unmet patient needs. Yet, the status remains still in early development, while several scientific, regulatory and cost-effectiveness issues, impose considerable hurdles to achieve marketing authorization, technology adoption and patient accessibility. In the context of this global landscape, Regenerative Dentistry, although achieving breakthrough innovations during the past years in TE of several dental and oral tissues in pre-clinical models, has hardly harnessed research progress to integrate innovative regenerative treatments into clinical practice. This presentation will disseminate our Institutional experience on the development of TE constructs tailored for application as ATMPs for oral tissue regeneration. It will also provide a brief overview of current clinical, regulatory and commercial status of cell-based therapies and will discuss the main hurdles to overcome to foster wider application in Regenerative Dentistry.

References

Bakopoulou A. Prospects of Advanced Therapy Medicinal Products-Based Therapies in Regenerative Dentistry: Current Status, Comparison with Global Trends in Medicine, and Future Perspectives. *J Endod.* 2020 Sep;46(9S):S175-S188. doi: 10.1016/j.joen.2020.06.026.

* abakopoulou@dent.auth.gr

Anti-bacteria Ti- based alloys for bone implants

Y. Fortouna, A. Balerba, Ch. E. Lekka*

*Department of Materials Science and Engineering, University of Ioannina
Institute of Materials Science and Computing, Univ.of Ioannina, Ioannina, Greece*

J.J. Gutierrez-Moreno

BSC – Barcelona Supercomputing Center, Barcelona, Spain

L. A. Alberta, M. Calin

*Institute of Complex Materials, IFW Dresden, Helmholtzstraße 20, 01069
Dresden, Germany*

Bacteria colonization and biofilm formation on orthopaedics or dental implants usually appears after an implant surgery causing serious infections while resist highly to conventional antibiotic treatment. For these reasons, innovative materials that will fruitful the metallic implants' requirements such as low Young moduli, high corrosion resistance and minimal cytotoxicity along with anti-bacterial properties are urgent/important to be designed. [1,2]

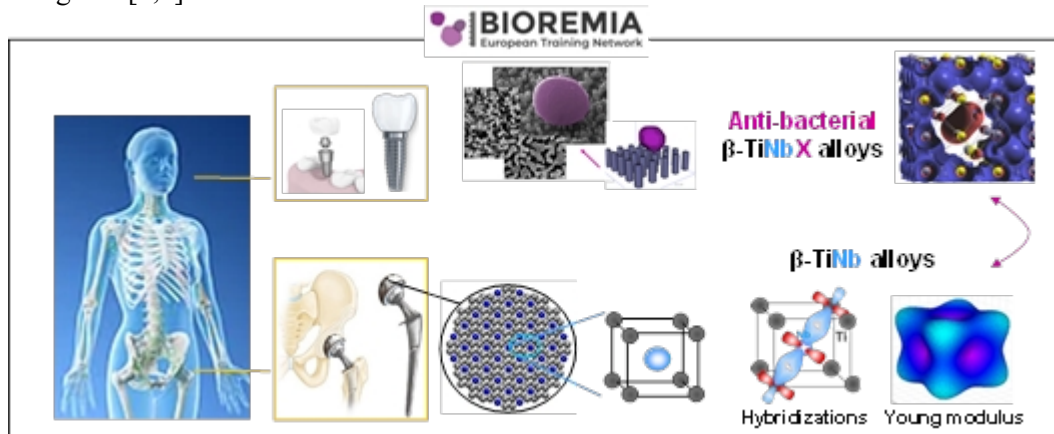


Figure 1: Structural, electronic and mechanical properties of Ti based alloys for hard tissue implants applications

The β -type Ti-Nb alloys have been suggested as promising materials for replacing the widely used TiAl_6V_4 implants while their enrichment with elements showing antibacterial properties like Ga, Cu and Ag might cause antibiofilm activity [2,3,4].

The results of this work could be of use in the design of antibacteria, low rigidity β -type Ti-alloys with non-toxic additions, suitable for orthopedic and orthodontics applications.

Acknowledgements

This work is supported by the Bioremia (H2020-MSCA-ITN-2019, No 861046, 2020-2024) and BioTiNet (FP7-PEOPLE-2010-ITN No 264635, 2011-2014).

References

- [1] Mitsuo Niinomi, Metals for biomedical devices. Woodhead Publishing Limited (2010)
- [2] Lekka, Gutiérrez-Moreno, Calin, J. Phys. Chem. Solids 102 (2017) 49
- [3] Gutiérrez Moreno, Panagiotopoulos, Evangelakis, Lekka, (2020), 13,1–11, 1288
- [4] Alberta, Fortouna, Vishnu, Gebert, Lekka, Calin (to be submitted)

* chlekka@uoi.gr

3D bioprinted constructs for bone tissue regeneration

Konstantinos Loukelis^{1,2}, Georgia-Ioanna Kontogianni^{1,2}, Dimitris Vlassopoulos^{1,2}, Maria Chatzinikolaidou^{1,2}

¹ Department of Materials Science and Technology, University of Crete, 70013 Heraklion, Greece

² Foundation for Research and Technology Hellas (FORTH)-Institute of Electronic Structure and Laser (IESL), 70013 Heraklion, Greece

Keywords: bioprinting, gellan gum, hydroxyapatite, bioink, bone

Bioprinting is one of the most versatile 3D printing techniques in the field of tissue engineering, combining cells and biomaterials into constructs with desired geometry. The success of a bioink is governed by many factors such as its biocompatible nature, its mechanical properties and its capacity to promote cell proliferation. This in turn leads to an increasing demand for the development of new combinations of biomaterials and biological constituents in order to produce biomimicking devices, optimal for tissue regeneration [1,2]. In this work, we prepared two different compositions of bioinks comprising gellan gum (GG) and polyvinyl alcohol (PVA) [3,4] with the osteoinductive compound nanohydroxyapatite (HAP) [5], to assess their mechanical properties, and their osteogenic potential when mixed with MC3T3-E1 pre-osteoblasts.

By mixing a 10% w/v PVA, a 4% w/v GG and a 15% w/v HAP solution in different ratios, four compositions were prepared in total: (i) 50-50 GG/PVA, (ii) 70-30 GG/PVA, (iii) 50-50 GG/PVA with 2.5% w/v HAP (50-50 GG/PVA/HAP) and (iv) 70-30 GG/PVA with 2.5% w/v HAP (70-30 GG/PVA/HAP), with the 50-50 and 70-30 indicating the ratios of the gellan gum to PVA solutions volume. The solutions were mixed with MC3T3-E1 pre-osteoblastic cell suspensions at a ratio of 5×10^6 cells/ml, formulating the bioink constructs and crosslinked by using a 1% w/v CaCl_2 solution. The biological evaluation of the bioinks includes the visualization of the living cells by the Live/Dead assay, the morphological characterization of cells and extracellular matrix (ECM) by the nuclei/actin cytoskeleton stain using DAPI/rhodamine phalloidin, and ECM collagen and glycosaminoglycans, as well as alizarin red staining to determine the levels of calcium mineralization. Moreover, the bioinks have been mechanically characterized by examining their biodegradation rate and their rheological properties by employing protocols such as dynamic strain sweep (DSS), dynamic frequency sweep (DFS), calculation of $\tan\delta$, recovery rate after applying extreme stress and viscosity levels.

At day 1, the cells were visibly round and stressed but on day 3 they had an increased proliferation in all compositions, with the HAP scaffolds having a more prominent effect. At day 7, bioinks had evident extracellular matrix formation, with the HAP containing bioinks depicting greater levels. Regarding the biodegradation rate, the 50-50 GG/PVA bioink retained values between 14% and 28%, the 70-30 GG/PVA, 7% and 23%, the 50-50 GG/PVA/HAP, 9% and 17% and finally the 70-30 GG/PVA/HAP, 5% and 16% for days 7 and 21, respectively. The rheological analysis showcased that the presence of HAP only slightly affected the examined quantities. Specifically, the yield points ranged between 11 and 28 kPa for the various compositions, with the DFS analysis validating the G' and G'' values. $\tan\delta$ which is indicative of the ratio between the elastic and the viscous part of the material, ranged between 0,11 and 0,71. Finally, all bioinks retained a recovery rate of at least 89% of their viscosity levels after the application of a 200% strain.

Novel bioinks containing gellan gum, PVA, and hydroxyapatite were constructed to assess their role in bioinks' biomechanical traits. The 3D bioprinted constructs were mixed with pre-osteoblasts to form bioinks for bone tissue growth. Their rheological properties support their excellent bioprintability, while their biocompatible attributes promote bone regeneration.

REFERENCES

1. Ozbolat I., Ozbolat W.P.V., *Drugs Discovery Today*. 1257-1271, 2016
2. Decante D. et al, *Biofabrication*. 13 032001, 2021
3. Oliveira T. et al, *Tissue Engineering Part A*. 343–353, 2010
4. Kumar, A., & Han, S., *International Journal of Polymeric Materials and Polymeric Biomaterials*. 159–182, 2016
5. Zhou H., Lee J., *Acta Biomaterialia*. 2769-2781, 2011

Incorporation of Moxifloxacin-Loaded Silica-Based Mesoporous Nanocarriers in Electrospun PLGA Fibers for Periodontal Regeneration

G.K. Pouroutzidou*,

Advanced Materials and Devices Laboratory, School of Physics

E. Kontonasaki

Department of Prosthodontics, School of Dentistry

D. Bikiaris

School of Chemistry

Aristotle University of Thessaloniki, 54124 Thessaloniki, Greece

Mesoporous silica-based nanoparticles (MSNs) are unique drug carriers due to their ordered pore structure, which allows high drug loading and release capacity. [1] Calcium (Ca), magnesium (Mg) and strontium (Sr) doped MSNs are capable of inducing in vitro osteogenesis and in vivo bone formation through the release of Ca, Mg, Sr, and Si ions, which compel their use for bone scaffolds fabrication. [2] Electrospun membranes are promising materials for guided tissue regeneration (GTR) as they provide a suitable framework for the formation of new functional periodontal tissues. [3] The fabrication of multifunctional local drug delivery systems for sustained and prolonged drug release can be used in periodontal applications such as interventions to simultaneously prohibit epithelium downgrowth and proper healing and regeneration of damaged periodontal tissues. [4] The aim of this study was the development and characterization of novel composite membranes from poly(lactic-glycolic acid) (PLGA)/Moxifloxacin-loaded MSNs through electrospinning. Degradation, swelling, drug release, biocompatibility in human periodontal ligament cells and erythrocytes, as well as mechanical and physicochemical properties were evaluated. The incorporation of moxifloxacin-loaded MSNs in PLGA led to a sustained and prolonged release while maintaining satisfactory mechanical strength. The increase in the amount of the polymer yielded more uniform fibers with large diameters and pores. During the electrospinning process, the increase of the applied voltage and the rotation speed of the collector led to more uniform fibers with larger diameters and pores. The composite membranes were found to be hemocompatible at masses less than 1 mg after exposure to healthy erythrocytes. The morphology, physicochemical, and biological properties of the fabricated membranes yield them promising for periodontal tissue regeneration.

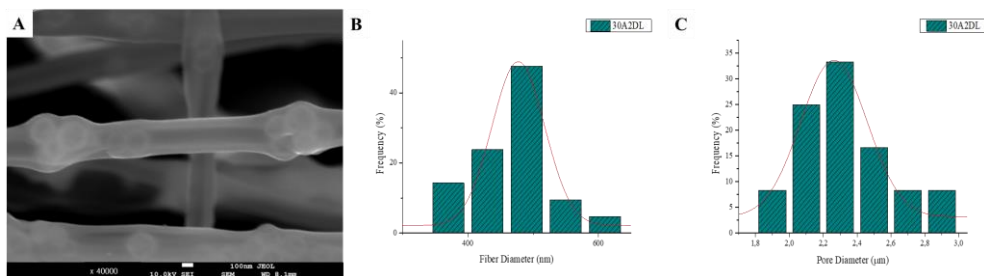


Figure 1: SEM microphotograph (A) and fiber (B) and pore (C) diameter distribution of composite membranes.

References

- [1] Bharti, et. Al. *Int J Pharm Investig* 5(3):124 (2015).
- [2] Pouroutzidou GK, et Al., *Int J Mol Sci* Jan 8;22(2):577 (2021).
- [3] Bottino, et. Al., *Dent Mater* Jul;28(7):703–21 (2012).
- [4] Pouroutzidou, et. Al., *Nanomaterials* Mar 2;12(5):850 (2022).

* gpourout@physics.auth.gr

3D scaffolds via Multi-Photon Polymerization for the directed neurite development in co-culture systems

Antonis Kordas^{1,2,*}, Phanee Manganas¹, Anthi Ranella¹, Maria Farsari¹

¹*Institute of Electronic Structure and Laser, Foundation for Research and Technology-Hellas (FORTH-IESL), 100 Nikolaou Plastira Street, Heraklion, 70013, Greece*

²*Department of Materials Science and Technology, University of Crete, Vassilika Vouton, Heraklion, 71409, Greece*

Multi-Photon Polymerization (MPP), a Direct Laser Writing (DLW) technique, has found application in the field of Tissue Engineering (TE), due to the ability of fabrication of high precision scaffolds that can be used as a cell culture substrate [1, 2]. Of great importance is the Peripheral Nervous System (PNS) Tissue Engineering which shows increasing potential as an alternative to established methods, namely surgery and grafts, that aim to counter PNS-related diseases and damage. A novel bridge-shaped 3D scaffold design was fabricated using a femtosecond fibre laser operating at 780nm (pulse duration: 120fs, repetition rate: 80MHz) using an already established organic/inorganic hybrid material [3]. The fabricated scaffolds had suitable dimensions (400 μ m x 400 μ m x 60 μ m) for the mono- and co-cultures of murine neuronal N2a and glial Schwann (SW10) cells at three timepoints (7, 14, 21 days). The cultures exhibited scaffold-dependent cell and neurite directionality compared to flat glass cultures which were used as controls and showed a completely random orientation. This highlighted the impact of scaffold topography in cell behavior which was significantly influenced in the presence of scaffolds. Additionally, longer neurites have been favored in scaffold co-culture systems compared to N2a scaffold mono-cultures after 21 days (a percentage of 31.4% \pm 5.5% compared to a percentage of 15.4% \pm 5.4% respectively), indicating a synergistic effect of scaffold topography and SW10 cells [4]. These findings support the ability of controlling neurite directionality and length, properties deemed crucial for practical applications such as treatment of PNS damage and are expected to contribute to the development of an *in vitro* model for the study of neurodegenerative diseases and understanding of key cellular responses such as myelination.

Keywords: Multi-photon polymerization (MPP), Tissue regeneration, Co-culture system, Scaffold Topography, Cell Orientation, Neurite Directionality

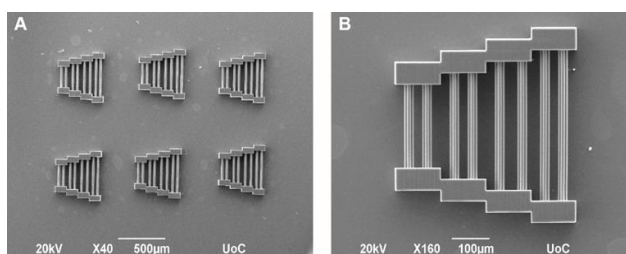


Figure 1: SEM image of 3D scaffolds for cell cultures. A: typical coverslip with 6 scaffolds for cell cultures. B: Magnification of a single scaffold [4].

References

- [1] Sun, H.B. and Kawata, S., Eds., ed Berlin, Heidelberg: Springer Berlin Heidelberg, (2004), 170: 169-273
- [2] Nguyen, A. K. and Narayan, R. J., (2017), *Materials Today*, 20, (6):314-322
- [3] Ovsianikov A. et al., (2008), *ACS Nano.*, 2:2257-2262
- [4] Kordas A., Manganas P. et al., (2022), *Materials*, 15: 4349-4365

* antkor89@iesl.forth.gr

Micro and nano-engineered silicon for high energy density lithium ion cells

F. Farmakis

*Micro- and Nanotechnology Lab, Electrical and Computer Engineering Dept.
Democritus University of Thrace, Vas. Sofias 12, Xanthi, Greece*

Lithium-ion Batteries (LIBs) are currently the most prominent choice for energy storage applications, especially for portable electronic devices, cordless power tools and electric vehicles thanks to their high energy density, long cycle life and low weight, compared to other energy storage technologies. However, there is a continuous need to improve the overall electrochemical performance of lithium-ion batteries, as the constant technological advances in the fields of automotive industry and portable communication device industry demand higher specific energy and energy density (>400 Wh/kg and >800 Wh/L) than actually commercially available cells.

Commonly, LIBs use graphite-based anodes (negative electrode), which have a capacity limitation due to the theoretical specific capacity of graphite versus Li/Li^+ , ~ 372 mAh/g, with a lithiation phase of LiC_6 . The most promising material to replace graphite is silicon (Si) with a maximum specific capacity, at room temperature, of 3579 mAh/g at the lithiation phase of $\text{Li}_{15}\text{Si}_4$, offering, in addition, a low potential vs Li/Li^+ , abundance, non-toxicity and huge know-how processing from the microelectronic industry. However, pure silicon anodes are not ready to be commercialized, as silicon expands during lithiation (up to 300% of its initial volume) resulting to electrode cracking, material pulverization and Solid Electrolyte Interphase (SEI) fracture and regrowth. Consequently, electrodes demonstrate a continuous capacity fading upon cycling leading to limited cell cycle life. During the past years, there has been extensive ongoing research on improving the cycle life of silicon electrodes. Different approaches have been adopted to address silicon's expanding problem, by focusing on different aspects of the electrode. One approach has been the preparation and investigation of Si nanostructures that can accommodate the volume expansions during cycling, by manipulating the size, the surface and morphology of silicon particles. Furthermore, in order to enhance the electrical conductivity of silicon and offer a protective layer for SEI formation, the use of carbon-based coatings has been proposed, preventing the continuous cracking and growth of SEI. A promising approach focuses on combining two of the above-mentioned strategies, i.e. the creation of silicon nanostructures and the use of a carbon-based shell/coating. By managing to create a void space in between silicon and the carbon shell the nanoparticle can swell during lithiation without fracturing the outer shell and the corresponding SEI that is formed on the carbon shell surface.

The scope of this work is to present a brief summary of the technological challenges towards a silicon-based anode with high specific capacity and long-term stability.

Lithionic two-terminal resistive switching devices with analog memory and a nanobattery architecture based on $\text{Li}_{1-x}\text{CoO}_2$ cathode, SiO_x electrolyte and $\text{Li}_{4+3x}\text{Ti}_5\text{O}_{12}$ anode

P. S. Ioannou^a, E. Kyriakides^a, O. Schneegans^b and J. Giapintzakis^a

^a Complex Functional Materials Laboratory, Department of Mechanical and Manufacturing Engineering, University of Cyprus, 75 Kallipoleos Ave., 1678, Nicosia, Cyprus

^b Laboratoire de Génie Electrique et Electronique de Paris, CentraleSupélec, CNRS, Université Paris-Saclay, Sorbonne Université, 11 rue Joliot-Curie, 91192, Gif-sur-Yvette, France

Memristor technologies are emerging as the most viable successor to CMOS-based transistor technologies for the implementation of neuromorphic computing, due to their two-terminal design which allows the non-von Neumann architecting of bioinspired artificial neural networks (ANN's), enabling the reduction of the energy- and silicon “real-estate”- costs [1].

A new class of ion migration-based resistive switching (RS) devices, that rely on the electrochemical Li^+ migration to produce reversible changes in the device conductance, has shown potential as binary or analog memristors [2], and artificial synapses [3].

The insulator to metal transition of $\text{Li}_{1-x}\text{CoO}_2$ (LCO) during delithiation ($0 \leq x \leq 0.25$) has been utilized in thin film nanobattery devices based on LCO cathode, SiO_2 electrolyte and Si anode to produce multistate RS, through the reversible field-driven migration of Li^+ from the LCO cathode to the Si anode [4]. Recently, devices based on $\text{Li}_{4+3x}\text{Ti}_5\text{O}_{12}$ (LTO, $0 \leq x \leq 1$) with a Pt/LTO/Pt architecture have shown non-volatile RS with analog conductance modulation capabilities, through the electric field driven Li^+ migration which leads to a phase separation between insulating $\text{Li}_4\text{Ti}_5\text{O}_{12}$ and metallic $\text{Li}_7\text{Ti}_5\text{O}_{12}$ domains and the formation of conductive bridges between the two Pt electrodes [5].

Leveraging on mutually-beneficial electric field driven delithiation and lithiation of $\text{Li}_{1-x}\text{CoO}_2$ cathode and $\text{Li}_{4+3x}\text{Ti}_5\text{O}_{12}$ anode respectively in terms of conductance tunability, and the “zero”-strain property of LTO during lithiation in terms of endurance enhancement, the fabrication of Au/LCO/ SiO_x /LTO/Pt RS nanobattery devices is hereby examined. Such devices are capable of non-filamentary, non-volatile, and analog RS with prolonged retention ($\sim 10^5\text{s}$) and endurance ($\sim 10^4$ cycles). On the other hand, a small memory window ($I_{\text{on}}/I_{\text{off}} < 10$), strong potentiation/depression asymmetry, and indications of environmental-related degradation have been observed.

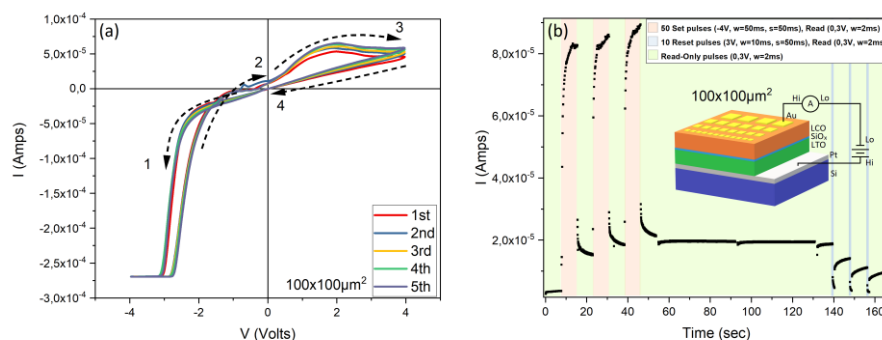


Figure 1: Current-Voltage characteristic curves of a typical Au/LCO/ SiO_x /LTO/Pt device, showing reversible RS (a). Pulsed voltage characterization of this device showing non-volatile multistate conductance modulation (b).

References:

- [1] Lanza, Mario, et al. "Memristive technologies for data storage, computation, encryption, and radio-frequency communication." *Science* 376.6597 (2022)
- [2] Zhu, Yuntong, et al. "Lithium-film ceramics for solid-state lithionic devices." *Nature Reviews Materials* 6.4 (2021): 313-331.
- [3] Ioannou, Panagiotis S., et al. "Evidence of biorealistic synaptic behavior in diffusive Li-based two-terminal resistive switching devices." *Scientific reports* 10.1 (2020): 1-10.
- [4] Mai, V. H., et al. "Memristive and neuromorphic behavior in a Li_xCoO_2 nanobattery." *Scientific reports* 5.1 (2015): 1-6.
- [5] Gonzalez-Rosillo, Juan Carlos, et al. "Lithium-battery anode gains additional functionality for neuromorphic computing through metal-insulator phase separation." *Advanced Materials* 32.9 (2020): 1907465.

* ioannou.s.pan@gmail.com

High Performance Single-ion Polymer Electrolytes via Macromolecular Engineering

E. Glynos^{1,2*}, G. Nikolakakou,^{2,3} D. Kritsiotakis^{1,2}, C. Pantazidis,⁴ G. Sakellariou⁴

¹ *Department of Materials Science and Technology, University of Crete, 71003 Heraklion, Crete, Greece*

² *Institute of Electronic Structure and Laser, Foundation for Research and Technology-Hellas, P.O. Box 1385, 71110 Heraklion, Crete GR, Greece*

³ *Department of Chemistry, University of Crete, Heraklion, 700 13 Heraklion, Crete, Greece*

⁴ *Department of Chemistry, National and Kapodistrian University of Athens, Panepistimiopolis Zografou, 15771 Athens, Greece*

*eglynos@iesl.forth.gr, eglynos@materials.uoc.gr

Single-ion solid polymer electrolytes (SI-SPEs) represent the ultimate solution to the safety issues associated with the use of flammable and toxic liquid electrolytes in commercial Li-ion batteries and for the realization of high energy-density Li-metal batteries. In spite of the considerable research effort in SI-SPEs, the realization of their potential has been hindered by the inability to design materials that possess simultaneously, cation transference number close to unity (i.e. single-ion solid polymer electrolytes, $r_+ = 1$), good mechanical properties, and high ionic conductivity. In this talk, we introduce the use of novel, stiff/glassy nanostructured polyanion particles, composed of polyanion miktoarm star copolymers of poly(styrene-4-sulfonyltrifluoromethylsulfonyl) imide lithium, PSTFSILi, arms that are complement to longer ion conducting poly(ethylene oxide), PEO, arms, (PSTFSILi)_n(PEO)_n, where $n \approx 22$, attached to a poly(divinylbenzene), PDVB, crosslinked core as additives to liquid, oligomeric poly(ethylene oxide), PEO, electrolytes for the synthesis of SI-SPEs that are single-ion by design while exhibit an unparalleled combination of high shear modulus and Li-ion conductivity. Key to their performance is the morphology that stems from the ability of the (PSTFSILi)_n(PEO)_n nanoparticles to homogeneously disperse within the liquid PEO electrolyte, allowing the development of a highly interconnected network of pure liquid PEO and the profound effect of mikto arm architecture on the degree of ion dissociations that promotes high ionic conductivity.

Acknowledgments

This research has been co-financed by the European Union and Greek national funds through the Operational Program Competitiveness and innovation, under the call RESEARCH –CREATE –INNOVATE (project code: T1EΔK-02576, MIS5033805)



Ευρωπαϊκή Ένωση
Ευρωπαϊκό Ταμείο
Περιφερειακής Ανάπτυξης



Με τη συγχρηματοδότηση της Ελλάδας και της Ευρωπαϊκής Ένωσης

ΕΠΑνεΚ 2014–2020
ΕΠΙΧΕΙΡΗΣΙΑΚΟ ΠΡΟΓΡΑΜΜΑ
ΑΝΤΑΓΩΝΙΣΤΙΚΟΤΗΤΑ
ΕΠΙΧΕΙΡΗΜΑΤΙΚΟΤΗΤΑ
ΚΑΙΝΟΤΟΜΙΑ



Phase evolution of $V_{1-x}Fe_xO_2$, ($x=0, 0.5, 0.75, 1.0$ %) system as a function of temperature

D.K. Manousou^{*}, S. B. Atata, M. Calamiotou, S. Gardelis

Section of Condensed Matter Physics, Department of Physics, National and Kapodistrian University of Athens, Panepistimioupolis, Zografos, 15784 Athens, Greece

Y. J. Sohn^a, K. Friese^{b,c}

^a Institute of Energy and Climate Research IEK-1, Forschungszentrum Jülich GmbH, 52425, Jülich, Germany

^b Jülich Centre for Neutron Science-2 and Peter Grünberg Institute-4 (JCNS-2/PGI-4), Forschungszentrum Jülich GmbH, 52425 Jülich, Germany

^c Institute of Crystallography, RWTH Aachen University, 52066 Aachen, Germany

Vanadium dioxide (VO_2) is a strongly correlated material that has attracted much attention over the last years, as it exhibits a remarkable Metal-Insulator Transition (MIT) at $T_{MIT} \approx 68^\circ\text{C}$, which is accompanied by a reversible Structural Phase Transition (SPT) between the monoclinic (M1) insulating phase and high-temperature rutile (R) metallic phase [1]. At T_{MIT} , a dramatic change of the electrical resistance and a strong modification of the optical transmittance in the near infrared region take place. Displacing T_{MIT} at lower or higher values is a very challenging issue. The main method that has been widely investigated is the introduction of carriers or strain by elemental doping. High valence dopants (Nb^{5+} , Mo^{6+} , W^{6+}) is expected to reduce the T_{MIT} while low valence dopants (Al^{3+} , Cr^{3+} , Fe^{3+}) is expected to increase it [2-4]. Up to now the phase diagram of the $V_{1-x}Fe_xO_2$ system remains controversial, especially in the low concentration region $x \leq 1\%$.

We have investigated the phase evolution of $V_{1-x}Fe_xO_2$, ($x=0, 0.5, 0.75, 1.0$ %) system by in-situ X-Ray Powder Diffraction (XRPD) and Diffuse Reflectance in infrared region in the temperature range $25-90^\circ\text{C}$ to resolve the unclear characteristics of the phase diagram in the low concentration region. The XRPD patterns have been analysed by the Le Bail method using the JANA2006 software [5]. The appearance of the insulating M1 and the metallic R as well as the intermediate triclinic (T) and monoclinic (M2) phases could be monitored in the above temperature range while diffuse reflectance measurements as a function of temperature showed the MIT. The phase diagram of the $V_{1-x}Fe_xO_2$ system in the low concentration region (Fig.1(a)), could be thus unambiguously resolved. We have also observed that the stabilized by Fe dopant intermediate M2 and T phases have been vanished after further annealing the samples under N_2 /vacuum at high temperature 800°C (Fig.1(b)). The results will be discussed in respect to Vanadium – Oxygen (V-O) defects [6].

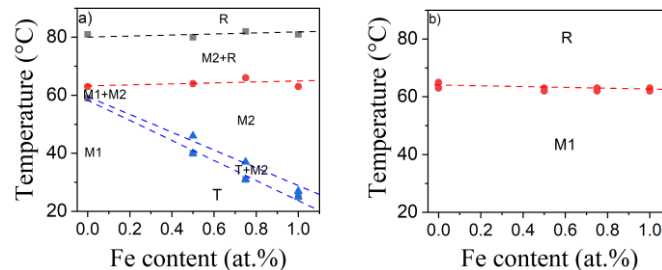


Figure 1: Phase diagram of $V_{1-x}Fe_xO_2$, ($x=0, 0.5, 0.75, 1.0$ %) before (a) and after (b) annealing under N_2 /vacuum at 800°C .

References

- [1] Z. Tao et al, Phys. Rev. Lett. 109, 166406, (2012).
- [2] R. Zhang et al, Ceram. Int. 42, 0272-8842, (2016).
- [3] J.-L. Victor et al, J. Phys. Chem. Lett. 12, 7792-7796, (2021).
- [4] E. Strelcov et al, Nano Lett. 12, 6198–6205 (2012).
- [5] V. Petricek et al, Z. Kristallogr. 229(5), 345-352 (2014).
- [6] S. Joshi et al, Sci. Rep. 10, 17121 (2020).

* dimmanous@phys.uoa.gr

Advanced photonic processes for low-cost and safe perovskite-based energy storage devices

A. Kostopoulou^{a,*}, K. Brintakis^a, D. Vernardou^b, E. Stratakis^{a,c}

^a *Institute of Electronic Structure and Laser, Foundation for Research and Technology - Hellas, Heraklion, 71110, Crete, Greece*

^b *Department of Electrical & Computer Engineering, School of Engineering, Hellenic Mediterranean University, Heraklion, 710 04, Crete, Greece*

^c *Physics Department, University of Crete, Heraklion, 710 03 Crete, Greece*

Metal halide perovskites have been recently proposed as promising anode materials for energy storage applications.^{1,2} Despite their quite important electrochemical characteristics, all perovskite-based anodes are synthesized at high temperatures (90–150 °C) and with reaction durations of the order of tens of hours. In this work, we present perovskite materials synthesized with room temperature, simple and fast approaches for high-performance and stable electrodes for Li-air batteries. Hexagonally shaped nanocrystals capped with ligands³ and ligand-free microcubes⁴ synthesized with re-precipitation based protocols will be compared according to their storage capacity and stability.

Specifically, it is shown that the electrodes incorporating the ligand-free microcubes present outstanding stability at the same time with high specific capacity compared to the ligand-capped nanoparticulate system. These could be attributed to the high crystal quality of the materials and thus enhanced electrical conductivity, even under operation with an aqueous electrolyte. The large interfacial area between the perovskite material and the electrolyte along with the increase of the active sites on the exposed microcubes facets favor the Li ion intercalation. In addition, the absence of capping ligands contributes further to the enlargement of contact area and facilitates the ion penetration compared to ligand capped nanocrystals. The good crystallinity of the microcubes enhances the Li-ion intercalation and the electron transportation. The microcubes performance is the best among all the anodes utilizing metal halide perovskite nanostructures, reported to date.

We also discuss the photo-induced processes used for the coverage of the perovskite storage material in order to increase the stability of the anodes or that used for conjugation of perovskite nanocrystals with 2D materials in order to obtain anodes for Zn-air batteries. [5] The role of the shape and size of the metal halide perovskites, but also the conjugation with the 2D materials in the performance and the stability of the anodes will be discussed. The photo-induced deposition of the TiO₂ layer found that was crucial for the stability of the anodes in all the tested anodes

References

- [1] Kostopoulou et al., *Journal of Materials Chemistry A* **6**, 9765 (2018).
- [2] Kostopoulou et al., *Nanophotonics* **8**, 1607 (2019).
- [3] Kostopoulou et al., *Nanoscale* **11**, 882 (2019).
- [4] Kostopoulou et al., *Journal of Power Sources Advances* **3**, 100015 (2020).
- [5] Kostopoulou et al., *Nanomaterials* **10**, 747 (2020).

Acknowledgments

FLAG-ERA Joint Transnational Call 2019 for transnational research projects in synergy with the two FET Flagships Graphene Flagship & Human Brain Project - ERA-NETS 2019b (PeroGaS: MIS 5070514).

* akosto@iesl.forth.gr

Mechanochemical synthesis, processing and printability of $\text{La}_{1-x}\text{Sr}_x\text{Ti}_{1-y}\text{Mn}_y\text{O}_{3\pm\delta}$ perovskites as mixed ion-electron conducting (MIEC) materials

L. Zouridi^{1,2*}, E. Gagaoudakis², E. Mantsiou², A. Vourros³, J. Garagounis³,
G.E. Marnellos^{3,4}, V. Binas^{1,5**}

1 Department of Materials Science and Technology, University of Crete, Herakleion, Greece;
2 Institute of Electronic Structure and Laser, Foundation for Research and Technology-Hellas;
3 Chemical Process & Energy Resources Institute, Centre for Research & Technology Hellas,
Thessaloniki, Greece; *4 Department of Mechanical Engineering, University of Western*
Macedonia, Kozani, Greece; *5 Department of Physics, University of Crete, Herakleion, Greece*

Mixed ion-electron conductors (MIEC) have been studied in the past decades as electrodes for solid state electrochemical devices and as active materials for heterogeneous catalytic reactions, most notably in the high temperature regime ($> 900^\circ\text{C}$). Due to their high electronic and oxygen ion (O^{2-}) conductivity, MIEC metal oxides have been proposed and employed in a variety of applications including gas separation membranes, solid state batteries, solid oxide cell electrodes, and gas sensors. Perovskite metal oxide materials with a general formula of ABO_3 exhibit such conductive properties, with notable examples such as SrTiO_3 . Additionally, in the field of solid oxide fuel cells and electrolysis cells (SOFC/SOEC) mixed oxide perovskite MIECs such as LaMnO_3 and Sr-doped derivatives have been extensively utilized as oxygen/air electrodes for the oxygen reduction reaction of molecular oxygen to oxide ion.

Conventional synthesis and deposition methods of such ceramic oxides for fabrication of solid state devices include sol-gel, solvothermal, and combustion synthesis, along with slot casting, screen-printing, chemical vapour deposition and electrodeposition, respectively. However, novel solvent-free synthetic routes of high yields, low toxicity and lower energy consumption, as well as contact-less direct deposition have been reported in recent years, in order to address scalability, cost reductions and sustainability of the manufacturing process.

In this work we present our most recent results on the solvent-free mechanochemical synthesis of a series of oxide perovskite ceramics, Sr-doped Lanthanum Manganates and Titanates with a general formula of $\text{La}_{1-x}\text{Sr}_x\text{Ti}_{1-y}\text{Mn}_y\text{O}_{3\pm\delta}$ (with $x, y = 0, 0.5$ or 1), and their processing for ink formulation towards thin film deposition via inkjet printing. The structure and morphology of powdered materials have been physicochemically characterized (XRD, SEM, EDS). Additionally, powders were processed into colloidal inks in order to examine their printability by means of viscometry, particle size analysis (via DLS), surface tension characteristics and interfacial behaviour (via contact angle) on different substrates. Furthermore, deposition of synthesized materials as colloidal inks was achieved by inkjet printing, utilizing a Dimatix® Fujifilm printer, after the optimization of deposition parameters. For comparison, some conventional deposition techniques have been used, depending on the substrate (spin-coating, and/or screen-printing). The printed ceramic thin films were processed by thermal sintering and characterized physicochemically in order to define their structural and morphological properties. Finally, printed devices of MIEC perovskite ceramics were assessed for their applicability as electrodes in SOFC and gas sensing devices.

Acknowledgements This research was supported by “NSRF-EPAnEK” proposals “SMARTPACK” (T2EAK-02373), “LIGBIO-GASOFC” (T1EAK-01894) and “NANOLEFINS” (TAEAK-06169).

*l.zouridi@iesl.forth.gr

** binasbill@iesl.forth.gr

Integration of two-dimensional materials-based perovskite solar panels into a stand-alone solar farm

George Viskadouros, Konstantinos Rogdakis, Ioannis Kalogerakis, Emmanuel Spiliarotis and Emmanuel Kymakis

Department of Electrical & Computer Engineering, Hellenic Mediterranean University, Heraklion, Crete, Greece.

kymakis@hmu.gr

During the past decade, there was intensive research on the development of perovskite solar cells (PSCs), which have emerged as an alternative efficient energy harvester for both IoT devices and solar farms. The power conversion efficiency (PCE) of PSCs has rapidly increased and is now approaching the state-of-the-art PCE of 26.1%¹ obtained by crystalline-silicon PVs. However, this impressive PCE obtained on small-area cells and in laboratory conditions should be also valid to large-area PV panels in real outdoor conditions. Interface engineering, using solution processable 2D materials (e.g., graphene and transition metal dichalcogenides) is an effective approach to increase the readiness of this technology for manufacturing. The incorporation of the 2D materials improves the charge dynamics of the interfaces and most importantly protects the perovskite layer against diffusion of external agents, such as oxygen and moisture and the metal ion migration². In this context, the Graphene Flagship partners University Rome Tor Vergata, BeDimensional S.p.A, Greatcell and Hellenic Mediterranean University demonstrated the validity of this technology through the entire value chain, from materials development, perovskite modules and panels fabrication and their integration in an autonomous solar farm, to outdoor field tests, and assessment of the real energy production output. The main validation of the proposed approach is the realization of an autonomous solar farm, consisting of 5m² perovskite PV panels in the HMU campus at Crete³. A continuous monitoring of the solar farm was performed through in-house developed maximum power point trackers, coupled with a correlation of the environmental conditions, recorded by a weather station, with the outdoor performance of farm. The assembled solar farm delivered peak power exceeding 260W, proving the scalability of the proposed technology. The energy production of the solar farm was monitored for 12 months, demonstrating a remarkable 20% reduction (T_{80}) of the PV performance over 8 months of operation. Moreover, the solar farm's electrical characteristics were monitored as a function of temperature and light intensity. The data analysis demonstrated that the perovskite panels enabled by 2D materials are promising for outdoor operation at elevated temperatures, such as in high-irradiance global locations.

References

- [1] <https://www.nrel.gov/pv/assets/images/efficiency-chart.png>
- [2] Bellani, et al. Chem. Soc. Rev. 50, 11870– 11965 (2021)
- [3] Sara Pescetelli, Antonio Agresti, George Viskadouros, et al. Integration of two-dimensional materials-based perovskite solar panels into a stand-alone solar farm, Nature Energy (2022)10.1038/s41560-022-01035-4.



Figure 1: A photograph of the solar farm

Authors: Rafail Frantzeskakis, John Van Dyke, Sophia Economou and Edwin Barnes

Title: Time-crystalline behavior in central-spin models with Heisenberg interactions

Abstract:

Time crystals, non-equilibrium phases of quantum matter induced by periodic driving and many-body interactions, have been experimentally realized recently in trapped ion systems and superconducting circuits [1,2]. Such phases can also occur in solid-state spin systems, including ensembles of NV centers [3] or nuclear spins [4] in diamond and quantum dot spin chains [5-7].

Here, we show how to create time crystal phases in central-spin models with Heisenberg interactions, which can describe a single dot or defect system or star-shaped dot arrays. Such interactions are generally present in electron-nuclear spin systems due to hyperfine couplings [8,9]. We show how to use time crystal physics to stabilize multi-qubit short-range correlated states in the presence of Heisenberg interactions by using either magnetic field gradients or additional pulses on the central spin. Both approaches effectively convert the Heisenberg interactions into Ising form [5,10], enabling the subharmonic response characteristic of time crystalline behavior to emerge. Our results can be used to design new schemes for state preservation or robust quantum information processing in quantum dot and defect systems that exploit periodic driving and many-body interactions [7].

References:

- [1] Zhang Jiehang, et al. "Observation of a discrete time crystal." *Nature* 543.7644 (2017): 217-220.
- [2] Mi Xiao, et al. "Time-crystalline eigenstate order on a quantum processor." *Nature* 601.7894 (2022): 531-536.
- [3] Choi Soonwon, et al. "Observation of discrete time-crystalline order in a disordered dipolar many-body system." *Nature* 543.7644 (2017): 221-225.
- [4] Randall J., et al. "Many-body-localized discrete time crystal with a programmable spin-based quantum simulator." *Science* 374.6574 (2021): 1474-1478.
- [5] Barnes Edwin, John M. Nichol, and Sophia E. Economou. "Stabilization and manipulation of multispin states in quantum-dot time crystals with Heisenberg interactions." *Physical Review B* 99.3 (2019): 035311.
- [6] Qiao Haifeng, et al. "Floquet-enhanced spin swaps." *Nature communications* 12.1 (2021): 1-9.
- [7] Van Dyke John S., et al. "Protecting quantum information in quantum dot spin chains by driving exchange interactions periodically." *Physical Review B* 103.24 (2021): 245303.
- [8] Assali Lucy VC, et al. "Hyperfine interactions in silicon quantum dots." *Physical Review B* 83.16 (2011): 165301.
- [9] Pezzagna Sébastien, and Jan Meijer. "Quantum computer based on color centers in diamond." *Applied Physics Reviews* 8.1 (2021): 011308.
- [10] Li Bikun, et al. "Discrete time crystal in the gradient-field Heisenberg model." *Physical Review B* 101.11 (2020): 115303.

Magnetic field effect on the thermoelectric properties of semiconducting $\text{LaNi}_{0.2}\text{Co}_{0.8}\text{O}_3$ and metallic $\text{LaNi}_{0.7}\text{Co}_{0.3}\text{O}_3$

Z. Viskadourakis*, G. Kenanakis

Institute of Electronic Structure and Laser (IESL), Foundation for Research and Technology – Hellas (FORTH), N. Plastira 100, Vassilika Vouton, Heraklion GR 70013, Greece

J. Giapintzakis

Department of Mechanical Manufacturing, University of Cyprus, 75 Kallipoleos Ave., P.O. Box 20537, Nicosia 1678, Cyprus

The thermal transport properties for two members of the $\text{LaNi}_x\text{Co}_{1-x}\text{O}_3$ solid solution, i.e., $x = 0.2$ and $x = 0.7$, have been investigated in the absence and presence of external magnetic field. Negative magneto-thermopower is observed for the $x = 0.2$ sample, along with a reduction in thermal conductivity below 100K. On the other hand, positive magneto-thermopower is found for the $x = 0.7$ sample, whereas thermal conductivity is unaffected, resulting to a noticeable improvement of the thermoelectric figure of merit, in the low temperature regime. In both cases the observed thermoelectric behavior is explained considering the $\text{LaNi}_x\text{Co}_{1-x}\text{O}_3$ magnetic structure, which is based on $\text{Co}^{3+}/\text{Co}^{4+}$ mixed spin state configurations. It is revealed that the thermoelectric performance of cobaltites can be effectively improved by tuning their magnetic structure.

* zach@iesl.forth.gr

Skyrmions in antiferromagnets

S. Komineas*, N. Papanicolaou
University of Crete, Heraklion, Greece

P.E. Roy

Hitachi Cambridge Laboratory, Hitachi Europe Limited, Cambridge CB3 0HE, U.K.

Magnetic skyrmions are swirling configuration of the magnetic order parameter that are stable in materials with the Dzyaloshinskii-Moriya (DM) interaction. They are commonly observed in magnetic films, typically extending a few or tens of nanometers laterally, and their nontrivial topology makes them robust against perturbations. Skyrmions exhibit particle-like dynamics which, together with their small size, lead to properties that make them suitable as the constituent information carriers in memory and logic devices or memristor elements in artificial synapses for neuromorphic computing architectures.

The chiral DM interaction is crucial also for the dynamics of solitons, in addition to its role in their stabilization. We study antiferromagnetic skyrmions described via the Néel vector, that is the appropriate order parameter. In the first example [1], we show that skyrmions in chiral antiferromagnets can be traveling as solitary waves with velocities up to a maximum value that depends on the DM parameter. We calculate the traveling skyrmion configuration, as shown in Fig. 1a. The solitonic behavior of skyrmions in antiferromagnets is in stark contrast to the dynamical behavior of their ferromagnetic counterparts.

In the second example [2], we study breathing oscillations of skyrmions in the nonlinear regime, and the features of larger amplitude oscillations. We predict theoretically and observe numerically skyrmion collapse and subsequent annihilation events, as shown in Fig. 1b. The process is efficient when the skyrmion is mildly excited so that its radius initially grows, while the annihilation event of the topological texture is eventually induced by the internal breathing dynamics.

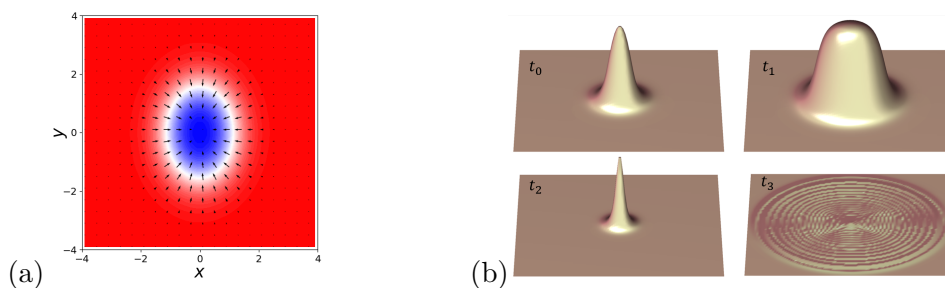


Figure 1: (a) A skyrmion traveling along the x direction represented via the projection of the Néel vector on the plane. (b) Snapshots for a skyrmion annihilation event represented via surface plots of the perpendicular component of the Néel vector.

References

- [1] S. Komineas and N. Papanicolaou, SciPost Phys. 8, 086 (2020).
- [2] S. Komineas and P. E. Roy, arXiv:2203.04157 (2022).

*komineas@uoc.gr

Fe-based Superconductors: Structural Phase Transitions Tuned by Electronic Fluctuations

Myrsini Kaitatzi^{1,2,*}, Alexandros Deltsidis^{1,2}, Aleksandr Missiul³, Emil S. Bozin⁴,
Alexandros Lappas¹

¹ *Institute of Electronic Structure and Laser, Foundation for Research and
Technology-Hellas, Vassilika Vouton, 71110 Heraklion, Greece*

² *Department of Materials Science & Technology, University of Crete, Voutes,
71003 Heraklion, Greece*

³ *CELLS - ALBA synchrotron, 08290 Cerdanyola del Vallès, Catalonia, Spain*

⁴ *Condensed Matter Physics and Materials Science Department, Brookhaven
National Laboratory, Upton, NY 11973, USA*

In-depth studies elaborating on hybrid iron chalcogenide superconductors are of a great interest to the condensed matter physics community due to their intriguing behaviors arising from structural modifications and electronic correlations upon intercalation. Intercalation of the 8 K FeSe superconductor with organic molecules leads to a substantial enhancement of the critical temperature (T_c) up to 42 K [1]. In effect, in such hyper-expanded lattice superconductors subtle local distortions in their nanoscale environment are introduced (Fig.1). Our team has developed solvothermal synthesis pathways for $\text{Li}_x(\text{C}_5\text{H}_5\text{N})_y\text{Fe}_{2-z}\text{Se}_2$ intercalated samples with the purpose to investigate them with state-of-the-art synchrotron science tools. In one hand, high Q-resolution X-ray diffraction, over a broad temperature range (10-300 K) is utilized to shed light on possible structural phase transitions, taking place at the average level when the materials cross the T_c . Rietveld analysis suggests that their high- T_c relates to the tetragonal ThCr_2Si_2 -type structure. On the other hand, complementary high-energy synchrotron X-rays enable a wide-Q field of view, appropriate for total scattering insights [2]. When combined with pair distribution function (PDF) analysis, correlated local distortions, pertaining to the electronic active Fe-selenide layers, are identified as the outcomes of the electron donor moieties, accommodated in the interlayer space. The structural insights acquired from these studies are highly valuable in an effort to draw materials-design principles that help to optimize the electronic structure for attaining even higher T_c .

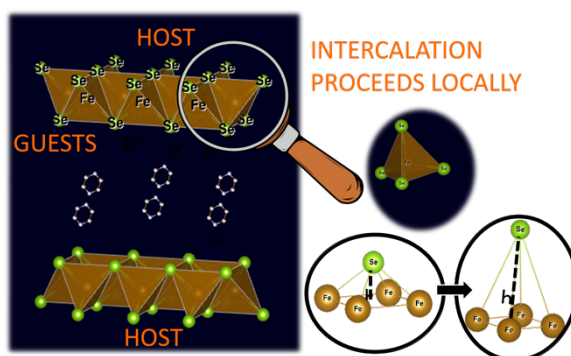


Figure 1: Interplay among lattice distortions doping and superconductivity.

References

- [1] A. Krzton-Maziopa et al., *J. Phys.: Condens. Matter* **30** 243001 (2018).
- [2] I.C. Berdiell et al., *Inorg. Chem.* **61**, 4350 (2022).

* myrsinik@iesl.forth.gr

COMSOL simulations of assemblies of sub-millimeter NdFeB -based magnets

O. Manos¹, A. Sigalos¹, D. Niarchos^{1,2}

¹Amen New Technologies, Athens, Greece

²INN, NCSR Demokritos, Athens, Greece

A. Lixanrdu and C. Vogler

Huawei Technologies Austria GmbH, Vienna, Austria

Magnetic measuring offers numerous advantages over other positioning and measuring methods for industrial applications allowing the measurement of a distance with high accuracy attributed to the magnetic field's irrelevance to the non-magnetic disturbances such as dirt, dust, or liquid droplets. A typical measuring solution consists of a measuring head with a magnetic field sensor and a magnetic linear scale composed of a highly accurate pattern of magnetic North(N) and South(S) poles. Via counting the number of NS alternations the distance is determined with high accuracy and sensitivity.

Ferrite-based micromagnets are the building block materials of the current state-of-the-art magnetic scale applications presenting a favorable compromise between the desired properties and costs. However, these structures provide the lowest magnetic field strength of all permanent magnetic materials with a direct consequence on the sensitivity of magnetic scale applications. In addition, the current magnetic scale fabrication processes aim to fabricate discreet micromagnets involving several fabrication steps which complicate the production procedures and increase the production time and costs significantly.

We propose the replacement of Ferrite-based micromagnets with NdFeB ones which deliver up to 20 times stronger magnetic field per unit volume leading to enhanced sensitivity and accuracy of these structures. Our new generation NdFeB-based magnetic scales present smaller pole pitch, improved tolerance, and position accuracy compared to their Ferrite-based counterparts. Simulated results using a COMSOL software will be compared with experimental data.

Here some simulations

Figure 1. a) The simulated B_z profile contributions of our home-built magnetizer. b) B_z profile patterned on the unmagnetized NdFeB rod.

Metal oxides and organic molecules for interface engineering in high performance polymer solar cells

L.C. Palilis,^{1,*} E. Polydorou,² M. Verouti,^{1,2} A. Soultati,² K.-K. Armadorou,² A. Verykios,² P.-P. Filippatos,^{2,3} K. Turlouki,² M. Tountas,⁴ S. Panagiotakis,² F. Nunzi,⁵ A. Chroneos,³ A. Charisiadis,⁶ V. Nikolaou,⁶ M. Papadakis,⁶ G. Charalabidis,⁶ E. Nikoloudakis,⁶ E. Kymakis,⁴ A.G. Coutsolelos,⁶ F.D. Angelis,⁵ M. Nazeeruddin,⁷ P. Argitis,² D. Davazoglou,² A. Fakharuddin,⁸ A.R.B.M. Yusoff⁹ and M. Vasilopoulou²

¹ *Department of Physics, University of Patras, Rio – Patras, 26504, Greece*

² *INN, NCSR Demokritos, Aghia Paraskevi - Athens, 26504, Greece*

³ *Faculty of Engineering, Environment and Computing, Coventry University, Priory Street, Coventry CV1 5FB, United Kingdom*

⁴ *Department of Electrical & Computer Engineering, Hellenic Mediterranean University, Estavromenos, Heraklion, Crete GR-71410, Greece*

⁵ *Department of Chemistry, Biology and Biotechnology University of Perugia Via Elce di Sotto 8, Perugia 06123, Italy*

⁶ *Department of Chemistry, University of Crete, Laboratory of Bioinorganic Chemistry, Voutes Campus, Heraklion, Crete 70013, Greece*

⁷ *Institute of Chemical Sciences and Engineering, École Polytechnique Fédérale de Lausanne (EPFL), Rue de l'Industrie 17, Sion CH-1951, Switzerland*

⁸ *Department of Physics, University of Konstanz, 78457 Konstanz, Germany*

⁹ *Department of Chemical Engineering, Pohang University of Science and Technology (POSTECH), Pohang, Gyeongbuk 37673, Republic of Korea*

Polymer solar cells (PSCs) are one of the most attractive solar cell technologies as they combine the controlled functionalization and optoelectronic properties of conjugated polymers with solution processability, flexibility and low cost. One of the most critical components that affects device efficiency and stability is the functionality of the interfaces between the electrodes and the organic layers employed. To this regard, various interfacial engineering strategies have been exploited to control charge injection/extraction, transport and recombination, and improve device performance. [1] Herein, we investigate in detail representative inorganic and organic compounds, namely metal oxides such as fluorine-doped tantalum pentoxide [2] and organic small molecules such as functionalized boron-dipyromethenes (BODIPYs) [3], that can be deposited at low temperatures or processed directly from orthogonal solvents (with regard to conjugated polymers) as highly effective interfacial layers for improved hole and electron transfer/extraction, respectively, in PSCs. As a result, significant improvements in both efficiency and stability of bulk heterojunction PSCs based on various commercially available organic semiconductors was achieved as a result of improved interfacial energetic level alignment facilitating charge transport/extraction.

References

[1] L.C. Palilis, A. Verykios, A. Soultati, E. Polydorou, P. Argitis, D. Davazoglou, A.R. bin M. Yusoff, M. Vasilopoulou and M.K. Nazeeruddin, *Advanced Energy Materials* **10**, 2000910 (2020).

[2] E. Polydorou, M. Verouti, A. Soultati, K.-K. Armadorou, A. Verykios, P.-P. Filippatos, G. Galanis, K. Turlouki, N. Kehayias, I. Karatasios, N. Kuganathan, A. Chroneos, V. Kilikoglou, L.C. Palilis, P. Argitis, D. Davazoglou, A. Fakharuddin, A.R.B.M. Yusoff and M. Vasilopoulou, *Organic Electronics*, 2022, DOI: 10.1016/j.orgel.2022.106607.

[3] A. Soultati, F. Nunzi, A. Fakharuddin, A. Verykios, K.K. Armadorou, M. Tountas, S. Panagiotakis, E. Polydorou, A. Charisiadis, V. Nikolaou, M. Papadakis, G. Charalabidis, E. Nikoloudakis, K. Yanakopoulou, X. Bao, C. Yang, A.D.F. Dunbar, E. Kymakis, L.C. Palilis, A.R.B.M. Yusoff, P. Argitis, A.G. Coutsolelos, F.D. Angelis, M. Nazeeruddin and M. Vasilopoulou, *Advanced Materials Interfaces*, 2022, DOI: 10.1002/admi.202102324.

* **lpalilis@physics.upatras.gr**

'Breathing' 2D Hybrid Double Halide Perovskites consisting of non-toxic elements

Maria Maniadi ^a, Bruno Cucco ^b, Xiaobin Wang ^c, Shunran Li ^c, Apostolos Pantousas ^a, Mikaël Kepenekian, ^b, Peijun Guo ^c, George Volonakis ^b, Constantinos C. Stoumpos ^a

^a Department of Materials Science and Technology, University of Crete, Heraklion 70013, Greece

^b Univ Rennes, ENSCR, INSA Rennes, CNRS, ISCR (Institut des Sciences Chimiques de Rennes), UMR 6226, France

^c Department of Chemical and Environmental Engineering, Yale University, New Haven, Connecticut 06511, United States

Email: marimani99@materials.uoc.gr

Lead halide perovskites AMX_3 ($A^+ = Cs, CH_3NH_3$ or $HC(NH_2)_2$, $M^{+2} = Pb, Sn$ or Ge and $X^- = Cl, Br$ or I) have taken the semiconductor field by storm in the last decade, guided by the immense development of efficient photovoltaics that have reached power-conversion efficiencies $>25\%$.^[1] A notable class among them is dimensionally reduced two-dimensional (2D) perovskites that offer much greater sensitivity to moisture that boosts the devices' performance, in addition to the exotic photo physics they possess relative to their stable excitonic features at room temperature. Further branching out in the class of 2D perovskites, recent reports have shown that it is possible to stabilize double 2D perovskites consisting of two metal ions in an ordered periodic arrangement.^[2] These compositions due to the absence of lead atoms have demonstrated a variety of interesting physical qualities which in combination with their low toxicity make them an alternative direction towards the discovery of novel inorganic semiconductors.

In this work, we demonstrate that 2D hybrid double halide perovskites based on mixed metal Ag-In, Ag-Bi and Ag-Sb compositions, with a general chemical formula $(4AMP)_2AgM^{III}Br_8 \cdot 0.5H_2O$, ($4AMP^{2+}$ is the dication of 4-aminomehtyl piperidine, M^{III} is In, Sb or Bi), can be obtained in good yield and high chemical purity using low-temperature wet chemistry. The new compounds, which possess the Ruddlesden-Popper structure-type, have been characterized by single-crystal and powder X-ray diffraction and their optical properties at room temperature were determined (Figure 1). The compounds possess a strong optical absorption in the visible likely deriving from a slightly indirect band gap transition. Another feature that these compounds possess, is that they are "breathing". All three compounds contain 0.5 H_2O molecules in the unit cell, and can be dehydrated reversibly with thermal treatment and water vapor exposure, respectively. Solid solutions with a combination of three different metals, Ag-Sb-Bi, have also been obtained and characterized. The above properties render these mixed-metal 2D hybrid halide perovskites suitable for integration so much into environmentally friendly optoelectronic devices, as much in small molecule sensing in their dehydrated form.

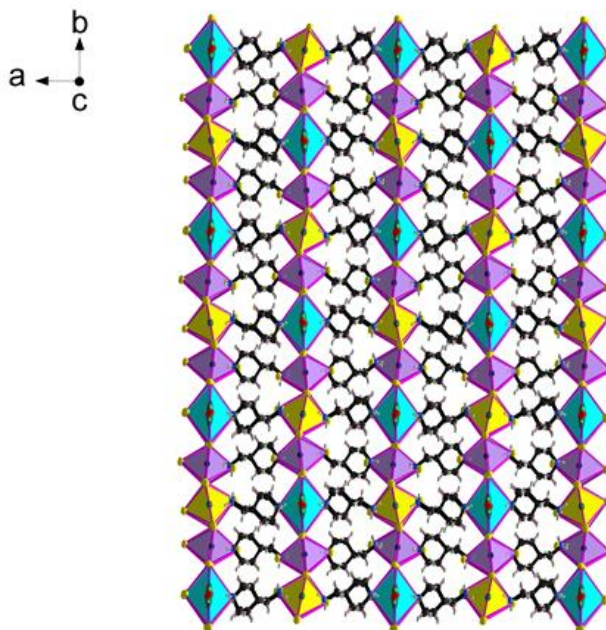


Figure 1: Representative layer stacking of a hybrid 2D double halide perovskite $(4AMP)_2AgM^{III}Br_8 \cdot 0.5H_2O$. Yellow octahedra are Ag-atom centered, blue ones are disordered Ag atom centered and purple polyhedra consists are $M(III)$ -atom centered. The organic cations interdigitate between the two-dimensional sheets in quintuple conformation ordering

1. Aryal, U.K., et al., *2D materials for organic and perovskite photovoltaics*. Nano Energy, 2022. **94**: p. 106833.
2. Li, X., et al., *Bismuth/Silver-Based Two-Dimensional Iodide Double and One-Dimensional Bi Perovskites: Interplay between Structural and Electronic Dimensions*. Chemistry of Materials, 2021. **33**(15): p. 6206-6216.

On the effect of SOI substrate in silicon nitride resistance switching MIS structures

A.E. Mavropoulis^{a,*}, N. Vasileiadis^{a,b}, T.Tsiamis^a, C. Theodorou^c, L. Sygellou^d, P. Normand^a, G. Ch. Sirakoulis^b, P. Dimitrakis^{a,*}

^a Institute of Nanoscience and Nanotechnology, NCSR “Demokritos”, Ag. Paraskevi 15341, Greece

^b Department of Electrical and Computer Engineering, Democritus University of Thrace, Xanthi 67100, Greece

^c Univ. Grenoble Alpes, Univ. Savoie Mont Blanc, CNRS, Grenoble INP, IMEP-LAHC, 38000 Grenoble, France

^d Institute of Chemical Engineering Sciences, FORTH/ICE-HT, Patras 26504, Greece

Several resistive memory technologies (RRAMs) are prominent, but few are fulfilling the requirements for CMOS integration and meet the commercialization standards. SiN_x was found to exhibit competitive resistance switching (RS) properties and attractive SiN-based RRAM devices have been recently demonstrated [1-3]. In the majority of the publications, the RS SiN_x structures are metal-insulator-semiconductor (MIS), meaning that the bottom electrode was n⁺⁺ Si. In this work, the fabrication and electrical characterization of a fully compatible CMOS process on SOI substrate of 1R silicon SiN-based resistance switching MIS devices is presented. The RS characteristics are compared with the same devices previously fabricated on bulk silicon. The scope of this work is to benchmark the use of thin SOI film as bottom electrode compared to bulk Si substrates in single MIS RS cells (1R) utilizing low-frequency noise, DC and AC measurements.

Typical round sweep I-V curves are presented in Fig. 1, where the current switching is evident due to the formation (+eV, SET)/ destroy (-eV, RESET) of a conductive filament made of nitrogen vacancies. The series resistance of the bottom electrode was found to be higher on SOI compared to Si wafer, while the SOI substrate devices exhibited self-compliance characteristics as revealed by I-V voltage sweeps and AC impedance measurements. Device-to-device variability of SET and RESET voltages suggest better uniformity for SOI substrates. Low-frequency noise spectral analysis indicated that there is no additional group of characteristic traps related to the SOI substrate.

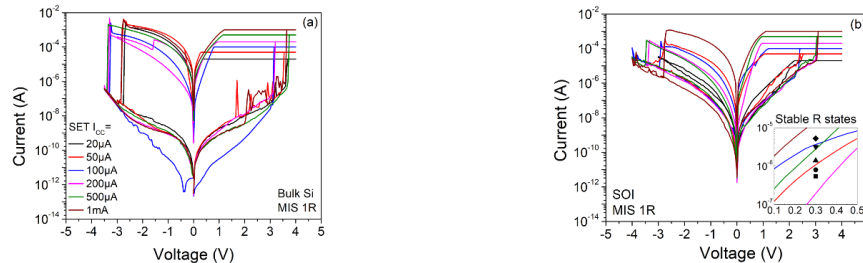


Figure 1: I-V switching characteristics at different I_{CC} for a) bulk Si substrate, b) SOI substrate 1R cells. c) SET/RESET voltage statistics.

Acknowledgements

This work was supported in part by the research projects “3D-TOPOS” (MIS 5131411)

References

- [1] N. Vasileiadis, et al., IEEE Trans. on Nanotechnology 20 (2021): 356-364
- [2] N. Vasileiadis, et al., Materials 2021, 14, 5223
- [3] N. Vasileiadis, et al., Chaos, Solitons & Fractals 153 (2021): 111533

* a.mavropoulis@inn.demokritos.gr

Electrospinning of TiO₂ based semiconductor nanofibers with enhanced photocatalytic properties

P. Pascariu¹, L. Georgescu², E. Koudoumas² and M.P. Suchea^{2,3*}

¹*“Petru Poni” Institute of Macromolecular Chemistry, 700487, Iasi, Romania*

²*Center of Materials Technology and Photonics, School of Engineering, Hellenic Mediterranean University, Heraklion, Crete, 71410, Greece*

³*National Institute for Research and Development in Microtechnologies (IMT-Bucharest), Bucharest, 023573, Romania*

The photocatalytic materials are important for various applications, such as antifouling, self-cleaning, antifogging and antibacterial actions as well as deodorization or decomposition or removal of pollutant, applications requiring the development of a broader range of smart functional materials. The most widely used semiconductor photocatalysts are TiO₂ and ZnO, because of their high photosensitivity, photochemical stability, large band gap, strong oxidizing power and non-toxic nature. In particular, anatase TiO₂ has been reported as the most extensively used semiconductor photocatalyst for industrial applications and pollution clean-up since 1970s. The successful exploitation of such photocatalysts requires the development of appropriate techniques for controlling their size, morphology, structural and surface characteristics, in an effort to enhance their photochemical response to visible/solar illumination.

This presentation concerns the development and optimization of inorganic nanocomposite fibrous materials, fabricated by electrospinning followed by electrospinning-calcination and suitable for nano-environmental applications, having high photocatalytic activity against various water pollutants in the presence of ultraviolet and visible light. These fabrication methods are of low cost and easy to scale up and can lead to materials having the photocatalyst immobilized in a felt-like structure exhibiting remarkable photocatalytic activity for the degradation of a large number of common water pollutants. At the same time, these felt-like structures are easy to recover and rejuvenate for re-use. In this work, the fabrication of pure and doped TiO₂ membranes will be presented. Moreover, characterization of the fabricated nanocomposites will be shown, such as X-ray diffraction (XRD), scanning electron microscopy (SEM), Raman spectroscopy, ultraviolet–visible spectroscopy (UV–vis) as well as their involvement in the photocatalytic degradation of common water pollutants.

Acknowledgements: PP contribution to this work was partially supported by a grant of the Romanian Ministry of Research, Innovation and Digitization, CNCS/CCCDI – UEFISCDI, project number PN-III-P1-1.1-TE-2019-0594, within PNCDI III. M.P.S. contribution was partially financed by the Romanian Ministry of Research, Innovation and Digitalisation through „MICRO-NANO-SIS PLUS” core Programme.

Superhydrophilic low temperature TiO₂ ultra thin films deposited on CSP mirrors by magnetron sputtering

N. Mouti*, A. Kaidatzis, K. Giannakopoulos

Institute of Nanoscience and Nanotechnology, N.C.S.R. "Demokritos", Athens, Greece

Soiling of mirrors increases concentrated solar thermal power (CSP) maintenance costs. Previous approaches with self cleaning coatings have failed to fully address the challenges posed by the surfaces' nature and interaction with their environment, such as desert dust [1]. During the present work, we prepare by magnetron sputtering and characterize TiO₂ thin films on Guardian Glass CSP mirrors [2], in order to take advantage of their superhydrophilic self cleaning character. Hydrophilicity has been shown to be a purely surface property after being tested in a variety of film thicknesses. We report here results from thin films of various thicknesses, the best of which was at about 8 nm, with uniform and stable mirror coverage, as seen in optical profilometry. Aiming at low deposition temperatures for fabrication cost reasons, we managed to reach 120° C. The contact angle we achieved was <1°, without the UV treatment that is usually needed. Because maximum mirror reflectivity is also a major requirement, we achieved up to 100 percent film transmission, as the O₂ during the sputtering process increases and the thin film's thickness decreases [1]. The superhydrophilic property and transmittance measurements of representative samples are shown below.

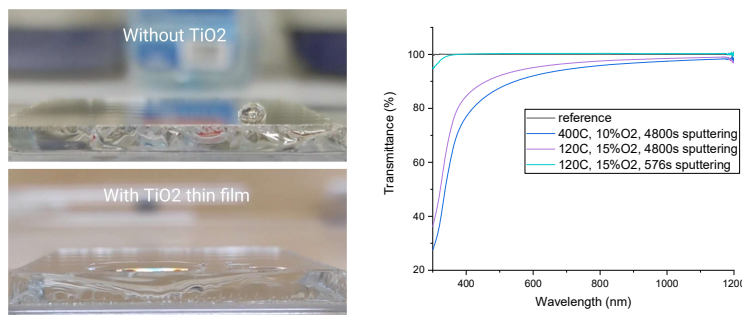


Figure 1: Demonstration of CSP mirror hydrophilicity before and after the sputtered deposition TiO₂ thin film. Transmittance UV-IR measurements of TiO₂ sputtered films.

References

- [1] P. Bellmann, F. Wolfertstetter, R. Conceição, and H. G. Silva, *Sol. Energy* **197**, 229–237 (2020)
- [2] M.-K. Lee and Y.-C. Park, *Thin Solid Films* **638**, 9–16 (2017)

Acknowledgements

Project Nano4CSP is supported under the umbrella of [SOLAR-ERA.NET](#) Cofund 2 by GSRT – General Secretariat for Research and Development (Greece), RIF – Research and Innovation Foundation (Cyprus) and FFG – Austrian Research Promotion Agency. [SOLAR-ERA.NET](#) is supported by the European Commission within the EU Framework Programme for Research and Innovation HORIZON 2020 (Cofund ERA-NET Action, N° 786483)

* n.mouti@inn.demokritos.gr

Quantum droplets in mixtures of cold atomic gases

G. M. Kavoulakis

Hellenic Mediterranean University

Self-bound, macroscopic, droplets are often observed in various physical systems, with the most familiar example being that of water droplets. Furthermore, droplets appear on microscopic length scales, as e.g., in atomic nuclei and in liquid-helium nanodroplets.

In this talk I will present results on recent experimental and theoretical work on “quantum” liquid droplets in an ultracold mixture of bosonic atoms. These are self-bound states, which become possible due to many-body effects stemming from quantum fluctuations. Quantum fluctuations, which are typically very small, become significant in this system when two different species are mixed, and the couplings for inter- and intra-component interactions are tuned appropriately.

In my talk I will first describe the basic physics of these systems. Then, I will present some recent experimental results. Finally, I will discuss the ground state and the rotational response of quasi-two-dimensional droplets which are confined in a harmonic potential, and also of quasi-one-dimensional droplets which are confined in a ring-like potential.

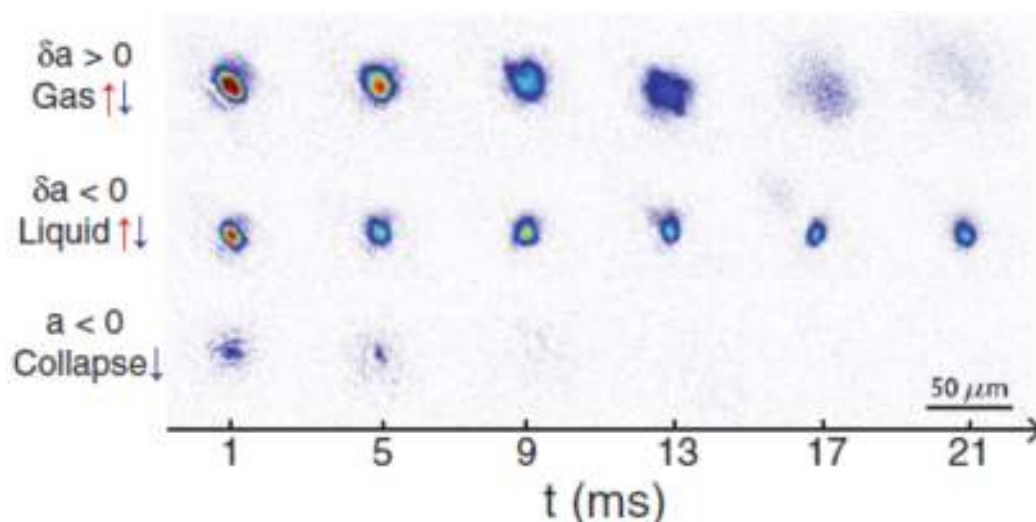


Figure 1: In situ density distribution of the atoms after the removal of the confinement. *C. R. Cabrera, L. Tanzi, J. Sanz, B. Naylor, P. Thomas, P. Cheiney, L. Tarruell, Science* **359**, 301 (2018)

Evaluation of the Tesla valve as a micromixer for Fe_3O_4 nanoparticles and contaminated water

E.G. Karvelas^a, Christos Liosis^b, Ioannis Sarris^c and T.E. Karakasidis^{a,*}

^a*Department of Physics, University of Thessaly, Greece*

^b*Department of Civil Engineering, University of Thessaly, Volos, Greece*

^c*Department of Mechanical Engineering, University of West Attica, Greece*

Plenty microfluidic applications are based on effective mixing among them water purification, where contaminated water needs to be mixed with water loaded with nanoparticles. In accordance with this, here, series of simulations are performed to succeed an effective mixing of iron oxide nanoparticles and contaminated water in the duct. The selected geometry for the simulations is the Tesla valve which is an alternative for usage as micromixer (Fig.1). In the present work, a stream loaded with Fe_3O_4 nanoparticles and a stream with contaminated water is numerically studied for various inlet velocity ratios and initial concentrations of the two streams. The Navier-Stokes equations are solved for the water flow while the discrete motion of particles is evaluated by a Lagrangian method. Outcomes are very promising since mixing efficiency reached up to 63% for $V_p/V_c=20$ under various inlet nanoparticles rates for two Tesla units (Fig. 2). Moreover, nanoparticles occupied a large percent of the height and the width of the micromixer near the common exit. In addition, the quantification of results exhibits a significant role of inlet rates to mixing efficiency for lower velocity ratio. Additionally, the crucial factor for mixing efficiency is the velocity ratio, which acquires a decisive role as increases.

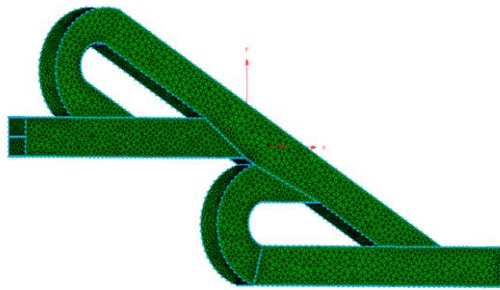


Fig. 1: Micromixer geometry with computational mesh.



Fig. 2: Distribution of nanoparticles ($D = 13.5 \text{ nm}$) into micromixer for rate equal to 1000 particles/s under $V_p/V_c = 20$

Acknowledgment: This work is supported by the research program : Enhancing ICT research infrastructure in Central Greece to enable processing of Big data from sensor stream, multimedia content, and complex mathematical modelling and simulations (MIS 5047244) which is implemented under the Action Reinforcement of the Research and Innovation Infrastructure, funded by the Operational Programme Competitiveness, Entrepreneurship and Innovation (NSRF 2014–2020) and co-financed by Greece and the European Union (European Regional Development Fund).

References

- [1] Karvelas, E.; Liosis, C.; Benos, L.; Karakasidis, T.; Sarris, I. Micromixing Efficiency of Particles in Heavy Metal Removal Processes under Various Inlet Conditions. *Water (Switzerland)* **2019**, *11* (6), 1135. <https://doi.org/10.3390/w11061135>.
- [2] Liosis, C.; Karvelas, E.; Karakasidis, T.; Sarris, I. Numerical study of magnetic particles mixing in water under an external magnetic field, *Journal of Water Supply: Research and Technology - AQUA*, 2020, *69*(3), pp. 266–275.

Artificial multiresonant sheet materials for broadband wave manipulations

O. Tsilipakos*, M. Kafesaki, E. N. Economou

Institute of Electronic Structure and Laser, FORTH, Heraklion, Crete, 70013, Greece

C. M. Soukoulis, T. Koschny

Ames Laboratory—U.S. DOE and Dept. of Physics and Astronomy, Iowa State Univ. Ames, Iowa 50011, USA

Metasurfaces, ultrathin artificial materials composed of subwavelength resonant meta-atoms, promise to replace bulky conventional optical components, offering significant technological advantages (size & weight reduction, planar fabrication) and the ability to tailor their response at will by engineering the underlying meta-atoms. However, they typically suffer from narrowband response. By judiciously combining multiple meta-atom resonances in the unit cell, we demonstrate that metasurfaces can be made to exhibit arbitrarily broadband (achromatic) response. This is exemplified by delaying broadband pulses without distortion [1], Fig. 1(a). If the supplied group delay is spatially modulated [strips of different delay τ_1, τ_2, \dots in Fig. 1(b)], achromatic wavefront manipulation can be achieved [2]. The proposed concept has been experimentally verified in GHz frequencies by a multiresonant unit cell comprising five resonant meta-atoms (three electric and two magnetic dipole resonances) on a three-metallization layer printed circuit board [3], Fig. 1(c).

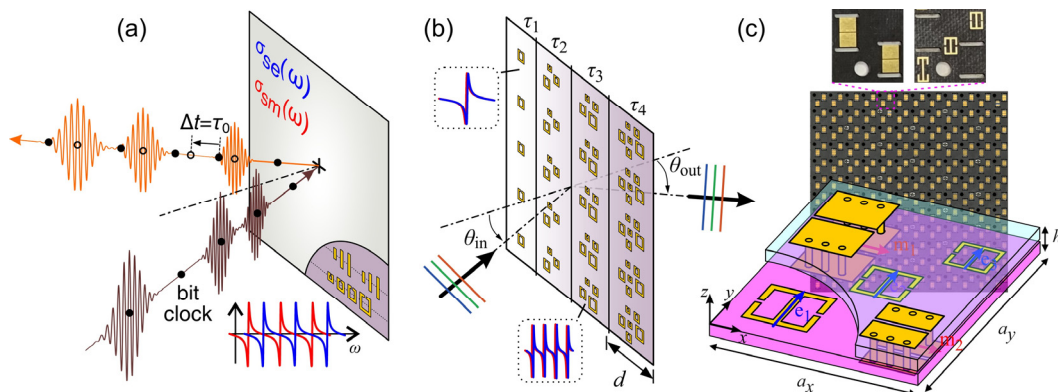


Figure 1: (a) Multiresonant metasurface for broadband pulse delay [1]. Operation in reflection requires spectrally interleaved resonances in the electric and magnetic surface conductivities. (b) By spatially modulating the supplied group delay, the metasurface can implement achromatic wavefront manipulation (e.g. beam steering) [2]. Operation in transmission requires spectrally overlapping electric and magnetic resonances. (c) Physical implementation of multiresonant unit cell for microwave frequencies. ELC and SRR resonators implement electric and magnetic dipole resonances, respectively [3]. Views of the fabricated printed circuit boards.

Acknowledgments: Support by the Hellenic Foundation for Research and Innovation under the “2nd Call to support Post-Doctoral Researchers” (Project Number: 916, PHOTOSURF).

References

- [1] O. Tsilipakos, T. Koschny, C. M. Soukoulis, *ACS Photonics* **5**, 1101-1107 (2018)
- [2] O. Tsilipakos, M. Kafesaki, E. N. Economou, C. M. Soukoulis, T. Koschny, *Advanced Optical Materials* **8**, 2000942 (2020)
- [3] O. Tsilipakos, L. Zhang, M. Kafesaki, C. M. Soukoulis, T. Koschny, *ACS Photonics* **8**, 1649 (2021)

* otsilipakos@iesl.forth.gr

Hybrid Graphene – Gold Metasurfaces for Enhanced Third Harmonic Generation Efficiency

A. Theodosi^{*,a,b}, O. Tsilipakos^b, C. M. Soukoulis^{b,c}, E. N. Economou^{b,d}, M. Kafesaki^{a,b}

a. Dep. of Materials Science and Technology, Univ. of Crete, Heraklion, 70013, Greece

b. Institute of Electronic Structure and Laser, FORTH, Heraklion, Crete, 70013, Greece

c. Ames Laboratory U.S. DOE and Dep. of Physics and Astronomy, Iowa State Univ. Ames, Iowa 50011, USA

d. Department of Physics, Univ. of Crete, Heraklion 70013, Greece

Graphene is a unique nonlinear material for THz applications due to its strong third order nonlinearity in combination with the capability to support tightly-confined surface plasmons [1]. The short wavelength of propagating graphene plasmons enables the design of metasurfaces (MSs) supporting higher-order resonances, while the lattice constant remains subwavelength even for higher harmonic frequencies avoiding diffraction effects. A proven approach for boosting the efficiency of third harmonic generation (THG) process is to carefully align the fundamental (FF) and third-harmonic (TH) frequencies with MS resonances, a strategy which has been termed double-resonant enhancement [2]. In our previous work [3], we studied MS structures where the graphene was patterned into rectangular patches and reported third harmonic generation conversion efficiency (CE) of -20dB (at input intensity of 0.1 MW/cm²) [3]. In this work, we target an implementation that is friendlier to an experimental demonstration and, at the same time, aims to further increase the efficiency.

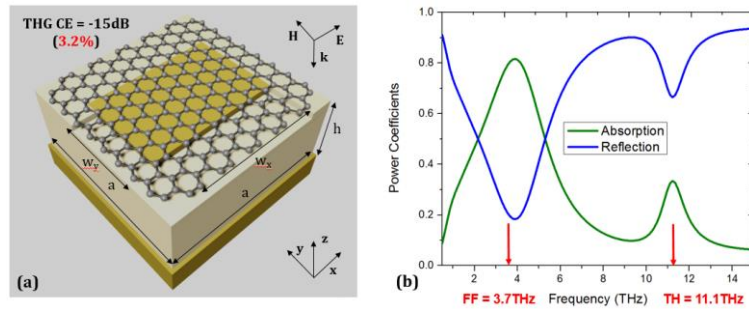


Figure 1: (a) Metasurface structure with gold patches covered with a uniform graphene layer (b) Linear plane-wave scattering spectrum (Reflected and Absorbed power coefficients) for the optimum geometrical parameters of the structure, with $w_x = 0.95a$ and $w_y = 0.65a$. The fundamental frequency and the third harmonic frequency (red arrows) are aligned with absorption peaks.

Our proposed MS [Fig. 1(a)] is composed of a uniform graphene layer on top of gold patches (with size $w_x \times w_y$), rectangular in the optimal case, residing on a dielectric substrate (thickness $h = 8.3 \mu\text{m}$), backed by a gold backreflector. The lattice constant is $a = 5.6 \mu\text{m}$. To optimize the structure response, a parametric study with respect to the length and width of the resonating patches, w_x and w_y . The CE is calculated under continuous wave (CW) conditions with a frequency-domain finite element method by using two linear simulations, at the FF and TH frequencies, respectively [4]. The optimum point in the w_x - w_y map resulted in a conversion efficiency $\text{CE} = -15\text{dB}$ (3.2%) for the E_x polarization.

This work was supported by the Hellenic Foundation for Research and Innovation under the “2nd Call to support Post-Doctoral Researchers” (Project Number: 916, PHOTOSURF)

References

- [1] Hafez H. A.; Kovalev S.; Tielrooij K. et al. *Terahertz Adv. Opt. Mat.* **8**, 1900771 (2020).
- [2] You J. W. et al. *Philos. Trans. R. Soc. A Math. Phys. Eng. Sci.* **375**, 20160313 (2017).
- [3] Theodosi A; Tsilipakos O.; Kafesaki M; et al. *Opt. Exp.*, **30**, 460-472 (2022).
- [4] Christopoulos T.; Tsilipakos O.; Sinatkas G. et al. *Phys. Rev. B*, **98**, 235421 (2018).

The synergy of electromagnetic effects and thermophysical properties of metals in the formation of laser induced periodic surface structures

G.D.Tsibidis^a, P.Lingos^a, E.Stratakis^{a,b}

^{a1} Institute of Electronic Structure and Laser (IESL), Foundation for Research and Technology (FORTH), N. Plastira 100, Vassilika Vouton, 70013, Heraklion, Crete, Greece

^b Department of Physics, University of Crete, 71003 Heraklion, Greece

¹Corresponding author: tsibidis@iesl.forth.gr

Femtosecond pulsed lasers have been widely used over the past decades for precise materials structuring at the micro- and nano- scales. In order, though, to realize efficient material processing and account for the formation of laser induced periodic surfaces structures (LIPSS), it is very important to understand the fundamental laser-matter interaction processes. A significant contribution to the LIPSS profile appears to originate from the electromagnetic fingerprint of the laser source. In this work, we follow a systematic approach to predict the *pulse-by-pulse* formation of LIPSS on metals due to the development of a spatially periodic energy deposition that results from the interference of electromagnetic far fields on a non-flat surface profile. On the other hand, we demonstrate that the induced electromagnetic effects, alone, are not sufficient to allow the LIPSS formation, therefore, we emphasize on the crucial role of electron diffusion and electron-phonon coupling on the formation of stable periodic structures (Fig.1). Gold and stainless Steel are considered as two materials to test the theoretical model while simulation results appear to confirm the experimental results that, unlike gold, fabrication of pronounced LIPSS on stainless Steel is feasible.

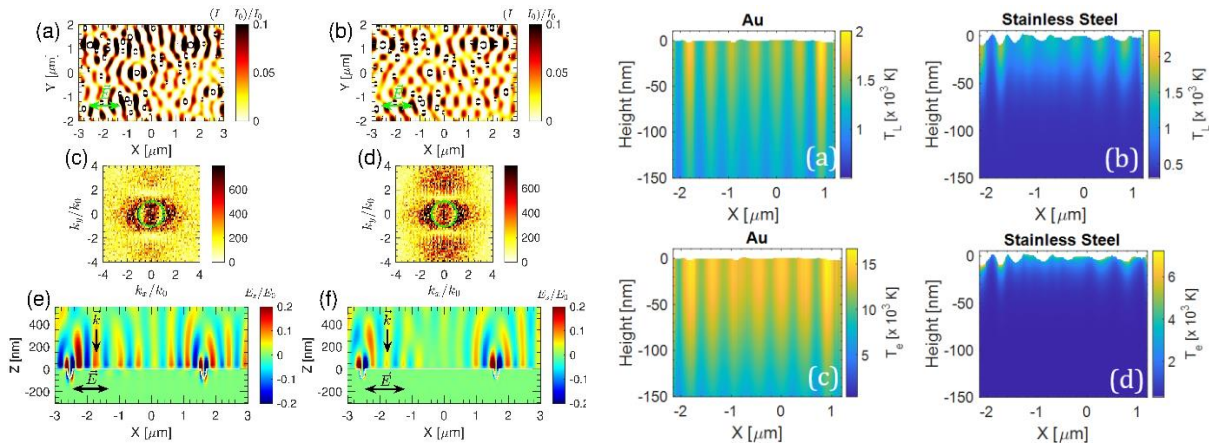


Fig.1: Absorbed energy distributions on the transverse plane for Au (*first* column) and Stainless Steel (*second* column) surfaces. Thermal effects on Au (*third* column) and Stainless Steel (*fourth* column) after four pulses.

References

G.D.Tsibidis, P.Lingos, E.Stratakis, ‘The synergy of electromagnetic effects and thermophysical properties of metals in the formation of laser induced periodic surface structures’ (submitted) [arXiv:2206.02351](https://arxiv.org/abs/2206.02351)

Nanostructured Systems of Diphenylalanine Peptides and Graphene Sheets: an Atomistic Simulation Study

M. Arnittali^{1,2,3,*}, A.N. Rissanou^{1,2,3}, V. Harmandaris^{1,2,3}

¹*Computation-Based Science & Technology Center, The Cyprus Institute, Nicosia Cyprus;*

²*Institute of Applied and Computational Mathematics (IACM), Foundation for Research and Technology Hellas (FORTH), IACM/FORTH, GR-71110 Heraklion, Crete;*

³*Department of Mathematics and Applied Mathematics, University of Crete, GR-71409 Heraklion, Crete, Greece.*

In the current work, the self-assembly of diphenylalanine peptides (FF) on a graphene layer, in aqueous solution, is investigated, through all-atom Molecular Dynamics simulations [1]. The effect of graphene surface on the self-assembly propensity of peptides, as well as on the formed structure, as it has been observed in a corresponding solution of FF in water [2], is examined. Two interfacial systems are studied, with different concentration of dipeptides at room temperature. Atomistic details about the conformational preferences, the orientation of peptides with respect to the surface and the hydrogen bond network are given. Length and time scales of the formed structures are quantified providing important insight into the adsorption mechanism of FF onto the graphene surface. A hierarchical formation of FF structures is observed involving two sequential processes: first, a stabilized interfacial layer of dipeptides onto the graphene surface is formulated, followed by the development of a structure of self-aggregated dipeptides on top of this layer. The whole procedure is completed in almost 200ns, whereas self-assembly in the system without graphene is accomplished much faster; in less than 50ns cylindrical structures, signal of the macroscopic fibrillar ones, are formed. Strong $\pi - \pi^*$ interactions between FF and the graphene led to a parallel to the graphene layer orientation of the phenyl rings. Reduction in the number of hydrogen bonds between FF peptides is observed because of the graphene layer, since it disturbs their self-assembly propensity.

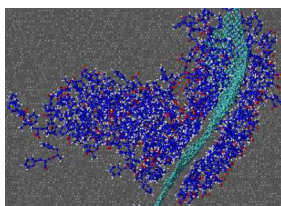


Figure 1: Graphical representation of a model system.

References

- [1] Rissanou, Keliri, Arnittali and Harmandaris, *Physical Chemistry Chemical Physics*, **22**, 27645-27657 (2020).
- [2] Rissanou, Georgilis, Mitraki, and Harmandaris, *The Journal of Physical Chemistry B*, **117**, 3962-3975 (2013).

Case-Studies for Computer-aided Materials Design: alloyed Hausmanites and Gold Nanoparticles

E. Pervolarakis^{1,*}, D. Katerinopoulou^{2,3}, G. Kiriakidis³, Z. Łodziana⁴,
E. Iliopoulos^{2,3}, G. A. Tritsarlis⁵, P. Rosakis^{6,7}, I. N. Remediakis^{1,3}

¹ Department of Materials Science and Technology, University of Crete

² Physics Department, University of Crete

³ Institute of Electronic Structure and Laser, FORTH

⁴ Institute of Nuclear Physics, Polish Academy of Sciences, Kraków, Poland

⁵ J. A. Paulson School of Engineering Applied Sciences, Harvard University, USA

⁶ Department of Mathematics and Applied Mathematics, University of Crete

⁷ Institute of Applied & Computational Mathematics, FORTH

We employ hierarchical multi scale calculations, with Density-Functional Theory (DFT) coupled to continuum models and machine learning algorithms, in order to unravel the transport mechanism in manganese oxide alloys and provide methodology for reliable edge-energy calculation for metal nanoparticles.

We study Mn_3O_4 alloyed with Zn and Ni, both in the Hausmanite and the inverse spinel structures. Experimental investigation has shown that these alloys exhibit impressive non-Arrhenius dependence of conductivity on temperature, and can thus be used as temperature sensors. The experimental results can be explained through extensive DFT calculations coupled to a model of polaron hopping in an inhomogeneous energy landscape [1].

We calculate edge energies of gold nanoparticles using a data-informed machine-learning (ML) multiple linear regression algorithm. The algorithm was provided with structural data for the nanoparticles along with the total energy as was calculated using either interatomic potentials or Density Functional Theory (DFT). The predicted edge energies are well converged with respect to the sample size. Moreover, we present for the first time vertex energies of gold nanostructures [2].

This research is co-financed by 1) European Social Fund- ESF (MIS 5050587) 2) Hellenic Foundation for Research and Innovation (HFRI-FM17-1303) 3) National Infrastructures for Research and Technology S.A. (pr009029-NANO-COMPDESIGN).

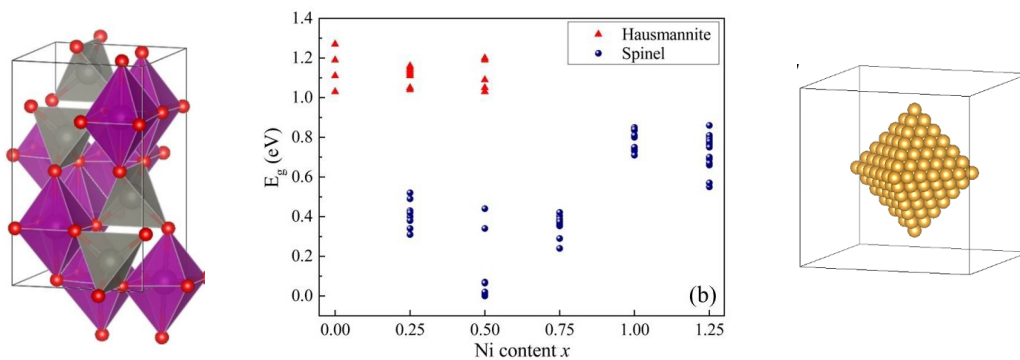


Figure 1: Left: The Hausmanite crystal structure. Center: Calculated band-gaps of the most stable structures for $Zn_{0.5}Ni_xMn_{2.5-x}O_4$. Right: An octahedral Au nanoparticle.

References

- [1] D. Katerinopoulou, E. Pervolarakis, C. Papakonstantinou, B. Malic, H. Gelinck, G. Kiriakidis, Z. Łodziana, I. N. Remediakis and E. Iliopoulos, *J. Appl. Phys.*, in press.
- [2] E. Pervolarakis, G. A. Tritsarlis, P. Rosakis, I. N. Remediakis, arXiv:2206.12239.

* emper@materials.uoc.gr

Modelling catalyst materials for CO₂ reduction: from metal nanoparticles to halide perovskites

Rafaela Maria Giappa^{1,*}, Apostolos Pantousas¹, George Kopidakis^{1,2}, Ioannis N. Remediakis^{1,2}, Constantin C. Stoumpos¹

¹*Department of Materials Science and Technology, University of Crete, Greece*

²*Institute of Electronic Structure and Laser, Foundation for Research and Technology-Hellas (IESL-FORTH)*

Two urgent, interconnected problems of our times are the exhaust of conventional energy resources and the need to reduce CO₂ emissions and move towards a sustainable carbon emission free economy. Environmentally-friendly reduction of CO₂ to fuels might serve as a solution to both problems. The use of electrocatalysis or photocatalysis for this reaction will result in green fuel production that could rely on renewable energy sources alone. Up to now, CO₂ reduction is at the forefront of catalysis science and is challenged by selectivity and stability issues in the existing catalytic materials and processes.

Aiming to design optimized anode materials for electrochemical CO₂ reduction to fuels, our quest on electrocatalytic CO₂ reduction is twofold; we explore the catalytic properties of two classes of materials, transition metals and perovskite semiconductors, by means of first principles calculations. Our starting point is the best-known catalyst for CO oxidation towards CO₂, which is gold nanoparticles [1]. We employ Density Functional Theory (DFT) calculations and the Nudged-Elastic Band (NEB) method to locate reaction transition states and identify minimum-energy paths (MEPs) for chemical reactions on 10-atom gold nanoclusters. We discuss energetics of the reactions and provide insight into the conditions that favour one reaction over the other, thus helping improving catalyst selectivity. We compare to standard CO₂ reduction catalysts such as single-crystal Cu.

For the second family of materials, metal halide perovskites and their 2D structures and nanostructures have emerged in the last decade as superb semiconducting materials, mainly driven by their high output in photovoltaics. Many side applications have already branched out, with one being their applications in electrocatalytic and photocatalytic fuel cells [2]. Due to their superior optical absorption and their ability to operate for a wide range of bandgaps depending on how one varies their chemical composition [3], metal halide perovskites can be tailored to the needs of each specific photoelectrocatalytic process. We mainly focus on 2D perovskites with bulky hydrophobic cations between the sheets of corner-connected octahedra. We perform DFT electronic-structure calculations for such systems and comment on their potential uses in environmentally-friendly catalytic processes.

References

- [1] IN Remediakis, N Lopez, JK Nørskov, *Angew. Chemie Intern. Ed.* 44, 1824-1826 (2005).
- [2] L. Mao, C. C. Stoumpos, and M. G. Kanatzidis, *J. Am. Chem. Soc.*, 141, 1171 (2019).
- [3] C. C. Stoumpos and M. G. Kanatzidis, *Acc. Chem. Res.*, 48, 2791 (2015).

This research work was supported by the Hellenic Foundation for Research and Innovation (HFRI) under the projects "MULTIGOLD" (HFRI-FM17-1303, KA 10480) and the 3rd Call for HFRI PhD Fellowships (Fellowship Number: 5706, KA 11033)

* rafaalagiappa@materials.uoc.gr

Novel Conducting Trimers for In Vivo Electronic Functionalization of Tissues

D. Mantione, E. Istif, L. Vallan,
*Laboratoire de Chimie des Polymères Organiques, Université de Bordeaux,
Bordeaux INP, CNRS, France*

G. Dufil, D. Parker, E. Stavrinidou
Laboratory of Organic Electronics, Linköping University, Sweden

E. Pavlopoulou*
*Institute of Electronic Structure and Laser, Foundation for Research and
Technology – Hellas, Greece*

Electronic materials that can self-organize in-vivo and form functional components along the tissue of interest can result in seamless integration of the bioelectronic interface. We have designed and synthesized three new trimers based on 3,4-ethylenedioxythiophene (EDOT) and thiophene that can be used as conducting building blocks in bioelectronics.[1] The trimers comprise an EDOT-thiophene-EDOT or an all-EDOT backbone and are functionalized by the addition of side groups that bear anionic or cationic moieties. Functionalizing the side groups with anions or cations proves to be an efficient way to tailor the doping level, as well as the oxidation potential, which consequently affects the polymerization kinetics. In addition, we successfully performed the chemical, electrochemical and enzymatic (in physiological pH) in vitro polymerization of the three trimers. Furthermore, the trimers were efficiently polymerized in vivo along the roots of living plants due to the presence of native peroxidase enzymes. The localization of the resulting polymer in the roots depends on the trimers structure. This work not only offers to the bioelectronics community a set of new water-soluble EDOT-based materials for interfacing living tissue, that complements nicely the currently used ETE-S trimer, but, most importantly, paves the way for rational design of electronic materials that can self-organize in vivo for spatially-controlled electronic functionalization of living tissue.

References

[1] D. Mantione, et al., ACS Appl. Electron. Mater. **2**, 4065 (2020).

Phase transitions and electric dipole moments in hybrid halide perovskite single crystals

Giannis G. Gkikas^{1,2,3,*}, Violeta Spanou^{2,4}, Constantinos C. Stoumpos², Alexandros Lappas¹

¹ Institute of Electronic Structure and Laser, Foundation for Research and Technology - Hellas, Vassilika Vouton, 71110 Heraklion, Greece

² Department of Materials Science and Technology, University of Crete, Voutes Campus, Heraklion 70013, Greece

³ Electrical and Computer Engineering Department, Hellenic Mediterranean University, Heraklion 71004, Greece

⁴ Department of Chemistry, University of Crete, Voutes, 70013 Heraklion, Greece

Halide perovskites AMX_3 ($A^+ = Cs, CH_3NH_3$ or $HC(NH_2)_2$, $M^{+2} = Pb, Sn$ or Ge and $X^- = Cl, Br$ or I), are amongst the leading emerging materials in the past decade towards optoelectronic and environmental remediation applications, including devices such as solar cells, light-emitting diodes, hard radiation detectors and photocatalytic modules. What makes these semiconductor materials so attractive for optoelectronic devices is their superb absorption across the visible and near-infrared region ($E_g = 1.1-3.0\text{eV}$) and their high charge-carrier mobility and long charge-carrier diffusion lengths. An important research branch of halide perovskites focuses in the understanding of the underlying physicochemical origins of these fascinating properties, which is currently lacking. Such understanding will be beneficial not only from the fundamental science perspective but also crucial for the rational enhancement of the optoelectronic performance.

In this work, single-crystals of $CH_3NH_3PbX_3$ (Figure 1) were grown using a wide variety of growth techniques, from solution supersaturation and non-solvent vapor diffusion to inverse temperature growth, while the response of the electric moments of the crystals were studied with dielectric spectroscopy. All the studies were performed on well-faceted, mm-sized crystals, painted with gold electrodes. High-precision capacitance measurements were undertaken with a custom-made probe station, operating in the 80-320 K temperature range, utilizing an AC excitation voltage in a broad frequency range ($f = 20\text{Hz}-2\text{MHz}$). The measurements on single-crystalline specimens offer significant benefits in terms of device responsivity, because of the higher charge-carrier mobility and electrical contact uniformity.¹ AC current measurements permit investigating both the impact of the electric field stimulus on the lattice dynamics, as well as the lattice relaxation dynamics correlated with the consecutive structural phase transitions ($140 < T < 170\text{K}$) emerging when the materials are cooled to lower temperatures.²

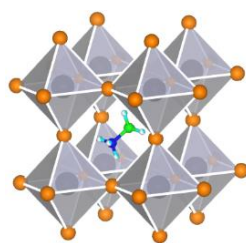


Figure 1. Crystal Structure of $CH_3NH_3PbX_3$.

References

1. Wang, X.-D., Li, W.-G., Liao, J.-F. & Kuang, D.-B. Recent Advances in Halide Perovskite Single-Crystal Thin Films: Fabrication Methods and Optoelectronic Applications. 27 (2019).
2. Onoda-Yamamuro, N., Matsuo, T. & Suga, H. Calorimetric and IR spectroscopic studies of phase transitions in methylammonium trihalogenoplumbates (II)†. *J. Phys. Chem. Solids* **51**, 1383–1395 (1990).

* janis.gkikas@iesl.forth.gr

Nature as an inspiration for printing angle-insensitive structural colors using two-photon polymerization

G. Zyla*¹, S. Gorb², A. Ostendorf³

¹*IESL-FORTH, N. Plastira 100, Heraklion, 70013 Crete, Greece*

²*Functional Morphology & Biomechanics, Christian-Albrechts-Universität, 24098, Kiel, Germany*

³*Applied Laser Technologies, Ruhr-Universität Bochum, 44801 Bochum, Germany*

In nature, colors that result from the interaction of light with structures on the micro- and nanoscale are referred to as structural colors. Typically, these colors are used by animals or plants to generate functions that ensure their survival, such as camouflage, mimicry, or communication [1]. For this purpose, organisms have developed sophisticated surface structures on their epidermis that often produce unique optical properties due to a combination of regular and irregular structural features, which delimits them from classical photonic crystals [2]. In this context, the most famous examples are the blue butterflies of the genus *Morpho*, whose color is produced by multilayers. However, the color surprisingly appears almost angle-insensitively due to specific disorder characteristics within the photonic structures [3].

Inspired by those butterflies, this work presents how a transparent photosensitive material can be processed by two-photon polymerization to mimic the angle-insensitive blue coloration. The morphology and optical properties of the biological and biomimetic surface structures were analyzed using scanning electron microscopy and angle-resolved spectroscopy. In addition, the great design freedom of the 3D printing technique enabled the processing of different structural geometries on the microscale and different feature sizes on the nanoscale in such a simple workflow not achievable by any other manufacturing technique. Therefore, it was possible to simultaneously tune the color hue and set the direction in which angle-insensitive colors appeared to an observer. As a result, numerous opportunities are conceivable to generate a broad diversity of highly complex patterns for counterfeit protection.

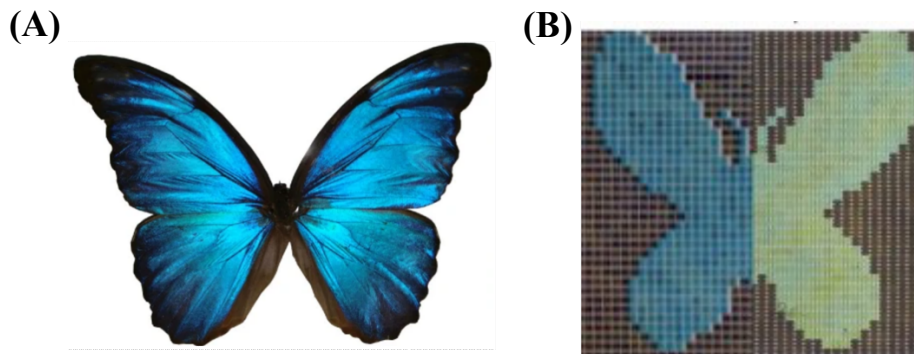


Figure 1: (A) The structural color of a *Morpho didius*. (B) Structural color generated by *Morpho*-inspired structures using two-photon polymerization.

References

- [1] W. Wickler. *Nature* **208**, 519–521 (1965).
- [2] P. Vukusic, J.R. Sambles. *Nature* **424**, 852–855 (2003)
- [3] S. Kinoshita, S. Yoshioka, J. Miyazaki. *Rep. Prog. Phys.* **71**, 076401 (2008).

* zyla@iesl.forth.gr

Design and Development of Functionalized Pillar-Layered MOFs

K. Papadopoulos^{*1}, K. Manousakis¹, G. K. Angeli¹, C. Tsangarakis¹, E. Loukopoulos¹, P. N. Trikalitis¹

¹Department of Chemistry, University of Crete, Heraklion 70013, Greece
ptrikal@uoc.gr

Metal-Organic Frameworks (MOFs) represent a diverse class of porous materials that can be truly designed in terms of their inorganic and organic components, offering a wide spectrum of tuneable properties. Despite being solids, such materials have shown unique structural flexibility phenomena under external stimuli (e.g. temperature, host-guest interactions, pressure and light), paving the way to state-of-the-art responsive materials for applications such as selective gas separation [1]. In particular, pillar-layered (PL) MOFs have attracted great interest in terms of their framework flexibility [2]. More specifically, DUT-8(M) (M: Ni, Co, Cu, Zn) is a representative PL-MOF family with a typical “gate-opening” behaviour that has shown to hold great promise for separation applications [3]. This mixed-ligand framework consists of 2D grids (layers) formed by paddle-wheel metal clusters which are connected by naphthalene dicarboxylate (NDC) ligands. These grids are pillared by a tertiary diamine, DABCO, leading to an open 3D structure with **pcu** topology (Figure 1). The flexible behaviour arises from the ability of the inorganic node to act as a “hinge”, and thus the alteration of the metal centres has enabled the fine tuning of the framework’s flexibility [4]. Despite the study of the metals’ nature effect, to the best of our knowledge, the effect on the flexibility of the nature of the organic ligand, in terms of their functional groups, which has been shown to have an impact on the flexibility phenomenon in similar systems [5], hasn’t been investigated for DUT-8.

Herein, we explore for the first time the layer-forming ligand functionalization of the DUT-8 framework. Three novel structures were successfully synthesized and characterized by introducing different functionalities on the organic linker. One of them lead to a topologically identical framework as the DUT-8(M) system (Figure 1), while the other two resulted to completely different topologies with intriguing properties. Synthetic conditions, crystal structures, stability investigations and sorption properties will be presented and discussed.

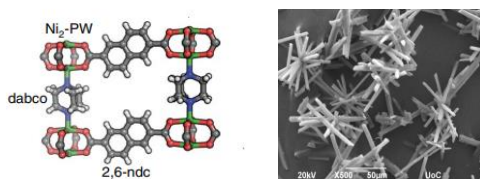


Figure 1: (Left) DUT-8(Ni) Pillar-Layered structure (Right) Representative SEM image of the isostructural DUT-8 single crystals.

References

- [1] Giasemi K. Angeli, Edward Loukopoulos, Konstantinos Kouvidis, Artemis Bosveli, Constantinos Tsangarakis, Emmanuel Tylianakis, George Froudakis, and Pantelis N. Trikalitis, *J. Am. Chem. Soc.*, **143**, 10250-10260 (2021).
- [2] S. Ehrling, E. M. Reynolds, V. Bon, I. Senkovska, T. E. Gorelik, J. D. Evans I, M. Rauche, M. Mendt, M. S. Weiss, A., E. Brunner, U. Kaiser, A. L. Goodwin and S. Kaskel, *Nature Chemistry*, **13**, 568–574 (2021).
- [3] Linda Bondorf, Jhonatan Luiz Fiorio, Volodymyr Bon, Linda Zhang, Mariia Maliuta, Sebastian Ehrling, Irena Senkovska, Jack D. Evans, Jan-Ole Joswig, Stefan Kaskel, Thomas Heine, Michael Hirscher, *Science Advances*, **8**, eabn7035, (2022).
- [4] Nicole Klein, Herbert C. Hoffmann, Amandine Cadiou, Juergen Getzschmann, Martin R. Lohe, Silvia Paasch, Thomas Heydenreich, Karim Adil, Irena Senkovska, Eike Brunner and Stefan Kaskel, *J. Mater. Chem.*, **22**, 10303, (2012).
- [5] Sebastian Henke, Andreas Schneemann, Annika Wütscher, and Roland A. Fischer, *J. Am. Chem. Soc.*, **134**, 9464–9474 (2012).

Acknowledgements

This research work was supported by the DeSulfur program titled "Advanced nanoporous materials for the Deep deSulfurization of liquid fuels via adsorption in mild conditions (project code: T2EAK-01976)"

Co-catalyst assisted mesoporous II-VI metal sulfide nanocrystal assemblies for highly efficient photochemical water-splitting and hydrogen production

I. Vamvasakis, E. K. Andreou, G. S. Armatas
Department of Materials Science and Technology, University of Crete
Vassilika Vouton, 71003 Heraklion, Greece

Photocatalytic water splitting for hydrogen (H₂) production has been one of the hot subjects in recent decades as a result of the global energy crisis. Key element of this approach is the development of cost-effective functional catalysts with high activity and long-term stability.[1] To that end, II-VI metal-sulfide colloidal nanocrystals (NCs), such as CdS and ZnS, have attracted enormous research attention because of their interesting optical, electronic and catalytic attributes.[2] However, conventional metal sulfides suffer from low charge-carrier separation and poor chemical stability that restrain their photocatalytic efficiency. A well-established approach to overcome these limitations and achieve improved catalytic performance is to employ functional co-catalysts and create heterostructures with open-pore architecture at the nanoscale.[3,4] Here, we report the design and fabrication of two novel mesoporous materials comprised of CdS and CdS/ZnS nanocrystal assemblies (NCAs) and demonstrate their photocatalytic performance for H₂-generation from water. The resultant materials consist of a highly porous network (BET surface area up to 260 m² g⁻¹) of linked ~5 nm-sized metal-sulfide NCs that is perforated by uniform mesopores (ca. 6 nm in size). When coupled with low-cost active co-catalysts, such as nickel hydroxide or nickel phosphides, the formed mesoporous heterostructures exhibit a remarkable photocatalytic H₂-production activity associated with a quantum yield (QY) up to ~70% at 420 nm. Photocatalytic experiments combined with UV-vis/NIR, photoluminescence and electrochemical impedance spectroscopy studies suggest that the outstanding photocatalytic performance of these catalytic systems mainly arises from the accessible 3D open-pore structure and the favorable band-alignment of metal sulfide with the respective co-catalyst, which suppresses carrier recombination and promotes efficient charge-transport at the junction interfaces.

References:

- [1] S. Chen, et al., *Nat. Rev. Mater.*, 2 (2017) 17050
- [2] A. Vaneski et al., *J. Photochem. Photobiol. C: Photochem. Rev.*, 19 (2014) 52
- [3] I. Vamvasakis et al., *Adv. Funct. Mater.*, 26 (2016) 8062
- [4] I. Vamvasakis et al., *ACS Catal.*, 8 (2018) 8726
- [5] We acknowledge support from the Hellenic Foundation for Research and Innovation (H.F.R.I.) under the “1st Call for H.F.R.I. Research Projects to support Faculty Members & Researchers and the Procurement of High-cost research equipment grant” (Project Number: 400).

Spray Deposition of LiFePO₄ on Al foil as cathode for Li-ion batteries

C. Floraki^{1*}, K. Brintakis², A. Kostopoulou², E. Stratakis², D. Vernardou^{1,3}

¹*Department of Electrical and Computer Engineering, School of Engineering, Hellenic Mediterranean University, 71410 Heraklion, Greece*

²*Institute of Electronic Structure and Laser, Foundation for Research & Technology-Hellas, P.O. Box 1527, Vassilika Vouton, 71110 Heraklion, Greece*

³*Institute of Emerging Technologies, Hellenic Mediterranean University Center, 71410 Heraklion, Greece*

**corresponding author, e-mail floraxris@gmail.com*

The high energy demand of energy storage applications has led to the discovery of sustainable energy storage devices such as the Li-ion batteries, which are one of the most promising solutions. However, Li-ion batteries present a low energy density, which cannot meet the actual requirements of storage systems. In order to improve their electrochemical performance, cathode materials such as LiFePO₄ (LFP) have been investigated. LFP presents good cycle performance, high safety and stability, and theoretical capacity of 170 mAh g⁻¹. Nevertheless, the existing fabrication methods of LFP, which have been utilized primarily for the growth of powders are time consuming and use organic solvents.

In order to overcome all the aforementioned limitations, a simple one-step spray growth of LiFePO₄ on Al-foil has been performed through an aqueous solution of LiFePO₄ (1:1:1) for the fabrication of the cathodes for Li-ion batteries. The structural and morphological features of the electrodes have been investigated before and after the consecutive scans using an aqueous LiSO₄ electrolyte. The stability and efficiency of the electrodes using the aqueous electrolyte have also been evaluated through cyclic voltammetry analysis.

Mesoporous Architectures of Spinel Chalcogenide Nanoparticles Coupled with Transition Metal Phosphides for Photochemical Water Splitting and Hydrogen Production

Evangelos K. Andreou*, Ioannis Vamvasakis, Gerasimos S. Armatas
*Department of Materials Science and Technology, University of Crete, Heraklion
70013, Greece*

The photochemical water splitting for hydrogen production has been proven as an attractive solution to the rising problem caused by the excessive fossil fuel consumption. This photochemical process of producing solar fuels, such as hydrogen, has a positive impact on the environment due to the zero emission of harmful byproducts. Hydrogen is a promising future energy source thanks to its high gravimetric energy density and efficient conversion to electricity with zero carbon emission. However, until now over 95% of hydrogen is produced from fossil fuels with significant amount of greenhouse gas evolution. To this end, there has been a strong effort from the research community to devise new photocatalytic materials that combine high solar-to-chemical conversion efficiency, low cost of production and high chemical stability. Our research group and others have already projected the potential of mesoporous assemblies of metal chalcogenide nanoparticles as outstanding photocatalysts for hydrogen evolution from water.[1] Recently, we found that the co-existence of two types of materials, the spinel chalcogenides and transition metal phosphides, in the same structure can be considered as an ideal candidate for the photochemical water splitting and hydrogen generation. Herein, we report for the first time a low temperature synthesis of CdIn₂S₄ nanocrystals of size 5-10 nm and their conversion to mesoporous architectures with large internal surface area (>135 m²g⁻¹) and outstanding photocatalytic activity for hydrogen evolution (100 μmol h⁻¹). Furthermore, when Ni₂P nanosheets recombine on the CdIn₂S₄ mesoporous surface to produce Ni₂P/CdIn₂S₄ heterostructures the photocatalytic H₂ evolution rate rises to 400 μmol h⁻¹, affording an apparent quantum yield over 50% at 420 nm for water splitting, which is the highest ever reported activity for thiospinel-based systems.

References

- [1] I.Vamvasakis et al, *Adv. Fun. Mat.* **26**, 2016, 8062-8071; *ACS Catal.* **8**, 2018, 8726-8738.
- [2] The authors acknowledge support from the Hellenic Foundation for Research and Innovation (H.F.R.I.) under the “1st Call for H.F.R.I. Research Projects to support Faculty Members & Researchers and the Procurement of High-cost research equipment grant” (Project Number: 400).

* vaggelisandr@gmail.com

Novel Metal Organic Frameworks for Desulfurization of Oil based Fuels

Giasemi K. Angeli, Constantinos Tsangarakis and Pantelis N. Trikalitis
Department of Chemistry, University of Crete, Voutes71003 Heraklion, Greece

Regardless the continuous efforts towards renewable energy sources, fossil fuels, especially petroleum based, are still crucial for the development of science, technology and are an undeniable prerequisite to carry out our daily activities. Therefore, many countries have set strict standards regarding fuels' sulfur content, to avoid the highly undesirable environmental and economic effects that they can cause. Acid rain, equipment corrosion and catalyst poisoning are only a few of the negative effects that sulfur organic compounds can create. On these terms ultra deep desulfurization is gaining increasing attention both from academia and industry in order to establish alternative methods for efficient deep desulfurization at low cost [1, 2].

Intensified research has been done and a plethora of materials were tested, among them Metal Organic Frameworks (MOFs) have emerged as promising candidates due to their diverse and tunable, highly porous nature. MOFs are a novel class of porous materials presenting intriguing characteristics as high surface area, diverse pore size and shape, open metal sites and tunable functionality. These make them suitable both for adsorptive removal of sulfur containing oil contaminants but also excellent heterogeneous catalysts which can be used in oxidative desulfurization procedures. However, despite the promising nature of MOFs, literature examples are limited mainly due to stability issues that were reported for early MOFs [3,4].

In this work we attempt to enrich the state of art regarding different MOFs' performance in desulfurization processes. Herein we present the results of diverse examples of MOFs based on different metal clusters (Zr (IV), Rare Earths (III), Cr (III)), diverse framework topologies, different pore shapes and sizes, carefully chosen functionalities (such as $-SO_2$ groups) and open metal sites [5-7]. All MOFs are examined both for their adsorption ability as well as their performance in oxidation of dibenzothiophene (DBT) and dimethyl-dibenzothiophene (DMDBT). MOFs were fully characterized before use, through PXRD and SCXRD experiments, SEM microscopy and detailed N_2 at 77 K or Ar at 87 K sorption experiments, to verify their phase purity and porosity. Their desulfurization performance was estimated through GC and 1H -NMR experiments. Finally, the MOFs that were used were re-examined with PXRD experiments and SEM microscopy, after the desulfurization procedure to examine their stability throughout the process.

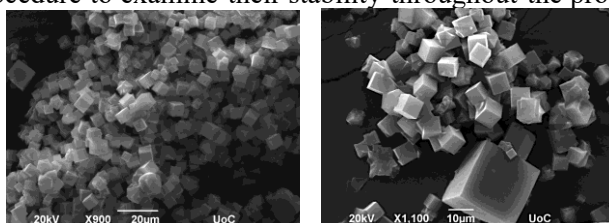


Figure 1: SEM images of a Zr based MOF after oxidative desulfurization of DMDBT.

References

- [1] Liberty L. et al, *Journal of Cleaner Production*, **323**, 129196 (2021)
- [2] Salete S. Balula*, *Chem. Commun.*, **51**, 13818 (2015)
- [3] Yiping Guo. et al, *Separation and Purification Technology*, **285**, 120287 (2022)
- [4] Leiduan Ha., et al, *Catalysis Today*, **350**, 64-70 (2020)
- [5] P.N.Trikalitis., et al, *J. Am. Chem. Soc.* **138**, 5, 1568–1574 (2016)
- [6] P.N.Trikalitis., et al, *J. Am. Chem. Soc.* **142**, 37, 15986–15994 (2020)
- [7] P.N.Trikalitis., et al, *ACS Appl. Mater. Interfaces* **14**, 19, 22242–22251 (2022)

Acknowledgements: This research work was supported by the DeSulfur program titled "Advanced nanoporous materials for the Deep deSulfurization of liquid fuels via adsorption in mild conditions (project code: T2EAK-01976)"

Phase diagram and Fredericks transition in nanocomposites of a liquid crystal and quantum dots

S.B. Atata, I. Lelidis

Section of Condensed Matter Physics, Department of Physics, National and Kapodistrian University of Athens, Panepistimioupolis, Zografos, 15784 Athens, Greece

We investigate the effect of quantum dots on the ordering of liquid crystals by means of polarized optical microscopy and electrooptical measurements. Specifically, nanocomposites of the 4-cyano-4'-octylbiphenyl liquid crystal with core-shell CdSe/ZnS quantum dots were prepared. The phase diagram of the nanocomposites as function of the quantum dots' concentration was constructed. A narrowing of the nematic phase temperature window was measured along with a drop of the clearing temperature. Microphase separation effects and the formation of a network of quantum dots appear above a critical concentration. The Fredericksz threshold, switch-on and switch-off times were determined as a function of the quantum dots' concentration. The influence of the quantum dots' size was evaluated.

Scaling up the synthesis of single layer MoS₂ crystals

N. Balakeras^{1*}, K. Filintoglou^{1,2}, A. Michail^{3,4}, K. Stergiou¹, I. Parthenios⁴,
and K. Papagelis^{1,4}

¹*School of Physics Department of Solid-State Physics, Aristotle University of Thessaloniki, Thessaloniki 54124, Greece*

²*HENANOTEC, Komnion 17, Thessaloniki 54624, Greece*

³*Department of Physics, University of Patras, Patras 26504, Greece*

⁴*FORTH/ICE-HT, Stadiou st. Platani, Patras 26504, Greece*

Among the family of 2D TMDCs, MoS₂ is an exceptional member due to its thickness-dependent optical and electronic properties. MoS₂ crystals have been fabricated via the Atmospheric Pressure Chemical Vapor Deposition (APCVD) method, using elemental Mo, MoO₂, and MoO₃ as a molybdenum source under continuous sulfur vapors carried by N₂ gas flow. In most cases, samples produced with those precursors suffer by inhomogeneous nucleation and low substrate coverage. Furthermore, after process refinement, the quality and the size of the 2D crystals have increased from a few microns to single crystals with lateral dimensions of hundreds of μm [1]. In this work, we have successfully employed a novel vapor - liquid APCVD method [2], that uses Na₂MoO₄ as a Mo precursor. First, the growth parameters (growth temperature and precursor concentration) were optimized to achieve almost 100% substrate coverage with 50% monolayer crystals. By fine tuning of other parameters of the fabrication process, such as the spin coating time and acceleration, the monolayer coverage can be increased from 50% to almost 80% (Figure 1). To extract useful metrics from optical microscope images of the grown MoS₂ films, an image processing software specialized in 2D materials was developed. The program utilises several techniques such as k-means clustering method to perform proper image segmentation leading to identification of single-layer, few layer and bulk domains.

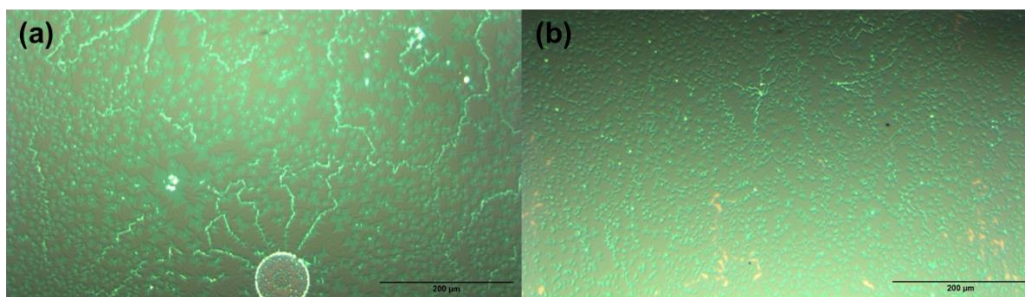


Figure 1: Optical images of MoS₂ grown on Si/SiO₂ after: (a) 2 min and (b) 6 min precursor of spin-coating.

References

- [1] Lee, Y.-H. *et al.* *Advanced Materials* **24**, 2320–2325 (2012)
- [2] Michail A. *et al.* *2D Materials* **5**, 035035 (2018)

*nmpalake@auth.gr

Laser-assisted processes on metal halide perovskite nanocrystals: Shape/dimensionality transformations and conjugation with 2D materials

K. Brintakis^{a,*}, A. Kostopoulou^a, E. Stratakis^{a,b}

^a *Institute of Electronic Structure and Laser, Foundation for Research and Technology - Hellas, Heraklion, 71110, Crete, Greece*

^b *Physics Department, University of Crete, Heraklion, 710 03 Crete, Greece*

Photonic processes such as photothermal, photochemical or photophysical were implemented in colloids in order to fabricate nanocrystals of different morphologies or to modify the size or morphological features of pre-formed nanocrystals. Besides the plethora of reports on laser-based fabrication or size/structure modification of nanocrystals of different -materials, only a few works referred to metal halide perovskite nanocrystals. The limited results have led to poor knowledge/understanding on the interactions of the laser irradiated photon with these materials in these dimensions. These limited works concern the pulsed laser fragmentation in liquid environment, starting from material in powder to form nanocrystals or the alteration of the nanocrystal stoichiometry via an anion exchange with the halides originated from the solvent (dihalomethane). [1,2]

Till now, different morphologies and structures of metal halide perovskite nanocrystals have been synthesized by tuning the parameters of the chemical synthesis such as ratio between the precursors, the time of the reaction, the quantity of the ligands and the temperature of the synthesis. In order to obtain nanocrystals of different morphologies for comparing their properties or application performance, different syntheses have to be carried out, which is a time- and chemicals consuming process. Here we report on a simple and rapid photo-induced method to modify the shape and the dimensionality of metal halide nanocrystals via ultrashort-pulsed laser irradiation of their colloids. [3] Furthermore, conjugations of metal halide nanocrystals with 2D materials could be obtained by similar photo-triggered method. [4]

This rapid and single-step room temperature method provides unique opportunities for the cost-effective fabrication of single- or multi-phase nanostructures with controllable size, shape, and dimensionality. The transformation from one to another nanostructure and the conjugation of two distinct material allows new fundamental studies on the impact of dimensionality and morphology to the final physical properties as well as to new synergetic effects.

References

- [1] Dong et al., *J. Phys. Chem. Lett.* **10** (15), 4149 (2019).
- [2] Parobek et al., *J. Am. Chem. Soc.* **139** (12), 4358 (2017).
- [3] Kostopoulou et al., *Nanomaterials* **12** (4), 703 (2022).
- [4] Kostopoulou et al., *Nanomaterials* **10** (4), 747 (2020).

Acknowledgments

FLAG-ERA Joint Transnational Call 2019 for transnational research projects in synergy with the two FET Flagships Graphene Flagship & Human Brain Project - ERA-NETS 2019b (PeroGaS: MIS 5070514).

* kbrin@iesl.forth.gr

Formation of Black Titania by Ammonolysis for Photocatalytic Hydrogen Production

M. Charalampakis^{1,2}, E. Loukopoulos², E. Skliri¹, G. Kyriakidis¹, P. N. Trikalitis²,
V. Binas¹

¹Institute of Electronic Structure and Lasers, FORTH, Heraklion 70013, Greece

binasbill@iesl.forth.gr

²Department of Chemistry, University of Crete, Heraklion 70013, Greece

ptrikal@uoc.gr

White titanium dioxide (W-TiO₂) has been considered a great semiconductor photocatalyst for various photocatalytic applications due to its abundance and favourable properties such as low cost, low toxicity, good photocatalytic activity and chemical stability. However, optical absorption is confined to the ultraviolet region (UV) owing to its broad bandgap (3.0 eV for rutile and 3.2 eV for the anatase phase) thus rendering it active for only 5% of solar radiation [1]. By using different gas treatment methods, oxygen vacancies and other surface modifications can occur, leading to an effective alteration of the optoelectronic and catalytic properties [2] and the subsequent formation of black coloured titanium dioxide (B-TiO₂). As a result, black titania possesses narrower band gap or mid-gap states compared to white TiO₂ which enhances its visible light absorption. Additionally, the highly defective structure can suppress electron-hole recombination and facilitate charge transfer processes [1].

In this work, black titania was formed by thermally treating white titanium dioxide powders under ammonia (NH₃) atmosphere at different temperature protocols. The effect of annealing protocol on the formation and characteristics of black titania was studied after treatment at 450°C, 500°C, 550°C, 600°C, and 650°C. The samples have been characterized using techniques such as X-Ray diffraction, SEM/EDS analysis and XPS measurements before and after treatment. Finally, the powders were evaluated as catalysts for water splitting and hydrogen gas (H₂) production under solar light radiation. The photocatalytic experiments were carried out using a Shimadzu gas chromatographer (GC) equipped with a thermal conductivity detector (TCD) to determine the best photocatalyst powders.



Figure 1: (a) White and (b) Black titania formed by ammonolysis

References

- [1] X. Liu, G. Zhu, X. Wang, X. Yuan, T. Lin, F. Huang, *Adv. Energy Materials*, 1600452 (2016).
- [2] S. S. Sahoo, S. Mansingh, P. Babu, K. Parida, *Nanoscale Adv.* **3**, 5487 (2021).

Acknowledgements

This research work was supported by the “Water2Hy” program titled “A novel and rational design of surface and interface oriented heterostructures for sustainable solar-driven photocatalytic hydrogen conversion” part of the Bilateral and Multilateral S&T Cooperation Greece-China (Code: T7ΔKI-00369).

Development of novel Nanostructured surfaces using Residual Layer Free Nanoimprint Lithography and Metal Assisted Chemical Etching

Nefeli Dimogerontaki^{1,3}, Konstantina Tourlouki², Efstratios Svinterikos², Nikolaos Kehagias³,

1. Department of Physics, School of Applied Mathematical and Physical Sciences
National Technical University of Athens, Zografou Campus, GREECE

2. Nanotypos, Technopoli ICT Business Park Thessaloniki, Bld. C2, 55535, Pylea,

3. NCSR Demokritos, Institute of Nanoscience & Nanotechnology, P. Grigoriou 27 &
Neapoleos Str., 15341 Ag. Paraskevi, Greece

The fabrication of nano scale structures is important in many fields of technology such as photonics, electronics, energy conversion, energy storage, biosensors and biomimetic surfaces and many others. Therefore, the development and optimization of efficient and low-cost methods for the realization of nanostructured surfaces is very important. One of the most promising and efficient methods to produce and reproduce in a high throughput manner is nanoimprint lithography (NIL)¹. Depending on the targeted (final) application, replicating nano structures by NIL without a residual layer is highly desirable in nanoimprint lithography and can greatly simplify the overall manufacturing processes². In this work we discuss the imprinting conditions needed to achieve residual layer free (RLF) imprints when using thermal NIL and demonstrate micro/nano structured silicon wafers when combining RLF-NIL with Metal-Assisted Chemical Etching³ (MACE). To achieve our final silicon nano patterned surfaces, after RLF-NIL a thin (30 nm) Au layer is deposited followed by a lift-off process to create Au patterns on our Si wafer. In the next step the samples were submerged into an aqueous solution mixture of HF: H₂O₂: H₂O. By emerging the Au/Si nano-patterned samples into the HF: H₂O₂: H₂O solution bath, the Au film acts as a catalyst so the Si beneath the Au film is etched. As a result, the pattern is transferred to the Si substrate.

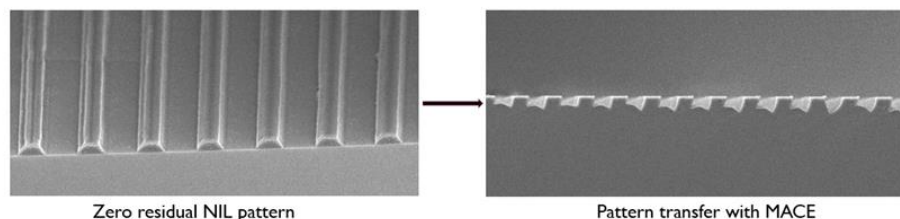


Figure 1: Cross section scanning electron microscope (SEM) images of Zero residual layer NIL patterns (left) and pattern transfer with MACE technique (right).

References

1. Schiff, H. Nanoimprint lithography: An old story in modern times? A review. *J. Vac. Sci. Technol. B Microelectron. Nanom. Struct.* **26**, 458 (2008).
2. Yoon, H., Lee, H. & Lee, W. B. Toward residual-layer-free nanoimprint lithography in large-area fabrication. *Korea Aust. Rheol. J.* **26**, 39–48 (2014).
3. Han, H., Huang, Z. & Lee, W. Metal-assisted chemical etching of silicon and nanotechnology applications. *Nano Today* **9**, 271–304 (2014).

Acknowledgments: This work has been funded under the national research programme of General Secretariat for Research and Innovation, Project acronym: Nanoroll, Project grant number: T6YBII-00254

Electronic structure of photocatalytic materials: doped ZnO and gold-perovskite interfaces.

A. Douloumis*, C. C. Stoumpos, G. Kopidakis, I. N. Remediakis
*Dept. of Materials Science and Technology, University of Crete,
University Campus Voutes, 70013 Heraklion, Crete, Greece*

Modern environmental applications call for functional surfaces and interfaces that can be used in photocatalysis and electrocatalysis. To this end, we simulate surfaces and interfaces of two widely used materials: doped ZnO and halide perovskites. Using Density-Functional-Theory (DFT) simulations, we focus on the surface of ZnO and the interface of perovskites with gold. For Mn-doped ZnO, we consider various dopant concentrations at the out-most (surface) layer of Zn atoms, while the interior of the material is kept at the ideal wurtzite structure. For each system, we calculate surface energy and surface workfunction. We discuss trends in surface stability and surface electronic structure of this material, as well as its applications in photocatalysis. Gold is used as a cathode in the majority of perovskite solar cells, however a direct gold-perovskite interface is little studied in literature. We perform first-principles calculations for a gold-perovskite interface, focusing on the energetics and the electronic structure of the system.

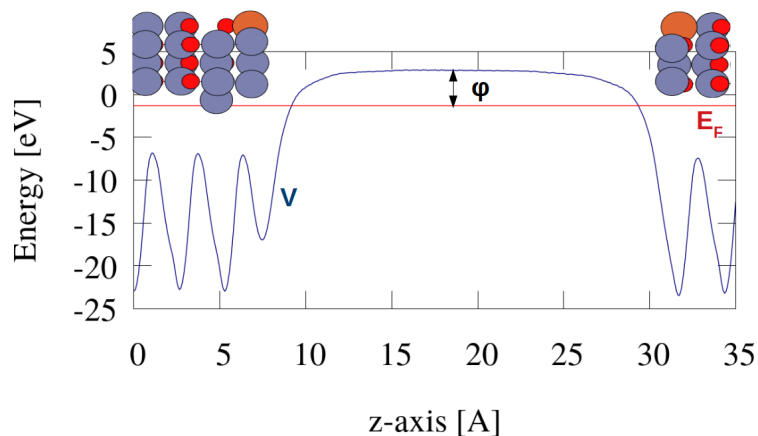


Figure 1: Electronic potential energy as a function of distance from the surface for a periodic simulation of Mn-doped ZnO(0001) slabs. Red, gray and orange spheres represent O, Zn and Mn atoms, respectively. The local potential of the slab (V), Fermi energy (E_F) and workfunction (ϕ) are shown.

This work was supported by the Hellenic Foundation for Research and Innovation (HFRI) under project "MULTIGOLD" (HFRI-FM17-1303, KA 10480) and by the Research Committee of the University of Crete (KA10136).

*adouloumis@materials.uoc.gr

Implementation of Hard-Soft Chemistry for one-Pot Synthesis of Bimetallic MOFs Suitable for Xe/Kr Separation

Konstantinos G. Froudas*, Giasemi K. Angeli, Pantelis N. Trikalitis

*Department of Chemistry, University of Crete, Voutes, Heraklion 71003, Greece
chemp1161@edu.chemistry.uoc.gr*

Metal-Organic Frameworks (MOFs) constitute a unique class of multifunctional, open-framework solids with prospective applications pertaining to energy and environmental sustainability. [1] To their vast majority, MOFs consist of inorganic and organic molecular building units, whose embedded geometrical information allows their regulated assembly under the principles of reticular chemistry. [2] Nevertheless, the systematic generation of more intricate structures, composed of two or more different metal ions by the practice of the aforementioned designing approach encounters noticeable limitations, mostly due to deviations in reaction kinetics.

In the present work, we report the one-pot rational construction of a mixed-metal-organic framework (M²MOF) by the deliberate implementation of hard and soft acid and base (HSAB) theory. [3] In particular, a bifunctional ligand comprised of a hard carboxylate and a soft pyrazolate moiety was purposely selected, aiming at the preferential binding of the former to a hard Lewis acid (M⁴⁺) and the latter to a soft Lewis acid (M²⁺). The resultant 3D framework with the rare **scu** underlying topology features comfortably accessible, 1D polygonal channels, while the synergism emerging from the highly polar pore environment (arising from different functionalities) and distinct structural characteristics is responsible for its notable performance in Xe/Kr separation.

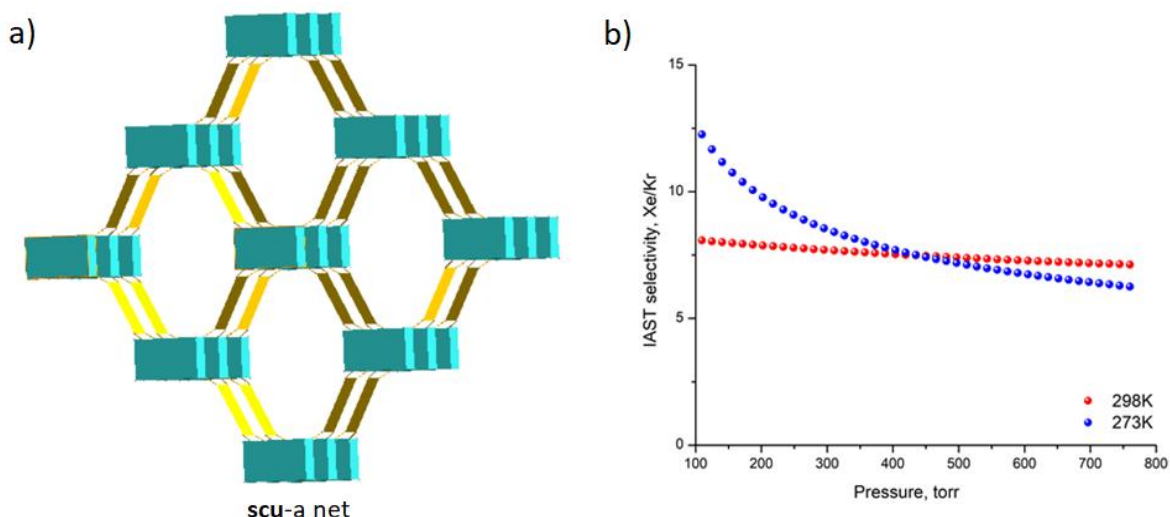


Figure 1: (a) The augmented **scu**-a net (b) Selectivity of Xe over Kr at 298 K and 273 K as predicted by IAST for a 10/90 Xe/Kr molar mixture.

References

- [1] Furukawa, K.E.; Cordova, K.E.; O’Keeffe, M. et al. *Science* **341**, 1230444 (2013).
- [2] Jiang, H.; Alezi, D.; Eddaoudi, M. *Nat. Rev. Mater.* **6**, 466-487 (2021).
- [3] Froudas, K.G.; Angeli, G.K.; Trikalitis, P.N. submitted (2022).

Dispersibility Determination of Stable g-C₃N₄ Colloidal Suspensions in Common Solvents

Kosmas Giannaris^{1,2,*}, Sofia Stefa^{1,3}, V. Binas^{1,3}, M. M. Stylianakis^{1,4}, K. Chrissopoulou¹ and S. H. Anastasiadis^{1,5}

¹*Institute of Electronic Structure and Laser, Foundation for Research and Technology-Hellas, Heraklion, Greece.*

²*Dept. of Materials Science and Technology, Univ. of Crete, Crete, Greece.*

³*Industrial, Energy and Environmental Systems Lab (IEESL), School of Production Engineering and Management, Technical University of Crete, GR-73100 Chania, Greece.*

⁴*Dept. of Nursing, Hellenic Mediterranean University, Heraklion Crete, Greece*

⁵*Dept. of Chemistry, Univ. of Crete, Heraklion, Greece.*

The present study intends to investigate the dispersion behavior of graphitic – Carbon Nitride (g-C₃N₄) in a wide variety of solvents. In this context, twenty (20) different solvents were utilized, covering a broad range of physicochemical characteristics (e.g. polarity, boiling point etc.). The synthesized g-C₃N₄ was extensively characterized in powder form by Attenuated Total Reflectance (ATR-IR), Ultraviolet-visible (UV-vis) and Raman spectroscopy, as well as X-ray diffraction (XRD) in order to confirm its layered structure. Next, stable dispersions were prepared through a tip-assisted ultrasonication process, followed by centrifugation and careful isolation of the supernatant from the sediment. The final concentration of the dispersed and exfoliated g-C₃N₄ flakes in each solvent was determined according to the Beer-Lambert's law. It should be highlighted, that this is the first time in the literature that stable g-C₃N₄ dispersions were prepared in various solvents by tip-ultrasonication instead of the conventional bath-assisted one, while the Hansen Solubility Parameters (HSP) of the material were calculated. [1,2] The acquired knowledge will be exploited to prepare and characterize waterborne polyurethane (PU)/C₃N₄ nanocomposites, expecting that the formation of multiple hydrogen bonds within the PU will endow the nanocomposites with improved mechanical and self-healing properties.



Figure 1: g-C₃N₄ dispersions in Acetone, Acetic Acid, Butanol, Ethylene Glycol.

Acknowledgements: This research has been supported by the European Union and Greek national funds through the Operational Program Competitiveness, Entrepreneurship and Innovation, under the call RESEARCH CREATE INNOVATE (SELFNANOPUD, MIS: 5067612).

References

- [1] M. Ayán-Varela, J.I. Paredes, L. Guardia, S. Villar-Rodil, J.M. Munuera, M. Díaz-González, C. Fernández-Sánchez, A. Martínez-Alonso and J.M.D. Tascón. *ACS Applied Materials & Interfaces* **7**, 24032 (2015).
- [2] K. Anagnostou, M.M Stylianakis, G. Atsalakis, D.M. Kosmidis, A. Skouras, I.J. Stavrou, K. Petridis and E. Kymakis, *J. Col. Interf. Sci.* **580**, 332 (2020).

*kosmas_g@iesl.forth.gr

Development of Functional Materials Surfaces

*F. Gojda,^{1,2} L. Papoutsakis,¹ M. Loulakis,¹ S Tzortzakis,^{1,3} K. Chrissopoulou,¹ and Spiros H. Anastasiadis^{1,4}

¹*Institute of Electronic Structure and Laser, Foundation for Research and Technology-Hellas, Heraklion Crete, Greece*

²*Department of Physics, University of Crete, Heraklion Crete, Greece*

³*Department of Materials Science and Technology, University of Crete, Heraklion Crete, Greece*

⁴*Department of Chemistry, University of Crete, Heraklion Crete, Greece*

Superhydrophobic surfaces have attracted significant scientific interest due to their importance in both fundamental research and practical applications [1, 2]. In this work, the development of a superhydrophobic and in certain cases water repellent surface is reported utilizing a simple, fast and economical way [3]. The material used was a smooth Ti6Al4V metal alloy that is widely utilized in several applications however its surface is considered hydrophilic. The surface of the material was initially irradiated by a femtosecond (fs) laser, without following a specific pattern, in order to acquire the necessary roughness. Following the irradiation, the effect of different parameters like temperature, pressure as well as residence time under heating or vacuum on the surface properties was investigated and the results were compared to the respective ones of a smooth surface. Contact angle and contact angle hysteresis measurements were performed to evaluate the wetting properties. The surface morphology was imaged by Scanning Electron Microscopy (SEM) whereas the surface chemical composition was evaluated by Energy Dispersive X-Ray spectroscopy (EDS). A just-irradiated surface exhibits superhydrophilic behavior, nevertheless its residence in an oven at different temperatures results in an alteration of its surface characteristics and in the manifestation of a hydrophobic behavior especially for temperatures higher than 120°C. A similar effect was observed in the case that an irradiated surface was placed in a vacuum chamber (pressure 10⁻² mbar); after a minimum of 3 hours the surface was converted to a superhydrophobic one, which additionally possessed water repellent properties, exhibiting very high contact angle and very low contact angle hysteresis. The observed behavior can be understood if one considers the change in the surface morphology and surface chemical composition.

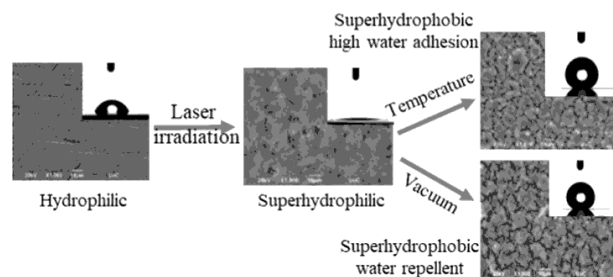


Figure 1: Schematic representation of the surface modification procedure.

References:

- [1] S. H Anastasiadis, *Langmuir* **29**, 9277–9290, (2013).
- [2] L. R. J Scarratt, U. Steiner and C. Neto, *Adv. Colloid Interface Sci.* **246**, 133–152 (2017).
- [3] F. Gojda, M. Loulakis, L. Papoutsakis, S. Tzortzakis, K. Chrissopoulou and S. H. Anastasiadis, *Langmuir* **38**, 4826-4838, (2022).

Polymer / Graphene Oxide Nanocomposites: Investigating the Effect of the Interfacial Interactions on Structure and Properties

I. Karnis ^{1,2*}, F. Krasanakis ¹, A. N. Rissanou ¹, K. Chrissopoulou ¹

¹*Institute of Electronic Structure and Laser, Foundation for Research and
Technology Hellas, Heraklion, Crete, Greece*

²*Department of Chemistry, University of Crete, Heraklion Crete, Greece*

K. Karatasos ³

³*Department of Chemical Engineering, Aristotle University of Thessaloniki,
Thessaloniki, Greece*

Polymer nanocomposites have been in the focus of interest of the research community due to their improved properties compared to the ones of the pure polymers. In this work, nanohybrids which consist of hyperbranched polymers of different generation and graphene oxides (GO) with different degree of oxidation were developed in a broad range of compositions to investigate the effect of the varying polymer/GO interactions on the final material structure and properties. Initially, the change of the GO oxidation degree was achieved by altering either the oxidation time or the mass of the oxidation agent, however it is only the latter that is found to play a role on the hybrid structure. Subsequently, nanohybrids were synthesized utilizing hyperbranched polyester polyols and the GOs with varying oxidation degrees. A gradual change from a phase separated to a fully intercalated structure was obtained using X-ray diffraction (XRD), as shown in Figure 1. Moreover, Differential Scanning Calorimetry (DSC) and Thermogravimetric Analysis (TGA) measurements revealed that the nanohybrids thermal properties were affected by the nanocomposite structure as well as the composition since there is a significant effect on the thermal transitions, the thermal stability of the polymer and on the reduction temperature of the GO.

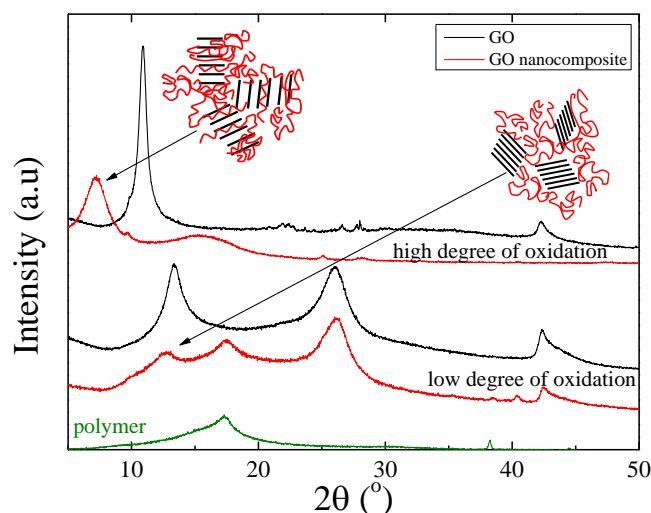


Figure 1: X-ray diffraction measurements of nanohybrids composed of GO of different degree of oxidation. The neat materials are shown as well.

Acknowledgements

This research has been co-financed by Greece and the European Union (European Social Fund- ESF) through the Operational Programme «Human Resources Development, Education and Lifelong Learning 2014-2020» in the context of the project "POLYGRAPH" (MIS 5050562).

*gkarnis@iesl.forth.gr

Photochemically doped MoSe₂ monolayers

D. Katrisioti^{1,2,*}, E. Katsipoulaki^{1,3}, E. Stratakis^{1,3}, and G. Kioseoglou^{1,2}

¹FORTH/IESL, Heraklion, 71110, Crete, Greece

²Department of Materials Science and Technology, University of Crete, Heraklion, 71003 Crete, Greece

³Department of Physics, University of Crete, Heraklion, 71003, Crete, Greece

The discovery of graphene [1] has created a new class of materials, the so-called two-dimensional (2D) materials, with such strong optical properties. Transition metal dichalcogenides (TMDs) have the form of MX₂ (where M=Mo or W and X=S, Se, Te). The fact that these indirect band gap bulk crystals are transformed to direct band gap semiconductors at their monolayer form [2-3], makes them the forefront of research for many optoelectronic applications. Here, monolayers of molybdenum diselenide (MoSe₂) are investigated after photochemical doping with spectroscopic methods such as photoluminescence, differential reflectivity, Raman spectroscopy and spin valley polarization. This doping process includes UV laser irradiation at chlorine environment that leads to an e-density reduction (p-type doping) on MoSe₂, as predicted from theory [4]. The PL can be significantly enhanced after photochlorination and it is dominated by the neutral exciton emission (Fig.1a) as a consequence of the adsorption of electron-withdrawing chlorine adatoms that strongly suppress the electron concentration. Differential reflectivity measurements performed in the same monolayer are in remarkable agreement with the micro-PL data (Fig.1b).

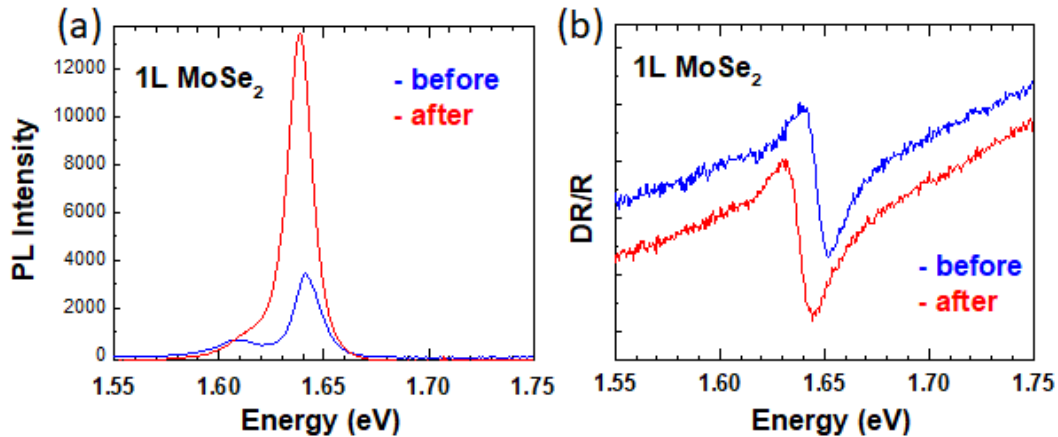


Figure 1: Photoluminescence (a) and differential reflectivity (b) spectra taken at 78K, before (blue curve) and after (red curve) photochlorination treatment. The PL is significantly enhanced after photochlorination and it is dominated by the neutral exciton emission.

Acknowledgements

Authors acknowledge financial support from the Hellenic Foundation for Research and Innovation (H.F.R.I.) under the 'First Call for H.F.R.I. Research Projects to support Faculty members and Researchers and the procurement of high-cost research equipment grant' project No: HFRI-FM17-3034.

References

- [1] K.S. Novoselov, et al., *Science* **306**, 666 (2004)
- [2] S.K. Geim and I. Grigorieva, *Nature* **499**, 419 (2013)
- [3] K.F. Mak and J. Shan, *Nat. Photonics* **10**, 216 (2016)
- [4] Y. Guo, et al., *AIP Advances* **9**, 025202 (2019)

* danai_kat@materials.uoc.gr

Control of electron density in WSe₂ monolayers via photochlorination

E. Katsipoulaki^{1,2,*}, I. Demeridou^{1,2}, E. Stratakis^{1,2}, and G. Kioseoglou^{1,3,*}

¹ FORTH/IESL, Heraklion, 71110, Crete, Greece

² Department of Physics, University of Crete, Heraklion, 71003, Crete, Greece

³ Department of Materials Science and Technology, University of Crete, Heraklion, 71003

Transition Metal Dichalcogenides (TMDs) of the form MX₂ (where M=Mo or W and X=S, Se, Te), are a special class of 2D-layered materials [1]. Unlike their 3D-counterparts that are indirect gap semiconductors, single layers of MX₂ have a direct-gap, with tremendous consequences in the PL quantum yield [2]. In addition, TMDs are characterized by valley dependent optical selection rules that make them ideal candidates to store and process quantum information (valleytronics), due to broken inversion symmetry in combination with time reversal symmetry [3,4]. In this work, the effect of doping (i.e., the electron/hole density) on the optoelectronic properties of single layers of WSe₂ is investigated. Photochemical doping is realized by intense UV laser pulses in a gas environment that provides the dopant atoms or molecules. By controlling systematically, the irradiation parameters, it is possible to control the doping level and consequently the electronic band structure of the monolayer crystal [5]. In the case of WSe₂, photochlorination induces n-type doping that is a partially reversible process achieved by a raster scanning procedure using a continuous wavelength laser. In addition, a significant increase in the spin valley polarization was achieved in accordance with an increase of the electron density after the photochemical doping [6,7].

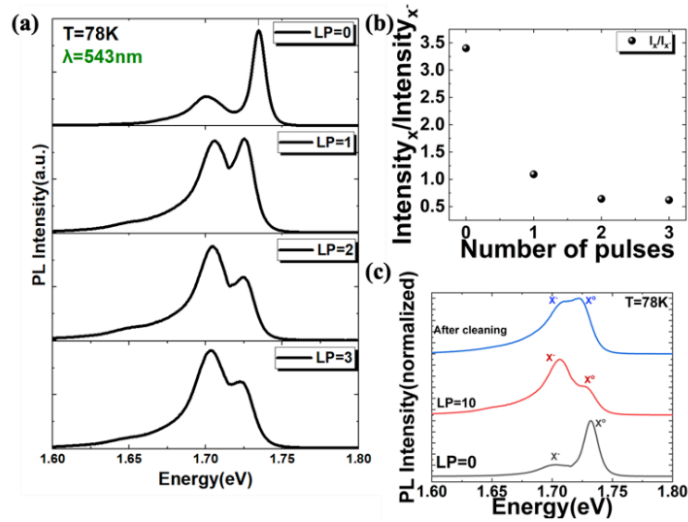


Figure 1: (a) Evolution of the PL spectra of 1L-WSe₂ at 78K, with the number of UV pulses. (b) The ratio of normalized intensities of the X and X* peaks as a function of the number of UV pulses, at 78K. (c) PL spectra of a pristine 1L-WSe₂ (grey curve), photochlorinated for 10 UV pulses (red curve) and dechlorinated (blue curve), at 78K.

Acknowledgements

E.K acknowledge support by the European Regional Development Fund of the European Union and Greek national funds through the Operational Program Competitiveness, Entrepreneurship and Innovation, under the call RESEARCH – CREATE – INNOVATE (SMARTPACK). I.D. acknowledge support by the European Union’s Horizon 2020 research and innovation program through the project NEP, EU Infrastructure, GA 101007417 – INFRAIA-03-2020 and by the synergy grant SPIVAST funded by FORTH. G. Kio., acknowledge funding by the Hellenic Foundation for Research and Innovation (H.F.R.I.) under the ‘First Call for H.F.R.I. Research Projects to support Faculty members and Researchers and the procurement of high-cost research equipment grant’ project No: HFRI-FM17-3034.

References

- [1] K. Novoselov, et al. *Proc. Natl. Acad. Sci* **102**, 10451 (2005); [2] K.F. Mak, et al. *PRL* **105**, 136805 (2010); [3] G. Kioseoglou, et al. *APL* **101**, 221907 (2012); [4] K.F. Mak, et al. *Nat. Nanotechnology* **7**, 494 (2012); [5] I. Demeridou, et al. *2D Materials* **6**, 015003 (2018); [6] I. Demeridou, et al. *APL* **118**, 123103 (2021); [7] S. Konabe, *APL* **109**, 07310 (2016).

* ekatsip@physics.uoc.gr

SiNWs/Ag nanostructures fabricated by a single step MACE process for the detection of biological substances

I. Kochylas, M.A.Apostolaki, V.Likodimos, S.Gardelis

Section of Condensed Matter Physics, Department of Physics, National and Kapodistrian University of Athens, Panepistimiopolis, 15 784, Greece

A.Dimitriou, L.Patsiouras, M.C. Skoulikidou, N.Papanikolaou

Institute of Nanoscience and Nanotechnology, National Center for Scientific Research "Demokritos", 15341 Agia Paraskevi, Athens, Greece

G.Geka, A.Kanioura, P.Petrou

Institute of Nuclear & Radiological Sciences & Technology, Safety & Energy, National Center for Scientific Research "Demokritos", 15341 Agia Paraskevi, Athens, Greece

Silicon nanowires (SiNWs) made by metal-assisted chemical etching (MACE) produce 3D surfaces offering a high surface-to-volume ratio with numerous applications in photonics, photovoltaics, nanoelectronics and sensor applications [1]. In the present work, we developed SiNWs by MACE and decorated them with silver nanoparticles in order to explore their potential as active substrates for sensitive molecule detection by Surface-Enhanced-Raman-Scattering (SERS) and Photoluminescence (PL) taking advantage of the local electric field enhancement within the nanogaps between silver nanoparticles [2]. The right choice of the laser wavelength and the metal determines the optimal enhancement in both techniques as the excited plasmons must be at resonance with the laser wavelength. In order to evaluate the substrates' performance, SERS measurements were carried out for two oxidative stress markers Glutathione (GSH) and Malondialdehyde (MDA). The substrates demonstrate strong SERS signals at low concentrations of the substances under investigation. Furthermore, PL measurements were carried out for the immunochemical detection cancer biomarker CA-125. Our results show that Ag decorated SiNWs fabricated by MACE offer a promising substrate for SERS and PL detection of biological analytes



Figure 1: SEM images of the silver nanoparticles grown on SiNWs.

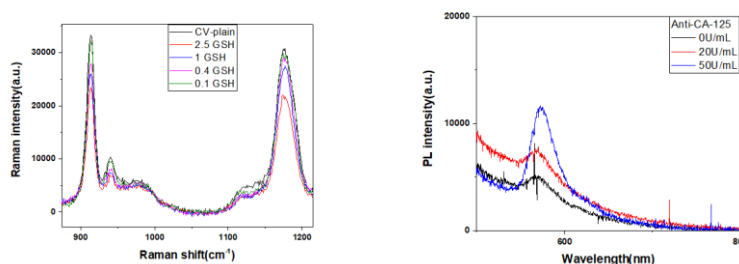


Figure 2: a) Raman spectra of GSH, b) PL spectra of Anti-CA-125

References

- [1] I. Kochylas, S.Gardelis, V.Likodimos, K.P.Giannakopoulos, P.Falaras, A.G. Nassiopoulou, *Nanomaterials* 11 (2021) 1760
- [2] Q. Fu, D. Zhang, Y. Chen, X. Wang, L. Han, L. Zhu, P. Wang and H. Ming, *Appl. Phys. Lett.* xxx (2013)

* gianniskohilas@gmail.com

Identification of non-uniform strain in WS₂ monolayers using P-SHG

G. Kourmoulakis^{1,2,*}, S. Psilodimitrakopoulos^{1*}, G. M. Maragkakis^{1,3},
L. Mouchliadis¹, A. Michail^{4,5}, J. A. Christodoulides⁶, J. Parthenios⁵,
K. Papagelis^{5,7}, E. Stratakis^{1,3*}, and G. Kioseoglou^{1,2}

¹ FORTH/IESL, Heraklion, 71110, Crete, Greece

² Dept. of Materials Science and Technology, Univ. of Crete, Heraklion, 71003 Crete, Greece

³ Department of Physics, University of Crete, Heraklion Crete 71003, Greece

⁴ Department of Physics, University of Patras, Patras, 26504, Greece

⁵ FORTH/ICE-HT, Stadiou str Platani, Patras 26504 Greece

⁶ Naval Research Laboratory, 4555 Overlook Ave SW, Washington, DC 20375-5320, U.S.A

⁷ School of Physics, Dept. of Solid-State Physics, Aristotle University of Thessaloniki

Strain in Transition Metal Dichalcogenide (TMD) monolayers (ML) changes the interatomic distances and the band structure, providing a new degree of freedom that allows manipulating their electronic properties, introducing the field of straintronics. Having an all-optical, minimally-invasive tool that rapidly probes strain in large areas of TMD MLs, would be of great importance in the research and development of novel 2D devices [1-3]. Here, we use polarization-resolved second harmonic generation (P-SHG) optical imaging to identify strain, induced in a single, spatially differentiated WS₂ ML placed on a pre-patterned Si/SiO₂ substrate with cylindrical wells. By fitting the P-SHG data pixel-by-pixel, we produce spatially resolved images of the crystal armchair direction. In the regions where the WS₂ monolayer is under non-uniform strain, we reveal a characteristic cross-shaped pattern in the armchair image. The presence of strain in these regions is independently confirmed using combination of atomic force microscopy and Raman mapping.

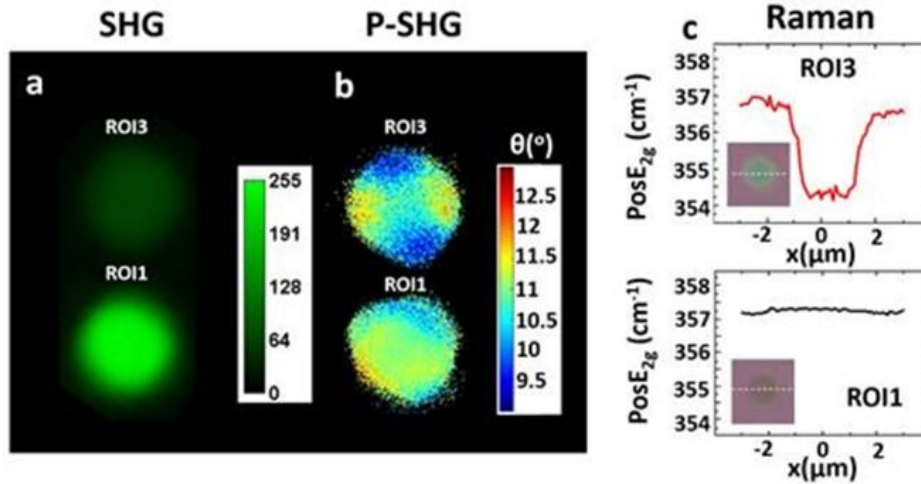


Figure 1: a) SHG intensity color map of strained (ROI3) and suspended (ROI1) ML WS₂, b) P-SHG color map of the corresponding crystal armchair orientation for the two ROIs, and c) Raman mapping for same ROIs: strained (ROI3) and suspended (ROI1)

Acknowledgements

G. Ko., L.M. and G. Kio., acknowledge funding by the Hellenic Foundation for Research and Innovation (H.F.R.I.) under the ‘First Call for H.F.R.I. Research Projects to support Faculty members and Researchers and the procurement of high-cost research equipment grant’ project No: HFRI-FM17-3034. AM, JP, and KP acknowledge financial support by the synergy grant SPIVAST funded by Foundation for Research and Technology Hellas

References

- [1] L. Mennel et al., Nat Comm 9, 516 (2018)
- [2] K. Beach et al., Phys Rev B 101, 155431 (2020)
- [3] J. Liang et al., Nano Lett, 17, 7539 (2017)

*) geokourm@iesl.forth.gr

Enhancing of CO uptake in Metal-Organic Frameworks by linker functionalization; A Multi-scale theoretical study

C.G. Livas*, G.E. Froudakis

*Department of Chemistry, Voutes Campus, University of Crete, GR-71003
Heraklion Crete, Greece*

E. Tylianakis

*Department of Materials Science and Technology, Voutes Campus, University of
Crete, GR-71003 Heraklion Crete, Greece*

MOFs are one of the most promising materials for gas adsorption, owing their big scientific interest to their intrinsic properties such as their large surface areas and porosity. The purpose of this study was to propose new materials for high Carbon Monoxide (CO) adsorption. Initially, the interaction strength of CO with a set of 42, strategically selected, functionalized benzenes was calculated in the MP2/6-311++G** level of theory [1]. Our results reveal that phenyl hydrogen sulfate (-OSO₃H) showed the highest interaction with CO (-19.5 kJ/mol), approximately 3 times stronger compared with the unfunctionalized benzene (-5.3 kJ/mol) [2]. Moreover, the three top-performing functional groups (-OSO₃H, -OPO₃H₂, -SO₃H) were selected to modify the organic linker of IRMOF-8 and test their ability to capture CO at 298K for a wide pressure range. Our Grand Canonical Monte Carlo (GCMC) simulations showed a significant increase in the CO uptake in the functionalized MOFs, compared with the parent IRMOF-8. Distinctive is that for the volumetric uptake a 60x increase was observed at 1 bar and 2x at 100 bar. The proposed functionalization strategy can be applied for improving the CO uptake performance not only in MOFs but also in various other porous materials.

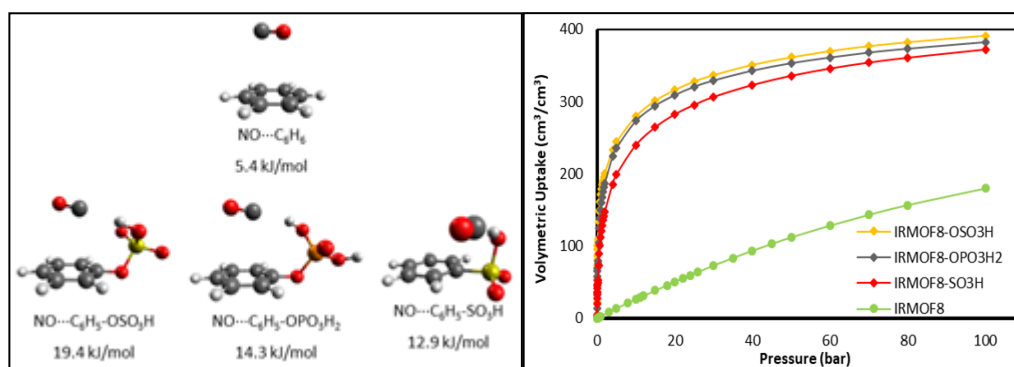


Figure 1: Left: Optimized geometries and the corresponding binding energies of the C₆H₅-X (X: -H, -OSO₃H, -OPO₃H₂, -SO₃H) calculated at the MP2/6-311++G** level of theory, Right: Absolute Volumetric isotherms for IRMOF8 and IRMOF8-n (n: -OSO₃H, -OPO₃H₂, -SO₃H) at T=298 K and pressure ranges up to 100 bar

References

- [1] C. Møller and M. S. Plesset, Phys. Rev. 46, 618 (1934).
- [2] C.G. Livas, E. Tylianakis, G.E. Froudakis Chemistry 4, 603-614 (2022).

* livas.charalampos@gmail.com

Development of TiO₂/MOF Nanostructured Composites Towards Photocatalytic Hydrogen Conversion

E. Loukopoulos^{*1}, M. Charalampakis^{1,2}, K. Papadopoulos¹, E. Skliri², V. Binas²,
P. N. Trikalitis¹

¹Department of Chemistry, University of Crete, Heraklion 70013, Greece

ptrikal@uoc.gr

²Institute of Electronic Structure and Lasers (IESL), FORTH, Heraklion, Greece

binasbill@iesl.forth.gr

The emergence of hydrogen as a potential green and renewable fuel has provided an ideal solution to address the global challenges towards clean forms of energy. Solar-driven, photocatalytic water splitting is one of the most promising and sustainable methods for H₂ production and has received considerable attention due to its simplicity and cost-effective design [1]. In the constant search for potential photocatalytic systems, porous metal-organic frameworks (MOFs) display large promise [2], as their high porosity, stability and hybrid inorganic-organic nature are important assets towards the formation of stable heterostructured composites with improved photocatalytic activity.

In this work, we report the preparation of several TiO₂/MOF nanostructured composites (Figure 1) and the investigation of their photocatalytic hydrogen conversion performance, using MIL-101 (Cr) as the MOF template. The materials have been characterized through an extensive series of techniques including X-Ray diffraction measurements, SEM/EDS studies, as well as gas sorption experiments with accurate porosity measurements, demonstrating the incorporation of TiO₂ within the framework. Photocatalytic experiments for hydrogen production by water splitting were then carried out in the solar light radiation spectrum using a solar simulator. The evolved gas was analysed using a Shimadzu gas chromatographer (GC) to evaluate their photocatalytic activity.

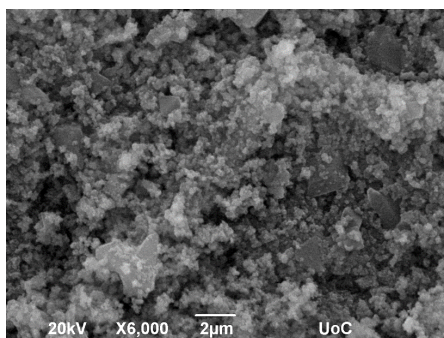


Figure 1: Representative SEM image of the synthesized TiO₂/MIL-101 nanostructured composites in this work.

References

- [1] H. Ahmad, S. K. Kamarudin, L. J. Minggu, M. Kassim, *Renew. Sustain. Energy Rev.* **43**, 599 (2015).
- [2] L. H. Nguyen, *Adv. Materials* **34**, 2200465 (2022).

Acknowledgements

This research work was supported by the “Water2Hy” program titled “A novel and rational design of surface and interface oriented heterostructures for sustainable solar-driven photocatalytic hydrogen conversion” part of the Bilateral and Multilateral S&T Cooperation Greece-China (Code: T7ΔKI-00369).

Heterostructured Au/Ag-MoS₂-TiO₂ inverse opal photocatalysts

S. Loukopoulos^{*}, S. Gardelis, V. Likodimos

Section of Condensed Matter Physics, Department of Physics, National and Kapodistrian University of Athens, Athens, Greece

Z. Sideratou, F. Katsaros, E. Sakelis, A. G. Kontos

Institute of Nanoscience and Nanotechnology, National Center for Scientific Research "Demokritos", Athens, Greece

Heterostructured Au/Ag-MoS₂-TiO₂ inverse opal photonic films were fabricated using the evaporation induced co-assembly of polystyrene colloidal spheres with a hydrolysed Ti alkoxide precursor, MoS₂ nanosheet and Au/Ag nanoparticle suspensions, in order to enhance the photocatalytic activity of TiO₂ in the visible range, where titania is inactive because of its wide band gap [1]. Liquid cascade centrifugation was used in order to select MoS₂ nanosheets of smaller sizes [2], which were then loaded on the mixed precursor at variable amounts. SEM measurements showed that low concentrations of MoS₂ during synthesis preserve the integrity of the inverse opal structure (Figure 1). The incorporation of MoS₂ and Au/Ag nanoparticles in the nanocrystalline TiO₂ skeletal walls was investigated by TEM, EDX, and Raman measurements. Photoluminescence and electrochemical measurements were employed to evaluate charge transfer for MoS₂-TiO₂ in combination with plasmonic effects. Specular reflectance measurements showed that controlling the inverse opal diameter can fine-tune the photonic band gap position, allowing to combine photonic amplification with the optimal film composition that maximizes photocatalytic performance for salicylic acid degradation.

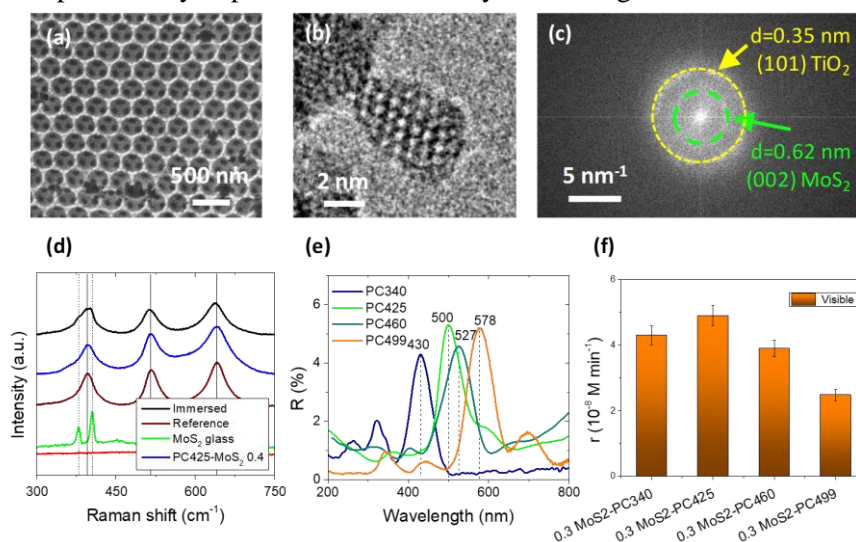


Figure 1: (a) SEM and (b) TEM images for PC425-MoS₂ inverse opals and (c) the corresponding FFT pattern. (d) Raman and (e) specular reflectance spectra of MoS₂-TiO₂ films. (f) Reaction rates of salicylic acid degradation under visible light.

Acknowledgements

The research work was supported by the Hellenic Foundation for Research and Innovation (H.F.R.I.) under the "First Call for H.F.R.I. Research Projects to support Faculty members and Researchers and the procurement of high-cost research equipment grant" (Project Number: 543).

References

- [1] V. Likodimos, Appl. Catal. B Environ. **230**, 269 (2018).
- [2] K. Synnatschke, P. A. Cieslik et al., Chem. Mater. **31**, 10049 (2019).

^{*} sloukop@phys.uoa.gr

Study of the thermochromic performance of hydrothermally synthesized Vanadium dioxide powder for energy efficient buildings

E. Gagaoudakis^{1,*}, **E. Mantsiou**¹, L. Zouridi^{1,2}, X. Maragaki^{1,3}, E. Aperathitis¹, G. Kiriakidis¹, V. Binas^{1,3}

¹*Institute of Electronic Structure & Laser, Foundation for Research and Technology (FORTH-IESL), Heraklion, Greece*

²*Department of Materials Science and Technology, University of Crete, Heraklion, Greece*

³*Department of Physics, University of Crete, Heraklion, Greece*

Thermochromic materials are known to modify their optical properties upon heating. Vanadium dioxide (VO₂) is by far the most studied thermochromic material, undertaking a first order Metal to Insulator Transition-MIT at a critical transition temperature of T_C = 68°C, close to room temperature. This electrical transition is accompanied by structural as well as optical changes. Thus, it can be used in numerous applications such as thermochromic coating on “smart” windows, thermal switch in electronic circuits, etc. [1]. VO₂ in powder form can be potentially used as a thermochromic coating in polymer matrix [2] as well as in thermochromic paints. In the present work, the thermochromic performance of hydrothermally synthesized VO₂ powder was investigated. In particular, the effect of the reducing agent during synthesis and the duration of post-processing ball-milling on the thermochromic properties were studied. X-Ray Diffraction (XRD), Scanning Electron Microscopy (SEM) and Differential Scanning Calorimetry (DSC) characterization techniques were employed to determine the structure, morphology and thermochromic performance of VO₂, respectively. Oxalic acid, among other reducing agents, was found to be the reducing agent that led to VO₂ powders with the better thermochromic performance. Moreover, the duration of the post-processing ball-milling seems to strongly affect the morphology (Fig. 1) as well as the thermochromic properties of synthesized VO₂.

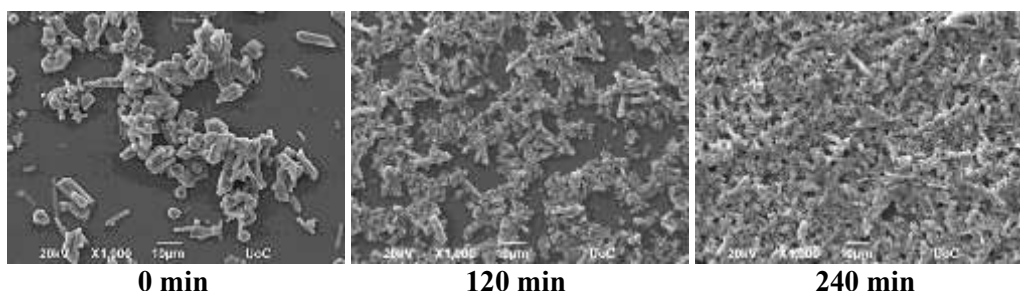


Figure 1: Effect of the ball-milling duration on the morphology of hydrothermally synthesized VO₂ powders.

Acknowledgements

This work was supported by LIFE VISIONS project (LIFE19 ENV/GR/000100) with the contribution of the LIFE Programme of the European Union. This work reflects only the authors' view and CINEA is not responsible for any use that may be made of the information it contains. This research is co-financed by Greece and the European Union (European Social Fund- ESF) through the Operational Programme «Human Resources Development, Education and Lifelong Learning» in the context of the project “Reinforcement of Postdoctoral Researchers - 2nd Cycle” (MIS-5033021), implemented by the State Scholarships Foundation (IKY).

References

- [1] P. Kiri, G. Hyett, and R. Binions, (2010), *Adv. Mat. Let.* 1(2): 86–105.
- [2] M. Xygkis, E. Gagaoudakis, L. Zouridi, O. Markaki, E. Aperathitis, K. Chrissopoulou, G. Kiriakidis, V. Binas, (2019), *Coatings* 9: 163

*mgagas@iesl.forth.gr

Nonlinear Optical Imaging of In-Plane Anisotropy in Two-Dimensional SnS

George Miltos Maragkakis^{1,2*†}, Sotiris Psilodimitrakopoulos^{1†}, Leonidas Mouchliadis¹, Abdus Salam Sarkar¹, Andreas Lemonis¹, George Kioseoglou^{1,3}, and Emmanuel Stratakis^{1,2}

¹FORTH/IESL, Heraklion, 71110, Crete, Greece

²Department of Physics, University of Crete, Heraklion, 71003, Crete, Greece

³Department of Materials Science and Technology, University of Crete, Heraklion, 71003

Two-dimensional (2D) tin(II) sulfide (SnS) crystals are orthorhombic, semiconducting group IV monochalcogenides, which are characterized by remarkable properties, such as in-plane anisotropic optical and electronic response [1]. This anisotropic response is exhibited along the in-plane armchair (AC) and zigzag (ZZ) crystallographic directions, offering an additional degree of freedom in manipulating their behavior [1]. Here, we perform polarization-resolved second harmonic generation (P-SHG) nonlinear imaging on liquid phase exfoliated SnS containing monolayer and bilayer crystals [2, 3], which lack inversion symmetry and produce SHG [4, 5]. We fit pixel-by-pixel the P-SHG experimental data with a nonlinear optics model, that allows us to calculate and map with high-resolution the AC/ZZ direction of several 2D SnS flakes belonging in the same field of view [2]. It is found that the P-SHG intensity polar patterns are associated with the crystallographic axes of the flakes and with the relative strength of the second order nonlinear susceptibility tensor in different directions. Therefore, our method provides quantitative information of the optical in-plane anisotropy of orthorhombic 2D crystals [2], offering great promise for performance characterization during device operation in the emerging optoelectronic applications of such crystals.

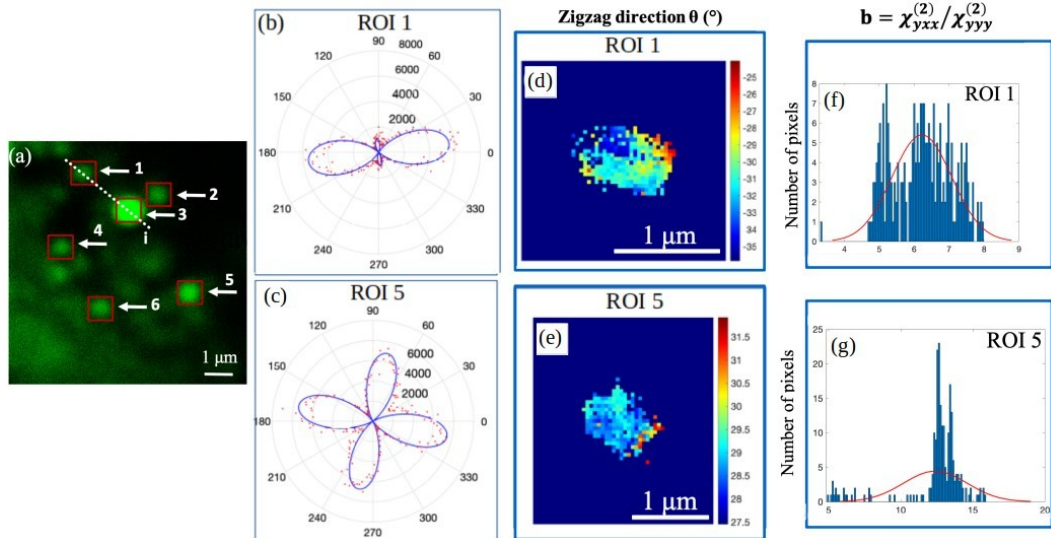


Figure 1: (a) SHG image of 2D SnS crystals. (b, c) Experimental data (in red dots) and fitting (blue line) of the P-SHG intensity, for the ultrathin SnS crystals 1, 5 depicted in (a). The P-SHG intensity is presented in polar plots as function of the linearly polarized excitation angle. (d, e) Pixel-by-pixel spatially resolved mapping of the ZZ crystallographic direction, and (f, g) histograms of the fitted $\chi^{(2)}$ parameter b , for the ultrathin SnS crystals 1, 5 depicted in (a).

Acknowledgments

† These authors contributed equally to this work. This research is co-financed by Greece and the European Union (European Social Fund-ESF) through the Operational Programme "Human Resources Development, Education and Lifelong Learning 2014-2020" in the context of the project "Crystal quality control of two-dimensional materials and their heterostructures via imaging of their non-linear optical properties" (MIS 5050340). This work was supported by the European Project TINKER (grant agreement n°958472) funded from the European Union's Horizon 2020 research and innovation program. This work has been supported by the EU's H2020 framework programme for research and innovation under the NFFA-Europe-Pilot project (Grant No. 101007417).

References

- [1] A. S. Sarkar & E. Stratakis. *Adv. Sci* **7**, 21, 2001655 (2020); [2] G. M. Maragkakis, et al. *Adv. Optical Mater.* **10**, 10, 2270038 (2022); [3] A. S. Sarkar, et al. submitted; [4] H. Wang & X. Qian. *Nano Lett.* **17**, 8, 5027-5034 (2017); [5] Zhu M., et al. *Adv. Optical Mater.* **9**, 22, 2101200 (2021).

* gmaragkakis@physics.uoc.gr

Ferromagnetic Resonance in Ru/Co/MoPt multilayers

P. Ntetsika^{1*}, R. Gupta², R. Brucas², P. Svedlindh², G. Mitrikas³,
I. Panagiotopoulos¹

¹ Department of Materials Science and Engineering, University of Ioannina, Ioannina 45110, Greece

² Department of Engineering Sciences, Uppsala University, Box 534, SE-751 21 Uppsala, Sweden

³ Institute of Nanoscience and Nanotechnology, National Centre for Scientific Research-Demokritos, Athens, Greece

Introduction

Synthetic antiferromagnets (SAFs) are based on the oscillatory RKKY interlayer exchange coupling of thin magnetic layers through metal, via the conduction electrons [1]. The low field tunability of the magnetic state in SAFs opened the route to spintronic devices [2]. It is the same tunability that makes them attractive for other applications such as tunable magnonics [3] and terahertz nano-oscillators [4]. In Ru/Co multilayers with in plane anisotropy we have observed hybridized modes of mixed optic-acoustic character. Here we extend the study to a perpendicular anisotropy system Ru/Co/MoPt.

Experimental Methods – Results

The multilayered $[\text{Ru}_6/\text{Co}_x/\text{MoPt}_4]_{12}$ (with $x=12-16$ Å) films have been deposited on rotating substrates, at room temperature by magnetron sputtering. The hysteresis loops show a weak perpendicular anisotropy with a smeared spin-flop transition about 5kOe. Angle dependent cavity FMR results support the conclusion that the samples exhibit a canted AF state up to 14kOe.

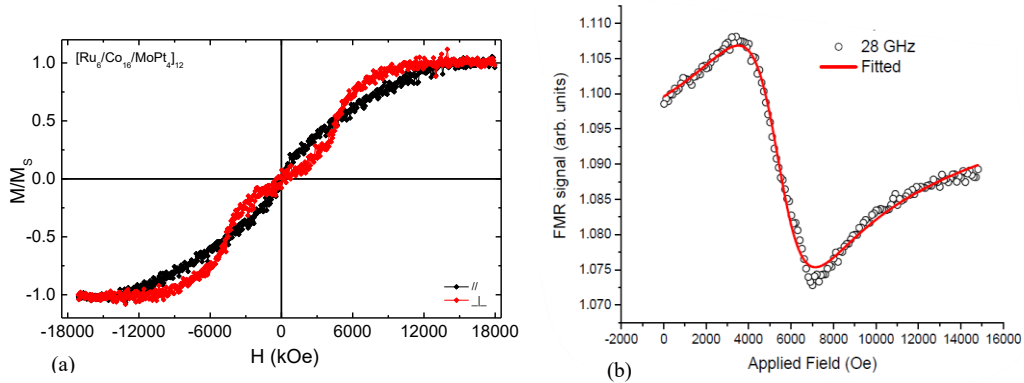


Figure 1: Typical (a) VSM magnetization curves and (b) FMR spectra for $[(\text{Ru}_6/\text{Co}_{16}/\text{MoPt}_4)_{12}]$ sample.

Acknowledgements

P. Ntetsika acknowledges funding by the Hellenic Foundation for Research and Innovation (HFRI) under the 3rd Call for HFRI PhD Fellowships (Fellowship Number: 5383).

References

- [1] P. Ntetsika, G. Mitrikas, G. Litsardakis, I. Panagiotopoulos, *Mater. Adv.*, **10**, 1039 (2022).
- [2] A. Fert, *Rev. Mod. Phys.*, **80**, 1517 (2008).
- [3] M. Ishibashi, Y. Shiota, T. Li, S. Funada, T. Moriyama, and T. Ono, *Science Advances*, **6**, 1-8 (2020).
- [4] T. Seki, H. Tomita, A. A. Tulapurkar, M. Shiraishi and T. Shinjo, *Appl. Phys. Lett.*, **94**, 212505 (2009).

* p.ntetsika@uoi.gr

Surface modification of Mo-BiVO₄ photonic crystal photocatalysts by Au and Ag plasmonic nanoparticles

M. Pylarinou*, S. Gardelis, V. Likodimos*

Section of Condensed Matter Physics, Department of Physics, National and Kapodistrian University of Athens, Athens, Greece

E. Sakellis, P. Tsipas, N. Boukos, A. Dimoulas

Institute of Nanoscience and Nanotechnology, National Centre for Scientific Research “Demokritos”, Athens, Greece

Bismuth vanadate (BiVO₄) has emerged as the most promising metal oxide photocatalyst for solar water splitting despite persistent electron-hole recombination and poor charge transport [1], which can be ideally combined with photonic crystals (PCs) structuring, metal doping and plasmonic nanoparticles to enhance light trapping, charge carrier generation and separation [2]. In this work, Mo-doped BiVO₄ inverse opals were surface modified by plasmonic Au and Ag nanoparticles in order to enhance visible light photocatalytic activity. Well-ordered Mo-doped BiVO₄ PC films were fabricated by the self-assembly of polystyrene spheres of different diameters and infiltration of appropriate metal salt precursor with the controlled addition of (NH₄)₆Mo₇O₂₄·4H₂O providing Mo⁶⁺ shallow donors substituting for V⁵⁺ cations, followed by calcination at 400 °C. Optimization of metal doping and light trapping was carried out using templating spheres of different diameters and Mo loadings evaluated on salicylic acid degradation after systematic investigation of their properties. TEM measurements along with elemental EDX mapping and XPS analysis identified the uniform distribution of metallic Ag (10 nm) and Au (5 nm) nanoparticles drop coated on the skeletal walls of the optimal Mo-BiVO₄-PC340 films. Diffuse reflectance spectra of the surface-modified PC films showed significant reduction of the reflectance peak due to the localized surface plasmon resonance, identified in the absorption spectra of the Ag and Au suspensions at 407 and 521 nm, respectively. Photocatalytic activity evaluation and photocurrent generation under visible light showed a marked enhancement for the Mo-BiVO₄ decorated by Au and Ag nanoparticles, respectively.

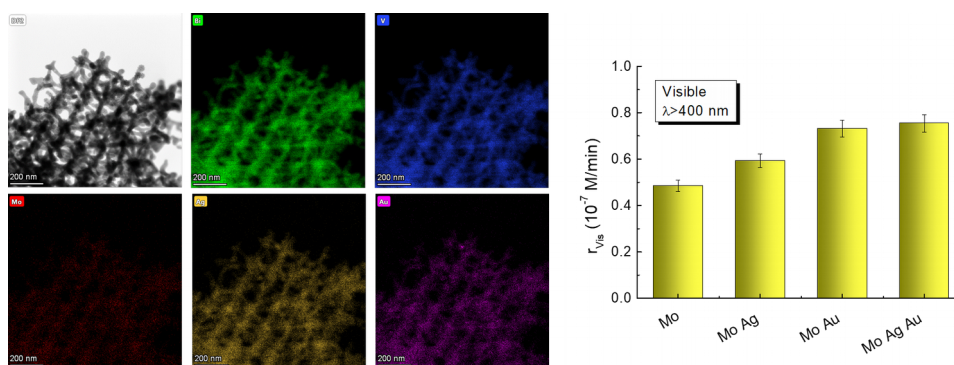


Figure 1: (left) TEM and EDX elemental maps of Ag-Au Mo-BiVO₄ PC340 inverse opal films and (right) salicylic acid degradation rates under visible light.

Acknowledgements

The research work was supported by the Hellenic Foundation for Research and Innovation (H.F.R.I.) under the “First Call for H.F.R.I. Research Projects to support Faculty members and Researchers and the procurement of high-cost research equipment grant” (Project Number: 543).

References

- [1] J. H. Kim, J. S. Lee, *Adv. Mater.* **31**, 1806938 (2019).
- [2] L. Zhang, C.-Y. Lin, V. K. Valev, U. Steiner, J. J. Baumberg, *Small* **10**, 3970 (2014).

* pylarin@phys.uoa.gr

Can accurate machine learning models pinpoint the best materials efficiently?

A.P. Sarikas*, G.S. Fanourgakis, G.E. Froudakis

Department of Chemistry, Voutes Campus, University of Crete, GR-71003
Heraklion Crete, Greece

The intrinsic properties of metal organic frameworks (MOFs), such as their large surface areas and porosity, render them as one of the most promising adsorbents for hydrogen storage systems. Additionally, their modular nature has led to an enormous expansion of the available material pool which in turns raises the question if an efficient identification of the best materials for a specific application, is feasible. In the recent years, Machine Learning (ML) techniques have been established as the main tool for the exploration of large material databases, since they can greatly accelerate this process. In this work, “traditional” ML models and self-consistent ML-based models [1] are compared with respect to their ability to efficiently pinpoint the best materials of a database. As a case study, we have used hydrogen adsorption in MOFs at different thermodynamic conditions. Despite their accuracy, traditional models struggle to identify the most promising materials without compromising computational cost. On the other hand, self-consistent models can even reduce by two orders of magnitude the amount of reference data required for the identification of the best materials compared to traditional approaches. Nevertheless, there are still factors that complicate the efficient pinpointing of novel materials.

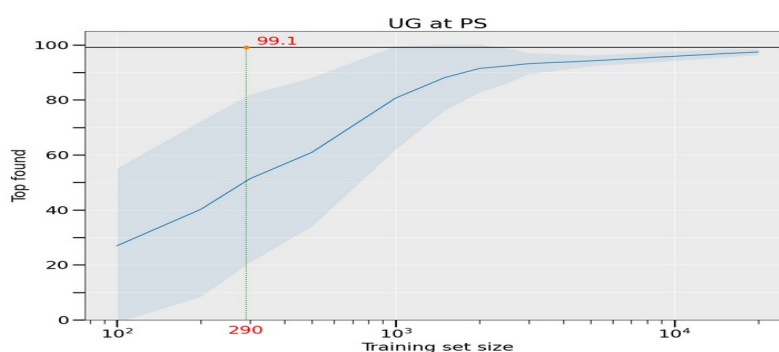


Figure 1: Blue line represents the number of the top 100 materials identified by the traditional model (y-axis) as function of the training set size (x-axis, logarithmic scale), while blue shaded area shows the respective standard deviation. The number of the top 100 materials that the SC model identifies and its training set size are represented by the black and green line, respectively (i.e. 290 materials are needed for training in order to identify 99 of the top 100 performing materials, while with traditional ML models you can find approximately 50 if using the same training set. Moreover, for obtaining 99 with traditional ML models you will need a training set of more than 10.000). UG and PS stand for usable gravimetric (capacity) and pressure-swing (conditions), respectively.

Acknowledgement

[1] This project has received funding from the European Union’s Horizon Europe research and innovation programme under grant agreement No 101058547 (MOST-H2).

References

[1] G. Fanourgakis, K. Gkagkas, E. Tylianakis and G. Froudakis, *The Journal of Physical Chemistry C*, **124**, 36 (2020).

* antonios.sarikas@gmail.com

Chemically modified carbon nanostructures as carriers of enhanced qualities for fabrics performing under critical operational conditions

Ioanna K. Sideri,^{a*} Antonia Kagkoura^a, Christina Stangel^a, Sozon Vasilakos^b,
Dionysios Siamidis^b, Silvia Pavlidou^c, Petros Perimenis^d, Nikolaos S.
Heliopoulos^d, Nikos Tagmatarchis^a

^aTheoretical and Physical Chemistry Institute, National Hellenic Research Foundation, 48 Vassileos Constantinou Avenue, Athens 11635, Greece.

^bSiamidis S.A., Industrial Zone, Inofita 32011 Viotia, Greece.

^cEBETAM A.E., Leoforos Eleftheriou Venizelou 4, 17676, Athens, Greece.

^d700 Military Factory, 18648, Piraeus, Greece

Hybridization of carbon nanostructures with fabric fibers enables the realization of multipurpose textiles featured in everyday life applications. [1] Herein, we strategically chemically modified carbon nanostructures to give them desired properties for their subsequent physisorption onto Kevlar, Nomex and VAR fibers. In detail, chitosan was utilized to provide antibacterial properties, benzotriazole for enhanced UV resistance and thiourea for flame retardancy (Figure 1). Following their complete characterization, the samples were tested for their ultraviolet radiation, flame retardant activity, and antibacterial properties respectively, validating our initial approach.[2] This work provides insights to the fabric industry in its quest to fulfil the current technical expectations on protective clothing and can bridge the gap between research and real life applications.

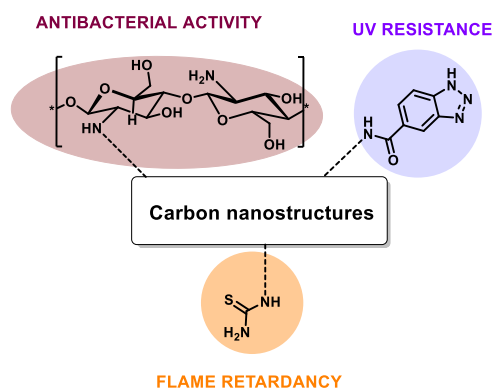


Figure 1: Chemically modified carbon nanostructures with enhanced UV resistance, flame retardancy and antibacterial activity.

Partial financial support by the European Regional Development Fund of the European Union and Greek national funds through the Operational Program Competitiveness, Entrepreneurship and Innovation, under the call RESEARCH-CREATE-INNOVATE (project code: T2EDK-01316) is acknowledged.

References

- [1] I. K. Sideri and N. Tagmatarchis, *Mater. Horiz.* **8**, 3187 (2021).
- [2] A. Kagkoura, C. Stangel, I. K. Sideri, R. Canton-Vitoria, S. Vasilakos, D. Siamidis, S. Pavlidou, N. Heliopoulos, P. Perimenis and N. Tagmatarchis, Manuscript in preparation.

* isideri@eie.gr

Highly active catalysts (Ni, Pt) supported on strontium titanate (SrTiO₃) for hydrogen evolution

A.P. Souri^{1,2*}, E. Skliri¹, I. Vamvasakis², G.S. Armatas², V. Binas^{1,3}

¹*Institute of Electronic Structure and Laser (IESL), FORTH, Vasilika Vouton, Heraklion, Greece*

²*Department of Material Science and Technology, University of Crete, Heraklion, Greece*

³*Department of Physics, University of Crete, Heraklion, Greece*

**asouri@materials.uoc.gr*

A critical point as far as energy consumption is concerned has been reached, thus clean and renewable energy sources are of paramount importance in order to meet the needs of the overgrown population. Photocatalytic water splitting is a safe and cost-effective way of converting solar energy into chemical fuels. Hydrogen (H₂) is thought of as a potentially important fuel because it is non-toxic, has high gravimetric energy density (~142 MJ/Jg) and can be produced utilizing renewable resources such as sunlight and water. In this regard, the research and development of robust and highly active semiconductor photocatalysts are of vital importance. Perovskite-type SrTiO₃ (STO) has been extensively studied as a photocatalytic water splitting semiconductor since it has a suitable conduction band edge position for water reduction and H₂ production. Furthermore, recent research has shown that the presence of co-catalysts such as metallic nanoparticles on the surface of STO is crucial to inhibit charge carrier recombination and improve photocatalytic hydrogen generation performance.^[1] More specifically, at the metal/semiconductor interface, a Schottky barrier is created that is responsible to assist transportation of electrons from the semiconductor to metal co-catalyst, which acts as an electron trap leading to improved H₂ evolution.

In this work, STO was successfully synthesized through hydrothermal polyol process and nanoparticles of Ni and Pt were deposited on its surface via a photochemical deposition method. A series of Pt and Ni-decorated STO materials with different wt% of metal loadings were synthesized. SEM and TEM images revealed the morphology of the prepared materials as well as the size of the deposited Ni and Pt nanoparticles. Moreover, UV-vis spectroscopy highlights the enhancement in the absorption towards the visible region of the spectrum. Photocatalytic experiments for hydrogen evolution were performed in an airtight Pyrex glass reactor using a 300 W Xe lamp as the irradiation source. The evolved gas was analysed using a gas chromatograph equipped with a thermal conductivity detector. The catalytic results indicated that the Pt/STO catalyst with 0.1% Pt reached a rate of 294 $\mu\text{moles h}^{-1}$ whereas the sample with a 0.25% Ni loading reached a rate of 63 $\mu\text{moles h}^{-1}$ for H₂ evolution, demonstrating a 14x and 3x times enhancement in photocatalytic performance, respectively, compared to the pristine STO sample (21 $\mu\text{moles h}^{-1}$).

References

[1] I. Tamiolakis *et al.*, “Mesoporous implantable Pt/SrTiO₃:C,N nanocuboids delivering enhanced photocatalytic H₂-production activity via plasmon-induced interfacial electron transfer”, *Appl. Catal. B Environ.*, 2018, 236, 338–347.

Acknowledgements

This research work was supported by the “Water2Hy” program titled “A novel and rational design of surface and interface oriented heterostructures for sustainable solar-driven photocatalytic hydrogen conversion” part of the Bilateral and Multilateral S&T Cooperation Greece-China (Code: T7ΔKI-00369).

Room temperature synthesis of hydrophilic, highly-fluorescent metal halide perovskite nanocrystals for biomedical applications

M. Splinaki^{a,b}, A. Kostopoulou^a, K. Brintakis^a, E. Stratakis^a

^a*Institute of Electronic Structure and Laser, Foundation for Research & Technology-Hellas, P.O. Box 1527, Vassilika Vouton, 71110 Heraklion, Greece*

^b*University of Crete, School of Medicine
P.O. Box 2203, Vassilika Vouton, 71003 Heraklion, Greece*

Metal halide perovskite nanocrystals that have the chemical formula ABX_3 , where the “A”, “B” cations are located in corner positions of the unit cell and at the center of the cell respectively and “X” anion is situated at the unit cell faces, due to their interesting optical properties (high PLQY, narrow FWHM, intense fluorescence, tunable emission), are investigated as potential probes with high sensitivity and rapid sensing capability in the fields of bio-imaging, bio-sensing and drug delivery. Among the different chemical phases, the $CsPbBr_3$ all-inorganic perovskites has the highest luminescence and stability (Goldschmidt factor ~ 0.92), but still remain hydrophobic and unstable in biological buffers [1,2]. An effective way to overcome the previously addressed issues is the encapsulation of the fluorescent nanocrystals into an inert silica (SiO_2) shell which is non-toxic and transparent to visible spectrum. According to this, the aim of this research was to fabricate hydrophilic perovskite nanocrystals well dispersed in aqueous and biological media using room temperature protocols. Two different silica precursors were used in order to develop a robust SiO_2 shell around the perovskite cores ($CsPbBr_3$): TMOS ($Si(OCH_3)_4$) in which the hydrolysis takes place rapidly in four directions ($-OCH_3$) resulting in a denser matrix and MPTMS ($HS(CH_2)_3Si(OCH_3)_3$) with two functional groups, the $-OCH_3$ (hydrolysis \rightarrow denser shell) and $-SH$ ($-PbS$ bond \rightarrow stability between the shell and the core). The optimum precursor quantities as well as the appropriate order of the injection in the reactant solution were carefully investigated. The stability through the time of the-perovskite-based core-shell nanocrystals in water (Figure 1a-b) and biological buffer (Figure 1c) were studied through PL spectroscopy. The aqueous colloidal solutions remained PL active even after 7h. Transmission Electron Microscopy revealed the spherical $CsPbBr_3@SiO_2$ structures “bubble-like morphology”- where the perovskite nanocrystals were included.

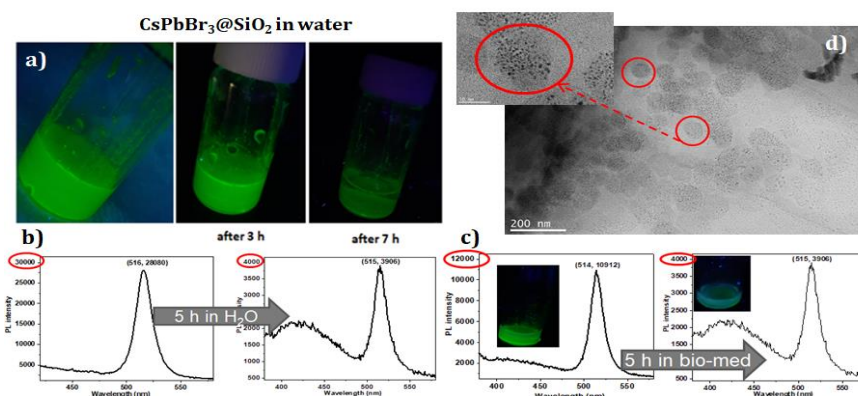


Figure 1: a) Aqueous dispersion of $CsPbBr_3@SiO_2$ nanoparticles upon time under UV lamp, b) PL spectra of the same solutions upon time, c) PL spectra of $CsPbBr_3@SiO_2$ nanoparticles in biological medium (HG DMEM with 10% FBS and 1% pIs), d) TEM images of $CsPbBr_3@SiO_2$ nanoparticles.

References

- [1] Hwang et al., *J Mater Chem C*, **6**, 972 (2018).
- [2] Lian et al. *Coordination Chemistry Reviews* **452**, 214313 (2022).

From Order to Disorder of Alkanethiol SAMs on Complex Au (211), (221) and (311) Surfaces: Impact of the Substrate

Dimitrios Stefanakis, Vangelis Harmandaris, Georgios Kopidakis, and Ioannis Remediakis

In our work, we investigate the impact of the substrate on the structural properties and the morphology of alkanethiol self-assembled monolayers (SAMs) on gold, using first principles calculations and atomistic molecular dynamics simulations. We consider hexadecanethiols on Au(211), Au(221) and Au(311) surfaces which contain few-atom wide terraces separated by monoatomic steps similar to the complex Au surfaces used in experiments. The structure of the SAMs is probed via several structural properties including tilt angles, mean C atom heights from the surface, precession angles, gauche defects, gyration tensors and relative shape anisotropy. Comparing these properties to those of the well-studied SAMs on Au(111), we observe similarities but also striking differences. A clear order to disorder transition is observed by changing the substrate: Well-ordered SAMs on (111) and (211) surfaces become mixed ordered-disordered structures on (311) and fully disordered on (221). The presence of steps on the Au surfaces also results in preferential tilt orientations with long-range order. Our results show that in addition to the expected grafting density dependence, the transition from order to disorder crucially depends on substrate morphology. The onset of ordering behavior is related to the atomic structure of the surface. The key parameter that affects long-range order is the energy for changing the dihedral angle between Au-S-C₍₁₎-C₍₂₎ of the adsorbed alkanethiol.

Thermoelectric properties of n-type PbS nanocrystals doped with two-dimensional lead bromide perovskites

Marios E. Trantafyllou-Rundell,^{a,b} Christine Fiedler^b, Constantinos C. Stoumpos,^a Maria Ibáñez^b

^aDepartment of Materials Science and Technology, University of Crete, Heraklion 70013, Greece

^bInstitute of Science and Technology Austria, Klosterneuburg 3400, Austria

Thermoelectric materials have been highly-sought-after materials since they promise to convert wasted heat energy into useful electrical power, using the so called Seebeck effect.^{1,2} The efficiency of a thermoelectric material is expressed by the figure of merit zT which is defined as $zT = S^2\sigma T/(\kappa_e + \kappa_L)$ where S is the Seebeck coefficient, σ is the electric conductivity, and κ_e and κ_L are the electron and lattice thermal conductivity, respectively. Lead chalcogenides have attracted most of the attention in the past decades, as they fulfill the requirements for achieving high figures-of-merit (high σ , small κ) while the temperature of optimal operation lies in the few hundred degrees Celsius, an ideal temperature to convert heat from combustion engine exhausts. PbS-based materials have attracted much attention for thermoelectric power generation due to their low-cost and earth-abundant features.

In this work we crystallized 2D metal halide perovskites on top of n-type PbS nanoparticles in order to dope (n-type) the PbS into PbS/perovskite composites. $(\text{HA})_2\text{PbBr}_4$ perovskite crystals (where HA stands for the protonated monoanionic form of hexylamine) dissolved in a suitable polar solvent were intermixed with PbS nanoparticles dispersed in the same solvent under controlled N_2 atmosphere. The addition of nonpolar solvent leads to the rapid recrystallization of the perovskite on the surface of the PbS nanocrystals. Thermal annealing and coalescence using Spark Plasma Sintering (SPS) conditions, followed by appropriate processing led to dense pellets of the composite material. Overall, halide perovskites succeed in increasing carrier concentration and electrical conductivity of PbS. Thereby, the power factor is improved ($\sim 15 \mu\text{W cm}^{-1} \text{K}^{-2}$) pushing the zT value up to ~ 0.8 at 850K. (Fig 1.)

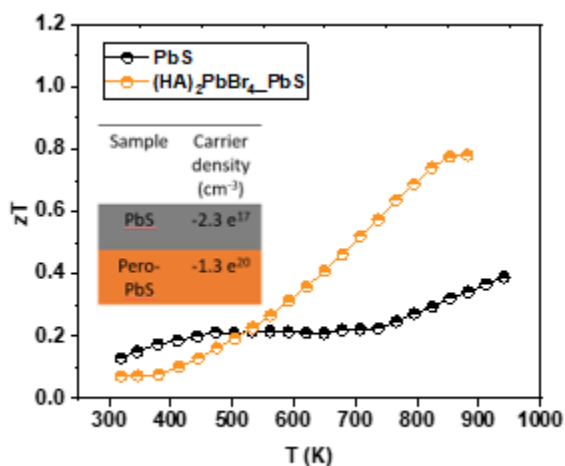


Figure 1. zT of the PbS pellet before and after the perovskite.

¹ Zhao, L.-D. *et al.* High Performance Thermoelectrics from Earth-Abundant Materials: Enhanced Figure of Merit in PbS by Second Phase Nanostructures. *J. Am. Chem. Soc.* **133**, 20476–20487 (2011).

² Hu, S., Ren, Z., Djurišić, A. B. & Rogach, A. L. Metal Halide Perovskites as Emerging Thermoelectric Materials. *ACS Energy Lett.* **6**, 3882–3905 (2021).

Performance and stability improvement of inverted perovskite solar cells by interface modification of charge transport layers using an Azulene-pyridine molecule.

Nikolaos Tzoganakis^{1,a}, Boxu Feng^{2,b}, Michalis Loizos^{3,a}, Konstantinos Chatzimanolis^{4,a}, Miron Krassas^{5,a}, Dimitris Tsikritzis^{6,a}, Xiadong Zuang^{7,b}, Emmanuel Kymakis^{8,a},

^a *Department of Electrical & Computer Engineering, Hellenic Mediterranean University (HMU), Heraklion 71410, Crete, Greece*

^b *Meso-Entropy Matter lab, State Key Laboratory of Metal Matrix Composites Shanghai Key Laboratory of Electrical Insulation and Thermal Gaining, School of Chemistry and Chemical Engineering, Frontiers Science Center for Transformative Molecules, Shanghai Jiao Tong University, Shanghai 200240, P. R. China.*

Abstract:

In this work, a two-fold interface engineering approach is proposed by implementing an Azulene-Pyridine molecule (AzPy) deposited over the hole and electron charge transport layers (HTL and ETL). Extensive characterization and analyses revealed that the surface engineering of HTL with AzPy improves the perovskite formation, thus increasing light absorption and reducing non-radiative recombination, while protecting the perovskite from the degradation species derived from the HTL. The stability tests of the devices revealed that the PCBM/BCP/Ag interface is the weak interface, in terms of stability, under thermal and light stress and the thermal stress induces a burn-in phenomenon i.e., a rapid decrease in power conversion efficiency (PCE) in few hours. This problem was mitigated, through the second engineering approach, by developing an AzPy layer onto the ETL, thus the performance and stability of the devices under ambient conditions and thermal or light stress were considerably improved. Moreover, a surface treatment of perovskite surface with n-hexylammonium bromide was employed, resulting to devices with PCE over 20%. By combining all the proposed interface engineering approaches, the optimized devices deliver a PCE up to 20.42% and retain 90% of their initial PCE for more than 1200 h under ambient conditions, while the thermal and light stabilities of the devices improved substantially in comparison to the reference.

Greece-China joint R&D project Calypso (T7ΔKI-00039), co-financed by Greece, the EU Regional Development Fund and the Chinese Ministry of Science and Technology

Surface engineering of charge transport in inverted perovskite solar cells with azulene derivatives

Dimitris Tsikritzis^{1,3}, Nikolaos Tzoganakis¹, Boxu Feng², Michalis Loizos¹, Miron Krassas¹, Xiaodong Zhuang² and Emmanuel Kymakis^{1,3}

¹*Department of Electrical & Computer Engineering, Hellenic Mediterranean University (HMU), Heraklion 71410, Crete, Greece.*

²*Meso-Entropy Matter lab, State Key Laboratory of Metal Matrix Composites Shanghai Key Laboratory of Electrical Insulation and Thermal Gaining, School of Chemistry and Chemical Engineering, Frontiers Science Center for Transformative Molecules, Shanghai Jiao Tong University, Shanghai 200240, P. R. China*

³*Institute of Emerging Technologies (i-EMERGE) of HMU Research Center, Heraklion 71410, Crete, Greece*

Perovskite solar cells (PSCs) have reshaped the thin-film photovoltaic technology owing to their exceptional high power conversion efficiency (PCE) in conjunction with their low-cost and facile production¹. The inverted PSCs although exhibit lower PCEs compared to normal ones, they show negligible hysteresis, better stability, and prolonged lifetime. In this work, novel azulene derivatives, namely Az-4TPA and biAz-4TPA, were synthesized and incorporated in inverted PCEs. The energy levels of the new molecules favour the hole charge extraction and by forming a thin biAz-4TPA/PTAA bilayer, the optimized devices reached a PCE up to 18.48% due to the improved energy level alignment at the hole extraction side of the device. Moreover, the devices incorporated the biAz-4TPA/PTAA bilayer show improved stability. We demonstrate a simple method for reducing the dependence for PTAA in inverted devices by using ultrathin PTAA films between a novel azulene derivative and perovskite layers. The optimal PTAA concentration of 0.75 mg mL⁻¹ corresponds to more than 62% less PTAA used for the fabrication of the device, while delivering higher PCE and stability. The results show that the hydrophobic substrate is essential for perovskite growth in inverted PSCs and the potential new HTLs must conform with this, or interface engineering is needed to modify the wettability of the surface. Finally, we show that azulene derivatives have the potential to be used as HTLs for PSCs and their functionalization and molecular tuning is expected to deliver improved devices.

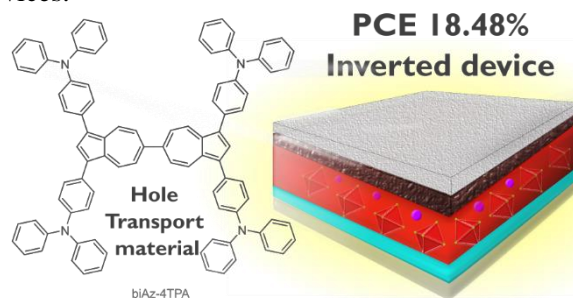


Figure 1: A novel π -conjugated azulene molecule was used as efficient Hole Transport Layer in inverted perovskite solar cells delivering PCE up to 18.48%.

References

1. Jeong, J. *et al.* Pseudo-halide anion engineering for α -FAPbI₃ perovskite solar cells. *Nature* **592**, 381–385 (2021).

Electronic band structure of Gr/MS₂ (M=Mo, W) and WX₂/MoX₂ (X=S, Se) van der Waals heterostructures

G. Vailakis*, G. Kopidakis

Department of Materials Science and Technology, University of Crete, 70013
Heraklion, Greece

Institute of Electronic Structure and Laser, Foundation for Research and
Technology–Hellas, 71110 Heraklion, Greece

Van der Waals heterostructures (vdWh) are vertically stacked two-dimensional materials with remarkable properties. Superconductivity of twisted bilayer graphene at the magic angle, interlayer excitons in transition metal dichalcogenide (TMD) heterostructures, and optoelectronic properties of TMD/graphene heterostructures, are examples, among others, where vdWh significantly differ from their monolayer constituents. Ab-initio electronic structure calculations for vdWh and their interpretation are challenging as different crystal lattices combine into a single material (Fig. 1a,b) and large simulation cells are required. We have developed a methodology for unfolding and analyzing the electronic band structure of vdWh in a way that a clear comparison with the electronic bands of each monolayer can be made (Fig. 1c,d). Our results show that composition of monolayers, twist angles, and stress in the heterostructures have a strong influence on their observable optoelectronic properties. The effect of band hybridization occurring from the coupling of the monolayers is identified and discussed. TMD/TMD heterostructures are type II semiconductors when the band hybridization does not change the valence band maximum from K to Γ .

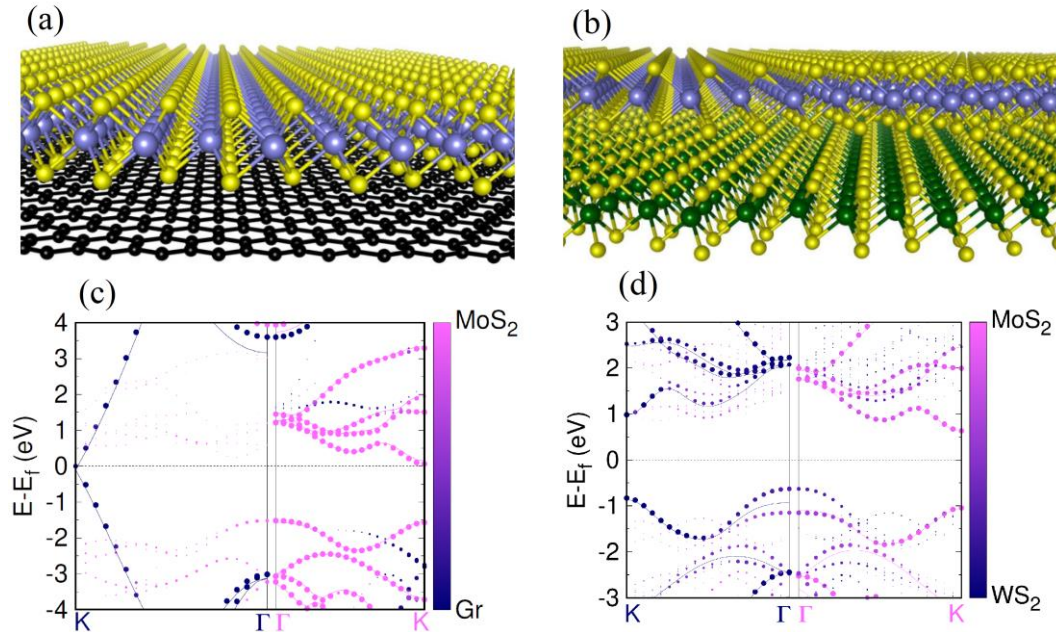


Figure 1: Van der Waals heterostructures, Gr/MoS₂ (a) and WS₂/MoS₂ (b). The unfolded band structures on the 1st Brillouin Zones of the bottom monolayer (dark blue K and Γ) and top monolayer (magenta K and Γ) for Gr/MoS₂ (c) and WS₂/MoS₂ (d), where the solid lines represent the band structures of the isolated monolayers and the points depict the unfolded electronic states of the heterostructure.

* gvailakis@materials.uoc.gr

Multiscale Computational study of 5- Fluorouracil delivery by Zeolite Imidazole Frameworks (ZIFs)

M. Vlachos^a, E. Tylianakis^b, E. Klontzas^c, M. Severi^d, G. Turtù^d, F. Zerbetto^d, G. Froudakis^a

^a Dept. of Chemistry, University of Crete, Voutes, Greece

^b Dept. of Materials Science and Technology, University of Crete, Voutes, Greece

^c National Hellenic Research Foundation, Athens, Greece

^d Dept. of Chemistry "G. Ciamician", Alma Mater Studiorum - Università di Bologna, Bologna, Italy

Zeolitic Imidazolate Frameworks (ZIFs) are considered as potential nanocarriers in biomedical applications such as storage and transportation of drugs, due to their low toxicity, high internal load and controlled release. In this work, the interaction of selected ZIFs with the anticancer drug 5-Fluorouracil (5-FU) is studied, through semi-empirical computational techniques (PM7), Grand Canonical Monte Carlo simulations and also Molecular Dynamics. Our investigation is based on ZIF-8 which is characterized by pH-sensitive controlled drug release [1]. In order to improve the drug interaction with the framework and expand the parent ZIF-8, we replace imidazole with 3-(1H-pyrrol-3-yl)pyridine for each linker. This modified ZIF shows an interaction with 5-FU of 34 kcal/mol, where the parent ZIF-8 has only 12 kcal/mol. Furthermore, Grand Canonical Monte Carlo simulations were employed to determine the loading of 5-FU in both ZIF compounds under different thermodynamic conditions [2], and Molecular Dynamics simulations reveal a detailed comparison between the two ZIF materials.

References

- [1] Chun-Yi, S., Chao, Q., Xin-Long, W., Guang-Sheng, Y., Kui-Zhan, S., Ya-Qian, L., Zhong-Min, S., Peng, H., Chun-Gang, W., En-Bo, W. Zeolitic imidazolate framework-8 as efficient pH-sensitive drug delivery vehicle. *Dalton Trans* **2012**, 41, 6906-6909.
- [2] Tylianakis, E.; Froudakis, G. E. Grand Canonical Monte Carlo Method for Gas Adsorption and Separation. *Journal of Computational and Theoretical Nanoscience* **2009**, 6, 335-348.

3D printed photocatalysts against liquid laundry detergents

Nikolaos Rafail Vrithias

*Institute of Electronic Structure and Laser, Foundation for Research & Technology-Hellas, N. Plastira 100
Department of Materials Science and Technology, University of Crete, 70013
Heraklion, Greece*

Maria Sevastaki

*Institute of Electronic Structure and Laser, Foundation for Research & Technology-Hellas, N. Plastira 100
Department of Chemistry, University of Crete, 71003 Heraklion, Crete, Greece*

George Kenanakis

Institute of Electronic Structure and Laser, Foundation for Research & Technology-Hellas, N. Plastira 100

The last few years, there is an increasing research interest concerning the degradation of large amount pollutants in waste water, using semiconductor photocatalysts such as ZnO and TiO₂ under solar or artificial light. There are plenty of powder photocatalysts, having encouraging results, although there is a difficulty in their reuse [1]. Moreover, there are several experiments performed, employing stabilized photocatalysts in the form of thin films or nanostructures on various substrates, which offer reusability, while in most cases their dimensions cannot exceed some tens of mm [2].

A different approach, which has not be studied until now, is the synthesis of large scale and 3-dimensional photocatalytic samples/devices in the order of cm or tens of cm [3]. In this case, the active material could be either dispersed within, or located on the surface of device 3D scaffold. Following this approach, we fabricated 3D printed photocatalytic samples, for every day and large scale applications. In this work we chose the Fused Deposition Modeling (FDM) technique, which allows us to fabricate 3D samples with complex geometries in large scale (~20x20x20 cm³) with a spatial resolution of approximately 100 μm in z-axis and 11 μm in x and y.

In this work, ZnO and/or TiO₂ nano-powders were mixed with ABS or HDPE in several v/v concentrations reaching a maximum of 20% v/v and forwarded to a “Noztek Pro” (Noztek, Shoreham, West Sussex, UK) high temperature extruder, in order to be transformed to cylindrical filaments with a diameter of 1.75 ± 0.15 mm, suitable for 3D-printing, and several 3D geometries were fabricated by means of a dual-extrusion FDM-type 3D printer (Makerbot Replicator 2X; MakerBot Industries, Brooklyn, NY, USA).

The photocatalytic activity of the 3D printed samples was quantified by means of the decolorization of methylene blue (MB), and a typical Liquid Laundry Detergent (Dixan) in aqueous solutions. The decolorization of the above aqueous solutions was monitored by UV–Vis spectroscopy in absorption mode, while their degradation was checked by Raman spectroscopy, under UV illumination.

It is evidently shown that the 3D architectures result in a significant photocatalytic ability, due to their increased active surface area reaching an efficiency of ~ 95% after 60 min of UV irradiation (even ~ 85% in only 20 min) under UV irradiation, offering a novel low-cost alternative way for fabricating large-scale photocatalysts, suitable for practical applications.

References

- [1] Mills, J. Wang, J. Photochem. Photobiol., A 182, 181 (2006)
- [2] G. Kenanakis, N. Katsarakis, Journal of Environmental Chemical Engineering 2, 1748 (2014)
- [3] Z. Viskadourakis, M. Sevastaki, and G. Kenanakis, *Appl. Phys. A* 124, 585 (2018)

Structural and electronic properties of β Ti-based alloys by density functional theory

D. Fylaktooulou^{*}, K. Kamarakis, A. Tsanios, P.S. Selinof, A. Kassas, D. Delali, P.M. Kiritsi, S. Rentzis, Y. Fortouna, A. Balerba, Ch. E. Lekka
Department of Materials Science and Engineering, University of Ioannina
Institute of Materials Science and Computing, Univ.of Ioannina, Ioannina, Greece

The β -Ti-based alloys represent the second generation of biocompatible alloys that are suggested to be promising materials for replacing the widely used TiAl6V4 implants [1-2]. That is since the β -Ti-based metallic implants show lower Young moduli, higher corrosion resistance and minimal cytotoxicity. Nevertheless, in order to retain or improve these features and even include anti-bacteria properties further work is needed. This study consists of a systematic evaluation on the structural and electronic properties of the well known β -TiNb alloys in presence of biocompatible elements like Sn, In, Hf, Ga, Cu, Ag and Zr. Investigations on the ternary TiNbX (X= Sn, In, Ga) revealed that minor In or Sn additions (having sp valence electrons) introduce low energy states with s character that present antibonding features with the Ti first neighboring atoms as well as with the Ti-Nb second neighboring atoms thus weakening the chemical bonds and leading to elastic softening [2,3,4].

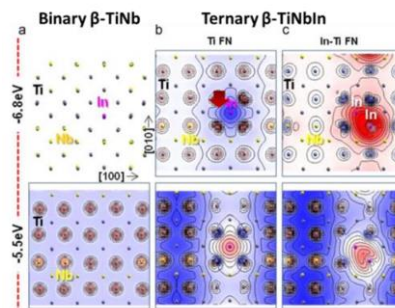


Figure 1: Electronic properties of β TiNbIn based alloys

On the contrary Hf substitution (sd valence electrons) in the orthorhombic Ti-Nb results in a phase transition to the β -phase due to Hf 5d contributions at the Fermi level and the Hf 6s hybridizations at low energies in the electronic density of states. Bonding–antibonding first neighbor features existing in the shifted plane destabilize the β -phase, especially at high Hf concentrations, while the covalent-like features in the first neighborhood stabilize the corresponding plane of the β -phase. New states close to the Fermi level are also introduced upon Cu substitution in the β -TiNb alloy. These results could be enlighten the design of β -type Ti-alloys suitable for metallic implants.

Acknowledgements

This work is supported by the Bioremia (H2020-MSCA-ITN-2019, No 861046, 2020- 2024) and BioTiNet (FP7-PEOPLE-2010-ITN No 264635, 2011-2014).

References

- [1] Mitsuo Niinomi, Metals for biomedical devices. Woodhead Publishing Limited (2010)
- [2] Lekka, Gutiérrez-Moreno, Calin, J. Phys. Chem. Solids 102 (2017) 49
- [3] Gutiérrez Moreno, Panagiotopoulos, Evangelakis, Lekka, (2020), 13,1–11, 1288
- [4] Alberta, Fortouna, Vishnu, Gebert, Lekka, Calin (to be submitted)

* stm02447@uoi.gr

Raman and NEXAFS study of the oxidation of Cu₃N thin films during their growth procedure

K. Mavridou, F. Pinakidou, M. Katsikini*, J. Arvanitidis, E. C. Paloura
School of Physics, Aristotle University of Thessaloniki, GR-54124, Thessaloniki,
Greece

M. Brzhezinskaya
Helmholtz-Zentrum Berlin für Materialien und Energie, Albert-Einstein-Str. 15,
12489 Berlin, Germany

M. Zervos
Nanostructured Materials and Devices Laboratory, School of Engineering,
University of Cyprus, PO Box 20537, Nicosia, 1678, Cyprus

Cu₃N thin films were grown by annealing of Cu under NH₃:O₂ flow. The Cu layers were deposited on different substrates by sputtering. The procedure followed is the one proposed by Matsuzaki *et al.* [1], where the O₂ molecules adsorbed on the Cu surface are transformed to oxygen species that selectively cause dehydrogenation of NH₃ creating adatoms on the surface that migrate into the bulk forming Cu₃N. The annealing temperatures were ranging from 300 to 800 °C. The samples were studied by Raman and N-K-edge Near Edge X-ray Absorption Fine Structure (NEXAFS) spectroscopies. Raman spectra were recorded using two different excitation wavelengths (647.1 and 514.5 nm) since resonance effects affect, to a different extent, the Raman peak intensities of copper oxides and Cu₃N, allowing for their better discrimination. Cu₂O surface oxide is formed in almost all the samples even at low annealing temperatures. On the other hand, the formation of CuO is generally observed at higher temperatures with the onset depending on the amount of O₂ in the gas mixture. However, high temperature is necessary to grow larger crystallites, as it is deduced by the narrowing of the high-frequency Raman peak (at ca. 650 cm⁻¹) of Cu₃N and SEM. N-K-edge NEXAFS spectra revealed that the formation of CuO, at elevated annealing temperatures, is accompanied by the creation of N₂ trapped in the sample. Molecular nitrogen is most probably formed by the N atoms originating from the dissociation of the Cu-N bonds.

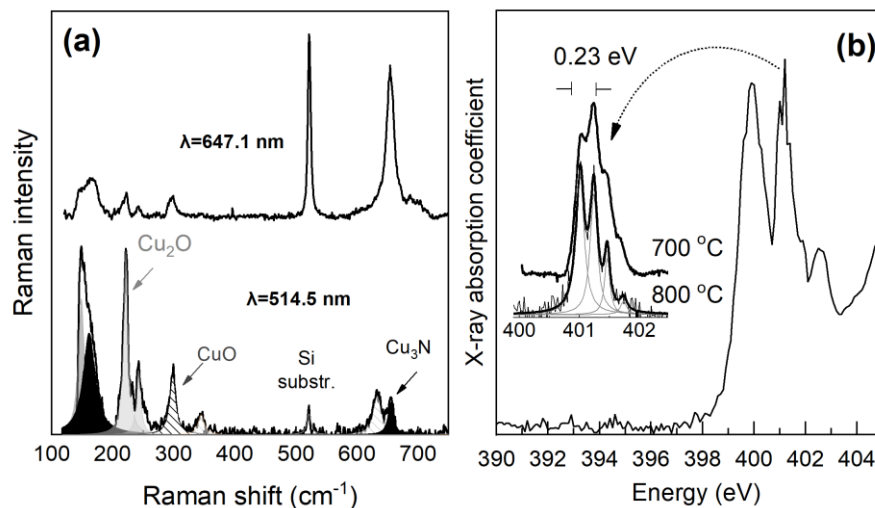


Figure 1: (a) Raman spectra of a sample annealed at 600 °C recorded using two different excitation wavelengths. (b) N-K-edge NEXAFS spectrum of a sample annealed at 700 °C. The inset shows the fine structure of the N₂ peak due to vibronic transitions.

Reference

[1] K. Matsuzaki, K. Harada, Y. Kumagai, S. Koshiya, K. Kimoto, S. Ueda, M. Sasase, A. Maeda, T. Susaki, M. Kitano, F. Oba, H. Hosono, *Adv. Mater.* **30**, 1801968 (2018).

* katsiki@auth.gr

A Highly Stable, Flexible Metal Organic Framework for Selective Sorption Applications

K. Manousakis^{*1}, K. Papadopoulos¹, G. K. Angeli¹, E. Loukopoulos¹, C. Tsangarakis¹, P. N. Trikalitis¹.

¹Department of Chemistry, University of Crete, Heraklion 70013, Greece
ptrikal@uoc.gr

In the emerging and vast field of Metal-Organic Frameworks (MOFs), particular attention has been given in flexible structures. This behaviour is often induced by a physical or chemical stimulus, including the sorption of gases and/or vapors. [1] This kind of flexible MOFs are promising materials for important applications including gas and vapor separation due to their ability to modify their structure in the presence of specific substances depending on their nature. [2]

In this work, we report the synthesis and characterization of a highly stable, flexible MOF, based on a carboxylate functionalized organic linker. The synthesis afforded good quality single crystals, suitable for structure determination using single crystal X-ray diffraction (Figure 1, left). The material has been extensively characterized using a variety of techniques including powder X-Ray diffraction and SEM/EDS. In addition extended gas and vapor sorption measurements using a state-of-the-art volumetric system, revealed a highly flexible behaviour upon sorption of polar vapors. The observed selective vapor sorption properties are very important towards industrially relevant separations processes.

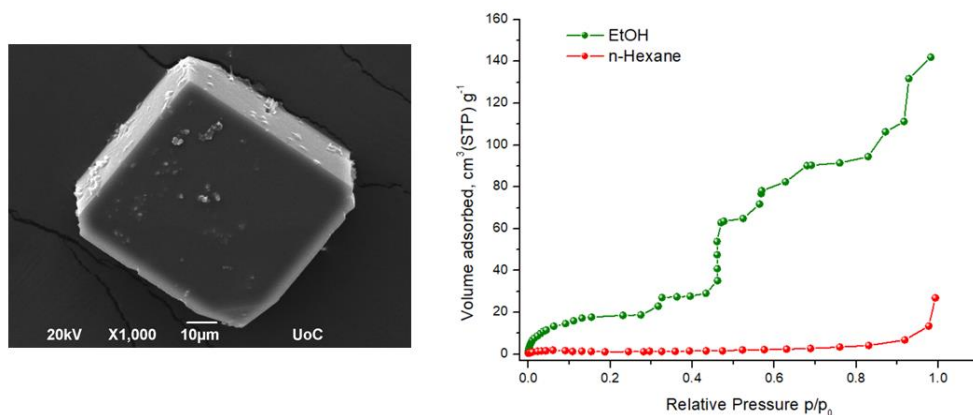


Figure 1: Representative SEM image of the as-synthesized flexible MOF (left). Adsorption isotherms of selected vapors recorded at 298 K up to the corresponding saturation pressure of the adsorbate (right).

References

- [1] Ehrling, S. Mendt, M. Senkowska, I. Evans, J. D. Bon, V. Petkov, P. Ehrling, C. Walenzus, F. Pöppl, A. Kaskel, S. Chem. Mater. , **32**, 5670– 5681(2020).
- [2] Jian-Rong Li, Ryan J. Kuppler, Hong-Cai Zhou , Chem. Soc. Rev., **38**, 1477-1504(2009).

Acknowledgements

This research work was supported by the DeSulfur program titled "Advanced nanoporous materials for the Deep deSulfurization of liquid fuels via adsorption in mild conditions (project code: T2EΔK-01976)".

*chemp1149@edu.chemistry.uoc.gr

Strain induced frequency shifts of the second order Raman modes of monolayer WS₂

A. Michail^{1,2*}, K. Filintoglou^{3,4}, N. Balakeras³, N. N. Lathiotakis⁵,
J. Parthenios² and K. Papagelis^{2,3}

¹*Department of Physics, University of Patras, Greece*

²*Institute of Chemical Engineering Sciences, Foundation for Research and Technology Hellas (FORTH-ICEHT), Patras, Greece*

³*School of Physics, Department of Solid State Physics, Aristotle University of Thessaloniki, 54124, Thessaloniki, Greece*

⁴*HENANOTEC, Komnion 17, Thessaloniki 54624, Greece*

⁵*Theoretical and Physical Chemistry Institute, National Hellenic Research Foundation, Vass. Constantinou 48, GR-11635, Athens, Greece*

Atomically thin transition metal dichalcogenides (2D - TMDCs) are an emerging class of materials with great prospect in fundamental as well as applied science. Importantly, their optical and vibrational properties can be significantly tuned by external stimuli, such as mechanical strain [1]. Despite the fact that the strain dependence of the first order Raman modes have been studied extensively, the impact of strain on the higher order Raman scattering remains rather unexplored. Important insight on the lattice dynamics can be obtained from higher order Raman modes, since phonons with non-zero momenta can be probed [2].

In this work, WS₂ monolayer single crystals, fabricated by an atmospheric pressure chemical vapor deposition method, are subjected to controlled biaxial deformations. *In-situ* Raman microscopy is employed to study the evolution of the second order Raman modes under various levels of mechanical strain. Under resonant excitation (2.41 eV) numerous higher order peaks emerge in the Raman spectrum of WS₂ attributed to many-phonon combination processes. In total, more than 15 higher order Raman modes are investigated, and their corresponding strain induced shift rates and mode Grüneisen parameters are determined. Using Density Functional Perturbation Theory, the two-phonon density of states was calculated and compared with the experiment.

References

- [1] F. Carrascoso, H. Li, R. Frisenda and A. Castellanos-Gomez, *Nano Research* **14**, 1698–703 (2021)
- [2] B. R. Carvalho and M. A. Pimenta, *2D Mater.* **7**, 042001 (2020)

* antmichail@upatras.gr

Ab initio calculations on β Ti-based implant surfaces

M.E. Nousia^{*}, S. Papadoniou Chatzis, B. Lontos, A. Mosxou, Ch. Kourti, A.X. Galani, A. Delaporta, A. Balerba, Ch. E. Lekka
Department of Materials Science and Engineering, University of Ioannina
Institute of Materials Science and Computing, Univ.of Ioannina, Ioannina, Greece

Implant surfaces are really critical for tissue engineering, osteogenesis as well as bacterial adhesion and proliferation [1-2]. Usually, polymeric coatings have been widely used for the manufacturing of the medical device's surfaces in order to tune the mechanical properties and biocompatibility. Nevertheless, the knowledge of the properties of the metallic implant or the oxide termination that will affect any coating adsorption or even bacteria deposition is critical. Therefore, aiming in a fundamental understanding of metallic implant surfaces, a detail study on the structural and electronic properties β -Ti based alloy surfaces with non-toxic and antibacterial element enrichment is needed. In this work a detail study of several β -TiX (X=Nb, Ga, Cu, Ag) low index surfaces in presence of antibacterial adatoms is presented. The energetically favored terminated layer is revealed for the order or disorder (001) and (110) surfaces. Surface contraction is found for all cases and the rippling effect is revealed for the mix terminated layers. Surface atoms introduce new surface energy states altering the bulk electronic density of states while the adatoms mainly interact with the Ti surface atoms.

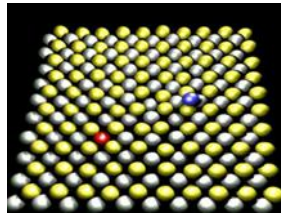


Figure 1: Metallic β -TiNb (110) surface in presence of Ga adatom

Furthermore, the structural and electronic properties of TiO₂ anatase and rutile surfaces are presented since this oxide layer is usually formed on top of any Ti-based implant. These results can be used as a guide for the design of novel low-rigidity alloys for biomedical applications.

Acknowledgements

This work is supported by the Bioremia (H2020-MSCA-ITN-2019, No 861046, 2020-2024).

References

- [1] Barfeie, Wilson, Rees, British Dental Journal, 218, E9 (2015)
- [2] Xu, Siedlecki, Advances in Polyurethane Biomaterials 2016, 247-284
- [3] Lekka, Gutiérrez-Moreno, Calin, J. Phys. Chem. Solids 102 (2017) 49

* stm02290@uoigr

Thermochemical properties of hybrid two-dimensional lead halide perovskites based on bulky aromatic spacer cations

Chrysostomos Papamichail, Constantinos C. Stoumpos

Department of Materials Science and Technology, University of Crete, Heraklion 70013, Greece

Hybrid halide perovskites have been studied extensively in the last decade given their remarkable photophysical properties. Nevertheless, these relatively new class of solid materials continues to surprise with the wealth of unconventional properties they possess, including a remarkable thermal expansion/contraction they possess that can be compared with those of viscous liquids [1]. The interest in the thermal properties of the material has been reinvigorated following the recent discovery that a certain variety of two-dimensional (2D) lead halide perovskites can undergo a reversible glass/crystalline transition upon moderate heating [2]. Because of this unique property, materials of this type have acquired a distinct research interest, targeting switchable phase change materials, towards volatile memory applications.

The purpose of this work towards this end was to synthesize a variety of 2D materials with bulky, asymmetric organic cations that are difficult to interdigitate between the inorganic perovskite sheets, as an attempt to trigger a potential glass-crystal transition in the solids. Thus, materials of the general formula A_2PbX_4 ($X = \text{Br, I}$ and $A = 2$ -Phenethylamine (PEA), 2 -(1-Naphthyl)ethylamine (1-NEA), 2 -(2-Naphthyl)ethylamine (2-NEA) and 2 -(4-Biphenyl)ethylamine (BPEA) were synthesized and structurally characterized by Single-Crystal and X-ray diffraction and their thermal properties were recorded via Thermogravimetric Analysis (TGA) and Differential Scanning Calorimetry (DSC). We find that the so much the conformation, as much as number of aromatic rings incorporated in the organic carbon chain strongly impact the thermal properties of the materials, either by manipulating the thermal stability of the materials or by shifting the temperature of the corresponding structural phase transition. Despite the fact that no clear glass-crystal transition was observed in the selected collection of halide perovskites, certain trends relating to the order of the phase transitions and the transition temperature range could be deduced by a careful analysis of the thermodynamic quantities, in comparison with those of the linear aliphatic spacer ammonium cations [3]. Moving forward, we propose a design of new ammonium cation that can be used to moderate the transition temperature and, ideally, inhibit the crystal-crystal transition in favor of a glass-crystal modifications, suitable for application in rewritable memory devices.

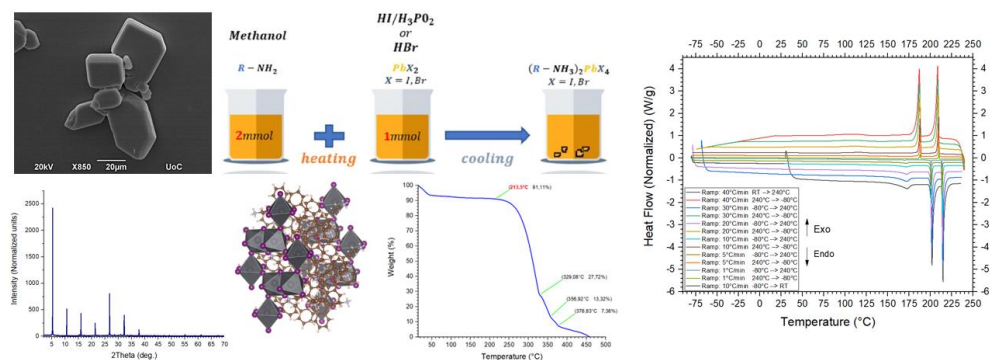


Figure 1. Design illustration of the synthetic process together with the SEM analysis, the powder and single – crystal XRD characterizations and the thermogravimetric analysis of the DSC and TGA data of the iodine and bromide perovskite compounds used in the above study.

References

1. D. H. Fabiani, C. C. Stoumpos, G. Laurita, A. Kaltzoglou, A. G. Kontos, P. Falaras, M. G. Kanatzidis, R. Seshadri, *Angew. Chem. Int. Ed.* 2016, 55, 15392.
2. Singh, A., Jana, M. K., Mitzi, D. B., Reversible Crystal–Glass Transition in a Metal Halide Perovskite. *Adv. Mater.* 2021, 33, 2005868.
3. Barman, S., Venkataraman, N. v., Vasudevan, S., & Seshadri, R. (2003). Phase transitions in the anchored organic bilayers of long-chain alkylammonium lead iodides ($C_nH_{2n+1}NH_3$) $_2PbI_4$; $n = 12, 16, 18$. *J.Phys. Chem. B*, 107(8), 1875–1883.

Si-Graphene Oxide Heterostructures as Anode Material in Li-air Energy Storage Devices: Effect of the Si Loading

M. Apostolopoulou^{1*}, C. Floraki¹, K. Anagnostou¹, A. Kostopoulou², K. Brintakis², E. Stratakis², E. Kymakis^{1,3}, D. Vernardou^{1,3}

¹*Department of Electrical and Computer Engineering, School of Engineering, Hellenic Mediterranean University, 71410 Heraklion, Greece*

²*Institute of Electronic Structure and Laser, Foundation for Research & Technology- Hellas, P.O. Box 1527, Vassilika Vouton, 71110 Heraklion, Greece*

³*Institute of Emerging Technologies, Hellenic Mediterranean University Center, 71410 Heraklion, Greece*

**corresponding author, e-mail mar.apostolopoulou31@gmail.com*

In recent years, due to the rapid development of technology, the demand of efficient storage devices is increasing. Silicon has attracted increasing interest as a promising anode material for lithium-ion batteries due to its high theoretical capacity and abundance in nature. However, it exhibits large volume changes during the charging/discharging cycles causing irreversible capacity losses. To overcome these problems and increase the lifetime of the energy storage devices, research attention is focused on combining Si with 2D materials such as graphene oxide.

In this work, anodes have been fabricated by growing a Si nanoparticulate layer on the top of graphene oxide layer. In particular, the graphene oxide prepared by a modified Hummer's method was deposited through a spray procedure on a Cu substrate and then a Si-layer was grown on it with the same procedure. The Si nanoparticles were commercially available and two Si-loadings were studied in order to find the optimum loading for the best capacity and lifetime of the storage devices.

The potential application of Si-GO heterostructures were studied and evaluated as efficient anodes for Li-ion water-based batteries via cyclic voltammetry through Li⁺ intercalation/de-intercalation consecutive scans. Furthermore, in order to investigate their stability over continuous Li⁺ intercalation/de-intercalation cycles in aqueous electrolyte, the structural and morphological properties of the anodes were evaluated through X-ray photoelectron spectroscopy, Scanning electron microscopy, Energy dispersive spectroscopy and Raman spectroscopy.

Keywords: Graphene Oxide, Si nanoparticles, Aqueous Li-ion electrolyte, Anode materials, Li-ion batteries, Cyclic voltammetry

3D printed composite materials with antifouling properties for aquaculture applications

Andrianna Bouranta¹, Ioan Valentin Tudose¹, Luciana Georgescu¹, Nikolaos Rafail Vrithias^{2,3}, George Kenanakis², Efsevia Sfakaki⁴, Nikolaos Mitrizakis⁴, George Strakantounas⁴, Nikolaos Papandroulakis⁴, Cosmin Romanitan⁵, Cristina Pachiu⁵, Oana Tutunaru⁵, Lucian Barbu -Tudoran^{6,7}, Mirela Petruta Sucheai^{1,5,*} and Emmanouel Koudoumas^{1,*}

¹ *Center of Materials Technology and Photonics, Hellenic Mediterranean University, Heraklion 71410, Greece;*

² *Institute of Electronic Structure and Laser, Foundation for Research & Technology-Hellas, Heraklion 70013, Greece;*

³ *Department of Materials Science and Technology, University of Crete, Heraklion 70013, Crete, Greece*

⁴ *Institute of Marine Biology, Biotechnology and Aquaculture, Hellenic Centre for Marine Research, Heraklion 71500, Greece;*

⁵ *National Institute for Research and Development in Microtechnologies (IMT-Bucharest), Bucharest 023573, Romania;*

⁶ *Electron Microscopy Center “Prof. C. Craciun”, Faculty of Biology & Geology, “Babes-Bolyai” University, 400006 Cluj-Napoca, Romania;*

⁷ *Electron Microscopy Integrated Laboratory, National Institute for R&D of Isotopic and Molecular Technologies, 400293 Cluj-Napoca, Romania*

Aquaculture is an industry of particular importance internationally, providing significant protein to an ever-increasing world population and offers the largest percentage of seafood consumed by humans. Its production infrastructure is based on a complex variety of components submerged in water, such as cages, nets, floats and ropes. However, all of these components are surfaces available for biofouling, as they provide the possibility of accretion in a wide variety of marine organisms, which acts as a source of parasites, and therefore has significant economic consequences. Current technology for preventing biofouling is based on the use of toxic, biocide-containing materials, which is a serious threat to marine ecosystems, as they affect both the targeted organisms and the environment around them. The purpose of this research is to develop alternative materials, which should be environmental friendly and combine low cost, durability, ease of production and efficiency for aquaculture applications. In recent years, there has been a strong interest in photocatalytic materials, such as TiO₂, because of their support to antifouling, self-cleaning and antibacterial action. TiO₂ seems to be one of the most active materials for photocatalytic action, as it also shows great stability due to its good resistance to corrosion.

Here we report on the development of new composite materials for aquaculture nets, using Acrylonitrile Butadiene Styrene (ABS)/TiO₂ and High-Density Polyethylene (HDPE)/TiO₂ with different metal oxide contents, so that the final material has antifouling properties, but also suitable mechanical behavior. The sample nets were developed employing extrusion and 3D printing, the obtained materials being characterized by SEM, XRD and Raman Spectroscopy, while, their antifouling properties were also evaluated. The antifouling response was determined by monitoring the prevention of growth of *Navicula* sp. diatoms and the monocellular algae *Chlorella* sp. on them. The results so far have shown that the HDPE/TiO₂ are quite good candidates for antifouling nets.

Acknowledgement: This work was funded by the Operational Program Fisheries and Maritime 2014–2020 in the framework of the project “Innovative materials for nets for fish farming with environmentally friendly antifouling action”, MIS 5029684.

* mirasuchea@hmu.gr and mira.suchea@imt.ro; koudoumas@hmu.gr

Carbon-red mud foam/paraffin hybrid materials for thermal energy storage and electromagnetic interference shielding applications

Christina Gioti¹, Ioannis Villis¹, Anastasios Karakassides¹, Sevasteia Gkiouzel¹, Georgios Asimakopoulos¹, Maria Baikousi¹, Constantinos E. Salmas¹, Zacharias Viskadourakis², George Kenanakis² and Michael A. Karakassides¹

¹*Department of Materials Science and Engineering, University of Ioannina, Ioannina, Greece*

²*Institute of Electronic Structure and Laser, Foundation for Research and Technology-Hellas, Heraklion, Crete, Greece*

Carbon-based porous materials are very promising candidates for Phase Change Materials (PCMs) shape stabilizers, because of their higher thermal conductivities when compared to the polymers or ceramic analogs. Also, their synthesis is not complex but more importantly requires low cost and abundant raw materials. In this work, host carbon-based porous foams matrices were synthesized utilizing the polymeric foam replication method. Green floral foam (phenol-formaldehyde foam) was used as a template, phenolic resin was used as a carbon source, while red mud was used as a filler. For this purpose a chemical and morphological investigation of the structure was carried out, along with the investigation of its porosity and mechanical properties. Carbon-red mud foam hybrid materials indeed exhibit open-cell structures with high porosity (>65%), with inorganic walls composed of various ceramic phases and partially graphitized carbon. The paraffins that were used as PCMs were n-octadecane, and the commercial RT18HC. After the incorporation, several spectroscopic and analytical techniques were used to obtain the paraffin loading and the thermal stability of the hybrid materials. Leaching tests of the hybrids indicated that the carbon foams can absorb and retain large PCM amounts, with adequate encapsulation efficiencies, whereas the investigated hybrids show also efficient electromagnetic shielding performance required for commercial applications. Their excellent thermal and EMI shielding performance, make the as-prepared samples promising candidates for use in thermal management and EMI shielding of electronic devices.

References

Christina Gioti, Anastasios Karakassides, Georgios Asimakopoulos, Maria Baikousi, Constantinos E. Salmas, Zacharias Viskadourakis, George Kenanakis and Michael A. Karakassides, Multifunctional Carbon-Based Hybrid Foams for Shape-Stabilization of Phase Change Materials, Thermal Energy Storage, and Electromagnetic Interference Shielding Functions, *micro* (2022) in press.

This work was co-financed by the European Union and Greek national funds through the Operational Program Competitiveness, Entrepreneurship and Innovation, under the call RESEARCH—CREATE—INNOVATE (acronym: SEMI-WEB; project code: T2EDK-02073).

MgO-C refractories containing nanoadditives: the effect of graphite content and of use modified graphite with Fe and Si.

Sevasteia Gkiouzel¹, Konstantinos C. Vasilopoulos¹, Ioanna Kitsou², Eleni Roussi², Efthimios Kagiaras³, Athena Tsetsekou², S.Agathopoulos¹ and Michael A. Karakassides¹

¹Department of Materials Science and Engineering, University of Ioannina, GR-451 10 Ioannina, Greece,

²School of Mining Engineering and Metallurgy, National Technical University of Athens, GR-15780, Athens, Greece

³Mathios Refractories S.A., Athens, Greece

Magnesia-carbon (MgO-C) refractories are widely used in basic oxygen furnaces, electric arc furnaces and steel ladles for their excellent corrosion resistance and other important properties. The amount of carbon has crucial role in these properties. Also, the idea of coated graphite seemed to improve corrosion resistance of the MgO-C refractories. This study reports on the graphite content and the use of modified graphite with Fe and Si in MgO-C refractories doped with nanoadditives such as magnesium, aluminum and titanium oxide. The graphite particles first purified and modified with an acid reagent (H₂SO₄/HNO₃ (3:1 v/v)) and then modified with Fe species and Si sources. Sol-gel *method* was applied to synthesize the Al₂O₃ and MgO NPs, whereas a microwave-assisted hydrothermal method via sol-gel process was used for the synthesis of TiO₂ NPs. The NPs were added in raw materials' mixture and in replacing equal amount of MgO fine powder (up to 7 wt.%). Cylindrical specimens with diameter 13mm and 30mm were formed by axial pressing at ~200 MPa and sintering was carried out at 1400 °C. The characterization of the produced ceramics showed that the use of 6 wt.% graphite (than 10 wt.%) resulting in refractory ceramics with higher density, lower porosity as well as higher cold crushing.

The artificial slags had a composition of 56CaO-11SiO₂-33Al₂O₃ (in wt.%). Typical wetting experiments were conducted at the temperature range of 1500-1650 °C for 15-120 min. This presentation will present and discuss the results regarding the influence of the chemical composition of the ceramics on the interfacial reaction and the refractory behaviour of the produced ceramics.

Acknowledgment: This work was carried out in the framework of the project "Advanced Aluminosilicate Refractories and Magnesite Refractories of High Efficiency using Nanotechnology" that is co-financed by the European Regional Development Fund in the context of the special action "Industrial Materials" of the Operational Programme "Competitiveness, Entrepreneurship & Innovation (EPAnEK)", ΕΣΠΑ 2014-2020 (acronym: NanoRefrMat; project code: T6YBP-00386).

Study of the electronic transport mechanism in Mn-Zn-Ni spinel oxides

D. Katerinopoulou^{1,2*}, E. Pervolarakis³, Z. Łodziana⁴, I.N. Remediakis^{2,3} and E. Iliopoulos^{1,2}

¹*Department of Physics, University of Crete, Greece*

²*Institute of Electronic Structure and Lasers, FORTH, Greece*

³*Department of Materials Science and Technology, University of Crete, Greece*

⁴*Institute of Nuclear Physics, Polish Academy of Sciences, Poland*

Manganese based spinel oxides are a class of ceramic materials with a broad range of industrial interest, in the area of sensors, electrochemical energy storage-conversion and (photo)catalysis.[1][2] Among them, nickel manganese oxides NiMn_2O_4 , represent a class of materials with negative temperature coefficient (NTC) of resistance, superb resistivity response, robustness and stability.[3]

In the current work, the ternary spinel system of nickel manganese oxide alloyed with zinc is studied. Transport in $\text{Zn}_{0.5}\text{Ni}_x\text{Mn}_{2.5-x}\text{O}_4$ pellets, as a function of Ni content ($0 \leq x \leq 1.25$) with two different cooling procedures was studied, along with structural characterization and theoretical calculations of their electronic and structural properties. The electronic transport mechanism in transition metal spinel oxides is usually associated with small polaron hopping.[4] In these alloys a super-Arrhenius temperature dependence of conductivity was observed, which cannot be accounted for by current small polaron hopping models. In respect of the structural properties, the coexistence of cubic Spinel and tetragonal Hausmannite was observed with relative phase ratio strongly dependent on composition. Ab-initio calculations pointed to the presence of metastable structures with similar formation energies but different electronic structure. In such inhomogeneous energy system Nearest-neighbour polaron hopping can account for the unconventional thermally activated conductivity behaviour. In conclusions, combing this peculiarity in conductivity along with the theoretical predicted electronic conformations, a model for the resistance functional dependence on temperature that consistently describes the experimental data deduced.

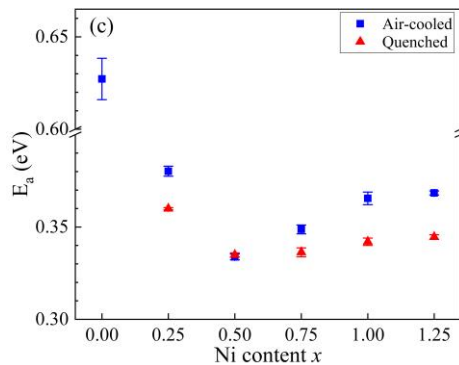


Figure 1: Calculated activation energies for all Ni content for both air-cooled and quenched pellets.

References

- ¹ A. Feteira and K. Reichmann, *Adv. Sci. Technol.* **67**, 124 (2010).
- ² K. Zhang, X. Han, Z. Hu, X. Zhang, Z. Tao, and J. Chen, *Chem. Soc. Rev.* **44**, 699 (2015).
- ³ D. Katerinopoulou, P. Zalar, J. Sweelssen, G. Kiriakidis, C. Rentrop, P. Groen, G.H. Gelinck, J. Van Den Brand, and E.C.P. Smits, **5**, 1800605 (2018).
- ⁴ B. Gillot, R. Legros, R. Metz, and A. Rousset, *Solid State Ionics* **51**, 7 (1992).

* dkaterin@iesl.forth.gr

Ultra-stable CoV_2O_6 hydrogen gas sensor, operating at room temperature

M.Moschogiannaki^{1,*}

¹Department of Materials Science and Technology, University of Crete, Herakleion, Greece

E. Gagaoudakis², G. Kiriakidis², V. Binas^{2,3}

²Institute of Electronic Structure and Laser, Foundation for Research and Technology-Hellas (FORTH-IESL)

³Department of Physics, University of Crete, Herakleion, Greece

The constantly increasing demand for flexible, reliable and stable gas sensors, operating at room temperature, which would be integrated with present electronic circuits for real life applications is a true fact. In the present work, the gas sensing properties of bimetallic cobalt-vanadium-oxide system (CoV_2O_6) under the effect of deposition method (spin coating, direct ink writing and drop-casting) as well as the type of substrate (glass, flexible PET), at room temperature were examined. The spin-coated sensor on glass substrate exhibited the higher response (65.2%) towards 1000 ppm H_2 at room temperature, compared to those that were deposited with the other methods, showing a response and recovery time of 94 s and 74 s, respectively. The CoV_2O_6 flexible PET sensor exhibited a response of 36.6% against 1000 ppm H_2 , at room temperature, with a response and recovery time of 120 s and 80 s, respectively. In addition, both operation under bending conditions at 180° and the reliability, in terms of repeatability of signal and stability after 1 year, were studied for the CoV_2O_6 flexible PET sensor. Finally, a sensing mechanism is proposed taking into account the thickness and architecture of the films as well as film variations and imperfections of the active sensing surface, such as micro-cracks, edges and pores. These parameters play a dominant role on the gas sensing performance far greater than that of the substrate or the metal electrodes. The realization of a CoV_2O_6 flexible sensor demonstrates its potential for real-life applications [1].

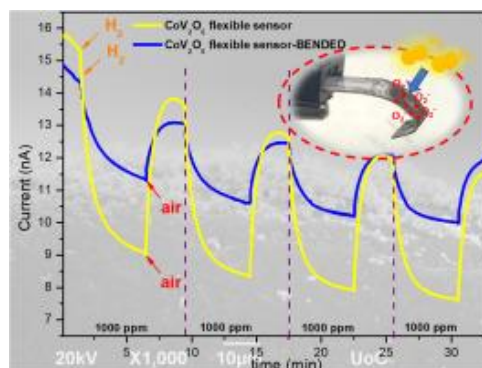


Figure 1: Gas sensing performance of flexible CoV_2O_6 bended sensor towards hydrogen, operating at room temperature

References

[1] M.Moschogiannaki et al., *Microelectronic Engineering*, **262**, 111819 (2022).

* marilenamosho@hotmail.com

Probing the Multi-Functional Performance of Magnetic Nanoparticles/Epoxy Resin Hybrid Nanocomposites

A. C. Patsidis*, S. Gioti, A. Sanida, G. C. Manika, G. C. Psarras
*Smart Materials & Nanodielectrics Laboratory, Department of Materials Science,
University of Patras, Patras 26504, Greece*

G. N. Mathioudakis
*Institute of Chemical Engineering Sciences (ICE-HT), Foundation for Research &
Technology-Hellas (FORTH), 26504 Patras, Greece*

Th. Speliotis
*Institute of Nanoscience and Nanotechnology, NCSR "Demokritos",
Athens 15310, Greece*

Polymer matrix nanocomposites is an important class of engineering materials for various technological applications. Multifunctional performance is achieved by integrating various desirable and supplementary properties/responses in a materials' system [1-3]. The latter should be able to respond under various loading conditions. Mechanical/thermal properties, tunable electric conductivity, variable electric polarization/dielectric permittivity, adjustable magnetic response, thermally induced phase changes contribute to the overall multifunctional performance. In the present study, magnetic nanoparticles (Fe_3O_4 , or ZnFe_2O_4 or $\text{SrFe}_{12}\text{O}_{19}$) with ferroelectric (BaTiO_3) particles or carbon nanotubes (CNTs) are used as fillers in a polymer matrix. BaTiO_3 particles provide functionality to the systems, via their thermally induced ferroelectric-to-paraelectric transition [4], while CNTs enhance mechanical endurance and electrical conductivity. Hybrid nanocomposites underwent structural, morphological characterization, and their thermo-mechanical, magneto-electric properties were investigated. The magnetic behaviour varying the employed magnetic filler type as well as the energy storing/retrieving ability of the studied systems is examined and discussed, aiming to determine the system exhibiting optimum performance.

References

- [1] Friedrich K. Routes for achieving multifunctionality in reinforced polymers and composite structures in Multifunctionality of Polymer Composites. Friedrich K., Breuer U., eds. Elsevier, 2015.
- [2] Song K., Guo J.Z. Liu C. Polymer-Based Multifunctional Nanocomposites and Their Applications. Elsevier, 2018.
- [3] Gioti S., Sanida A., Mathioudakis G.N., Patsidis A.C., Speliotis Th., Psarras G.C. *Materials*, 15, 1784, 2022.
- [4] Manika G.C., Andrikopoulos K.S., Psarras G.C. *Molecules*, 25, 2686, 2020.

Acknowledgments

The research work was supported by the Hellenic Foundation for Research and Innovation (H.F.R.I.) under the "First Call for H.F.R.I. Research Projects to support Faculty members and Researchers and the procurement of high-cost research equipment grant" (Project Number:2850).

Ceramic Inclusions/Epoxy Resin Hybrid Nanodielectrics: Development, Characterization and Multi-Functional Performance

S. Gioti, A. Sanida, G. C. Manika, A. C. Patsidis, G. C. Psarras
*Smart Materials & Nanodielectrics Laboratory, Department of Materials Science,
University of Patras, Patras 26504, Greece*

G. N. Mathioudakis
*Institute of Chemical Engineering Sciences (ICE-HT), Foundation for Research &
Technology-Hellas (FORTH), 26504 Patras, Greece*

Th. Speliotis
*Institute of Nanoscience and Nanotechnology, NCSR “Demokritos”,
Athens 15310, Greece*

In our days the scientific impact and technological demand of nanostructured and stimuli responsive materials is high and globally appreciated.

Multifunctionality is the combination of various desirable properties in a material or materials' system, targeting to develop a single material/system exhibiting all necessary responses under various loading conditions. Mechanical sustainability, suitable thermal response, tunable electric conductivity, variable electric polarization/dielectric permittivity, magnetic properties, thermally induced phase changes could be parts of the overall multi-functional behaviour [1-3].

The challenge of the present study concerns the development of a material/device exhibiting thermo-mechanical endurance, variable polarization/tunable dielectric response, adjustable conductivity, varying magnetic performance, and energy storing/recovering efficiency. For this reason, hybrid nanodielectrics of polymer matrix/ferroelectric particles (BaTiO_3)/magnetic nanoparticles (Fe_3O_4 , or ZnFe_2O_4 or $\text{SrFe}_{12}\text{O}_{19}$) were developed and studied under various loading conditions/external stimuli.

References

- [1] Friedrich K. Routes for achieving multifunctionality in reinforced polymers and composite structures in Multifunctionality of Polymer Composites. Friedrich K., Breuer U., eds. Elsevier, 2015.
- [2] Song K., Guo J.Z. Liu, C. Polymer-Based Multifunctional Nanocomposites and Their Applications. Elsevier, 2018.
- [3] Sanida A., Stavropoulos S.G., Speliotis Th., Psarras, G.C. Polymer, 236, 124311, 2021.

Acknowledgments

The research work was supported by the Hellenic Foundation for Research and Innovation (H.F.R.I.) under the “First Call for H.F.R.I. Research Projects to support Faculty members and Researchers and the procurement of high-cost research equipment grant” (Project Number:2850).

Mechanical and thermal properties of spinel refractories mixed with blast furnace waste slag

Aikaterini Symvoulidou^{1,2} and George Vekinis¹

¹Institute of Nanoscience and Nanotechnology, NCSR “Demokritos”, Agia Paraskevi, Greece

²Department of Physics, University of Ioannina, Ioannina, Greece

Steel-making waste slag is one of the most ubiquitous and intractable industrial waste materials in industrialised countries. It consists mainly of very hard semi-crystalline metal oxides with large amounts of oxides of iron and zinc as well as Na₂O and CaO and others, depending on the original composition of the ore mixture. It is essentially an inert material but, because of its very high hardness it has found few high value uses since it requires lots of energy to grind it to a usable size. It is mainly used as a road-filler and as a sand-blasting material. Over the years vast amounts have accumulated next to blast furnaces and steel-making plants which would only be reduced if a high-value application could be found.

In this work, an effort at utilising such slags has been made. Waste slag from steel-making plants was mixed with high temperature spinel refractory masses and tested to ascertain the effect on their mechanical and physical properties. Spinel refractory masses are used as bonding material in the construction of large kilns or furnaces for the production of ceramics and steel. The slag was first ground to various grain sizes and mixed up to 50% with the spinel refractory and sintered up to 1450°C. The specimens produced were tested under compressive and flexure load and by measurements of their thermal conductivity, thermal expansion, density, porosity and water absorption. The morphology of the starting materials and resulting specimens was examined by Scanning Electron Microscopy.

The results indicate that the use of up to 50% slag in spinel refractories does not affect the mechanical properties of the refractory and in some cases the strength is improved. At the highest sintering temperatures used the slag reacts with the spinel resulting in new high density, high strength refractories.

Cation and Anion co-doping of NiO for enhancing the UV-PV performance of NiO/TiO₂ heterostructures

Ch. Aivalioti^{1,2*}, E. Manidakis³, Z. Viskadourakis¹, N.T. Pelekanos^{1,3}, C.C. Stoumpos³,
M. Modreanu⁴, E. Aperathitis¹

¹IESL/FORTH, P.O. Box 1385, Heraklion 70013, Crete, Greece

²King Abdullah University of Science and Technology (KAUST) Thuwal 23955-6900 Saudi Arabia

³Dept. of Materials Science and Technology, University of Crete, 71003 Heraklion, Greece

⁴Tyndall National Institute-University College Cork, Lee Maltings, Cork, Ireland

The increasing energy consumption, produced from fossil fuels, and consequently the increase in air pollutants have led to phenomena such as global warming (greenhouse effect) with the well-known effects on the environment and human health. Buildings are responsible for consuming about 40% of the total produced energy, while windows are responsible for the loss of 10-25% of the thermal energy of buildings [1]. A properly designed “smart window” can control and modulate solar heat and lighting and it is possible, at the same time, to produce and store solar energy. The emerging class of wide gap oxide semiconductors can be fabricated as transparent solar cells, harvesting UV radiation and integrated into optoelectronics as power producers [2-4]. Thus, transparent solar cells can be used for energy-autonomous “smart windows” like electrochromics.

In this presentation, undoped NiO, single doped NiO with niobium (Nb) and nitrogen (N) (NiO:Nb, NiO:N) as well as co-doped NiO:(Nb,N) were fabricated by rf sputtering by employing metallic Ni and composite Ni-Nb targets in plasma containing % (Ar - O₂ - N₂) gases. The p/n heterostructures were fabricated by employing the fabricated p-type NiO and n-type TiO₂, namely p-NiO/n-TiO₂, to be investigated as UV solar cells. The TiO₂ layers consisted of a double mesoporous/compact TiO₂ film fabricated by spin coating, on FTO-covered glass substrates according to the standard procedure followed when TiO₂ is used as electron transfer layers for perovskites PVs. The TiO₂/FTO/glass configuration was the substrate used for forming NiO:Nb/TiO₂ and NiO:(Nb,N)/TiO₂ heterostructures (Fig. 1). The oxide layers were characterized by AFM, SEM-EDX, XRD, Raman, XPS, Hall and Seebeck effect and UV-Vis-NIR spectroscopy whereas the behavior of the heterostructures was characterized in the dark and photo I-V under UV illumination.

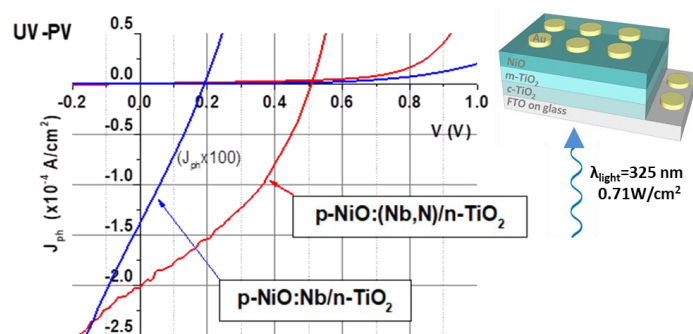


Figure 1: Dark and photo UV illumination

References

- [1] Karlsson J. “Control system and energy saving potential for switchable windows”, Proceedings of the 7th International IBPSA Conference, Rio de Janeiro, Brazil, August 13-15, 2001.
- [2] Wang Z, et al, Fusing electrochromic technology with other advanced technologies: A new roadmap for future development, *Mat. Sci. & Engineering R.* 2020;140:100524(26pp).
- [3] Manidakis E., et al “Hole transfer NiO layers with enhanced properties for all-inorganic perovskite solar cells”, Proceedings of the 37th EU PVSEC 2020, Lisbon, Portugal, September 7- 11, 2020
- [4] Aivalioti Ch., et al, “Transparent All-Oxide Hybrid NiO:N/TiO₂ Heterostructure for Optoelectronic applications”, *Electronics* 10 (2021) 988.

(*) corresponding & presenting author: Chrysa Aivalioti, chr.aivalioti@iesl.forth.gr.

Reduced Stark effect in CsPbBr₃ Perovskite Nanocrystals

N. G. Chatzarakis^{1,2}, A. Kostopoulos², G. Konstantinidis², G. Deligeorgis², G. Rainò^{3,4}, M. Bodnarchuk^{3,4}, M. V. Kovalenko^{3,4}, N. T. Pelekanos^{1,2}

¹Department of Materials Science & Technology, University of Crete, 70013 Heraklion, Greece

²Microelectronics Research Group, IESL-FORTH, 71110 Heraklion, Greece

³Department of Chemistry & Applied Biosciences, ETH Zürich, CH-8093 Zürich, Switzerland

⁴Empa-Swiss Federal Laboratories for Materials Science & Technology, CH-8600 Dübendorf, Switzerland

Lead halide perovskite nanocrystals (NCs), such as for instance CsPbBr₃ NCs, have shown great potential as single photon sources “on-demand”, exhibiting remarkable photon antibunching behaviour at room temperature but low single photon purity at low temperatures, contrary to what is typically observed in other semiconductor QD systems. Another particularity of these NCs is the absence of distinct biexciton lines in single dot spectroscopy experiments. This possibly suggests that the bi-exciton and exciton lines are close in energy, explaining the poor single photon purity at low temperatures. With increasing temperature, the hypothesis goes that some thermally-activated Auger process takes place, weakening the bi-excitonic emission and lowering drastically the $g_2(0)$ values at 300K. In order to clarify these hypotheses and deepen our understanding on the exciton transitions of these NCs [1-5], we present here a study on the emission properties of single CsPbBr₃ NCs under the influence of an external electric field. Toward this end, substrates with special inter-digitated contacts, shown schematically in Fig.1, were fabricated by standard photo-lithography. A thin film of polystyrene, containing dilute numbers of CsPbBr₃ NCs with 10nm edge length, was spin-cast over the electrodes. Micro-photoluminescence measurements on single CsPbBr₃ NCs under external electric field, exhibited typically very tiny Stark shifts of the main exciton peak (Fig. 2), in contradistinction with earlier work on CsPbI₃ NCs, where 20 times larger Stark shifts have been reported for similar fields [6]. In order to understand this result, further work focuses on the possible role of host-polymer in the observed Stark shifts and intends to extend the study to CsPbI₃ NCs.

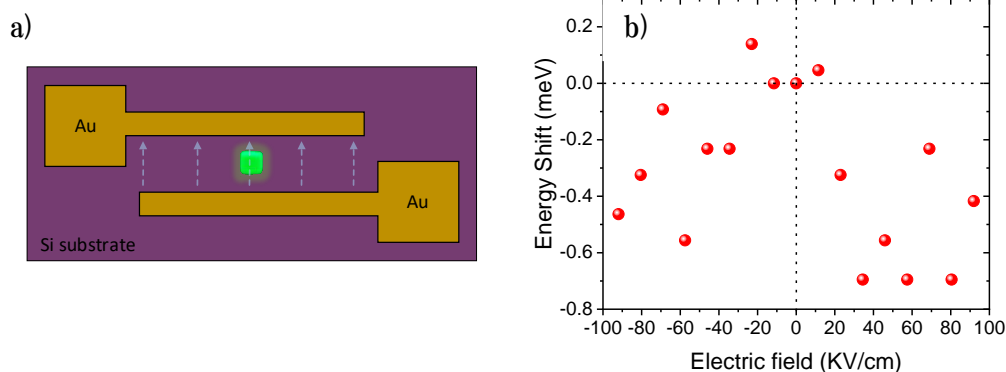


Figure 1: a) Schematic of the contact geometry used to apply electric field on CsPbBr₃ NCs, b) Energy shift of exciton line from a single CsPbBr₃ NC versus applied electric field

References

- [1] C. Yin et al., Phys. Rev. Lett. 119, 026401 (2017).
- [2] M. Fu et al., Nano Lett. 17, 2895 (2017).
- [3] J. Ramade et al., Appl. Phys. Lett. 112, 072104 (2018).
- [4] M. A. Becker et al., Nature 553, 189 (2018).
- [5] G. Rainò et al., Nano Lett. 19, 3648 (2019).
- [6] Bihu Lv et al. Phys. Rev. Lett. 126, 197403 (2021)

Electro-optic free-space ultrafast pulse-shaping in a graphene-loaded Bragg resonator

Alva Dagkli^{*}, Alma Chatzilari, Spyros Doukas, Eleftherios Lidorikis
Department of Materials Science and Engineering, University of Ioannina, 45110, Ioannina, Greece

Efficient ultrafast picosecond laser pulse-shaping in the near-IR, using saturable absorbers, is important for a variety of applications, from optical communications to signal processing. Graphene is an effective tunable absorber at high optical intensities, having the melting point at more than 4000 K and displaying wide-band operation, ranging from visible to THz [1-5]. In our analytical study we combine monolayer graphene with a single-port Bragg nanocavity, designed at $\lambda=1550$ nm, which operates in the reflection mode and shows 100% absorption at 300 K [6]. The free-space optical nanodevice is illuminated with high peak power pulses that manage to significantly increase graphene electronic and lattice temperatures. Under high incident power, intrinsic graphene absorptivity reduces, due to Pauli blocking effect, but results into a reflection increase, due to deviation from critical coupling. In our modelling scheme we explicitly study the formation of a hot electron gas in graphene, the phonon-mediated cooling, and the lattice temperatures. Manipulating graphene absorptivity through the appropriate combination of temperature, incident power and doping level, optical modulation is possible. Remarkably, the deviation of temperature- and doping- dependent graphene absorptivity from its critical value modulates the input pulse amplitude, duration and shape, resulting in single, double or even triple peaks.

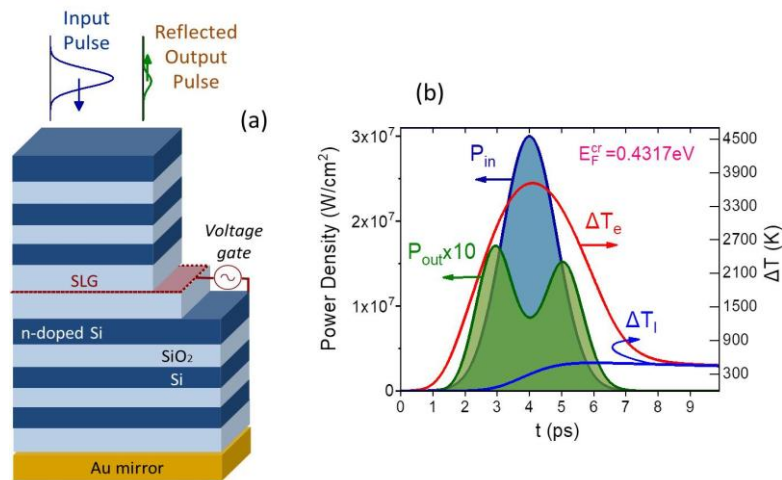


Figure 1: (a) Schematics of a single port asymmetric Bragg nano-cavity with a metal mirror on the backside for pulse-shaping. (b) Gaussian input (P_{in})/output (P_{out}) pulses with the respective electron (ΔT_e) and lattice (ΔT_l) temperature changes (from room temperature) as a function of time, for critical (~ 300 K) graphene doping.

References

- [1] Marini et al, PHYSICAL REVIEW B **95**, 125408 (2017)
- [2] Bao and Loh, ACS NANO **6**, 3677-3694 (2012)
- [3] Sun et al, NATURE PHOTONICS **10** (2016)
- [4] Ma et al, Applied Physics Reviews **6**, 041302 (2019)
- [5] Sun et al, ACS NANO **4**, 803-810 (2010)
- [6] Doukas et al, APPLIED PHYSICS LETTERS **113**, 011102 (2018)

* a.dagkli@uoi.gr

Hybrid GaAs nanowire/halide perovskite optoelectronic devices

E.M. Darivianaki^{*a}, M. Androulidaki^b, K. Tsagaraki^b, M. Kayambaki^b, G. Stavrinidis^b, G. Konstantinidis^b, E. Dimakis^c, N. T. Pelekanos^{a,b}, C. C. Stoumpos^a

^aDepartment of Materials Science and Technology, University of Crete, Heraklion, 71003, Greece

^bMicroelectronics Research Group, IESL-FORTH, Heraklion, 71110, Greece

^cInstitute of Ion Beam Physics and Materials Research, Helmholtz-Zentrum Dresden-Rossendorf, Dresden, Germany.

Perovskite solar cells attract much interest in photovoltaic applications nowadays, due to the high photovoltaic performance that they exhibit combined with the relative ease of fabrication. On the other hand, GaAs-based semiconducting devices are the best photovoltaic materials by most metrics, including, high absorption coefficient, direct bandgap, as well as high carrier mobility values [1]. For highly efficient solar cells, the choice of electron and hole transporting materials is of paramount importance to ensure efficient charge extraction with minimum recombination losses. As a norm, highly efficient perovskite solar cells make use of polycrystalline TiO₂ as the Electron Transporting Layer (ETL). Conceptually, considering the superb GaAs semiconducting properties, it is proposed that GaAs can be used as ETL, substituting conventional ETLs, aiming to drastically enhance electron extraction. This device design takes advantage of the discrete property of GaAs to have its conduction band lower in absolute energy than the perovskite conduction band, thus providing a favorable band alignment. In addition, intrinsic GaAs has extremely high electron mobility compared with polycrystalline TiO₂ [1],[2]. In this work, we focused on the fabrication of hybrid GaAs nanowire/perovskite diode devices, specifically choosing GaAs in its nanowire (NW) form to enhance the electrical contact area between the two materials (Figure 1a), intending to study the electrical properties of the device. The device architecture comprises (i) the GaAs NWs grown on an n-doped (111) Si wafer, (ii) an insulating layer (Cyclotene 3022-46 BCB) in between the NWs, preventing short-circuiting of the device, (iii) CH₃NH₃PbI₃, (iv) Spiro-OMETAD and (v) Au. The devices exhibited a clear diode response (Figure 1b), which is a promising result towards the fabrication of GaAs nanowire/perovskite photodiode devices, which can be made by substituting the top gold electrode with a transparent conducting oxide material.

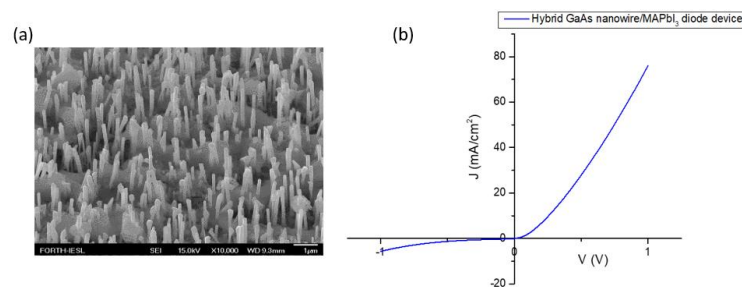


Figure 1: (a) SEM image of MAPbI₃ perovskite deposition around nanowires, (b) Current-voltage (I-V) curve of the diode device

Acknowledgements: This work was supported in part by the project “NANO-TANDEM” (MIS 5029191), co-financed by Greece and the European Regional Development Fund.

References

- [1] T.E. Sclesinger, Gallium Arsenide Encyclopedia of Materials: Science and Technology, 2nd edition; Editor: Buschow, Cahn, Merton C. Flemings, Ilschner, Kramer, Mahajan, Veyssiere, Publishers: Elsevier BV, p.3431-3435 (2001)
- [2] T. Bak.M.K. Nowotny, J.Phys. Chemistry.C **112**, 12981 (2008)

* elefdariv@materials.uoc.gr

High room temperature valley polarization in WS₂/Graphite

I. Demeridou^{1,2*}, M. Mavrotsoupakis^{1,3}, L. Mouchliadis¹, P. G. Savvidis^{1,3,4,5}, E. Stratakis^{1,2}, and G. Kioseoglou^{1,3,*}

¹ FORTH/IESL, Heraklion, 71110, Crete, Greece

² Department of Physics, University of Crete, Heraklion, 71003, Crete, Greece

³ Department of Materials Science and Technology, University of Crete, Heraklion

⁴ Key Laboratory for Quantum Materials of Zhejiang Province, Department of Physics, Westlake University, Hangzhou, China

⁵ Institute of Natural Sciences, Westlake Institute for Advanced Study, Hangzhou, China

Transition metal dichalcogenide (TMD) monolayers (1L) in the 2H-phase are 2D-semiconductors with two valleys in their band structure that can be selectively populated using circularly polarized light [1-3]. The role of the substrate for 1L-TMDs is an essential factor for the optoelectronic properties and for achieving a high degree of circular polarization at room temperature [4]. In this work, we investigate the room-temperature (RT) valley polarization of monolayer WS₂ on different substrates. The degree of polarization of photoluminescence in excess of 27% is found from neutral excitons in 1L-WS₂ on graphite at RT under on-resonance excitation. Using the photochlorination process [5], we modulate the polarization of the neutral exciton emission continuously from 27% to 38% for 1L-WS₂/Graphite. We show that valley polarization strongly depends on the interplay between the doping and the choice of the supporting layer of TMDs. Time-resolved PL measurements, corroborated by a rate equation model accounting for the bright exciton population in the presence of a dark exciton reservoir, support our findings. These results suggest a pathway towards engineering valley polarization and exciton lifetimes in TMDs, by controlling carrier density and choice of substrate.

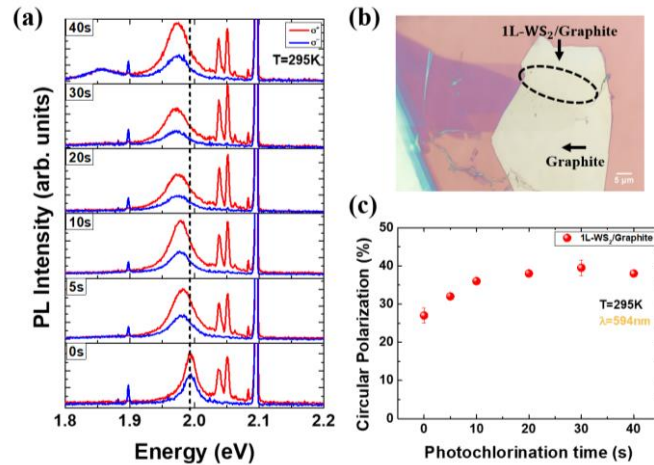


Figure 1: (a) Room temperature photoluminescence spectra of 1L-WS₂/Graphite analyzed for positive (σ⁺: red solid line) and negative (σ⁻: blue solid line) helicity as a function of photochlorination time (b) Microscope image of the monolayer 1L-WS₂/Graphite. (c) Circular Polarization of 1L-WS₂/Graphite as a function of photochlorination time.

Acknowledgements

I.D. acknowledge support by the European Union's Horizon 2020 research and innovation program through the project NEP, EU Infrastructure, GA 101007417 – INFRAIA-03-2020. L.M. and G. Kio., acknowledge funding by the Hellenic Foundation for Research and Innovation (H.F.R.I.) under the 'First Call for H.F.R.I. Research Projects to support Faculty members and Researchers and the procurement of high-cost research equipment grant' project No: HFRI-FM17-3034.

References

- [1] K.F. Mak, et al. *Physical Review letters* **105**, 136805 (2010)
- [2] G. Kioseoglou, et al. *Applied Physics Letters* **101**, 221907 (2012)
- [3] K.F. Mak, et al. *Nature Nanotechnology* **7**, 494 (2012)
- [4] I. Paradisanos, et al. *Applied Physics Letters* **116**, 203102 (2020)
- [5] I. Demeridou, et al. *2D Materials* **6**, 015003 (2018)

* idemer@physics.uoc.gr

Volatile Hybrid Organic/Inorganic Copper (I) Iodides/Polyiodides for Efficient Thin-Film Deposition of CuI

Konstantina Faka, Manolis G. Manidakis, Giannis Gkikas, Constantinos C. Stoumpos

Department of Materials Science and Technology, University of Crete, Heraklion 70013, Greece

P-type inorganic semiconductors are remarkably scarce when compared to their n-type counterparts, with notable examples found in the late 3d transition metal monoxides (i.e. Ni_{1-x}O) or the group 14 metal monochalcogenides (e.g. Sn_{1-x}Se). Among them, Cu(I) compounds, particularly the halides and the pseudohalides, stand out having been repeatedly employed as viable replacements to the best-performing organic p-type semiconductors, (*I*) based on triarylamine (e.g. PTAA) or thiophene (e.g. PEDOT:PSS) molecules commonly employed in photovoltaics.⁽²⁾ One of the most notable difficulties encountered in the use Cu(I) based compounds, however is their notorious insolubility in common solvents, thus making its solution processability limited.

In this work, we propose of a viable method of preparing high concentration precursor solutions in non-polar solvents than can subsequently be used for efficient deposition of CuI via standard spincoating techniques. Towards this end we have synthesized a series of hybrid organic/inorganic copper (I) iodides and polyiodides with diammonium cations (A = H₃N-(CH₂)_x-NH₃)²⁺) with general formulae A_xCu^I(I)_y(I_n)_z (Figure 1) with the aim of dissociating the insoluble sphalerite-type CuI lattice into smaller fragments that can be easily solution processed. Moreover, the presence of the organic ammonium cation, as well that of the polyiodides further assists in the increase of solubility due to the enhancement of non-polar interaction between the solvents and the solids. The excess of these components in the films can be easily removed during the post-deposition heating stage of the spincoating process, due to the volatile nature of the said components. Relevant to the perovskite solar cells, CuI shares the same halogen atom, which in turn is designed to facilitate the formation of a smooth interface between the active perovskite-layer and the p-type hole transporting layer.

Several hybrid organic/inorganic compounds have been synthesized and extensively characterized, both morphologically and spectroscopically, including the determination of the crystal structure via single-crystal X-ray diffraction. The thermal decomposition of the materials as well as their solubility tests in common organic solvents have also been performed. Ongoing work addresses the suitability of the materials as precursors in the CuI solution deposition process and evaluates their applicability in perovskite solar cells.

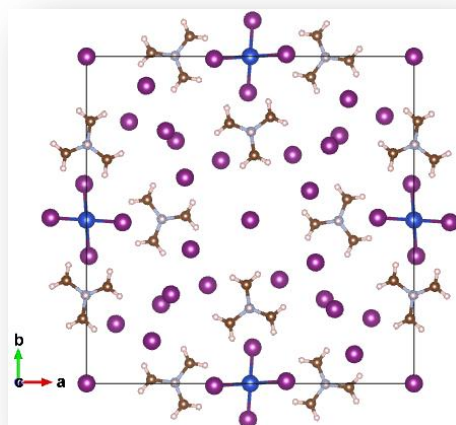


Figure 1. The crystal structure of the multicomponent hybrid organic/inorganic polyiodide iodocuprate based on the 1,4-diazabicyclo[2.2.2]octane dication.

References

1. N. Arora *et al.*, Perovskite solar cells with CuSCN hole extraction layers yield stabilized efficiencies greater than 20%. *Science* **358**, 768-771 (2017).
2. L. Calió, S. Kazim, M. Grätzel, S. Ahmad, Hole-Transport Materials for Perovskite Solar Cells. *Angew. Chem., Int. Ed.* **55**, 14522-14545 (2016).

Measuring optical forces using single beam optical tweezers

T. Giannakis^{1,2} and M. Kandyla^{*,1}

¹ National Hellenic Research Foundation, Theoretical and Physical Chemistry Institute, 48 Vasileos Constantinou Avenue, 11635 Athens, Greece

² National and Kapodistrian University of Athens, Department of Physics, University Campus, Zografou, 15784 Athens, Greece

*kandyla@eie.gr

Optical trapping, performed by optical tweezers (OT), is an innovative and highly sensitive method, which has the ability of measuring forces in the femto-Newton range, consequently, it can probe very small variations in biological properties. Using this method, we can capture at the focus of a laser beam microscopic objects like living cells, bacteria viruses, etc.[1], without physical contact and study their basic physical properties such as shear elastic constant and membrane viscosity.[2]

The most known way of calibration in an optical tweezer setup for spherical shaped-like specimens is based on the comparison between the trapping force and the Stokes' dragging force [3]. According to Stokes' law: $F_{drag} = 6\pi\eta ru$, where η is the medium viscosity coefficient, r is the radius of the specimen and u is the dragging velocity. In the equilibrium position the two forces are equals, so significant results such as trapping efficiency can be derived.

In this work, we build a single beam OT equipped with a homemade inverted microscope for biological and technological applications (Figure 1). We measure the optical forces exerted in the specimens from the optical trapping setup using the calibration method mentioned above for different specimen radii and different media viscosity coefficients.

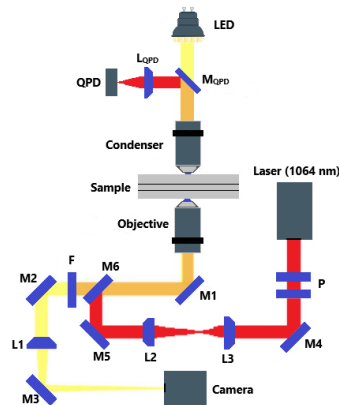


Figure 1: Schematic representation of the optical trapping setup

References

- [1] I. A. Favre-Bulle, A. B. Stilgoe, E. K. Scott, and H. Rubinsztein-Dunlop, "Optical trapping in vivo: Theory, practice, and applications," *Nanophotonics*, vol. 8, no. 6. De Gruyter, pp. 1023–1040, 2019. doi: 10.1515/nanoph-2019-0055.
- [2] C. N. Lima *et al.*, "Evaluating viscoelastic properties and membrane electrical charges of red blood cells with optical tweezers and cationic quantum dots – applications to β -thalassemia intermedia hemoglobinopathy," *Colloids and Surfaces B: Biointerfaces*, vol. 186, no. November, p. 110671, 2020, doi: 10.1016/j.colsurfb.2019.110671.
- [3] R. Zhu, T. Avsievich, A. Popov, and I. Meglinski, "Optical Tweezers in Studies of Red Blood Cells," *Cells*, vol. 9, no. 3, p. 545, 2020, doi: 10.3390/cells9030545.

Formamidinium lead bromide perovskite as visible-light detector

A. Anastasopoulos¹, A. Kaltzoglou¹,
A. Sinani^{1,2}, A. Bogris², C. Riziotis¹, M. Kandyla^{1,*}

¹*Theoretical and Physical Chemistry Institute, National Hellenic Research Foundation, 48 Vassileos Constantinou Ave., 11635 Athens, Greece*

²*Department of Informatics and Computer Engineering, University of West Attica, Aghiou Spiridonos, 12243 Egaleo, Athens, Greece*

Organic-inorganic halide perovskites have become a major research topic in the past ten years due to a variety of semiconducting applications, namely solar cells, luminescence, photocatalysis and photodetectors [1]. The current work deals in particular with the use of FAPbBr₃ (FA = (NH₂)₂CH) as a visible-light detector [2]. The polycrystalline compound was prepared by fusion of the precursor compounds PbBr₂ and FABr in solid state under vacuum. It was then pressed in the form of a pellet and two transparent fluorine-doped tin oxide (FTO) glasses were attached on both sides as electrodes. This air-stable, red-color compound exhibits a direct band gap of 2.15 eV and it has been proposed as a single-crystal detector for both for visible and X-ray photons [3,4].

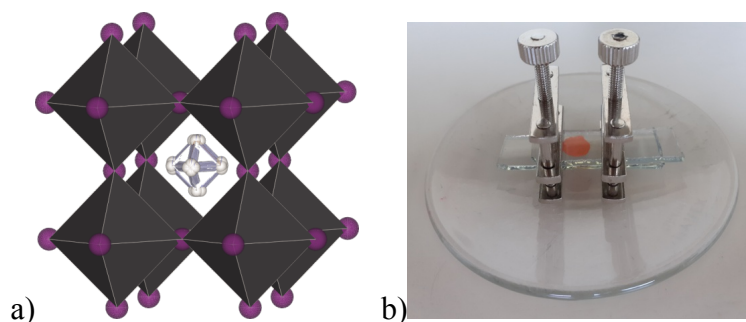


Figure 1: a) The crystal structure of the pseudo-cubic FAPbBr₃ with disordered C and N atoms. Hydrogen atoms are omitted. b) Photodetector device made of a FAPbBr₃ pellet sandwiched between two conducting FTO glasses.

We investigate the use of formamidinium lead bromide as a photodetector under various illuminating conditions, spanning the visible spectral range. The obtained I-V curves and spectral responsivity show a high sensitivity of the electrical resistance of the detector on the incident photon wavelength, in the range 550 – 600 nm. Photovoltage from the device under pulsed laser excitation at 405 nm wavelength allows for the measurement of the rise and fall time of the detector for various light pulse frequencies, in the range 1 Hz – 1 KHz. Overall, this work proposes polycrystalline FAPbBr₃ as a low-cost and readily prepared visible-light detector for optoelectronic applications.

References

- [1] Bin, Yusoff, Gao and Nazeeruddin, *Coordination Chemistry Reviews* **373**, 258 (2018).
- [2] Lu, Li, Zhang, Han, He, Zou and Xu, *Adv. Photonics Res.* **3**, 2100335 (2022).
- [3] Yao, Jiang, Xin, Ma, Wei, Zheng and Shen, *Nano Letters* **21**, 3947 (2021).
- [4] Dong, Fu, Yu, Jiang, Jin, Guo, Wang and Zhang, *CrystEngComm* **24**, 2100 (2022).

* kandyla@eie.gr

Enhanced chiral sensing using gain metamaterials

I. Katsantonis^{a,b,*} and M. Kafesaki^{a,b}

^a*Institute of Electronic Structure and Laser, Foundation for Research and Technology-Hellas, 70013 Heraklion, Crete, Greece*

^b*Department of Materials Science and Technology, University of Crete, 70013 Heraklion, Crete, Greece*

Detecting the chirality of molecules and biomolecules is of great interest for many branches of science and technology, especially for life sciences and pharmacology; in the latter, very often, only one of the two enantiomers of a chiral substance is associated with therapeutic action while the other can be even toxic. Therefore, an efficient discrimination of the different enantiomers of a chiral substance is of crucial importance. Since chiral light-matter interactions are extremely weak (natural chiral materials have chirality parameter $\kappa \sim 10^{-4}$) this detection can be very challenging. A way to overcome this problem in optical detection schemes, as has been demonstrated in many recent studies, is the involvement of nanophotonic or metamaterials structures [1]. The capability of such structures to enhance the chiro-optical signal of molecules placed in their vicinity is connected mostly to their capability to create strong local chiral fields. The existing research has demonstrated a variety of structures associated with enhanced chiral near fields and, thus, enabling enhanced chiro-optical response, mainly enhanced *circular dichroism* (CD) signal (Note that $CD = A_{RCP} - A_{LCP}$ is the absorption (A) difference between left- and right-handed circularly polarized waves (denoted by LCP and RCP respectively) passing through a chiral medium; chiral materials of opposite helicity give opposite CD). Here we propose an alternative and novel approach towards chirality detection. This is involving active (gain) materials and components. As we show proper employment metamaterial structures incorporating gain materials (i.e. gain metamaterials) can greatly enhance the circular dichroism signal obtained by natural chiral media.

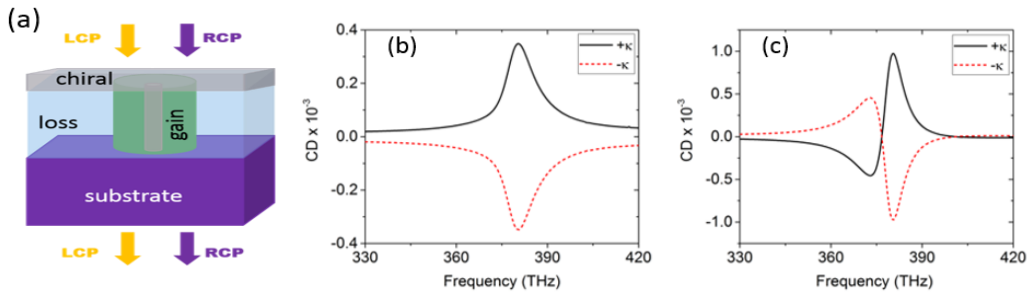


Figure 1: Panel (a) shows a potential setup (unit cell) of a chirality sensing platform/metamaterial composed of holey silicon disks (refractive index $n=3.5$) of diameter 300 nm, arranged periodically with a lattice constant of 500 nm and placed on top of a glass substrate with refractive index 1.5. The central holes are 20 nm in diameter and their height is the same as the disks ($l=130$ nm). The background medium on top of the glass substrate is considered of refractive index of 1.33. The thin chiral layer to be investigated (grey-color) is placed above the metamaterial structure and described by its refractive index ($n = 1.45+0.01i$), and chirality parameter $\kappa = \pm 5 \times 10^{-4}(1+0.1i)$. Panel (b) shows the CD for the system of Panel (a), where a thin chiral layer (of thickness 10 nm) is placed on top of the holey lossless silicon disk (without gain). Panel (c) shows the CD for the same system as panel (b) but with incorporation of gain ($n=3.5-0.02i$) in the holey silicon disk.

References

- [1] Mohammadi, E.; Tsakmakidis, K.L.; Askarpour, A.N.; Dehkoda, P.; Tavakoli, A.; Altug, H. Nanophotonic platforms for enhanced chiral sensing. *ACS Photonics*, **5**, 2696, (2018).
- [2] Katsantonis, I.; Droulias, S.; Soukoulis, C.M.; Economou, E.N.; Rakitzis, P.; Kafesaki, M. Chirality sensing employing Parity-Time-symmetric and other resonant gain-loss optical systems, *Phys. Rev. B*, **105**, 174112, (2022).

* katsantonis@iesl.forth.gr

Micro-optical elements fabricated onto an optical fiber adaptor for beam guidance

D.Ladika^{1,2*}, V. Melissinaki¹, G.D. Barmparis³, M. Farsari¹

¹*FORTH/IESL, Nik. Plastira 100, 70013 Heraklion, Crete, Greece*

²*Department of Materials Science and Technology, University of Crete, Greece*

³*Department of Physics, University of Crete, Greece*

Multi-photon lithography (MPL) is a powerful 3D printing technique which enables the direct writing of computer-designed structures within the volume of a photosensitive material[1]. Over the last decade, MPL has been a leading technique for rapid prototyping of 3D micro-optical elements to be fabricated directly onto the end-face of optical fibers[2] and photonic devices[3] or even for development of micrometric resonators[4].

Fabrication of fiber-coupled integrated photonic devices requires robust and reliable way in order to attached optical fibers to other structures, often with sub-micron accuracy[5]. Thus, we developed an optical fiber adaptor through MPL technique where micro-optical elements will be fabricated onto the adaptor, in order to achieve laser beam guidance. This device holds its novelty to the fact that can be easily handled in order to take measurements for a variety of optical fibers and applications.

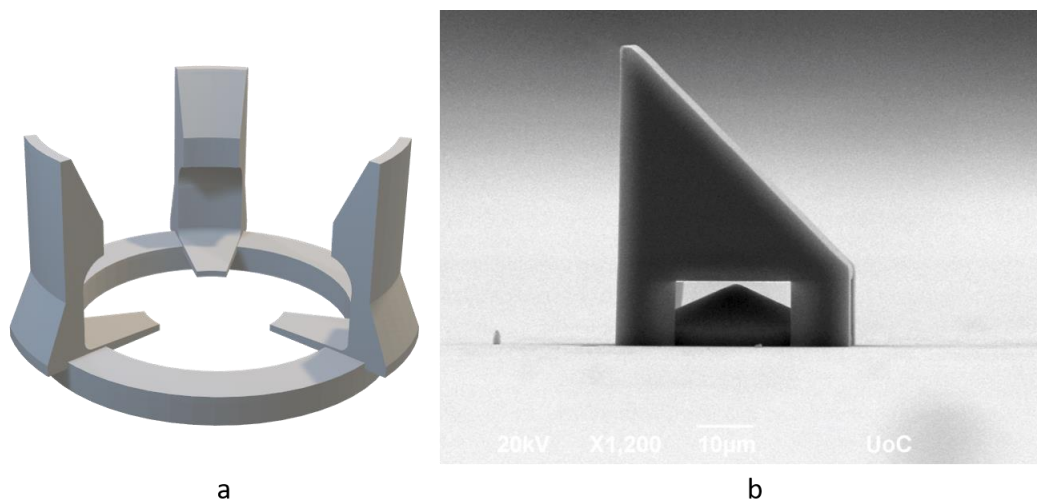


Figure 1: a. STL image of the optical fiber adaptor, b. SEM image of the micro-optical elements that will be attached to the adaptor

References

1. M. Farsari, M. Vamvakaki, and B. N. Chichkov, *J. Opt.* **12**, (2010).
2. V. Melissinaki, I. Konidakis, M. Farsari, and S. Pissadakis, *IEEE Sens. J.* **16**, 7094 (2016).
3. K. Y. Lee, N. Labianca, . H Lorenz, M. Despont, N. Fahrni, P. Renaud, P. Vettiger, ; G McBride, ; V Nazmov, E. Reznikova, J. Mohr, A. Snigirev, I. Snigireva, S. Achenbach, and V. Saile, *Opt. Express*, Vol. 19, Issue 23, Pp. 22910-22922 **19**, 22910 (2011).
4. V. Melissinaki, O. Tsilipakos, M. Kafesaki, M. Farsari, and S. Pissadakis, *IEEE J. Sel. Top. Quantum Electron.* **27**, (2021).
5. A. Bogucki, Ł. Zinkiewicz, W. Pacuski, P. Wasylczyk, P. Kossacki, J. Liu, B. Cai, J. Zhu, D. Chen, Y. Li, J. Zhang, G. Ding, X. Zhao, and C. Yang, *Opt. Express*, Vol. 26, Issue 9, Pp. 11513-11518 **26**, 11513 (2018).

Nonlocal effective medium (NLEM) for quantitative modelling of nanoroughness in spectroscopic reflectance

Eleftheria Lampadariou¹, Konstantinos Kaklamanis¹, Dimitrios Goustouridis², Ioannis Raptis² and Eleftherios Lidorikis^{1,3}

1 Department of Materials Science and Engineering, University of Ioannina, 45110, Ioannina, Greece; e.labadariou@uoi.gr; k.kaklamanis@uoi.gr;

2 ThetaMetrisis S.A, Christou Lada 40, Athens, 12243, Greece; dgoustouridis@thetametrisis.com; raptis@thetametrisis.com;

3 University Research Center of Ioannina (URCI), Institute of Materials Science and Computing, 45110 Ioannina; elidorik@uoi.gr;

Spectroscopic reflectance is a versatile optical tool for the characterization of transparent and semi-transparent thin films in terms of thickness and refractive index. The Fresnel equations are used to interpret the measurements, but their accuracy is limited when surface roughness is present. Nano-roughness can be modelled through a discretized multi-slice and effective medium approach, but up to date this offered mostly qualitative and not quantitative accuracy. Here we introduce an adaptive and nonlocal effective medium approach, which considers relative size and environment of each discretized slice. We develop our model using finite-difference time-domain simulation results and demonstrate its ability to predict nano-roughness size and shape with relative errors $< 3\%$ in a variety of test systems. The accuracy of the model is directly compared with the prediction capabilities of the Bruggeman and Maxwell-Garnett models, highlighting its superiority. Our model is fully parametrized and ready to use for exploring the effects of roughness on the reflectance without the need for costly 3D simulations, and to be integrated in the Fresnel simulator of spectroscopic reflectance tools.

Memristive perovskite solar cells for self-powered IoT edge computing

K. Rogdakis^{1,2,*}, M. Loizos¹, G. Viskadourous¹ and E. Kymakis^{1,2,*}

¹*Department of Electrical & Computer Engineering, Hellenic Mediterranean University (HMU), Heraklion 71410 Crete, Greece.*

²*Institute of Emerging Technologies (i-EMERGE) of HMU Research Center, Heraklion 71410, Crete, Greece.*

**e-mails: krogdakis@hmu.gr, kymakis@hmu.gr*

Abstract:

Mixed halide perovskites (HP) have been used as active layer in highly performing solar cells (PSC) that had led to efficient solar energy harvesting. Moreover, HP's rich dynamics enabled by the inherently coupled ionic and electronic degrees of freedom have also led to optoelectronic memristors emulating synaptic- and neural-like dynamics. A single printable material stack fabricated with low manufacturing cost at low temperature, combining both efficient solar energy harvesting and memristive functionalities would constitute a transformational breakthrough.

In our work we demonstrate an inverted PSC with an average power conversion efficiency (PCE) of ~17% (champion 17.97%) that upon appropriate electric bias procedure exhibits stable resistance switching characteristics without losing its PCE performance even after thousands of switching cycles (this device is termed as MemPVcell). MemPVcell demonstrates a light-tuneable High Resistance State (HRS) to Low Resistance State (LRS) ratio of up to 10^5 , fast switching cycles (in ms regime) with endurance of 3×10^3 cycles with no detectable HRS/LRS ratio drop. Corresponding PCE performance was monitored after multiple resistance switching loops and endurance cycles exhibiting a full PCE recovery to its initial value within few minutes of rest.

Electrochemically active supramolecular entities in layered hybrid halide perovskites

Eleni C. Macropulos^{*a}, Marios E. Triantafyllou Rundell^a, Linda Li^b,
Joseph Bennett^b, Peijun Guo^b, Mikael Kepenekian^c, Constantin C. Stoumpos^a

^a Department of Materials Science and Technology, University of Crete, Heraklion
70013, Greece.

^b Department of Chemical & Environmental Engineering, Yale University, West
Haven CT 06516, USA.

^c Institute of Chemical Sciences of Renne, University of Renne, Rennes F-35042,
France.

Halide perovskites are remarkable, unconventional semiconductors as they have high optical absorption coefficients, long charge carrier diffusion lengths, intense photoluminescence, and slow rates of non-radiative charge recombination [1]. Furthermore, layered hybrid halide perovskites ($A^I_2M^{II}X_4$ or $A^{II}M^{II}X_4$ (A=monovalent or bivalent cation, M=bivalent p-block metal, X=halide anion), consist of anionic sheets of corner-sharing metal-halide octahedra, selectively “partitioned” by organic cations to form crystallographically ordered nanoscale sheets. This arrangement generates natural multiple quantum wells that exhibit stable excitonic features with intense photoluminescence (PL) characteristics observable already at room temperature.

Some of the exotic properties of halide perovskites is also revealed in this class of materials since a handful of them exhibit broadband optical emission, generating white light as a result of the self-trapped exciton mechanism [2]. Understanding this type of trap-activated behavior requires careful design of the materials involving a variety of organic spacers that can potentially trigger or suppress this effect.

In this work, we have designed and synthesized a series of layered perovskites with electrochemically-active spacers, where the electrochemical state of the spacer can influence the optical emission of the bulk material. Concomitantly, the installation of a functional group in the spacer cation, further enhances the structural

complexity by engaging in weak supramolecular interactions which can use as “perturbation probes” to interrogate the optical response of the materials as a function of the electrochemical state of the spacer cation. Towards this end we have synthesized two sister A_2PbBr_4 compounds ($A^+=2,3$ dihydroxyphenylethylammonium((HO)₂-PEA) and 2-(3-aminoethyl)benzoic acid (HO₂C-PEA)) as a redox-active and redox-inert pair of compound with a similar supramolecular interaction environment. Interestingly, the redox-active compound spontaneously crystallizes in its partially oxidized semiquinone form undergoing a one-electron oxidation during the synthesis. In this form, the compound exhibits similar photoluminescence characteristics (strong blue-light emission at 400nm) with those of the redox-inert compound, suggesting that the chemically reactive radical has been quenched during the reaction. Ongoing work on the electrocatalytic reaction mechanism using cyclic voltammetry suggest that both the fully reduced form ((HO)₂-PEA)₂PbBr₄ and the fully oxidized ((O=C)₂-PEA)₂PbBr₄ are present in the solution, prompting further optical and structural characterization of these metastable halide perovskite species.

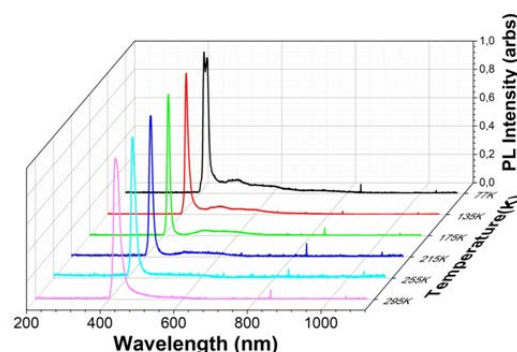


Figure 1: Temperature Dependent Photoluminescence of structure ((3,4-dihydroxy)PEA)₂PbBr₄.

References

- [1] C.C Stoumpos and M.G. Kanatzidis, Adv.Mater.**28**, 5778 (2016).
- [2] M. D. Smith and H. I. Karunadasa, Acc. Chem. Res.**51**, 619 (2018).

Hybrid Germanium Bromine Perovskites with Tunable Second Harmonic Generation

Yang Liu,¹ Shining Geng,² Ya-Ping Gong,³ Mei-Ling Feng,⁴ Despoina Manidaki⁵,
Constantinos C. Stoumpos⁵, Wei-Xiong Zhang,³ Zewen Xiao,² Lingling Mao¹

¹ Department of Chemistry, Southern University of Science and Technology, Shenzhen 518055, P. R. China

² Wuhan National Laboratory for Optoelectronics, Huazhong University of Science and Technology, Wuhan 430074, P. R. China

³ MOE Key Laboratory of Bioinorganic and Synthetic Chemistry, School of Chemistry, Sun Yat-Sen University, Guangzhou 510275, P. R. China

⁴ State Key Laboratory of Structural Chemistry, Fujian Institute of Research on the Structure of Matter, Chinese Academy of Sciences, Fuzhou, Fujian 350002. P. R. China.

⁵ Department of Materials Science and Technology, University of Crete, Vassilika Voutes GR-700 13 Heraklion, Greece

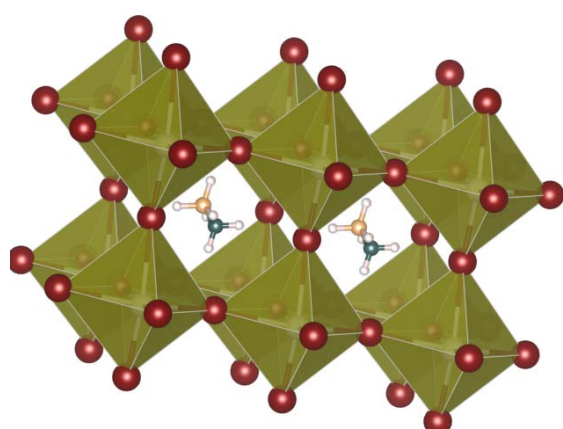


Figure 1: Crystal structure of the Methylammonium Germanium Bromide hybrid 3D perovskite. The $[\text{GeBr}_6]^{4-}$ units, form the corner – sharin octahedra.

Over the last decade, researchers have been particularly concerned with hybrid organic-inorganic halide perovskites, owing to their remarkable materials' chemistry and physics. Due to their exceptional semiconductor characteristics and charge-transport ability, they are one-of-a-kind optoelectronic materials. They've also been used to create photovoltaic devices with up to a 25% efficiency in power conversion.¹ Germanium-based perovskites, in particular, have attracted immense interest due to their ability to crystallized into non-centrosymmetric space groups,² which in turn enables the expression of strong nonlinear optical (NLO) properties. Second Harmonic Generation (SHG), in particular, is strongly amplified, corroborated by the presence of soft, highly polarizable atoms in

addition to the necessary pre-requirement of the absence of a crystallographic inversion symmetry. SHG is a property that is of paramount importance for the laser industry providing the ability to manipulate the wavelength of coherent monochromatic light.

In this work we present a series of new series of germanium-based bromide perovskites which crystallize in polar space groups and exhibit strong SHG responses relative to the commercially used compound potassium dihydrogen phosphate (KDP). The compounds possess a direct optical bandgap between 2.4-3.1 eV, possessing a relatively narrow SHG-transparent region to the Nd:YAG laser source (1064nm). Nevertheless, the particle size dependence of the SHG response suggests that all the materials possess a phase matchable behavior and are still promising candidates for use in their transparent SHG region. Ongoing work on the wavelength-dependent performance suggests that the efficiency of the SHG response can be strongly enhanced at longer excitation wavelengths.

References

1. Jeong, J. et al. Pseudo-halide anion engineering for α -FAPbI₃ perovskite solar cells. *Nature* **592**, 381–385 (2021).
2. Stoumpos, C. C. et al. Hybrid Germanium Iodide Perovskite Semiconductors: Active Lone Pairs, Structural Distortions, Direct and Indirect Energy Gaps, and Strong Nonlinear Optical Properties. *J. Am. Chem. Soc.* **137**, 6804–6819 (2015).

Strong passivation effect at the MAPbI₃/GaAs hetero-interface

Emmanouil G. Manidakis^{1,2}, Nikolaos G. Chatzarakis^{1,2}, Katerina Tsagaraki², Dimitris Tsikritzis³ Constantinos C. Stoumpos¹, Nikolaos T. Pelekanos^{1,2}

¹Department of Materials Science & Technology, University of Crete, Heraklion 71003, Greece

²Microelectronics Research Group, IESL-FORTH, Heraklion 71110, Greece

³Department of Electrical & Computer Engineering, Hellenic Mediterranean University, Heraklion 71410, Greece

Gallium Arsenide is the most heavily studied III-V semiconductor with excellent optoelectronic properties. It has a direct band gap at 1.42 eV, an ultra-high mobility of free carriers, as well as strong light emission and absorption phenomena, which make GaAs a very attractive material for applications ranging from solar cells to lasers and sensors. A well-known disadvantage of GaAs however, is the high non-radiative surface recombination velocity. Many works in the past have focused on the passivation of the GaAs surface with different approaches such as plasma treatment [1], chemical passivation [2] and deposition of another material on the surface as protection [3]. On the other hand, perovskite materials in the form of AMX₃ [A: monovalent cation (methylammonium (MA), formamidinium (FA), Cs), B: divalent metal cation (Sn, Pb), X: monovalent anion (I, Br, Cl)] [4] have recently attracted a lot of attention for a variety of optoelectronic applications, due to the low-cost and ease of fabrication, the direct and tunable bandgap, the relatively low exciton binding energy, long lifetimes and large diffusion length of the free carriers.

In this work, we merge the two material systems in view of novel hybrid devices. We investigate MAPbI₃ thin films deposited directly on undoped GaAs (100) substrates. We find that the presence of MAPbI₃ in contact with the GaAs surface, produces systematically a spectacular (nearly three-orders of magnitude) enhancement of the GaAs photoluminescence (PL) emission at low temperatures. We interpret this PL enhancement as due to some efficient passivation process of the GaAs surface caused by MAPbI₃.

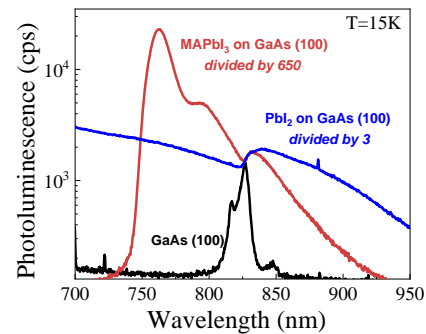


Figure 1 Low-T PL spectra of GaAs, MAPbI₃/GaAs and PbI₂/GaAs, divided where appropriate by the enhancement factor.

References

- [1] G. H. Yang, Y. Zhang, E. T. Kang, K. G. Neoh, W. Huang, and J. H. Teng, *J. Phys. Chem. B*, vol. 107, 8592 (2003).
- [2] D. Alexiev, D. A. Prokopovich, and L. Mo, *ArXivcond-Mat0407112*, (2004).
- [3] M. Hocevar *et al.*, *Appl. Phys. Lett.* 102, 191103 (2013).
- [4] C. C. Stoumpos and M. G. Kanatzidis, *Acc. Chem. Res.* 48, 2791 (2015).

Acknowledgments

This work was supported by Horizon 2020 Framework Programme (PULSE-824996) and “NANOTANDEM” (MIS 5029191) co-financed by Greece and the European Regional Development Fund.

Contact: mman@materials.uoc.gr

The effect of different architectures of TiO₂ as electron transport layer in perovskite solar cells

E.G. Manidakis^{1,2}, I. Syngelakis^{1,2}, Ch. Aivalioti^{1,2}, M. Androulidaki², K. Tsagaraki², C. C. Stoumpos¹, N.T. Pelekanos^{1,2}, G. Kenanakis^{1,2}, A. Klini², M. Farsari², E. Aperathitis²

¹*Department of Materials Science & Technology, University of Crete, 71003 Heraklion, Greece*

²*Institute of Electronic Structure & Laser, FORTH, Heraklion 70013, Greece*

Perovskite is a well-studied material over the last few years due to the excellent optoelectronic properties, the low fabrication cost and its application to low-cost high efficiency single and tandem solar cells. A conventional perovskite solar cell requires the use of an electron transport layer (ETL) for the efficient extraction of the photogenerated electrons. The basic criteria for ETL is the favorable band alignment with perovskite and the minimal parasitic optical absorption [1]. TiO₂ seems to be one of the most efficient ETL materials because it can effectively transfer the free electrons and at the same time repel the free holes, thus minimizing recombination effects.

In this work, we compare two different architectures of TiO₂ as ETL in perovskite solar cells. In a first realization, the standard alternation of compact and mesoporous TiO₂ is used as ETL, while in a second realization chemically-synthesized TiO₂ nanorods (NRs) are used instead, having different NR heights [2]. The main goal is to increase the effective area of the TiO₂/perovskite interface and take advantage of the enhanced transport properties of the enhanced structural quality of the TiO₂ NRs.

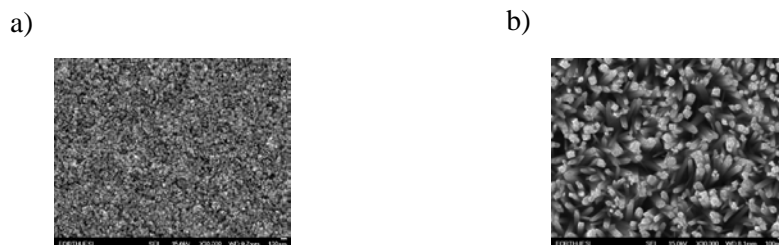


Figure 1. Top-view SEM images of the (a) mesoporous TiO₂ and (b) nanorods TiO₂ surface deposited/grown on FTO/glass.

The TiO₂ layers were characterized by AFM, SEM-EDX, XRD, PL and UV-Vis-NIR spectroscopy. The ETLs were employed in conventional perovskite solar cells [3] and their output performance were tested under AM1.5 solar illumination, compared and analyzed.

References

- [1] Q.-D. Ou, et al “Recent Advances in Energetics of Metal Halide Perovskite Interfaces,” *Adv. Mater. Interfaces*, vol. 4, no. 2, p. 1600694, 2017.
- [2] I. Syngelakis, “3D Laser Lithography with Applications in Photocatalysis”, Master thesis, 2022, Department of Materials Science and Technology, University of Crete.
- [3] Manidakis E., et al “Hole transfer NiO layers with enhanced properties for all-inorganic perovskite solar cells”, *Proceedings of the 37th EU PVSEC, Lisbon (2020)*.

Acknowledgements

This work was supported by Horizon 2020 Framework Programme (PULSE-824996) and “NANOTANDEM” (MIS 5029191) co-financed by Greece and the European Regional Development Fund.

Polariton lasing in 2D Perovskite Microcavities

M.Mavrotsoupakis^{1,2}, M.Triantafillou^{1,5}, M. Chairetis^{1,2}, G. Paschos^{3,4}, Constantinos C. Stoumpos^{1,5},
P. G. Savvidis^{1,2,3,4}

¹ Institute of Electronic Structure and Laser, Foundation for Research and Technology - Hellas, Heraklion, 71110, Crete, Greece

² Department of Materials Science and Technology, University of Crete, Heraklion, 71003 Crete, Greece

³ Key Laboratory for Quantum Materials of Zhejiang Province, Department of Physics, Westlake University, Hangzhou, China

⁴ Institute of Natural Sciences, Westlake Institute for Advanced Study, Hangzhou, China

⁵ Department of Chemistry, University of Crete, Heraklion, 71003, Crete, Greece

Exciton polaritons, with very low effective mass, are regarded as promising candidates to realize Bose–Einstein condensation in lattices for room temperature quantum simulations. Two dimensional (2D) organic–inorganic hybrid perovskites have properties that enable to sustain stable exciton polariton condensation, strong polariton–polariton interactions and long-range coherent polariton condensate flow at room temperature. The combination of huge exciton binding energies, enhanced stability, high tunability and ease of fabrication makes them ideal materials for achieving polariton condensation in optical microcavities. Here we present a fabrication of a microcavity, with layered, self-assembled perovskite (BA)₂(MA)₂Pb₃I₁₀ crystals as an active material sandwiched between two Bragg dielectric mirrors (DBRs). The structure of the material resembles multiple quantum wells with the perovskite layers representing the wells and the organic spacer (BA) the barriers. This natural confinement inherits perovskite excitons with huge electron-hole binding energies and makes them stable and observable even at room temperature. Initially the material is diluted as a supersaturated solution in hydrogen iodine at elevated temperature, then drop-casted on top of one DBR and lastly covered with the other DBR. The 2D crystals are formed once the sample is cooled with their width being dependent on the force acted upon the DBRs. This simple yet effective method results in the appearance of several cavity modes inside the microcavity with strong indication of anticrossing and polariton formation. At higher excitation energies, even signs of lasing can be seen from the photoluminescence measurements (Fig 1.) This microcavity fabrication method appears to be very promising for polaritonic applications and further research needs to be done for more clear and conclusive results.

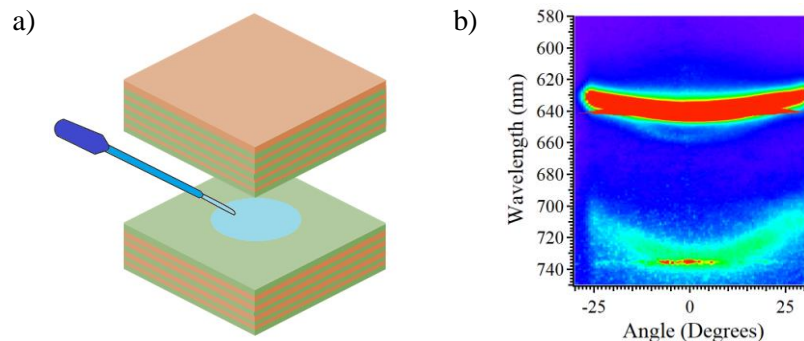


Figure 1: a) Fabrication of the sample with supersaturated perovskite material drop-casted between 2 DBR mirrors, b) Angle resolved photoluminescence measurements with indications of polariton formation and lasing

References

- [1] Kasprzak, J. et al., Nature 443, 409–414 (2006).
- [2] Gross, C. & Bloch., Science 357, 995–1001 (2017).
- [3] Schneider, C. et al., Rep. Prog. Phys. 80, 016503 (2016).
- [4] Lai, C. et al., Nature 450, 529–533 (2007).
- [5] Cerda-Méndez, E. et al., Phys. Rev. Lett. 105, 116402 (2010).
- [6] Jacqmin, T. et al., Phys. Rev. Lett. 112, 116402 (2014).
- [7] Stoumpos, C. et al., Chemistry of Materials 2016 28 (8), 2852-2867

Photonic nanojets fabricated by multiphoton polymerization technique

^{1,2}D. Ladika, ¹G. Zyla, ³G. Maconi, ^{1,*}V. Melissinaki, ³I. Kassamakov, ¹M. Farsari

¹*IESL/FORTH, Nikolaou Plastira 100, 70013 Heraklion, Crete, Greece*

²*Department of Materials Science and Technology, University of Crete Greece*

³*University of Helsinki, Helsinki, Finland*

Microsphere lenses are widely known for being able to focus light beyond the Abbe diffraction limit, a phenomenon known as a photonic nanojet [1],[2]. This work shows how to process novel photonic nanojet generating structures (PNGS) using maskless 3D printing by multiphoton lithography (MPL) and homemade organic-inorganic hybrid material [3]. Since MPL allows the fabrication of true 3D structures on the microscale with sub-100 nm resolution, it is possible to process arbitrary PNGS stacked on top of each other, such as multiple spheres with different diameters or a combination of a Fresnel-lens and a sphere (see Fig. 1). In addition, MPL enables the accurate and repeatable integration of novel PNS into a macroscopic supporting frame for easy manipulation and attachment. Thus, photonic nanojets generated by novel 3D-printed structures will enable fast super-resolution imaging of samples that would otherwise need to be analyzed using time-consuming scanning electron microscopy or atomic force microscopy.

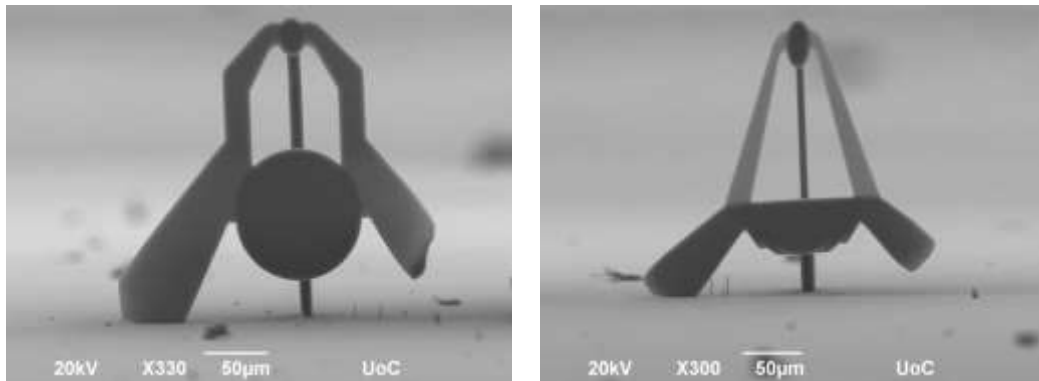


Figure 1: Scanning electron microscope image of the cross-section of photonic nanojet generating structures printed by MPL. The left image illustrates the combination of two spheres with a diameter of 20 μm and 100 μm . The right image shows the combination of a Fresnel-lens and a sphere with a diameter of 20 μm .

References

- [1] I. Kassamakov, S. Lecler, A. Nolvi, A. Leong-Hoi, P. Montgomery and E. Haggstrom. 3D Super- Resolution Optical Profiling Using Microsphere Enhanced Mirau Interferometry. *Scientific Reports* 7, Article number: 3683, (2017).
- [2] V. Heikkinen, I. Kassamakov, T. Viitala, M. Jarvinen, T. Vainikka, A. Nolvi, C. Bermudez, R. Artigas, P. Martinez, V. Korpelainen, A. Lassila and E. Haggstrom. Step height standards based on self-assembly for 3D metrology of biological samples. *Meas. Sci. Technol.*, 31, p. 094008, (2020).
- [3] M. Farsari, M. Vamvakaki, and B. N. Chichkov, *J. Opt.* 12, (2010).

$(\text{CH}_3(\text{CH}_2)_5\text{NH}_3)_2(\text{CH}_3\text{NH}_3)_{n-1}\text{Pb}_n\text{Br}_{3n+1}$: A homologous series of 2D halide perovskites with tuneable energy gap in the blue and green visible spectrum

Apostolos Pantouzas*, Constantinos C. Stoumpos*, Peijun Guo[†], Rafaela M. Giappa*

*Department of Materials Science and technology, Univeristy of Crete

[†] Yale school of engineering and applied science

Hybrid halide perovskites represent a new family of high-performance semiconductors with unconventional optoelectronic properties, thriving in photovoltaics and other aspects of optoelectronic technology^[1]. One derivative class of the materials are the dimensionally reduced two-dimensional (2D) perovskites which consists of periodic nanometer-thick layers of extended, anionic inorganic lattices separated by insulating organic cations. In this configuration, the materials behave as multiple quantum wells (MQW) naturally forming within single-crystals of the respective compounds. Because of this configuration, 2D halide perovskite form an excellent testbed for study of quantum phenomena, especially because the materials can stabilize excitons that are observable at room temperature^[2].

In this work, the $(\text{CH}_3(\text{CH}_2)_5\text{NH}_3)_2(\text{CH}_3\text{NH}_3)_{n-1}\text{Pb}_n\text{Br}_{3n+1}$ ($n = 1-5, \dots, \infty$) homologous series of 2D inorganic-organic lead-halide perovskites were investigated. Deriving from the bulk, three-dimensional (3D) lattice of the parent $\text{CH}_3\text{NH}_3\text{PbBr}_3$ perovskite (the $n = \infty$ end-member), a targeted synthetic approach using hexylammonium $\text{CH}_3(\text{CH}_2)_5\text{NH}_3^+$ cations as molecular scissors yields a new family of 2D perovskites with perovskite slices of quantized length, adjusted from the n -value of the chemical formula. The combination of alternating organic and inorganic layers affords both dielectric and quantum confinement in two dimensions. By controlling the number of layers in the inorganic plane, it is thus possible to tune the degree of the confinement, resulting in tuneable bandgap, in the range of 2.3-3.1 eV, and adjustable exciton binding energy of the photogenerated species. The excitons in the homologous series appear to follow the Mott-Wannier exciton series based on diffuse reflectance and photoluminescence measurements. Our results indicate that the general behavior of the bromide perovskites is analogous with that of the well-studied iodide-based perovskites family, with a notable difference that the excitonic features of the spectra persist even for the high n -value perovskites, suggesting larger exciton binding energy and a smaller exciton Bohr radius.

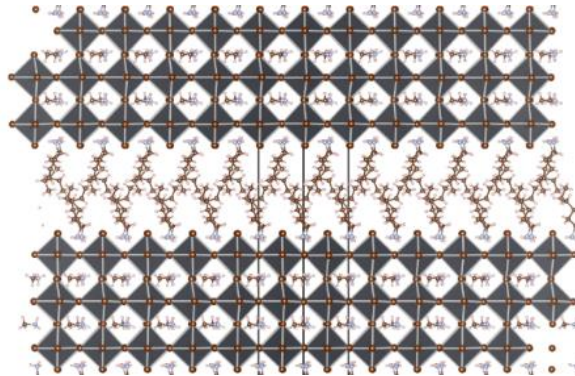


Fig. 1. The crystal structure of $(\text{CH}_3(\text{CH}_2)_5\text{NH}_3)_2(\text{CH}_3\text{NH}_3)_2\text{Pb}_3\text{Br}_{10}$ (the $n=3$ member). The structure is comprised of 3 layers of $\text{CH}_3\text{NH}_3\text{PbBr}_3$ perovskite sheets, separated by a bilayer of hexylammonium cations.

1. Huang L, Lambrecht WRL. Electronic band structure, phonons, and exciton binding energies of halide perovskites CsSnCl_3 , CsSnBr_3 , and CsSnI_3 . *Physical Review B* 2013;88(16).
2. Mazin II, Rashkeev SN. Effect of low symmetry on electron-phonon coupling in perovskite superconductors. *Solid State Communications* 1988;68(1).

A comparative study of Carbazole based polymer and Polyfluorene derivatives as emissive layer for blue emitting flexible PLED devices

K. Papadopoulos* , D. Tselekidou, S. Kassavetis, M. Gioti
*Nanotechnology Lab LTFN (Lab for Thin Films– Nanobiomaterials–
Nanosystems– Nanometrology), Aristotle University of Thessaloniki, 54124,
Thessaloniki, Greece*

V. Kyriazopoulos
*Organic Electronic Technologies P.C (OET), Antoni Tritsi 21B, GR–57001,
Thessaloniki, Greece*

A. K. Andreopoulou, K. Andrikopoulos, J.K. Kallitsis
*Department of Chemistry University of Patras, University Campus, Rio–
Patras GR–26504, Greece*

Electrically conductive polymers have proved to be very interesting materials in the development of various electronic and optical devices, such as solution processed Polymer Light-Emitting Diodes (PLEDs). Tremendous advances in the field of solution processed PLEDs have been achieved mainly through the synthesis of novel emitting materials. Blue light emission has been the most challenging notably due to the difficulty to inject charges in wide energy gap materials [1]. In this study, we compared promising lab scale blue emitting polymer bearing Carbazole moiety with commercially available Polyfluorene derivatives in terms of film forming ability, emission characteristics and color purity. The spin coating technique was implemented to produce functional layers, including the hole transport layer and emitting layer. The optical and photophysical properties of the solution processable thin films were thoroughly studied via NIR– Vis– far UV Spectroscopic Ellipsometry (SE) and Photoluminescence (PL) respectively, whereas the structural characteristics were examined by Atomic Force Microscopy (AFM). Subsequently, blue light PLED devices were fabricated, and they were evaluated using Electroluminescence (EL). From the analysis of the electrical data, valuable information was obtained for different current density characteristics under different bias voltage regimes. Emission bandwidths, color coordinates and the luminance were also derived in order to evaluate the devices' stability. Finally the printability of the polymer films to flexible substrates was investigated using slot die coating processes.

Acknowledgments

This research has been co-financed by the European Regional Development Fund of the European Union and Greek national funds through the Operational Program Competitiveness, Entrepreneurship, and Innovation, under the call RESEARCH–CREATE– INNOVATE (project code: T1EDK–01039)

References

- [1] Poriel, C., Rault–Berthelot, J., Blue Single–Layer Organic Light–Emitting Diodes Using Fluorescent Materials: A Molecular Design View Point. *Adv. Funct. Mater.* 2020, 30, 1910040

* kypapado@physics, auth. gr

Fabrication and analysis of 3D-printed metamaterials

Savvas Papamakarios^{1,2}, Maria Farsari¹

1) *Institute of Electronic Structure and Laser, Foundation for Research and Technology – Hellas (FORTH – IESL)
, 100 Nikolaou Plastira Street, Heraklio, 70013, Greece*

2) *Physics Department, University of Crete, Department of Physics, University of Crete, Vassilika Vouton,
Heraklion, 71409, Greece*

The creation of fascinating optical effects such as negative refractive, optical magnetism, and cloaking has become a human dream since the late 1940s, when artificially designed materials, so-called optical metamaterials, were investigated. Such materials enable strong light-matter interaction over a broad range of the electromagnetic spectrum not achievable by any existing material in nature. They are therefore highly interesting for many future applications in the field of telecommunication, optoelectronics, nanomaterials, and energy harvesting. However, the fabrication of 3D optical metamaterials, which would enable the use of their full potential, remains challenging due to the limitations of conventional manufacturing techniques. An approach that has been proved to be suitable to overcome this challenge is multi-photon lithography (MPL)¹, which is a true 3D printing technique with high resolution down to sub-100 nm. In this work, the high potential of using MPL for metamaterial research is further underlined by demonstrating a procedure to process metamaterials operating at THz frequency and generate novel devices for complete circuits or electronic devices such as perfect absorbers and electromagnetic waves attenuators that can be used in complete circuits and electronic devices. Simulation by Finite Differential Time Domain (FDTD) method were done to design the materials' geometry giving the best possible dimensions and properties for the structure, as FDTD is the most accurate way to solve precisely Maxwell's equations for electromagnetic waves interacting with matter. As a photosensitive material for the MPL an organic – inorganic photopolymer SZ2080 was used. SZ2080 has the best chemical and mechanical properties for the fabrication and development process. After MPL processing, the structures were further processed using selective electroless plating to cover the polymer material with silver via chemical procedure, so the spectral characterization (absorbance, transmittance, reflectance) can be done at THz frequencies.

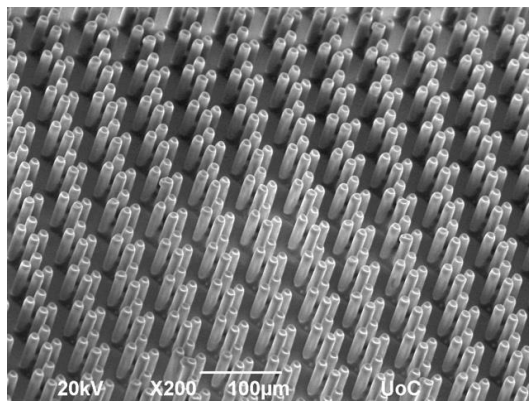


Figure 1: SEM image of the metasurface coated with silver via chemical procedure, showing the resolution of MPL method

¹ Farsari, M., Chichkov, B. Two-photon fabrication. *Nature Photon* **3**, 450–452 (2009), <https://doi.org/10.1038/nphoton.2009.131>

Photocurrent generation mechanisms for the description of Metal-Graphene-Metal photodetectors' responsivity.

A. Polymerakis, I. Vaggelidis and E. Lidorikis
*Department of Materials Science and Engineering, University of Ioannina,
Ioannina 45110, Greece*

Graphene is a promising material for visible to THz light detection, given its broadband absorption, which allows its use to many photodetection schemes and architectures. The graphene photodetectors with the simplest configuration are the Metal-Graphene-Metal (MGM), which can be considered as the fundamental building blocks for other photodetector architectures and stand out due to their easy fabrication and ultrahigh operating speeds. In such configurations, graphene is placed on a Si/SiO₂ substrate and is contacted by two metal electrodes, acting as source and drain. In this work we computationally investigate the various mechanisms of photocurrent generation such as the photothermoelectric (PTE), photovoltaic (PV), photoconductive (PC) and photo-bolometric (PB) effects on an MGM device, with Au contacts, in the spectral range spanning from visible to near infrared (500-1000nm). We demonstrate our methodology for a series of devices, assuming different channel length, i.e., the area between the two Au contacts, and different graphene doping inside the channel. We distinguish two different operation schemes, one with biased and one with unbiased conditions. Our results show that in the unbiased operation the PTE effect dominates, leading to a maximum responsivity of 15 mA/W, for long-channel architectures. As we apply bias voltage, the other photogeneration mechanisms start to contribute significantly to the photocurrent which further increases the device's responsivity, even for short-channel architectures where the PTE effect is negligible. [1]

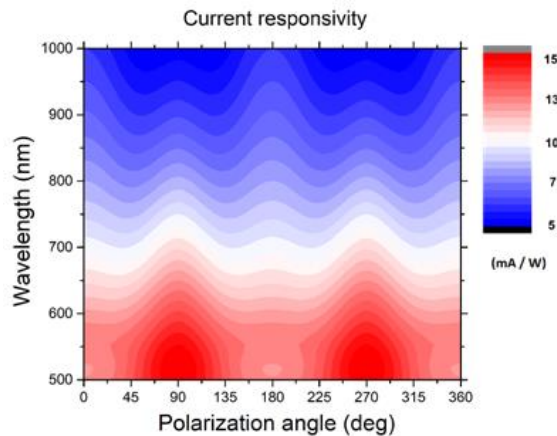


Figure 1: Photocurrent responsivity behaviour of the MGM photodetector

References

- [1] Echtermeyer, Tim & Nene, P. & Trushin, M. & Gorbachev, Roman & Eiden, A. & Milana, S. & Sun, Zicai & Schliemann, J. & Lidorikis, Elefterios & Novoselov, K. & Ferrari, A.. (2014). Photothermoelectric and Photoelectric Contributions to Light Detection in Metal-Graphene-Metal Photodetectors. *Nano letters*. 14. 10.1021/nl5004762.

Strong coupling phenomena in a CsPbBr₃ nanocrystal microcavity at 90K

C. Saitanidou^{1,2}, N. G. Chatzarakis^{1,2}, G. Kourmoulakis¹, G. Stavrinidis², G. Konstantinidis², G. Raino^{3,4}, M. Bodnarchuk^{3,4}, M. V. Kovalenko^{3,4}, N. T. Pelekanos^{1,2}

¹Department of Materials Science & Technology, University of Crete, 70013 Heraklion, Greece

²Microelectronics Research Group, IESL-FORTH, 71110 Heraklion, Greece

³Department of Chemistry & Applied Biosciences, ETH Zürich, CH-8093 Zürich, Switzerland

⁴Empa-Swiss Federal Laboratories for Materials Science & Technology, CH-8600 Dübendorf, Switzerland

Lead halide perovskite nanocrystals (NCs) have recently attracted wide interest based on their facile and low-cost synthesis, solution-processability and remarkable optical properties.¹ Considering their robust exciton binding energies (20-75 meV for CsPbX₃ NCs, with X=I, Br, Cl),² pronounced strong coupling and polariton lasing phenomena can be expected in properly configured NC-containing microcavities. In a recent work, polariton lasing has been observed up to room temperature using bulk-like 400nm-thick CsPbCl₃ platelets, sandwiched between dielectric mirrors.³ Achieving polariton lasing from a single layer of perovskite NCs is certainly more challenging compared to the bulk platelet case, but has a number of distinct advantages, such as precise position and thickness control of the active layer in the microcavity, relative ease of fabrication, and increased scalability of the produced polariton devices.

Here, we demonstrate for the first time, a full microcavity containing CsPbBr₃ NCs as the active medium, exhibiting strong-coupling effects at 90K. The microcavity consists of a $\lambda/2$ -polystyrene layer containing CsPbBr₃ NCs, 4% w/w, spin-cast onto a bottom distributed Bragg reflector (DBR). The microcavity is completed by placing on top, using a stamping technique, a transferrable top-DBR membrane,⁴ as schematically depicted in Figure 1. Evidence for strong coupling effects in the microcavity is presented in the angle-resolved photoluminescence measurement of Figure 2, showing a distinct discontinuity in the energy dispersion at about 20°, demonstrating the formation of lower and upper polariton branches. These novel polariton structures based on perovskite nanocrystals are very promising for the observation of polariton lasing at non-cryogenic temperatures, leading to a new generation of high temperature cost-effective nanophotonic devices.

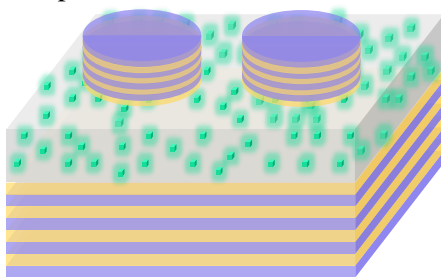


Figure 1: Schematic illustration of a microcavity containing CsPbBr₃ NCs.

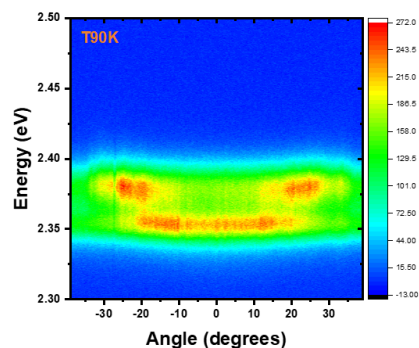


Figure 2: Angle-resolved photoluminescence of a CsPbBr₃ NCs microcavity

References

- [1] M. V. Kovalenko, L. Protesescu, M. I. Bodnarchuk, *Science* **358**, 745 (2017).
- [2] L. Protesescu,, M. V. Kovalenko, *Nano Lett.* **15**, 3692 (2015).
- [3] R. Su et al., *Nano Lett.* **17**, 3982 (2017).
- [4] E. A. Amargianitakis,, N.T. Pelekanos, *Microelectronic Engineering* **228**, 111279 (2020)

Triboelectric generators based on plasma-etched flexible surfaces

A. Segkos*, A. Bardakas, A. Zeniou, E. Gogolides, C. Tsamis
NCSR "Demokritos", Institute of Nanoscience and Nanotechnology,
15310 Aghia Paraskevi, Athens, Greece

Triboelectric generators (TEGs) have attracted significant scientific interest since the pioneering work of Fan et al. in 2012 [1]. The triboelectric phenomenon is based on contact electrification and electrostatic induction between two surfaces in relative motion. Several techniques have been proposed for controlling the surface roughness and thus triboelectric generator performance.

In this work, we investigate the modification of flexible surfaces (PET, Kapton®, etc.) using plasma processing on the electrical performance of TENGs. Etching and roughening of the sample surfaces was conducted in oxygen plasma with source power ranging from 300 to 1900W, bias power ranging from 50 to 300W and etching duration ranging from 40 to 240s, resulting in different surface roughness conditions (Fig. 1a).

Electrical characterization of the samples was performed in contact-separation mode. As a reference surface different types of electrodes were used for the triboelectric generator, corresponding to both "hard" and "soft" substrates, such as SiO₂, Kapton®, PET, PTFE, etc. The output voltage was monitored as a function of time using an oscilloscope. In addition, charging experiments were performed through a rectifier bridge and capacitor (0.47μF) circuit (Fig. 1b)

From the comparison of the voltages generated by the different triboelectric couples and the corresponding capacitor charging, conclusions are drawn regarding the matching of the different micro- and nano- structured surfaces and the effect of hard and soft reference electrodes.

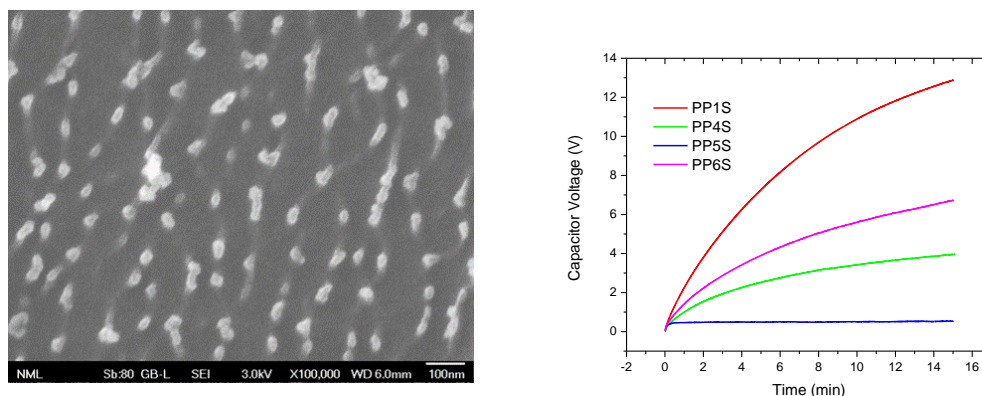


Figure 1 a) SEM images of PET surfaces after oxygen plasma-induced roughness and b) Capacitor voltage as a function of time for the four different PET samples.

Reference

[1] F. R. Fan, Z. Q. Tian, Z. L. Wang, *Nano Energy* 1 (2012) 328-334

Acknowledgment: This research has been co-financed by the European Union and Greek national funds through the Operational Program Competitiveness, Entrepreneurship and Innovation, under the call RESEARCH – CREATE – INNOVATE (EFOS, project code: T2EAK-00350).

* a.segkos@inn.demokritos.gr

Optical metasurfaces implemented by highly-ordered Laser Induced Periodic Surface Structures

A. C. Tasolamprou¹, E. Skoulas¹, G. Perrakis¹, M. Vlahou^{1,2}, Z. Viskadourakis¹, E. N. Economou^{1,3}, M. Kafesaki¹, G. Kenanakis¹ and E. Stratakis¹

¹*Institute of Electronic Structure and Laser, Foundation for Research and Technology Hellas, N. Plastira 100, 71110, Heraklion, Crete, Greece*

²*Department of Materials Science and Technology, University of Crete, Heraklion, 70013, Greece*

³*Department of Physics, University of Crete, Heraklion, 70013, Greece*

Metasurfaces are ultrathin electromagnetic periodic structures with a response that can be engineered through the architecture of their subwavelength elementary units, the meta atoms; they have been used for a variety of applications, from shielding and wavefront shaping to solar cell harvesting, operating from microwave to THz and the optical frequencies. An acclaimed scheme for implementing optical metasurfaces is the Gap Surface Plasmon metasurfaces, where light is confined in the dielectric spacer of a metal-insulator-metal-type configuration. These extraordinary thin structures have been shown to provide exceptional electromagnetic properties and a variety of applications, including wavefront-shaping, wave-mixing, polarization control, high-harmonic generation, perfect absorption, color printing, energy harvesting and others. Traditional methods to fabricate such structures usually include photolithography, particle beam lithography, direct-write lithography, pattern transfer and hybrid patterning lithography. In their majority these conventional techniques are inherently multistep and involve the extensive use of chemicals. Here, we demonstrate a versatile and tunable approach for the fabrication of Gap Surface Plasmon metasurfaces which consists of direct material processing using pulsed laser light. The approach is based on the controllable and selective generation of highly-ordered Laser Induced Surface Periodic Structures (LIPSS) on nanometre-thick films [1], which are backed by a grounded dielectric layer. LIPSS imprinting is inherently a single-step and large scale approach and so far it has been used in a variety of application such as surface enhanced Raman scattering, enhanced thermal radiation emission efficiency, cell growth, wetting, etc. We focus on shaping resonant gap plasmonic states with polarization-dependent enhanced or perfect absorption. As theory predicts and experiments verify, the produced metasurfaces exhibit well-defined and tunable resonances which are sensitive to the impinging wave polarization, leading to perfect absorption of either the normal to LIPSS polarization, a narrowband operation, or the parallel polarization, a broadband operation, in the near-IR and mid-IR [2].

References

- [1] E. Skoulas, A. C. Tasolamprou, G. Kenanakis, and E. Stratakis, "Laser induced periodic surface structures as polarizing optical elements," *Appl. Surf. Sci.*, vol. 541 p. 148470, 2021.
- [2] A. C. Tasolamprou, E. Skoulas, G. Perrakis, M. Vlahou, Z. Viskadourakis, E. N. Economou, M. Kafesaki, G. Kenanakis, and E. Stratakis, "Highly ordered laser imprinted plasmonic metasurfaces for polarization sensitive perfect absorption," under review, 2022.

Exciton polaritons for reconfigurable chirality

P.E. Stamatopoulou, N.A. Mortensen, C. Tserkezis*
Center for Nano Optics, University of Southern Denmark, Denmark

S. Droulias
Department of Digital Systems, University of Piraeus, Greece

Optical chirality (OC), i.e. the lack of mirror symmetry in the optical response of a specimen to left- or right-circularly polarised (L/RCP) light, is encountered widely in nature, e.g. in the study of biomolecules of medicines. Sensing and control of OC is thus of major importance for applications, and numerous activities in nanophotonics are focusing on providing photonic environments that facilitate measurements [1]. Because the intrinsic optical activity of natural chiral materials is weak, ways to e.g. enhance, spectrally shift, and measure circular dichroism (CD) signals—the differential absorption under LCP or RCP illumination—are highly in demand.

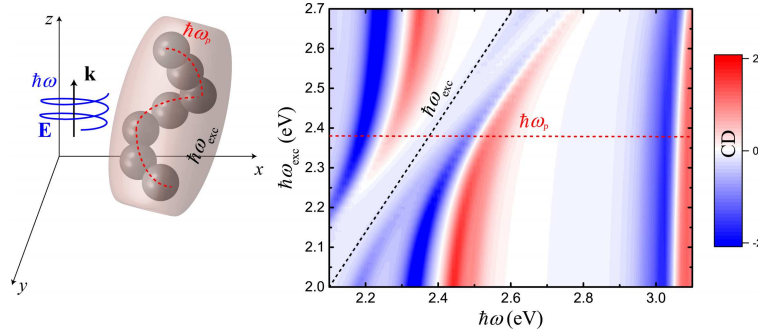


Figure 1: A metallic nanosphere helix that supports a collective plasmonic mode at energy $\hbar\omega_p$, embedded in an excitonic matrix characterised by a transition at $\hbar\omega_{exc}$. The entire system is illuminated by circularly polarised light of energy $\hbar\omega$. When the detuning between the two energies is small, the modes interact strongly, leading to an anticrossing in the optical spectra, including those for CD.

Here we suggest a means to manipulate and configure OC via strong coupling of the optical resonances of the sample with the excitons of an encapsulating or supporting medium [2]. We first show analytically, through the simple example of a chiral sphere coated with an excitonic layer, that strong coupling allows the emergence of two tuneable bands of strong CD signals (in place of the sole otherwise anticipated), whose energy depends on the excitonic material. This response is then verified with numerical calculations for a helix of metallic nanospheres embedded in an excitonic (itself achiral) matrix, as shown in Fig. 1. Strong coupling enables therefore post-fabrication flexibility for detecting CD signals and manipulating OC [3].

References

- [1] Warning et al., ACS Nano **15**, 15538 (2021).
- [2] Tserkezis et al., Rep. Prog. Phys. **83**, 082401 (2020).
- [3] Stamatopoulou et al., Nanoscale, *submitted*.

*ct@mci.sdu.dk

Tuning the emitting color of organic light-emitting diodes by dispersing the red dye DANS in the green emitter for biosensing applications

Apostolis Verykios^{a*}, Anastasia Soultati^a, Veroniki P. Vidali^a, Giorgos Pistolis^a,
Maria Vasilopoulou^a, Panagiotis Argitis^a

^a*Institute of Nanoscience and Nanotechnology, National Center for Scientific Research Demokritos, Agia Paraskevi, 15341, Athens, Greece*

Since the pioneering works on organic light-emitting devices (OLEDs) by the Kodak and Cambridge groups, extensive research works have been carried out to bring OLEDs into commercial applications in flat panel displays in the past decade [1,2]. Apart from optimizing device structure, another key approach for developing marketable OLEDs is the development of high-performance materials with additional desirable properties, such as the sensing ability [3]. In this work, we fabricated biosensors by using the changes in the emission spectrum of an OLED. In particular, the red emitting dye 4-dimethylamino-4'-nitrostilbene (DANS) embedded into an anthracene layer (M21), which is a wide bandgap organic green emitter served as the active layer of the device. Upon the addition of the fluorescent dye DANS into the M21, efficient Förster energy transfer takes place changing the green emission of M21 to red. For biosensing application, red OLED with M21+DANS active layer was fabricated and used as sensor to recognize analytes generated during meat spoilage. Analytes, such as acids diffused into the active layer of the OLED and led to change of color emission from red to green. This color change is attributed to the protonation of amine nitrogen atom in the amine group of the DANS occurring in an acidic environment resulted in the quenching of the intense red emission of the DANS molecule.

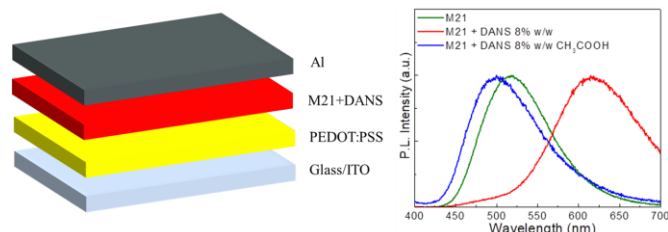


Figure 1: OLED architecture and photoluminescence spectra of emission layers showing color changes.

References

- [1] F. Elsamnah, A. Bilgaiyan, M. Affiq, C.-H. Shim, H. Ishidai, R. Hattori, *Biosensors* 2019, 9, 48.
- [2] Y. Sun, N.C. Giebink, H. Kanno, B. Ma, M.E. Thompson, S.R. Forrest, *Nature* 2006, 440, 908-912.
- [3] L.C. Palilis, M. Vasilopoulou, D.G. Georgiadou, P. Argitis, *Org. Electron.* 2010, 11, 887.

Acknowledgment

This research has been co-financed by the European Regional Development Fund of the European Union and Greek national funds through the Operational Program Competitiveness, Entrepreneurship and Innovation, under the call RESEARCH – CREATE – INNOVATE (project code:T2-EDK-04175-OLED-LUMIN-FOOD).

* verikios@hotmail.com

Low temperature tensile strength of Polylactic acid filled with ceramic nanopowders and glass bubbles

Panayiota Bousboura^{1,2} and George Vekinis¹

¹Institute of Nanoscience and Nanotechnology, NCSR “Demokritos”, AgiaParaskevi, Greece

²Department of Physics, University of Ioannina, Ioannina, Greece

Poly(lactic acid) (PLA) is a starch-based biopolymer considered the most promising candidate for replacing many fossil-based polymers for structural and functional applications. Because of its biodegradability it is already being used widely in many in-vivo medical applications as well as certain single-use packaging applications.

PLA displays very impressive strength and rigidity with satisfactory toughness at room temperature but its softening temperature is rather low, at about 55-65°C, restricting its use at higher temperatures. In this work we present a systematic study of the mechanical properties of PLA at low temperatures, as produced and with the addition of 1-3wt% fillers, either nano-structured ceramic powders or glass bubbles. Specimens were produced by filament extrusion of PLA-filler mixtures and subsequent 3D printing of tensile test coupons. The tensile strength and elongation at fracture were determined in tension at temperatures down to about -20°C and it was found that the tensile strength increases as the temperature decreases, for both the unfilled and filled materials, while the elongation at fracture decreases, without actually displaying clear brittle behavior.

The thermal conductivity and thermal expansion of the materials were also determined and it was found that they remained approximately constant irrespective of the type or amount of filler used. SEM observations showed that the filler materials were well-bonded to the matrix.

Generative Networks for Re-inserting Atomic detail in Coarse-grained Multi-component Macromolecules

E. Christofi^{1*}, V. Harmandaris^{1,2}, W. Li⁴, A. Chazirakis², M. Doxastakis³, M. A. Nicolaou¹, C. Chrysostomou¹

¹ *Computation-Based Science and Technology Research Center, The Cyprus Institute, Nicosia, Cyprus*

² *Department of Mathematics and Applied Mathematics, University of Crete, Heraklion, Crete, Greece*

³ *Department of Chemical and Biomolecular Engineering, University of Tennessee, Tennessee, USA*

⁴ *Institute for Chemical Reaction Design and Discovery (WPI-ICReDD), Hokkaido University, Sapporo, Japan*

* e-mail: e.christofi@cyi.ac.cy

Abstract

Despite the modern advances of the available computational resources, the length and time scales of the physical systems that can be studied in full atomic detail, via molecular simulations, are still limited. To overcome such limitations mathematical methods to reduce the dimensionality of the physical system under study are necessary. The most common technique to tackle this task is by developing systematic coarse-grained (CG) models for chemically-specific systems [1-2]. CG models have found practical applications in simulations of long entangled macromolecular systems. Restoring the atomistic detail from the CG description requires us to produce information from the physics and statistics of the system at the two representations considered. The methods proposed so far balance among accuracy, efficiency and general applicability [3-5]. Here, we introduce an efficient and versatile method for backmapping multi-component CG macro-molecules. By utilizing deep learning algorithms, we train a convolutional neural network to learn structural correlations (probability distribution functions) between polymer configurations at the atomistic and corresponding CG scales, obtained from atomistic simulations. The trained model was then utilized to get predictions of atomistic structures from input CG configurations. As an illustrative example we apply the new generative networks to polybutadiene copolymers of various microstructures, in which each monomer microstructure (i.e. *cis*-1,4, *trans*-1,4, and *vinyl*-1,2) is represented as a different CG particle type. Moreover, to examine the chemical transferability of the proposed method we modify the chemistry (CG particle types) of the input CG configurations, thus creating a set of well equilibrated polymer configurations of different microstructures (chemistry) than the one of the original CG configuration.

Keywords: Machine learning, Multi-scale modeling, Backmapping, Polybutadiene, Structural correlations

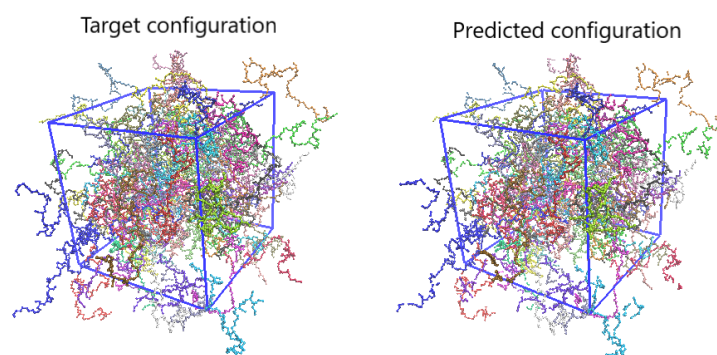


Figure 1: Target and predicted configurations of the UA model (polymer chains are unwrapped in the periodic simulation box and colored differently for visualization)

Acknowledgments

This work was supported by European Union's Horizon 2020 research and innovation program under grant agreement No810660.

References

- [1] VA Harmandaris, NP Adhikari, Nico FA van der Vegt, and Kurt Kremer. Hierarchical modeling of polystyrene: From atomistic to coarse-grained simulations. *Macromolecules*, 39(19):6708–6719, 2006.
- [2] VA Harmandaris and Kurt Kremer. Predicting polymer dynamics at multiple length and time scales. *Soft Matter*, 5(20):3920–3926, 2009.
- [3] Jakub Krajniak, Sudharsan Pandiyan, Eric Nies, and Giovanni Samaey. Generic adaptive resolution method for reverse mapping of polymers from coarse-grained to atomistic descriptions. *Journal of chemical theory and computation*, 12(11):5549–5562, 2016.
- [4] Andrzej J Rzepiela, Lars V Schäfer, Nicolae Goga, H Jelger Risselada, Alex H De Vries, and Siewert J Marrink. Reconstruction of atomistic details from coarse-grained structures. *Journal of computational chemistry*, 31(6):1333–1343, 2010.
- [5] Guojie Zhang, Anthony Chazirakis, VA Harmandaris, Torsten Stuehn, Kostas Ch Daoulas, and Kurt Kremer. Hierarchical modelling of polystyrene melts: from soft blobs to atomistic resolution. *Soft Matter*, 15(2):289–302, 2019.

Development of Polyurethane/r-GO Nanocomposites with Reinforced Self-healing Properties

E. Giannakaki^{1,2,*}, K. Giannaris^{1,3}, M. M. Stylianakis^{1,4}, A. Fidelli⁵, P. Krassa⁵,
K. Chrissopoulou¹ and S. H. Anastasiadis^{1,2}

¹*Institute of Electronic Structure and Laser, Foundation for Research and Technology-Hellas, Heraklion Crete, Greece.*

²*Dept. of Chemistry, Univ. of Crete, Heraklion Crete, Greece.*

³*Dept. of Materials Science and Technology, Univ. of Crete, Heraklion Crete, Greece.*

⁴*Dept. of Nursing, Hellenic Mediterranean University, Heraklion Crete, Greece.*

⁵*Megara Resins, Anastassios Fanis, S.A. Megara, Greece.*

In recent years, self-healing coatings have been the subject of increasing research interest due to their ability to self-repair local damages caused by external forces. Polymeric materials comprise one of the most promising materials to use towards this direction [1]. Waterborne polyurethane dispersions (WPUD) have attracted broad attention due to their advantage of low release of volatile organic compounds (VOCs). WPUD have a wide range of commercial applications in coatings, adhesives, and other consumer products. On the other hand, graphene derivatives are widely used to reinforce the mechanical and thermal properties of WPUDs. In the current work, reduced graphene oxide (r-GO) was incorporated within a waterborne polyurethane dispersion based on polycarbonate polyol to develop nanocomposites in different compositions and investigate its effect on the self-healing properties. Initially, the graphene oxide (GO) was synthesized via a modified Hummers method and was subsequently reduced using hydroiodic acid (HI) as a reducing agent to prepare the r-GO. The self-healing ability of the polyurethanes was found enhanced in the nanocomposites and the healing rate was found much higher compared to that of the pure polymer, as confirmed by microscopic and thermal analysis techniques, mainly due to better heat dissipation. The superior heat conductivity of r-GO allowed for the optimization of the self-healing ability with the incorporation of just a small amount of the additive (Figure 1), whereas its presence enhanced the mechanical properties of the nanocomposites after healing, as well.

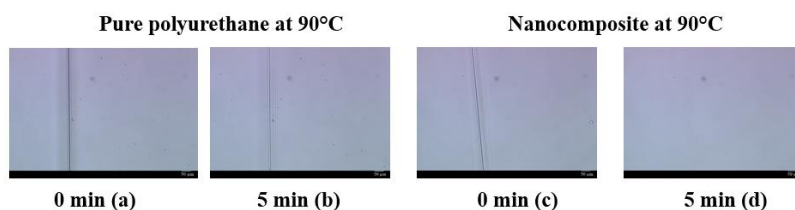


Figure 1: Optical Microscopy images of the self-healing of a crack in a pure polyurethane film (a and b) and a polyurethane/r-GO film (c and d).

References

[1] S. Utrera-barrios, R. Verdejo, M.A Lopez-Manchado and M. Santana, *Materials Horizons*, **7**, 2882–2902 (2020).

Acknowledgements: This research has been co-financed by the European Union and Greek national funds through the Operational Program Competitiveness, Entrepreneurship and Innovation, under the call RESEARCH-CREATE-INNOVATE (SELFNANOPUD, MIS: 5067612).

* evigian@iesl.forth.gr

Effect of topography and statin loaded micropatterned polymeric replicas on osteogenic differentiation

E. Kanakousaki*, P. Kavatzikidou, A. Manousaki, E. Stratakis, A. Ranella
*Foundation for Research and Technology - Hellas (FORTH), Institute of
Electronic Structure and Laser (IESL)*

E. Kanakousaki

Department of Biology, University of Crete, Greece

E. Stratakis

Department of Physics, University of Crete, Greece

Introduction: Engineered microenvironments are offering mechanistic insights into how the extracellular matrix (ECM) and physical forces regulate stem cells, revealing how these control self-renewal, proliferation and differentiation potentials. The cells sense the ECM mechanics and spread via transcription regulator proteins. YAP/TAZ are considered as nuclear relays of mechanical signals exerted by ECM rigidity and cell shape and as master regulator of cell-ECM interaction. Statins are inhibitors of cholesterol biosynthesis and studies demonstrated their effect on stimulation of new bone formation [1]. Ultrafast pulsed laser irradiation is considered as a simple microfabrication method to produce structures controlling the structure geometry and pattern regularity [2]. Such structures with an anisotropy discontinuous topographical nature could enhance cellular growth and alignment (eg neuronal [3,4]). Soft lithography has been successfully used to transfer micro-sized patterns from silicon (Si) to polymeric surfaces allowing the in-depth study on cell behavior [5]. The aim of this study is to investigate the effect of topography and statins on osteogenic differentiation.

Experimental Methods: A series of micro-patterned Si structures were fabricated by ultrafast laser irradiation. Positive replicas of polymers have been successfully reproduced from the Si structures via soft lithography (Figure 1). Statin-loaded replicas were then produced and characterized by Scanning Electron Microscopy. Finally, the cytocompatibility and cytotoxicity of the statin-loaded replicas was investigated with mouse Mesenchymal Stem Cells (MSCs) C57BL/6 was evaluated.

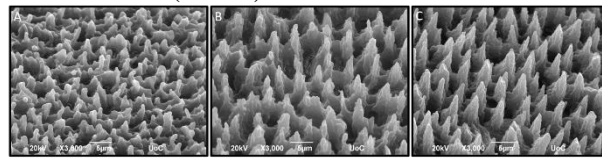


Figure 1: 10% cellulose acetate micropatterned polymeric replicas (A) Low Roughness, (B) Medium Roughness and (C) High Roughness and magnification (x3000).

Results and Discussion: Cell mechanotransduction was analyzed via the cytoskeleton/nuclear organization and YAP localization, on the replicas. The effect of the replicas on MSCs fate was also studied. The surface roughness had an effect on the MSCs mechanotransduction and differentiation. The chemical composition and degradation rate influenced cell morphology and cell nuclear mechanics. The ability of our technique to control the cellular behavior could be potentially useful in understanding disease pathogenesis and for the development of patient-specific applications.

Acknowledgments: The authors would like to thank the European Project NFFA-Europe-Pilot (n. 101007417 from 1/03/2021 to 28/02/2026) for providing financial support to this project.

References

- [1] Lee, T.-C. et al. *J Bioact Compat Polym.* **33**(2), 160–177 (2018).
- [2] Ranella A. et al. *Acta Biomaterialia* **6**, 2711 (2010).
- [3] Simitzi C. et al. *Biomaterials.* **67**, 115-128 (2015).
- [4] D Angelaki D. et al., *Mater. Sci. Eng. C.* **115**, 111144 (2020).
- [5] Babaliari E. et al. *Int. J. Mol. Sci.* **19**(7), 2053 (2018).

* ekanakousaki@iesl.forth.gr

Novel polymer resins for ultraviolet light assisted nanoimprint lithography applications

Charalampos Katsodridakis¹, Efstratios Svinterikos², Konstantina Turlouki², Nikolaos Kehagias¹, Panagiotis Argitis¹

1. NCSR Demokritos, Institute of Nanoscience & Nanotechnology, P. Grigoriou 27 & Neapoleos Str., 15341 Ag. Paraskevi, Greece

2. Nanotypos, Technopoli ICT Business Park Thessaloniki, Bld. C2, 55535, Pylea, Greece

Ultraviolet light assisted (UV)-nanoimprint lithography (UV-NIL) [1] is considered to be one of the edge cutting micro and nano-fabrication techniques by which nano structures can be replicated from a mold on to a suitable rigid or flexible substrate. An emerging variant of UV-NIL, which allows high-volume industrial scale application and commercialization, is the so-called ultraviolet light assisted roll-to-roll NIL (UV R2R NIL)[2]. During this process, an imprinter roller with a patterned surface is used to imprint into a thin photocurable resist material which has previously been coated on a flexible substrate.

In this paper, we present a library of photocurable solvent-free resins based on the two standard photocuring chemistries which are based on the cationic polymerization and free-radical polymerization mechanisms. A variety of acrylic and epoxy resins suitable for R2R NIL, which yield highly crosslinked polymers after exposure to UV light, have been developed by our research groups. These solvent-free formulations cure via free-radical and cationic polymerization processes respectively. In respect to the requirements of the final application, we discuss their tunable physical/chemical properties and present their unique functionality when combined with micro/nano structures.

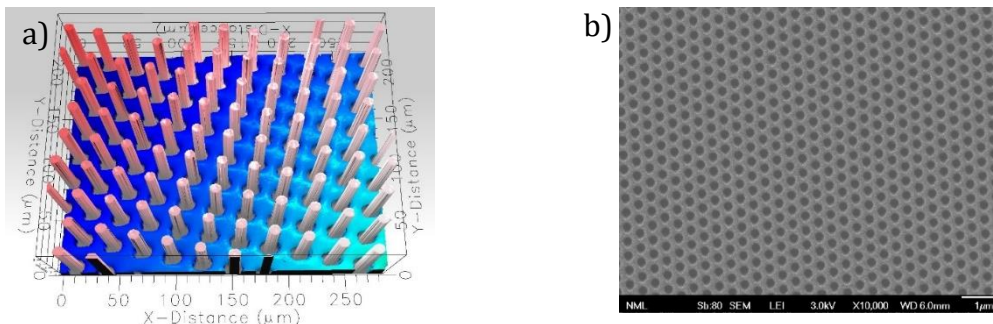


Figure 1: a) 3D optical profilometry image of micropillars imprinted on acrylic resin and b) SEM image of submicron-sized holes imprinted on epoxy resin

References

[1] Kooy et al. Nanoscale Research Letters 2014, 9:320

[2] J.J. Dumond, H.Y., Journal of Vacuum Science & Technology B 30, 010801 (2012)

Acknowledgments

This work was supported by the research project “Advanced inline nanometrology techniques for roll to roll nanoimprint lithography manufacturing processes, NanoMet” - MIS 5056202, funded by the Operational Programme (EPAnEK) "Competitiveness, Entrepreneurship and Innovation" (NSRF 2014-2020), under the special action "Industrial Materials" and co-financed by Greece and the European Union (European Regional Development Fund).

Co-culture of osteoblasts and osteoclasts in composite scaffolds support osteogenesis in vitro

Georgia-Ioanna Kontogianni^{1,2}, Amedeo Franco Bonatti³, Carmelo De Maria³, Raasti Naseem⁴, Catarina Coelho⁵, Giovanni Vozzi³, Kenneth Dalgarno⁴, Paulo Quadros⁵, Maria Chatzinikolaidou^{1,2}

¹ Foundation for Research and Technology Hellas (FO.R.T.H)-IESL, Heraklion, Greece

² Department of Materials Science and Technology, University of Crete, Heraklion, Greece

³ Research Center E. Piaggio and Dpt. of Information Engineering, University of Pisa, Pisa, Italy

⁴ School of Engineering, Newcastle University, Newcastle upon Tyne, United Kingdom

⁵ FLUIDINOVA, S.A., Maia, Portugal

Osteoporosis is a bone pathology caused by an imbalance in bone remodelling due to excessive osteoclast-mediated bone resorption and decreased action of osteoblasts. Bone tissue engineering (BTE) is an attractive strategy to treat long bone fractures using three dimensional (3D) constructs as bone graft substitutes mimicking the 3D porous environment of native bone [1, 2]. Fused deposition modeling (FDM) was used to process thermoplastic materials with mechanical properties close to those of the natural tissue [3]. In this study, polymeric blends of poly-L-lactic acid (PLLA), polycaprolactone (PCL) and poly(3-hydroxybutyrate-co-3-hydroxyvalerate) (PHBV) (90/5/5 % wt), blend+2.5%wt of nano-hydroxyapatite (nano-HA) and blend+2.5%wt of strontium-substituted-nano-HA (Sr-nano-HA) were fabricated into 3D scaffolds with specific geometry and evaluated for their osteogenic and osteoclastogenic potential using appropriate cell types.

Human bone marrow mesenchymal stem cells (hBM-MSCs, 2×10^4 cells/scaffold), were seeded onto the scaffolds and cultured for 13 days. Then, human peripheral blood mononuclear cells (hPBMCs) were added (50×10^4 cells/scaffold). Cell proliferation and morphology were monitored via a reduction-based cell viability assay, scanning electron microscopy (SEM) and confocal microscopy. Measurement of the alkaline phosphatase (ALP) and tartrate acid phosphatase (TRAP) activity was conducted to determine the effect of the polymeric scaffolds on the osteogenesis and osteoclastogenesis respectively. Quantitative polymerase chain reaction (qPCR) was applied to quantify changes in the gene expression of osteogenesis-related markers such as osteonectin, osteoprotegerin and osteocalcin, as well as osteoclastogenic markers including TRAP, dendritic cell-specific transmembrane protein and nuclear factor of activated T cells 1.

The cell viability assessment displays an excellent biocompatibility for all scaffold compositions allowing cells to proliferate. SEM and confocal microscopy images reveal well-spread cells depicting a physiological morphology. After 14 days, the ALP activity is more than two-fold higher in the co-culture compared to the hBM-MSC mono-culture. The TRAP activity results showed a significantly lower TRAP activity in the co-culture than in the hPBMC mono-cultures at all tested time points and materials. Osteogenesis related markers examined with qPCR were significantly higher in the co-culture than in the mono-cultures of hBM-MSCs.

The results confirm that hydroxyapatite and strontium as components of composite scaffolds with controlled spatial architecture enhance osteogenesis and reduce osteoclastogenesis in co-culture due to the communication of the two cell types in relation to the individual monocultures, suggesting their potential as implants to treat degenerative bone pathologies such as osteoporosis.

References

1. Langer, R. and J.P. Vacanti, *Science* **260** (5110): p. 920-6 (1993).
2. Danilevicius, P., *Applied Surface Science* **336**: p. 2-10 (2015).
3. Calore, A.R., *Methods Mol Biol* **2147**: p. 75-99 (2021).

PCDTBT: Accurate Force Field Derivation and Molecular Dynamics Simulation

K. Kordos, M. Andrea, D.G. Papageorgiou

Department of Materials Science and Engineering, University of Ioannina,
POB 1186, 45110, Ioannina, Greece

π -Conjugated polymers are essential building blocks in a bulk heterojunction architecture for organic solar cells. Polymer poly[N-9'-heptadecanyl-2,7-carbazole-alt-5,5-(4',7'-di-2-thienyl-2',1',3'-benzothiadiazole)] known as PCDTBT (Fig. 1a) is a carbazole based co-polymer, with a donor-acceptor structure. It consists of electron-donating and electron-withdrawing subunits and features a low band gap. In this work we apply ab-initio computations to construct an accurate force field for modelling PCDTBT at the fully atomistic level. More specifically, the LC- ω PBE long range corrected functional along with the 6-31G(d,p) basis set were employed to extract torsional profiles around the PCDTBT backbone. These were subsequently used to reparametrize the General Amber Force Field [1]. In order to validate the new parameterization a series of large-scale Molecular Dynamics simulations were performed at different chain lengths and different initial conditions. The calculated mass density at 300K is close to experimental measurements [2] and in addition, predictions on conformational properties namely persistence length (Fig. 1b), Kuhn length and conjugation length are compatible with existing experimental literature [3]. The outcome from Molecular Dynamics simulations suggests that the improved force field can reproduce successfully essential properties of PCDTBT which are relevant in further modelling of this polymer as a donor material in an organic photovoltaic device.

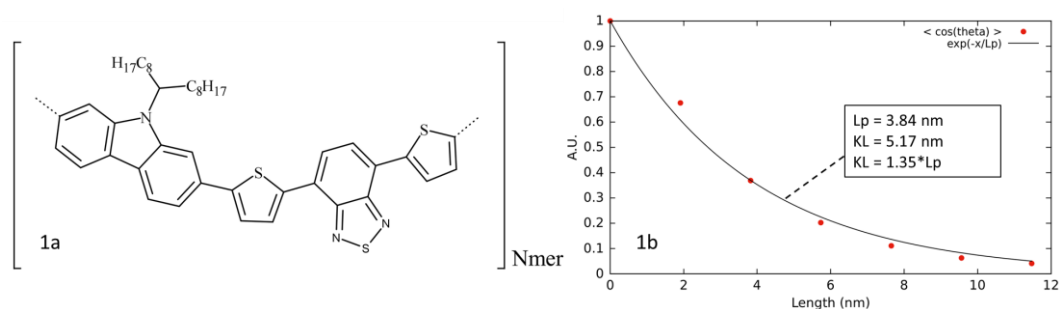


Figure 1: PCDTBT polymer (Fig. 1a) and PCDTBT persistence length (Lp) and Kuhn length (KL) (Fig. 1b).

References

- [1] Wang, J., Wolf, R. M.; Caldwell, et al. "Development and testing of a general AMBER force field". *J. Comput. Chem.*, **2004**, 25, 1157-1174.
- [2] Martin Streiter, Daniel Beer, Fabian Meier et al. "Homocoupling Defects in a Conjugated Polymer Limit Exciton Diffusion". *Adv. Func. Mater.*, **2019**, 29, 46.
- [3] Pieter van der Scheer, Ties van de Laar & Joris Sprakel. "Chain length-dependent luminescence in acceptor-doped conjugated polymers". *Sci. Rep.*, **2019**, 9, 11217.

Agricultural Plastics: Recent Developments in Waste management and Recycling

Marianna I. Kotzabasaki, Chrysanthos Maraveas and Thomas Bartzanas
*Farm Structures Lab., Department of Natural Resources and Agricultural
Engineering, Agricultural University of Athens,
11855 Athens, Greece*

Synthetic plastics are used in farms as mulching materials and shade materials/greenhouse covering materials (shade nets and plastic films) to protect plants from pests and extreme weather [1]. The properties of plastic materials make them one of the main pollutants in ecosystems, primarily because of their propensity to break down into small particles, such as microplastics and nanoplastics, and because of the emission of some chemical substances due to ultraviolet radiation from the sun that are added during the manufacturing process (additives) to improve the properties of the plastic (such as biophenol). Unfortunately, the practice of dumping plastic waste is widespread, with marine ecosystems experiencing the greatest rates of dumping, which has an impact on their flora and fauna, as well as the microbiome that goes along with it, as well as their physical environment.

Most of the time, the lack of sustainability generated by conventional agricultural production processes violates the 1992 United Nations (UN) principles for "*Sustainable or Lasting Development*." In addition, the European Union (EU) recently reformed its waste management regulations, which affect the treatment of agricultural plastics (hazardous and non-hazardous) [2, 3]. These regulations emphasize the reuse of waste generated during manufacturing processes by transforming it into by-products.

The various management methods for this waste stream include *Landfilling Burning or burial onsite (legally and illegally), Waste-to-Energy Incineration, Re-Use and Recycling*. During the last years, due to new technology developments on biotechnology, additive manufacturing and data management, new methods have been developed on waste management and recycling of plastics.

Aim of this work is the presentation of latest research developments and trends of agricultural plastics waste management and recycling, focused mainly on enzyme/microbial decomposition of plastics [4], re-use through 3D/4D printing technics [5], geospatial mapping of agricultural plastics [6] and discuss also their environmental and economic benefits.

References

- [1] Maraveas, C., Environmental Sustainability of Plastic in Agriculture, *Agriculture*, 10(8), 310 (2020).
- [2] European Union. Directive (EU) 2018/851 of the European Parliament and of the Council of 30 May 2018 amending Directive 2008/98/EC on Waste. *Off. J. Eur. Union L ser.*, **150**, 109–140 (2018).
- [3] European Union. Directive (EU) 2018/852 of the European Parliament and of the Council of of 30 May 2018 amending Directive 94/62/EC on packaging and packaging waste. *Off. J. Eur. Union L Ser.*, **150**, 141–154 (2018).
- [4] Anitha R., Maruthi R. and Sudha S., *Global Transitions Proceedings*, **3**(1), 100-103 (2022).
- [5] Maraveas C., Bayer I.S., Bartzanas T., *Biotechnology Advances*, **54**, 107785 (2022).
- [6] Mehta N., Cunningham E., Doherty M., Sainsbury P., Bolaji I., Firoozi-Nejad B., Smyth B.M., *Conservation and Recycling*, **179**, 106085 (2022).

Bias stress effect in organic thin film transistors operating in irradiation-activated electrolyte

I. Marinakis*, E. Kapetanakis

Department of Electronic Engineering, Hellenic Mediterranean University, 73133 Chania, Greece.

V. Saltas

Institute of Physics of the Earth's Interior & Geohazards, Hellenic Mediterranean University Research Center, 73133 Chania, Greece.

C. Katsogridakis, P. Argitis, P. Normand

Institute of Nanoscience and Nanotechnology, National Centre for Scientific Research "Demokritos", PO Box 60228, 15310 Athens, Greece.

In the present work, we report on solution-processed electrolyte-gated organic thin film transistors (EGOTFTs) stemming from in-situ photo-induced-generation of mobile ions in polymeric gate dielectrics. The latter are made of PMMA containing a photoacid generator (PAG) for producing upon UV irradiation an electrolyte with potentially mobile ions [1]. Particular emphasis is placed on the modulation of the source (S)-drain (D) output current (I_{DS}) of top-gate (PEDOT:PSS) bottom-contact (Au or ITO as S/D electrodes) p-type (P3HT)-based transistors operating in the linear regime under the application of fixed gate bias (V_{GS}). I_{DS} is recorded at the drain electrode by applying a square pulsed S/D voltage (-1V/0.2 s) at limited time intervals. Figure 1 shows the I_D - t characteristics in logarithmic representation of UV-irradiated devices with Au S/D electrodes, using a 350nm-thick PAG-PMMA layer formed onto a 20 nm-thick P3HT layer under fixed $V_{GS}=-25V$. Similar I_{DS} as time tends to infinity are recorded for devices with a channel length (CL) in the 0.5 - 10 μm range. As compared to the Au S/D electrode devices, UV-irradiated devices with interdigitated ITO electrodes (with variable 50-200 μm CL and channel width, $W=30$ mm), using a 350nm-thick PAG-PMMA layer formed onto a 20 or 50 nm-thick P3HT layer exhibit the same trend in the maximum recorded I_{DS} ($V_{GS}=-25V$) as depicted in the inset of Figure 2 for $V_{DS} = \pm 1V$. This clearly reveals that at long stress times, I_{DS} depends very little on the channel length and is dominated by S/D contact resistances. Figure 2 shows that I_{DS} as time tends to infinity decreases as the thickness of the P3HT increases, thus indicating an enhancement of the contact resistance with the P3HT thickness. Additional features of I_{DS} modulation with time as a function of the applied V_{GS} , V_{DS} , P3HT thickness, CL, and UV-exposure time will be presented at the conference.

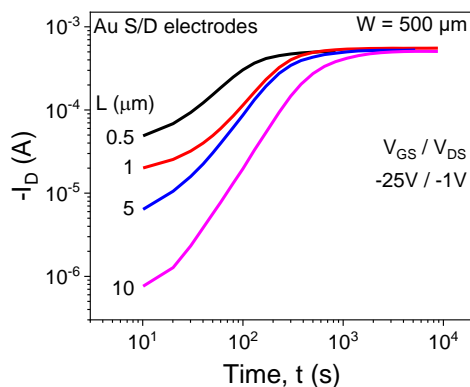


Figure 1: $\log(I_D) - \log(t)$ characteristics of UV-irradiated devices with Au S/D electrode for different channel lengths ranging from 0.5 to 10 μm , using an 80 $^{\circ}C$ -baked 350nm-thick PAG-PMMA electrolyte layer formed onto a 20 nm-thick P3HT layer under fixed $V_{GS}=-25V$.

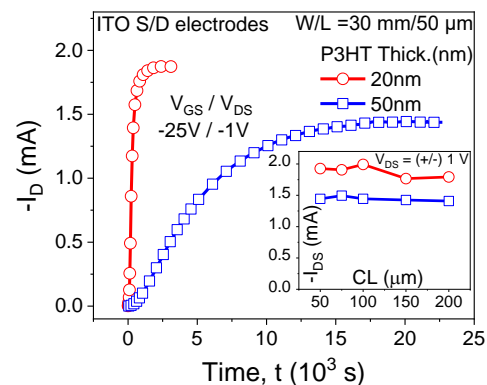


Figure 2: $I_D - t$ characteristics with interdigitated ITO electrodes, using a 20 or 50 nm-thick P3HT layer. Inset: I_{DS} vs CL characteristics of devices with L ranging from 50 to 200 μm ($W = 30$ mm) after stressing at $V_{GS}=-25V$ for $V_{DS} = \pm 1V$.

References

[1] E. Kapetanakis, Ch. Katsogridakis, D. Dimotikali, P. Argitis, and P. Normand, Adv. Electron. Mater. **6**, 2000238 (2020).

* ioanmarinakis@gmail.com

Effect of topography and cellulose nanocrystals on micropatterned polymeric replicas

A. Parlanis*, E. Kanakousaki, P. Kavatzikidou, A. Manousaki, E. Stratakis, A. Ranella

Foundation for Research and Technology - Hellas (FORTH), Institute of Electronic Structure and Laser (IESL)

A. Parlanis, A. Tsouknidas

Department of mechanical engineering, University of Western Macedonia, Greece

E. Stratakis

Department of Physics, University of Crete, Greece

Introduction: Cells make decisions on their responses depending on the stimuli relative to their surrounding environment. The extracellular matrix provides the necessary cues at micro and nano-scale for the cell adhesion, orientation/alignment, and proliferation. Furthermore, cells have the ability to sense the extracellular matrix (ECM) mechanics and spread via transcription regulator proteins. TAZ is characterised as a master regulator of cell-ECM interactions. Ultrafast pulsed laser irradiation is considered as a simple microfabrication method capable of producing anisotropy discontinuous topographical structures with control on geometry and pattern regularity [1, 2]. Soft lithography has been successfully used to transfer well-defined micro-sized patterns from silicon to polymeric [3, 4]. Cellulose nanomaterials (CN) based composites have emerged as promising materials in the field of Tissue Engineering and Regenerative Medicine due to their mechanical and chemical properties. The aim of this study is to investigate the effect of topography alongside the stiffness of the nanomaterials based composite replicas on cell morphology and osteogenic differentiation.

Experimental Methods: Replicas of polymers [Polycaprolactone (PCL) and their composites with Cellulose Nanocrystals (CNC)] have been successfully reproduced from the Si structures via soft lithography. Scanning Electron Microscopy (SEM) was performed for the morphological characterization of the polymeric replicas and their wetting profile was determined by contact angle. The degradation rate of the micropatterned replicas was also studied via SEM images, their weight loss as well as FTIR. The cell morphology, adhesion and differentiation of replicas of mouse Mesenchymal Stem Cells C57BL/6 were evaluated.

Results and Discussion: Cell mechanotransduction was analyzed via the cytoskeleton organization (shape), TAZ localization and cell nuclear profile on the replicas. The surface roughness had an effect on the MSCs morphology as shown in Figure 1. The chemical composition and degradation rate influenced cell responses.

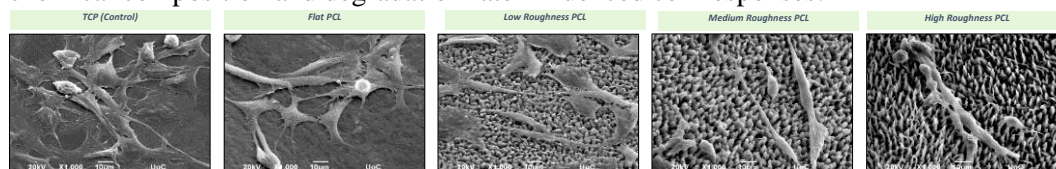


Figure 1: Scanning Electron Microscope (SEM) images of Mesenchymal Stem Cells (MSCs) on Polycaprolactone (PCL) scaffolds with four distinct topographies for 2 days of seeding.

ACKNOWLEDGMENTS

The authors would like to thank the European Project NFFA-Europe-Pilot (n. 101007417 from 1/03/2021 to 28/02/2026) for providing financial support to this project.

REFERENCES

1. Stratakis, E. et al., *Biomicrofluidics*. 5:013411, 2011
2. Simitzi C. et al. *Biomaterials*. 67:115-128, 2015
3. D Angelaki D. et al., *Mater. Sci. Eng. C*. 115:111144, 2020
4. Babaliari E. et al. *Int. J. Mol. Sci*. 19(7):2053, 2018.
5. Haishun Du et al., *Carbohydrate Polymers*. 209:130-144,2019.

* andreasparlanis@yahoo.com

3D bioprinted polysaccharide-based constructs for endothelial tissue engineering

Varvara Platania ^{1,2}, Konstantinos Loukelis ^{1,2}, Nikos Koutsomarkos ¹, Dimitris Vlassopoulos ^{1,2}, Maria Chatzinikolaidou ^{1,2}

1 Department of Materials Science and Technology, University of Crete, 70013 Heraklion, Greece

2 Foundation for Research and Technology Hellas (FORTH)-Institute of Electronic Structure and Laser (IESL), 70013 Heraklion, Greece

Introduction

Kappa-carrageenan is a natural linear polysaccharide derived from red seaweed with remarkable biocompatible properties [1]. Gellan gum is a biocompatible material produced by the bacterium *Sphingomonas paucimobilis*, which promotes the cell adhesion and proliferation capacity of various cells [2]. In recent years, a variety of different research studies in tissue engineering and regenerative medicine focuses on the construction of bioinks, which are structures comprising cells and other cellular constituents combined with biocompatible materials [3]. Our current work is based on the fabrication of a bioink containing kappa-carrageenan and gellan gum, which is tailored by employing extrusion 3D bioprinting to fabricate scaffolds with specific geometry facilitating a favorable 3D micro-environment for endothelial tissue growth.

Experimental methods

Two different blend compositions were prepared by mixing 4% w/v gellan gum (GG) with either 1.5% or 2% w/v kappa-carrageenan (K) in H₂O at 90°C for 4 h. The produced blend compositions are designated as GG-K1.5 and GG-K2 and used as inks. Subsequently, after cooling them at room temperature, the blends were mildly mixed with a volume of cell suspension (30x10⁶ cells/ml) in a ratio of 10:1 and the bioinks were loaded into extrusion cartridges for the 3D bioprinting process by means of a bioprinter (Inkredible+, Cellink). The produced bioinks have been placed in α MEM culture medium and stored in a humidified incubator at 37°C. Live/dead assay has been conducted with L929 fibroblasts to determine the cell viability and proliferation inside the bioink on days 1 and 7. Biodegradation studies have been performed on days 0, 7, 14 and 21 to assess the bioinks degradation rate in the presence of cells. Rheological analysis protocols have been executed to deduce the printability efficiency and the mechanical properties of the scaffolds including dynamic strain sweep (DSS), dynamic frequency sweep (DFS), recovery capability and viscosity of the developed bioinks. Ongoing experiments, evaluating functional endothelial markers including PECAM1 in bioprinted constructs are in progress.

Results and discussion

High cell viability of 90% has been validated for both scaffold compositions on day 1, while between days 1 and 7, a three-fold increase in cell number has been observed. No significant differences were detected between the two compositions regarding their biocompatibility. Additionally, the GG-K1.5 bioink depicted a biodegradation rate of 19% and 37% on days 7 and 21, respectively. The GG-K2 bioink exhibited lower biodegradation values of 15% on day 7, and 26% on day 21. Both blends displayed shear-thinning behaviour, a necessary characteristic for extrusion bioprinting. From the DSS tests, the yield points of the blends were calculated. The GG-K1.5 blend showed a yield point at 18 kPa, while the GG-K2 blend at 28 kPa. Both blends shared similar ranges for the loss tangent, 0.07-0.11 for the GG-K1.5 and 0.08-0.12 for the GG-K2 composition, indicating the predominance of elastic nature of both blends. A crucial condition for extrusion bioprinting is the material's ability to rapidly recover from the applied shear stress. The recovery of viscosity after 10 sec was measured at 97% for the GG-K1.5 and at 94% for the GG-K2 blend.

Conclusion

Two different bioink compositions containing kappa-carrageenan and gellan gum were fabricated through 3D extrusion bioprinting and promoted the growth of fibroblasts. Physicochemical and preliminary biological investigations confirm the constructs suitability for 3D bioprinting for soft tissue engineering.

References

- [1] Liu J. et al., *C. Polymers*. **121**, 27–36 (2015)
- [2] Sumi L. et al., *Inter. J. Biological Macromolecules*. **158**, 452–460 (2020)
- [3] Hospodiuk M. et al., *Biotechnology advances*. **35**(2), 217–239, (2017)

Acknowledgments

This research was funded by the Hellenic Foundation for Research and Innovation (H.F.R.I.) project number HFRI-FM17-1999.

Metamaterials as immunoengineering scaffolds

Stavros Skrepetos^{1,2}, George Flamourakis^{1,2}, Lina Papadimitriou¹, Anthi Ranela¹, Maria Farsari¹

1) Institute of Electronic Structure and Laser, Foundation for Research and Technology-Hellas (FORTH-IESL), 100 Nikolaou Plastira Street, Heraklion, 70013, Greece

2) Department of Materials Science and Technology, University of Crete, Vassilika Vouton, Heraklion, 71409, Greece

Macrophages play an important part in our immune system. They are immune system white blood cells that are engaged in the detection, phagocytosis, anti-bacterial capabilities, and the countering of other hazardous pathogen organisms that infiltrate the human body. The goal of this research is to monitor and comprehend how macrophages respond to auxetic, ultra – stiff, and ultra – light scaffolds. Scaffolds are created using multiphoton lithography, which enables free – form 3D printing of high resolution structures such as micro – optical elements and 3D scaffolds for tissue engineering and regenerative medicine applications. The scaffolds are based on the well – known re – entrant hexagonal geometry (bowtie), a novel auxetic scaffold named "shuriken," and the ultra – light – ultra – stiff Kelvin foam of different dimensions (small structures: approximately 10 μ m unit size and large structures: approximately 40 μ m unit size). Murine macrophages (RAW 264.7) were seeded on the scaffolds, and cell morphology and/or differentiation into M1 or M2 phenotypes were studied in response to the various mechanical conditions. Mechanical stimuli and topography influence important cellular responses such as morphology, directionality, orientation, and differentiation according to our findings. [1], [2]

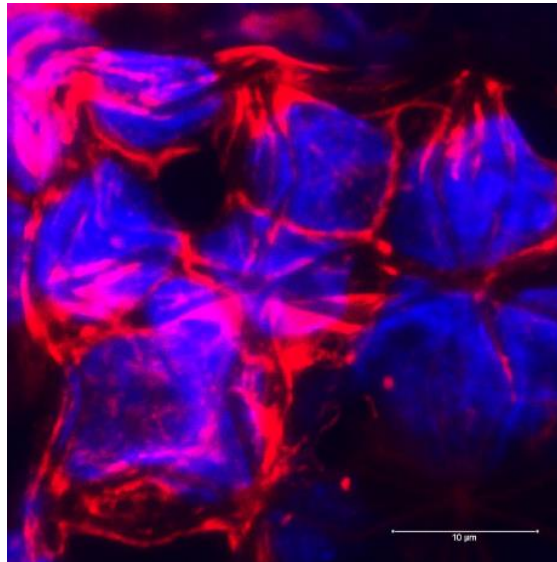


Figure 1: RAW 264.7 macrophages over structures with small pore size ($\sim 10\mu\text{m}$) on Shuriken lattice. Red channel: actin fibers and blue channel: nuclei of the cells. The spread-out actin fibres gives us the information that the cell has spread out trying to take up as much space on the unit cell as it can.

References

[1] G. Flamourakis *et al.*, "Laser-made 3D Auxetic Metamaterial Scaffolds for Tissue Engineering Applications," *Macromol. Mater. Eng.*, vol. 305, no. 7, pp. 1–9, 2020, doi: 10.1002/mame.202000238.

[2] R. Sridharan, A. R. Cameron, D. J. Kelly, C. J. Kearney, and F. J. O'Brien, "Biomaterial based modulation of macrophage polarization: A review and suggested design principles," *Materials Today*, vol. 18, no. 6, pp. 313–325, 2015, doi: 10.1016/j.mattod.2015.01.019.

Morphological, Structural, Thermal and Dielectric Properties of PLA/PCL based nanocomposites

V.M.V. Stavropoulou*, A.A. Barmdaki, E.E. Zavvou, P.K. Karahaliou
and C.A. Krontiras

Department of Physics, University of Patras, 26504 Patras, Greece

A. Giannakas

*Department of Food Science and Technology, University of Patras, 30100
Agrinio, Greece*

A. Ladavos

*Department of Food Science and Technology, University of Patras, 30100
Agrinio, Greece*

Poly (lactic acid) (PLA) is a biopolymer that has attracted scientific interest due to its good biodegradability, facile processability and excellent biocompatibility. In fact, the combination of good mechanical properties and reduced production cost, have made it the most suitable environmentally friendly material for the substitution of the traditional petroleum-based polymers. However, disadvantages like poor thermostability, high brittleness and low impact strength, are limiting its practical applications [1]. For this reason, blends of PLA with other polymers have been explored. In this orientation, polycaprolactone (PCL) is thought to be an appropriate candidate, since it is biocompatible, miscible with several polymers, easily processed and can be used in a wide range of applications, especially in tissue engineering, drug delivery and food packaging [2-4]. In the framework of this study, PLA/PCL blends were prepared via twin-screw extrusion in percentages of 90/10, 80/20, 70/30, 60/40 and 50/50 wt%. Scanning Electron Microscopy (SEM) was employed to assess the degree of dispersion of PCL and study the miscibility of the two polymers. Differential Scanning Calorimetry (DSC) reveals partial miscibility of the two components. X-Ray Diffraction (XRD) was also employed in order to study the crystal structure of the components. Furthermore, the dielectric behavior of the blends was studied by means of Broadband Dielectric Spectroscopy (BDS). A variety of relaxation mechanisms, attributed to PLA and PCL counterparts, were recorded and their dynamics was analyzed. Last, nanocomposites of PLA/PCL (80/20) and halloysite nanotubes (HNTs) in filler contents of 1, 3, 5, 7 and 10 wt% were prepared via twin-screw extrusion and studied using the same experimental techniques. HNTs were selected as nanofillers, since they have the potential to enhance the biocompatibility, they improve the mechanical properties of the polymer matrix and are good carriers of biologically active substances [5, 6]. The purpose of this addition was to investigate the effect of the nanofillers on the miscibility of PLA and PCL and possibly achieve the enhancement of the properties of these blends.

Acknowledgements

Authors acknowledge Prof. I. Iliopoulos for the XRD experiments.

References

- [1] Li et. al., *J Appl Polym Sci* **138**, 49668 (2021).
- [2] P.F.M. Finotti et al., *Journal of the mechanical behavior of biomedical materials* **68**, 155–162 (2017).
- [3] Z. N. Correa-Pacheco et al., *Appl. Phys. A* **120**, 1323–1329 (2015).
- [4] Terzopoulou et. al., *J Mater Sci* **53**, 6519–6541 (2018).
- [5] Alam et. al., *J Mater Sci* **56**, 14070–14083 (2021).
- [6] C. Venkatesh et. al., *J Polym Eng*; **41**(6), 499–508 (2021).

* v.stavropoulou@upnet.gr

Structural and dynamic properties of poly(ethylene oxide)/silica nanocomposites as studied by molecular dynamics simulations: Effects of temperature and silica concentration

I. Tanis*, V. Harmandaris

The Cyprus Institute, 20 Costantinou Kavafi St., 2121 Nicosia, Cyprus

Polymer nanocomposites (PNCs) prepared by introducing nanoparticles (NPs) (spheres, cylinders, plates) within a polymer matrix, have attracted significant scientific and technological interest since the addition of a small volume of nanofillers creates a great amount of interfacial area between polymer matrix and nanofillers, resulting in either improved or new properties without losing attractive properties inherent to pure polymers such as toughness, processability and optical transparency [1]. Molecular dynamics simulation is a complementary tool to experiments as it offers a detailed and direct insight into the properties of a polymer matrix embedded with spherical NPs. Motivated by pertinent experimental and numerical works, we examine structural and dynamic attributes of a poly(ethylene oxide)/silica PNC in a wide range of temperatures sampling both the melt and the glassy state. The effect of NP concentration is also addressed. Our results demonstrate that the dynamics of the adsorbed chains is slower compared to their non-adsorbed counterparts and reveal a coupling between the chain conformational states and their segmental dynamics.

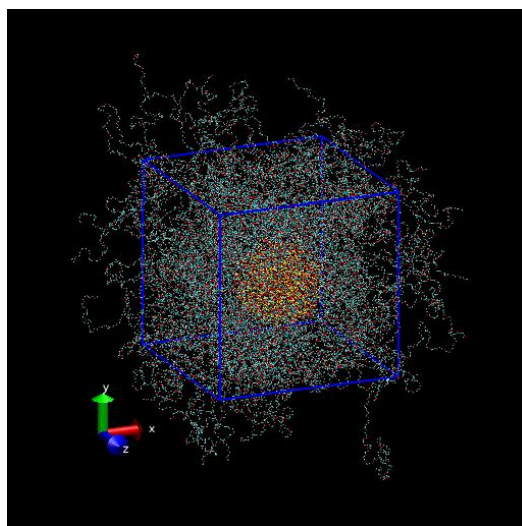


Figure 1: Atomistic representation of the PEO/Silica configuration at silica $v/v = 4.5\%$.

References

[1] Bailey E.J. and Winey K.I., *Progress in Polymer Science*, **105** 101242 (2020).

* i.tanis@cyi.ac.cy

Hyper expanded molecule intercalated iron selenides with robust superconducting response

Alexandros Deltsidis^{1,2,*}, Myrsini Kaitatzi^{1,2}, Laura Simonelli³, Alexandros Lappas¹

¹*Institute of Electronic Structure and Laser, Foundation for Research and Technology - Hellas, Vassilika Vouton, 71110 Heraklion, Greece*

²*Department of Materials Science and Technology, University of Crete, Voutes Campus, Heraklion 70013, Greece*

³*ALBA Synchrotron Light Source, Carrer de la Llum 2-26, 08290 Cerdanyola del Vallés, Spain*

Iron-chalcogenides along with the copper oxides constitute two families of 2D materials that exhibit high superconducting critical temperature (T_c). In these, magnetism and superconductivity typically coexist, and the superconducting state emerges when antiferromagnetic (AFM) order is suppressed by carrier doping, structural modifications under external pressure, or chemical pressure via isovalent substitutions. Since the parent materials of Fe-based superconductors have layered structures, doping by intercalation offers a facile avenue to suppress the AFM state with concomitant enhancement of the T_c . Electron donor molecules co-intercalated with alkalis in the β -FeSe (Fig. 1b) allow to study the impact on the electronic structure of the host, as the intercalation increases the interlayer separation and leads to a five-fold rise of the T_c (44 K). We have developed low-T solvothermal routes, for such high- T_c $\text{Li}_x(\text{C}_5\text{H}_5\text{N})_y\text{Fe}_{2-z}\text{Se}_2$ (Fig. 1a) [1] in order to study their structure-property relations by high-resolution synchrotron-based tools. Element-specific (Fe & Se K-edge) X-ray absorption (XAS) and emission (XES) spectroscopies were utilised to provide valuable insights on how the interlayer guests [Li-C₅H₅N] impact the evolution of (i) the FeSe₄ building blocks in the FeSe electronically active layers, including the Fe local moments, and (ii) the magnitude of T_c . The near edge region of the XAS confirmed doping-mediated local atomic rearrangements and progressive filling of orbital states, with concomitant reduction of empty levels near the E_F with respect to β -FeSe. The $K\beta$ XES point that the intercalated compounds, carry a low-spin state, as well as a somewhat reduced Fe local magnetic moment. Local structure assessments, based on modeling the EXAFS oscillations, suggest that while the Fe-Se bond remains stiff and covalent in nature, the Fe-Fe bond evolves to become softer for high Li content (x), due to raised Fe-site deficiency (Fig. 1c). The findings provide insights on the desirable combination of local electronic and structural parameters that tune the T_c in such strongly correlated electron systems, possibly offering an avenue to engineer robust superconducting state at elevated temperatures.

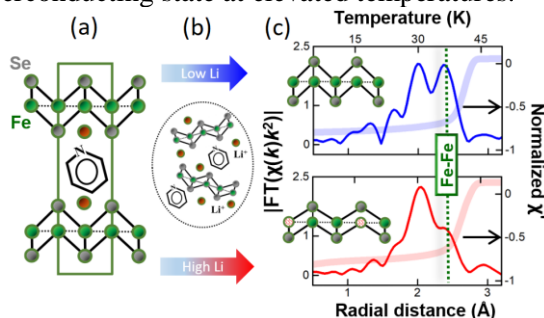


Figure 1: 2D iron-selenides, with large interlayer separation, probed by synchrotron XAS, bear Fe-vacancies with increased Li-content, but retain a robust superconducting state.

References

[1] Berdiell I. C. *et al.*, *Inorg. Chem.* **61**, 10 (2022).

* adeltsidis@iesl.forth.gr

Order parameters in underdoped copper oxides : charge and pair density waves

George Kastρινakis

Institute of Electronic Structure and Laser (IESL), Foundation for Research and Technology (FORTH), N. Plastira 100, Vassilika Vouton, 70013, Iraklio, Crete, Greece

kast@iesl.forth.gr

We use the formalism of the new fermion index, introduced a few years ago [1], in order to theoretically investigate order parameters in underdoped copper oxides. This fermion index is an additional degree of freedom for the electrons, which allows them to *participate simultaneously in several different pairs*. This is **impossible** without the new index. We use appropriate variational wavefunctions, which extend the well known BCS-type ones, while comprising a desired number of pairs of electrons for any given momentum. These yield a plethora of possible correlations, which are left unaccounted for in more traditional approaches. This is a self-consistent and strong coupling approach.

Applying the method to the underdoped copper oxides, we use a relevant model with one partially occupied energy band and one totally filled band. We consider a combination of electron **intra-band** and **inter-band** pairs. We use *realistic dispersion relations and electron-electron potentials*, in agreement with advanced first principles [2] etc. calculations.

We observe the emergence of charge (CDW) and pair density wave (PDW) orders, with characteristic finite momenta, in the low temperature limit. These may coexist with superconductivity. We make the connection with the results of X-ray scattering, NMR, etc. experiments [3],[4],[5], which probe these orders in the cuprates.

References

- [1] G. Kastρινakis, Annals of Physics **349**, 100 (2014)
 - [2] J.B. More'e et al., arxiv:2206.01510 (2022)
 - [3] W.-S. Lee, J. Phys. Soc. Jpn. **90**, 111004 (2021)
 - [4] R. Arpaia and G. Ghiringhelli, J. Phys. Soc. Jpn. **90**, 111005 (2021)
 - [5] S. Kawasaki et al., J. Phys. Soc. Jpn. **90**, 111008 (2021)
-

Skyrmion dynamics in ring-shaped synthetic antiferromagnetic racetracks

Dimitris Kechrakos*

Physics Laboratory, Department of Education, School of Pedagogical and Technological Education, Athens, Greece

Riccardo Tomasello

^aDepartment of Electrical Engineering, Technical University of Bari, Italy

Faye Gemenetzi

National Technical University of Athens, Athens, Greece

Giovanni Finocchio

Department of Mathematical and Computer Science, Physical Sciences and Earth Sciences, University of Messina, Messina, Italy

A racetrack memory where the information can be encoded in magnetic skyrmions seems to be a strong candidate for magnetic storage devices to succeed the conventional hard disk drives. Electrical current producing spin-orbit torques is a common means to drive skyrmions on a racetrack. Racetracks made of Synthetic Antiferromagnets (SAF) suppress the Skyrmion Hall Effect, which consists of a transverse displacement of skyrmions and their eventual annihilation at the racetrack boundary. In the present work we implement fully numerical micromagnetic simulations [1] of the current-driven dynamics of skyrmions in SAF racetracks with a ring shape. Circular racetracks have technological potentials as shift-register devices [2]. Due to the lack of transverse displacement in SAF systems, the skyrmions are shown to follow a stable circular motion with constant frequency. We study the dependence of the kinematic frequency on the material damping constant, the applied current and the size of the ring-shaped racetrack. We demonstrate that for rings with inner and outer diameters in the range of 100nm and 200nm, respectively and current density up to 300MA/cm² a circular motion with frequency of approximately 0.5GHz is supported. Envisaged applications of the skyrmion in a ring-shaped racetrack as a periodic electrical pulse GHz generator are discussed.

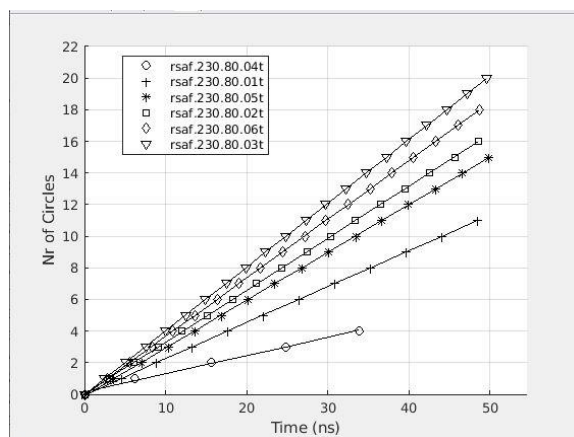


Figure 1: Number of of circles completed by the moving skyrmion as a function of time. The linearity of the data demonstrate the clock-functionality of the circular motion of skyrmions. Ring diameters are 460nm and 160nm. Different current densities applied are 50,100,150,200,250 and 300 MA/cm².

References

- [1] A.Giordano, G. Finocchio, L.Torres, M. Carpentieri, B. Azzerboni, J.Appl.Phys.**111** (2012) 07D112
- [2] Zhang, S.L., Wang, W.W., Burn, D.M. et al. Nat Commun **9** (2018) 2115

* dkehrakos@aspete.gr

C-doped L1₀-MnAl ferromagnetic thin films

A. Kaidatzis*, N. Mouti, K. Giannakopoulos, D. Niarchos
*Institute of Nanoscience and Nanotechnology, N.C.S.R. "Demokritos", Athens,
Greece*
André Thiaville
C.N.R.S. - Laboratoire de Physique des Solides, Orsay, France

Chemically ordered L1₀-MnAl alloys reveal high perpendicular magnetic anisotropy energy, small magnetic damping constant, and low magnetization (the latter being important for using low excitation currents in magnetic RAM applications) [1]. A key issue is to obtain such a material on commercial Si wafers, for ensuring compatibility to standard microelectronics processes and allowing the development of a low-cost, commercially viable spintronic devices technology.

In this work, we employed magnetron sputtering deposition of MnAl alloy with addition of carbon on heated single crystal Strontium Titanium Oxide (STO) substrates. Magnetostatic characterization was performed using the magneto-optical Kerr effect (MOKE), as well as Brillouin light scattering (BLS) for dynamic measurements. The results clearly show that a ferromagnetic phase appears. For obtaining the desired L1₀ phase on substrates compatible to microelectronics processes, we plan to deposit STO seed layers onto oxidized Si wafers and thereupon grow C-doped MnAl.

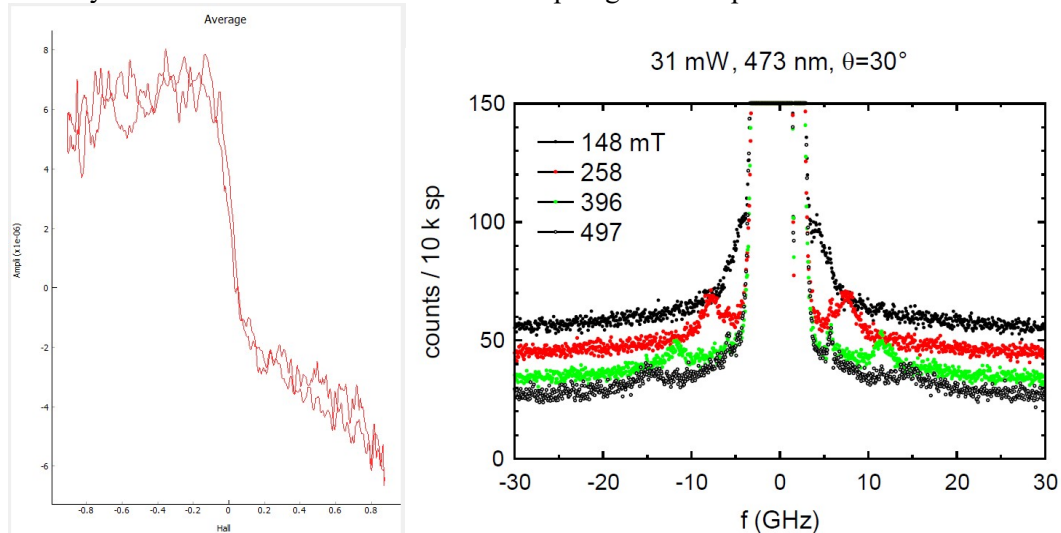


Figure 1 Representative magnetic characterization measurements. (Left) polar-MOKE measurements (out-of-plane field, values in T) of C-MnAl 100 nm thick film; A clear magnetization reversal with coercive field of ~60 mT is apparent in the perpendicular geometry. (Right) BLS measurements of the same sample. A (weak) peak is seen which shifts to higher frequencies when field (applied in the sample plane) is increased.

Funding: This work was supported by the NATO SPS programme in the framework of the Multi-Year Project "Spintronic Devices for Microwave Detection and Energy Harvesting Applications" (G5792).

References

[1] Takeuchi *et al.* Appl. Phys. Lett. **120**, 052404 (2022).

* a.kaidatzis@inn.demokritos.gr

Unravelling the ozone sensing mechanism of all-inorganic metal halide perovskites

A. Argyrou^{*a, b}, K. Brintakis^a, E. Gagaoudakis^a, V. Binas^a, A. Kostopoulou^a, E. Stratakis^{a, c}

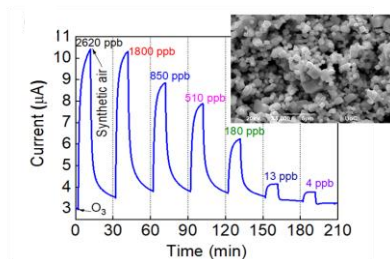
^aInstitute of Electronic Structure and Laser, Foundation for Research & Technology-Hellas, P.O. Box 1527, Vassilika Vouton, 70013 Heraklion, Greece

^bUniversity of Crete, Department of Chemistry, Vassilika Vouton, 70013 Heraklion, Greece

^cUniversity of Crete, Department of Physics, Vassilika Vouton, 70013 Heraklion, Greece

Gas sensors play an important role in many aspects of our lives due to their ability to detect a wide range of air pollutants, toxic and combustible gases. Therefore, there is an increasing demand for the development of novel materials that would provide new opportunities in terms of sensitivity, selectivity and stability. Furthermore, the fundamental understanding of the underlying sensing mechanism that involves the interaction between the target gasses and the sensing element needs further exploration.

Recently, metal halide perovskite crystals with the chemical formula ABX_3 , where A and B are two cations with very different sizes and X is a halogen anion, have appeared in gas sensing research since they can reversibly transduce any environmental stimuli into optical or electrical signal. According to the aforementioned, the aim of this research is the fabrication of sensitive perovskite-based sensing elements that would be able to detect ultra-low concentrations of the target gases. [1,2] Herein, we present the sensing performance of ligand-free all-inorganic $CsPbX_3$ (where X= Cl, Br or their mixtures) microcrystals to detect ultra-low concentrations of ozone. In comparison, doped systems with manganese have been fabricated with similar morphology in order to reduce the lead content and provide a more environmentally friendly sensing material. Both materials were grown by a cost-effective solution-based process under ambient conditions. Their sensing capability was evaluated by electrical measurements carried out under different gas concentrations, at room temperature operating conditions (Fig. 1a for the $CsPbBr_3$ sensing element). Remarkably, each sensor displayed enhanced sensing behavior upon time, providing information of the underlying sensing process. Additionally, the high performance of the μCs as O_3 sensing elements in terms of sensitivity and stability,



compared to the state-of-the-art semiconducting materials along with the fully elucidation of the sensing mechanism opens up new possibilities for environmental-friendly gas sensing materials.

Figure 1. Electrical response of $CsPbBr_3$ sensing elements upon different O_3 concentrations ranging from 2620 ppb to 4 ppb. Inset: SEM image of $CsPbBr_3$ microcubes.

References

- [1] Brintakis et al., *Nanoscale Adv.* **7**, 2699 (2019).
- [2] Argyrou et al., *J. Mater.* **8**, 446 (2022).

Acknowledgements

FLAG-ERA Joint Transnational Call 2019 for transnational research projects in synergy with the two FET Flagships Graphene Flagship & Human Brain Project - ERA-NETS 2019b (PeroGaS: MIS 5070514).

* kargyrou@iesl.forth.gr

Graphite-SiO_x electrodes with a biopolymeric binder for Li-ion batteries

Stavros X. Drakopoulos¹⁻³, Tom Cowell², Emma Kendrick^{2,3}

¹Department of Physics, University of Bath, United Kingdom

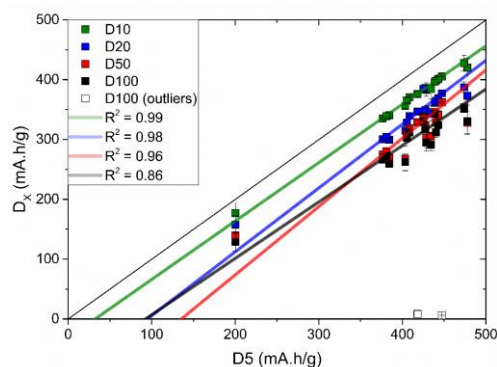
²The Energy Materials Group, University of Birmingham, United Kingdom

³The Faraday Institution, United Kingdom

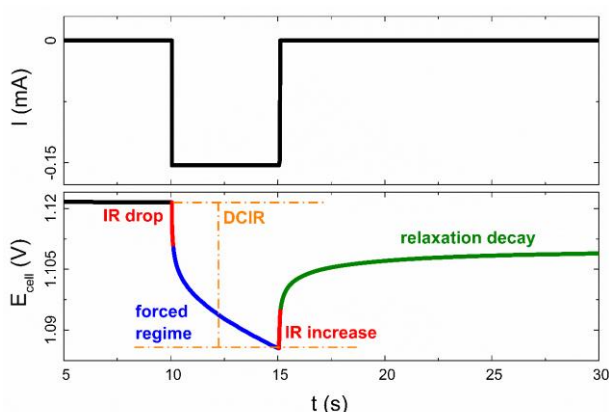
The rechargeable Li-ion battery is a fundamental necessity in modern society, being used in devices including cell phones, laptop computers, and digital cameras. Decades of incremental improvements have made today's rechargeable batteries longer-life with higher densities and are now being used in the emerging sector of electric vehicles. With this broad applicability of Li-ion batteries, it is important to take into account the environmental impact that they have and design the manufacturing, materials, processing and recycling with this in mind.

The most common anode material for Li-ion batteries is graphite, despite its relatively low energy storage density (372 mA.h/g), because of its cycle life stability attributed to its low volume expansion during lithiation and delithiation. In order to improve the specific capacity, but not compromise the volume expansion, silicon suboxide – SiO_x (1965 mA.h/g) can be mixed with graphite at low amounts to boost the specific capacity which is attractive for high-energy requirements. SiO_x is less conductive than graphite 6.7×10^{-4} S/cm compared to $\sim 10^4$ S/cm

and a conductive 3D network with carbon black, or alternative conductive additives, is used to increase the electrically conductive pathways and enable the electron transfer from the surface of the electrode to the current collector. The binder also increases the resistivity of the coatings and thus its presence is preferred at a minimum, however it is very important to the mechanical stability of the electrode since



In this work, carrageenan gum has been investigated as a potential green binder system for graphite-SiO_x anodes. A relationship between the physical properties and the electrochemical properties has been explored, with an end goal the cycle life performance. A simple current interrupt test elucidated and the contributing ohmic and charge transfer resistances showing increases for both, related to the mass loading, porosity and state of charge. This method may enable faster screening of electrode formulations, and prediction of cycle life of this and other electrode types.



it binds the active materials and conductive additive to the current collector and affects the electrode-current collector adhesion properties. In order to reduce cost, and improve the environmental impact of Li-ion battery electrodes, water-soluble binders can be utilized, most commonly carboxyl methylcellulose (CMC) and styrene-butadiene rubber (SBR). Other polymeric natural binders like carrageenan have been introduced and electrochemically investigated in the literature the past decade.

^{68}Ga -DPD- Fe_3O_4 as a dual-modality contrast agent: biodistribution study on mice and biocompatibility with peripheral human blood cells

M. A. Karageorgou^{*1,2}, P. Bouziotis¹ and D. Stamopoulos^{2,3}

¹INRASTES, NCSR "Demokritos", Ag. Paraskevi, 15341, Greece

²Department of Physics, NKUA, Zografou Panepistimioupolis, 15784, Greece

³INN, NCSR "Demokritos", Ag. Paraskevi, 15341, Greece

Radiolabeled Fe_3O_4 nanoparticles are promising candidates as dual-modality contrast agents (DMCA) for diagnostic applications. Accordingly, the biocompatibility of a DMCA is of significant clinical importance for subsequent *in vivo* applications. Thus, we focused on the realization of biocompatibility and biodistribution tests both *in vitro* and *in vivo*, of a DMCA, namely Fe_3O_4 nanoparticles radiolabeled with ^{68}Ga . The *in vitro* biocompatibility of the DMCA was performed after incubation with donated human blood cells, namely red blood cells (RBCs), white blood cell (WBCs) and platelets (PLTs) coming from five healthy individuals. The advanced atomic force microscopy (AFM) technique was employed for the investigation of the morphological characteristics of all blood cells at the nanoscopic level. The kinetics of the *in vivo* biodistribution of the DMCA was evaluated in normal mice. The obtained *in vitro* and *in vivo* data prove that the specific DMCA is biocompatible, thus promising for future *in vivo* applications [1, 2].

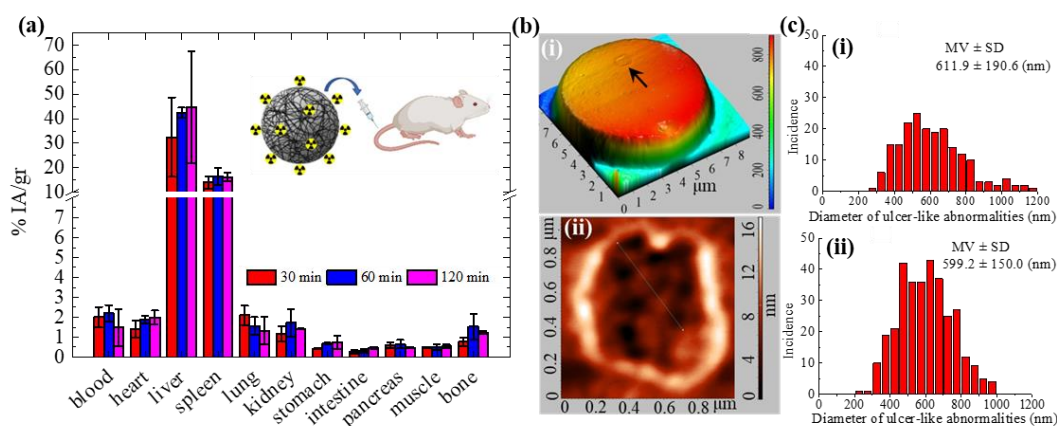


Figure 1: (a) The accumulation of [^{68}Ga]Ga-DPD- Fe_3O_4 DMCA in the organs of normal mice, expressed as percentage injected activity per gram of tissue (% IA/g) at 30, 60 and 120 min post injection. At each time point, the results are expressed as the mean value \pm standard deviation (MV \pm SD) of three mice. (b)(i) Three-dimensional AFM image of a DMCA-incubated RBC at $C_{\text{DMCA}}=0.1$ mg/ml (incubation at room temperature for 120 min). The arrow indicates an ulcer-like abnormality on the RBC membrane. (b)(ii) Two-dimensional topography of the ulcer-like abnormality observed on the RBC membrane in (b)(i). (c)(i)-(ii) Quantitative data of the diameter of ulcer-like abnormalities observed in RBCs coming from (i) DMCA-free after 120min incubation and (ii) DMCA-incubated samples at $C_{\text{DMCA}}=1$ mg/ml. The MV \pm SD expresses the mean value and standard deviation of all data obtained from five healthy donors.

References

- [1] Karageorgou M. A. et al., Mater. Sci. Eng. C. **115**, 111121 (2020).
 [2] Karageorgou M. A. and Stamopoulos D., Sci. Rep. **11**, 9753 (2021).

M. A. Karageorgou acknowledges the NKUA for financial support through the "S. Tsakirakis" Scholarship.

^{68}Ga -DPD- Fe_3O_4 as a dual-modality contrast agent: magnetic resonance imaging on mice

M. A. Karageorgou^{*1,2}, P. Bouziotis¹ and D. Stamopoulos^{2,3}

¹INRASTES, NCSR "Demokritos", Ag. Paraskevi, 15341, Greece

²Department of Physics, NKUA, Zografou Panepistimioupolis, 15784, Greece

³INN, NCSR "Demokritos", Ag. Paraskevi, 15341, Greece

Dual modality contrast agents (DMCAs), such as radiolabeled Fe_3O_4 nanoparticles, combine the advantages of each imaging modality (i.e., the high sensitivity of positron emission tomography or single photon emission computed tomography (PET or SPECT) with the high spatial resolution of magnetic resonance imaging (MRI)), providing a powerful imaging tool in diagnosis. Thus, taking into account the importance of the application of a DMCA in well-established imaging applications of clinical practice, we aimed to develop and evaluate both *in vitro* and *in vivo* a PET/MRI DMCA for diagnostic purposes. The DMCA we have studied consists of Fe_3O_4 nanoparticles, surface functionalized with 2,3-dicarboxypropane-1,1-diphosphonic acid (DPD) and radiolabeled with ^{68}Ga , that is ^{68}Ga -DPD- Fe_3O_4 . Here we demonstrate in detail, the physical properties of the specific DMCA (crystallographic, morphological and magnetic), as well as its *in vivo* imaging efficacy by means of MR imaging in normal mice [1, 2].

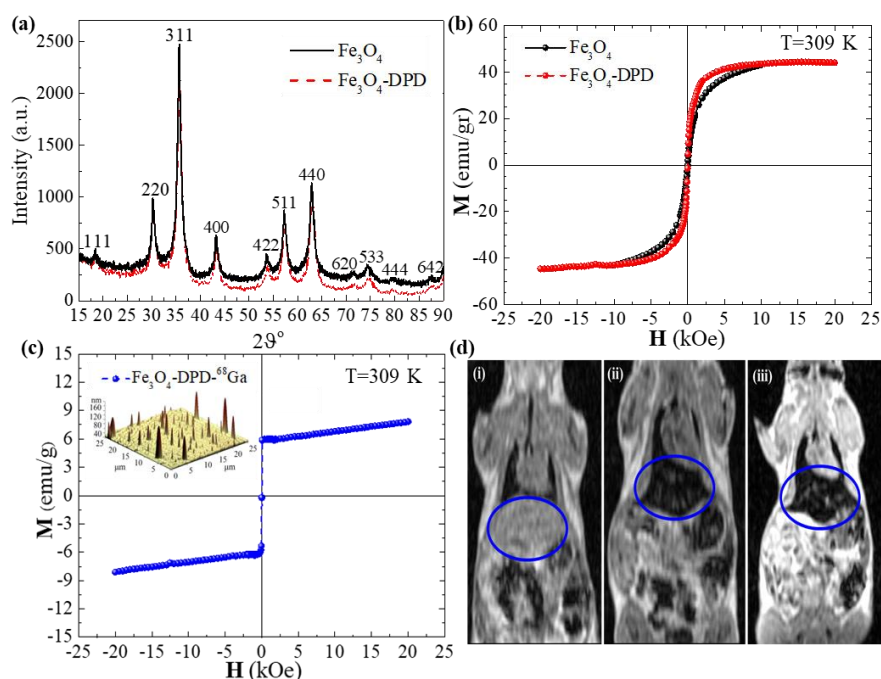


Figure 1: (a) XRD data of Fe_3O_4 and DPD- Fe_3O_4 contrast agents (CAs). (b) Magnetization data, $M(H)$, at $T= 309\text{K}$ of Fe_3O_4 and DPD- Fe_3O_4 CAs. (c) $M(H)$ measurements at $T= 309\text{K}$ of ^{68}Ga -DPD- Fe_3O_4 DMCA. The upper left inset illustrates a representative three-dimensional topographic atomic force microscopy image of the DMCA. (d) Representative T_1 -weighted coronal MRI data (6 h post injection) of $n = 3$ normal mice injected with ^{68}Ga -DPD- Fe_3O_4 DMCA at concentrations of: (i) $C_{\text{DMCA}}= 0.01\text{ mg/ml}$ and (ii) $C_{\text{DMCA}}= 0.1\text{ mg/ml}$, respectively and with (iii) non-radiolabeled DPD- Fe_3O_4 CA at $C_{\text{CA}}= 0.1\text{ mg/ml}$. The blue circles indicate the area of interest.

References

[1] Karageorgou M. A. et al., Contrast Media Mol. Imaging 6951240, 1-13 (2017).

[2] Karageorgou M. A. and Stamopoulos D., Sci. Rep. **11**, 9753 (2021).

M. A. Karageorgou acknowledges the NKUA for financial support through the "S. Tsakirakis" Scholarship.

Design and development of detachable water PLA filters using 3D printing

N.D. Dinas, A.X. Krestou^{*},

*Department of Mechanical Engineering, University of Western
Macedonia, Kozani, 50100, Greece*

A.Z. Stimoniaris

*Department of Chemical Engineering, University of Western
Macedonia, Kozani, 50100, Greece*

G. Ch. Kalogeropoulos,

*Department of Mechanical Engineering, f. W. Macedonia University of Applied
Sciences, Kila – Kozani, 50100, Greece*

The current paper describes the design and development of two detachable PLA water filters able to be attached in 5L and 500 ml bottles. The intended use of the former was the water filtration for settlements with poor or non-existent water systems, and of the latter the use for outdoor activities (i.e. camping, climbing). Polylactic Acid (PLA) was used as filament since it is synthesized by a naturally occurring L-lactic acid monomer derived from plant starch (i.e. corn, cassava, sugarcane) [1] that renders it a safe material for contact with potable water. The filters were designed using the Autodesk Fusion 360 programme, extracted in .stl format using the Cura Ultimaker programme and produced by means of the Creality Ender-3 v2 3D printer. The 5L model consisted of two ergonomically designed parts: the first part comprised of the elongated nozzle and the main filter chamber with side grooves for maximum flow while the second one was a detachable part for chamber sealing (Figure 1a). Maximum sealing was ensured by incorporating a user-removable grip that can be removed during the filtering media change process. The chamber is accessible and can be filled with the appropriate filter material through this grip. Holes were also formed in order to maintain the desired water flow. The dimensions of the 5L model were approximately 90,5mm x 57mm x 37mm (total length x nozzle diameter x filter diameter), implying a filter with large volume but at the same time with high durability. Portability and minimalism were the basic design principles for the 500ml model (500M). Being 52% smaller than the 5L one, this filter is light weighted and allows easy transport and storage. 500M filter consisted also of two parts: a nozzle and a chamber with holes (Figure 1b). The nozzle was modeled to look like a bottle cap for sports with ergonomic grooves on the sides for better grip, providing maximum flow. The dimensions of the 500M model were approximately 77mm x 32mm x 14mm (total length x nozzle diameter x filter diameter) and its minimal design renders it an excellent option for outdoor activities, allowing the user to carry it everywhere.



Figure 1: Nozzle and main filter chamber of the a) 5L filter and b) 500ml filter

References

- [1] Nadagouda, Ginn and Rastogi, *Current Opinion in Chemical Engineering* **28**, 173 (2020).

* akrestou@uowm.gr

Flexible 2D material transistors under controlled biaxial deformation

A. Michail^{1,2*}, J. A. Young³, K. J. Thompson⁴, C. A. Nattoo³, C. S. Bailey³,
A. Daus^{3,5}, E. Pop^{3,6}, J. Parthenios² and K. Papagelis^{2,7}

¹*Department of Physics, University of Patras, Greece*

²*Institute of Chemical Engineering Sciences, Foundation for Research and Technology Hellas (FORTH-ICEHT), Patras, Greece*

³*Electrical Engineering, Stanford University, Stanford, CA, 94305 USA*

⁴*Electrical and Computer Engineering, Ohio State University, Columbus, OH 43210, USA*

⁵*Chair for Electronic Devices, RWTH Aachen University, Aachen, 52074, Germany*

⁶*Materials Science and Engineering, Stanford University, Stanford, CA, 94305 USA*

⁷*School of Physics, Department of Solid State Physics, Aristotle University of Thessaloniki, 54124, Thessaloniki, Greece*

Semiconducting two-dimensional Transition Metal Dichalcogenides (2D - TMDCs) can sustain very large deformations before failure (up to 8%) while presenting large (1.5 to 2.0 eV) and extremely strain-sensitive (50–130 meV/%) direct bandgaps. Thus, this class of materials holds great promise in strain engineering applications. Over the decade, in the bulk of the published works, 2D - TMDC crystals have been tested under various types of strain [1–3]. However, with respect to flexible electronics, where a large number of interfaces is involved, the extend to which mechanical strains can be efficiently transferred to the 2D crystal requires further attention.

In this work it is shown that despite the larger number of interfaces occurring in a 2D material transistor, biaxial strain can be efficiently imposed on the devices in a controllable manner. In particular, WSe₂ and MoS₂ field effect transistors, fabricated on flexible polyethylene naphthalate (PEN) substrates are subjected to biaxial strain. The efficient strain transfer is verified using in-situ Raman mapping over the whole channel of several devices. Additionally, it is shown that in the spectroscopically difficult case of WSe₂, where the strain sensitive E' mode is accidentally degenerate with the more intense and strain insensitive A'_1 mode, the second order Raman active modes around 350 – 400 cm⁻¹ can be used as efficient strain indicators.

References

- [1] H. J. Conley, B. Wang, J. I. Ziegler, R. F. Haglund, S. T. Pantelides and K. I. Bolotin, *Nano Letters* **13**, 3626–30 (2013)
- [2] D. Lloyd, X. Liu, J. W. Christopher, L. Cantley, A. Wadehra, B. L. Kim, B.B. Goldberg, A. K. Swan and J. S. Bunch *Nano Letters* **16**, 5836–41(2016)
- [3] A. Michail, D. Anastopoulos, N. Delikoukos, J. Parthenios, S. Grammatikopoulos, S. A. Tsirkas, N. N. Lathiotakis, O. Frank, K. Filintoglou and K. Papagelis, *2D Materials* **8**, 015023 (2020)

*antmichail@upatras.gr

Band gap prediction & data analysis of inorganic halide perovskites using machine learning

Alaelddin Michailidis-Barakat^{*}, Emmanouil Pervolarakis, Constantinos C. Stoumpos, Ioannis N. Remediakis

Department of Materials Science and Technology, University of Crete, Heraklion 70013, Greece

Machine learning is a very prominent approach towards material discovery based on data mining and big data analysis. [1] This approach has been proven extremely successful in a wide range of research fields from medicine to artificial intelligence. In the field of solid-state chemistry, machine learning can provide us with a robust method of analyzing our experimental results and making predictions on the properties and synthesis of new materials. One such class of materials is perovskites, an innovative class of semiconductor materials, which has spiked the interest of the scientific community for many years. In this project, we utilize machine learning in order to assist with the discovery of new materials combining a computational approach to identify the materials and a synthetic materials chemistry approach to attempt to verify the computational results. We ultimately seek to discover new compounds with desirable optoelectronic properties in the visible spectrum range for employment in photovoltaic research. [2] We use machine learning as an alternative method to other computational as well as test-and-trial methods, and we find that our machine learning methodology provides a higher accuracy in the prediction of photoactive perovskites. By employing machine learning on analyzing and predicting properties of perovskites, we have successfully surpassed the effectiveness hurdles of conventional theoretical methods, such as DFT.

References

[1] Lu, *Materials Reports: Energy* **1** (3), 100047 (2021).

[2] Stoumpos and Kanatzidis, *Accounts of chemical research* **48** (10), 2791-2802 (2015).

^{*} aladdin@materials.uoc.gr

Fabrication and performance of electrochromic devices based on V₂O₅ and WO₃ thin films

K. Mouratis^{1,4,*}, I. V. Tudose^{1,5,6}, C. Romanitan², M. Popescu², G. Simistiras^{1,3}, S. Couris⁴, M. P. Suche^{1,2,*} and E. Koudoumas^{1,3,*}

¹ Center of Materials Technology and Photonics, School of Engineering, Hellenic Mediterranean University, 71410 Heraklion, Crete, Greece

² National Institute for Research and Development in Microtechnologies - IMT Bucharest, Voluntari, Ilfov, Romania

³ Department of Electrical and Computer Engineering, School of Engineering, Hellenic Mediterranean University, 71410 Heraklion, Crete, Greece

⁴ Physics Department, University of Patras, 26500 Patras, Greece

⁵ Chemistry Department, University of Crete, Heraklion, Greece

⁶ IESL-FORTH, Heraklion, Crete, Greece

V₂O₅ and WO₃ thin films were successfully fabricated and optimized using the air carrier spray pyrolysis method and integrated into functional lab-scale electrochromic devices, the characterization of the as-developed thin films being published previously [1-5]. The devices were based on an electrochromic film on one side, a film acting as an ion storage on the other side and an electrolyte between them in the form of a gel, all components being held together in a sealed setup with terminals for electrical connections. The design and the construction of the device was completed through 3D printing technology and their evaluation was based on the recording of transmittance spectra at 650 nm, by alternating the applied voltage on the working electrochromic film. The effects on the overall performance of the device in relation with the type of material used (V₂O₅ or WO₃) and the applied voltage were examined and found to be the key features of the device performance. The results were very promising for the upscaling of the devices.

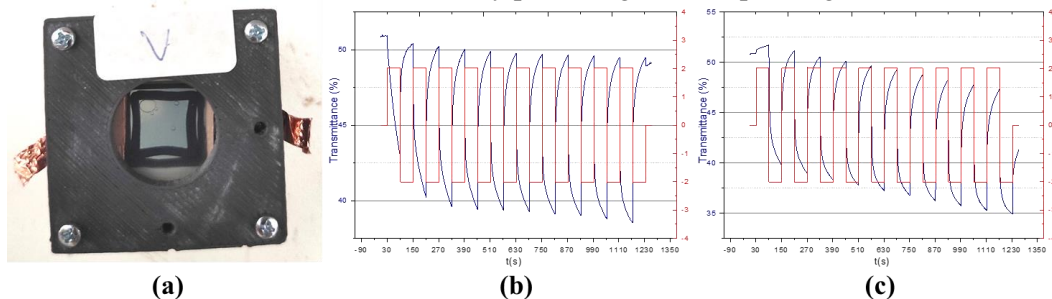


Figure 1: (a) Electrochromic lab-scale device with V₂O₅ film in one side and WO₃ on the other. Transmittance spectra of the device with (b) applied voltage on V₂O₅ and (c) on WO₃.

Acknowledgements: This research was co-financed by Greece and the EU (European Social Fund – ESF) through the Operational Program «Human Resources Development, Education and Lifelong Learning» project “Strengthening Human Resources Research Potential via Doctorate Research – 2nd Cycle” (MIS-5000432), implemented by the State Scholarships Foundation (IKY).

References

- [1] Mouratis, K.; et al. *Nanomater.* 2020, Vol. 10, Page 2397 **2020**, 10, 2397, doi:10.3390/NANO10122397. [2] Mouratis, K.; et al *Mater.* 2020, Vol. 13, Page 3859 **2020**, 13, 3859, doi:10.3390/MA13173859. [3] Pachiou, C. et al. *Proc. Int. Semicond. Conf. CAS* **2020**, 2020-*Octob*, 191–194, doi:10.1109/CAS50358.2020.9267972. [4] Romanitan, C.; et. al. *Phys. status solidi* **2021**, 2100431, doi:10.1002/PSSA.202100431. [5] Mouratis, K.; et al. *Coatings* 2022, Vol. 12, Page 545 **2022**, 12, 545, doi:10.3390/COATINGS12040545.

* kmouratis@hmu.gr; mirasuchea@hmu.gr; mira.suchea@imt.ro; koudoumas@hmu.gr

A laser-based technique for the classification of milk samples based on their animal origin

E. Nanou*, P. Kourelias, D. Stefas, S. Couris

Department of Physics, University of Patras & Institute of Chemical Engineering Sciences (ICE-HT), Foundation for Research and Technology, Hellas (FORTH)

V. Kokkinos, C. Bouras

Department of Computer Engineering & Informatics, University of Patras

E. Konstantinou

ELGO Demeter-Laboratory of Patras

E. Manolopoulou, E. Tsakalidou

Laboratory of Dairy Research, Department of Food Science and Human Nutrition, Agricultural University of Athens

The raw milk production of EU farms used for dairy products, in 2020, was about 160.1 million tonnes. Of that, 154.4 million tonnes were cow milk, 3 million tonnes were ewes' milk, 2.5 million tonnes were goats' milk and 0.3 million tonnes were buffalos' milk. On the opposite side, in Greece, being the largest producer of non-bovine milk in EU, 57% of the Greek farms' raw milk delivered to dairies is coming from ewes and goats. Usually, non-bovine milk is of higher cost value than bovine milk, as it originates from farming under geographical and climatic constraints, e.g., in high altitude or arid areas found mostly on islands or provincial areas. Moreover, ewe and goat milk are more nutritious than bovine milk and are frequently used to produce different dairy products, as e.g., cheese, yogurt, etc. Therefore, the rapid, in-situ and reliable identification/determination of the animal origin of milk is of high interest.

Laser Induced Breakdown Spectroscopy (LIBS), a laser-based technique, is proposed for the first time for the discrimination of raw milk samples from different animal origins, i.e., cow, goat, and sheep. In principle, a pulsed laser is used to create a micro plasma on the sample's surface. The spectral analysis of the plasma radiation can provide valuable information about the elemental composition of the sample. The measurements can be carried out in-situ, on-line and/or remotely. In addition, the combination of LIBS with machine learning allows the fast classification of the milk samples based on their animal origin.

In this work, the principles of LIBS technique will be presented, and its application for the determination of milk elemental composition and for the discrimination of milk samples of different animal origins, will be demonstrated and discussed. Finally, the general potential of the technique for food science and for food quality control will be discussed, as well.

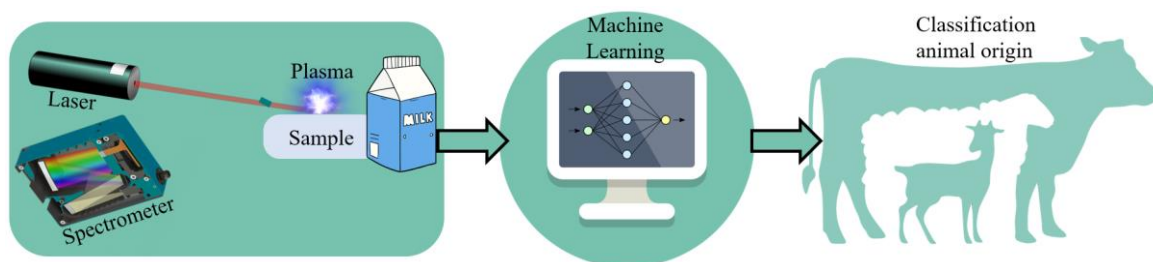


Figure: LIBS assisted by machine learning for the determination of milk's animal origin.

* e.nanou@iceht.forth.gr

A spectroscopic study for the characterization of high voltage composite insulators

D. Polygenis^{1,2*}, D. Stefanis^{1,2}, N.C. Mavrikakis^{3,4}, K. Siderakis^{3,4}, K. Mouratis^{1,5},
E. Koudoumas⁵ and S. Couris^{1,2}

¹ *Physics Department, University of Patras*

² *Institute of Chemical Engineering Sciences (ICE-HT), Foundation for Research and Technology, Hellas (FORTH)*

³ *Hellenic Electricity Distribution Network Operator S.A.*

⁴ *Laboratory of Energy and Photovoltaic Systems, Hellenic Mediterranean University*

⁵ *Center of Materials Technology and Photonics, Hellenic Mediterranean University*

The efficient operation of composite insulators in overhead high voltage power transmission lines and sub-stations is of great importance for the transportation of electrical energy. However, their aging and the deposition of environmental pollutants on their surface can deteriorate their operational characteristics causing serious problems on the electrical power grid operation. In that view, the use of a laser-based technique, namely Laser Induced Breakdown Spectroscopy (LIBS), is used for the classification of insulators in terms of their aging and other processes affecting their performance. LIBS is an analytical technique employing a high intensity laser beam to induce a micro-plasma on the sample's surface. LIBS features a range of advantages over other spectroscopic methods, including rapid multi-elemental analysis, while being marginally destructive to the targeted material. Furthermore, LIBS is capable of remote, real-time operation without requiring the removal of the insulator from the power grid. Such advantages, make LIBS an interesting tool for the evaluation of composite insulators.

In the present work, different LIBS experimental configurations (single and double pulse LIBS) assisted by machine learning are applied for the classification of composite high voltage insulators based on their ageing, surface degradation and pollution due to environmental stresses, and chemical composition. The LIBS results are compared with other results obtained according to established protocols, including FTIR, SEM and EDX.

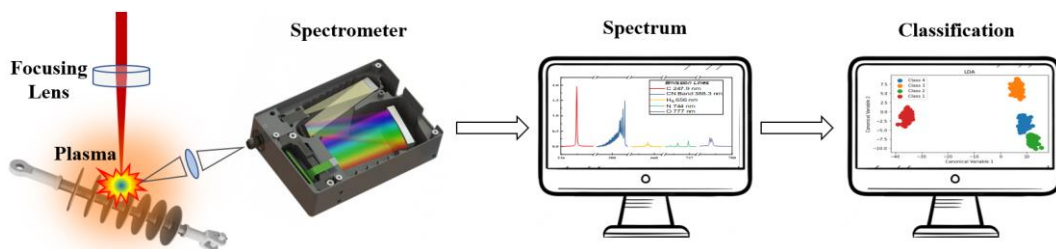


Figure 1: LIBS assisted by machine learning for the classification of high voltage insulators.

* d.polygenis@iceht.forth.gr

Mechanical and structural properties of FRP concrete: data-driven, machine learning approaches

F. Sofos*, T.E. Karakasidis

Condensed Matter Physics Laboratory, Department of Physics, University of Thessaly, Lamia, Greece

M. Valasaki, C.G. Papakonstantinou

Civil Engineering Department, University of Thessaly, Volos, Greece

Material properties extraction has been facilitated by the vast number of data stored in various electronic databases and being accessible in the research community, such as experimental, simulation, graphical, and various literature data. The application of statistical methods, and, especially, the incorporation of artificial intelligence and machine learning techniques, has given a new direction to the problem. Physical sciences and engineering have recently followed these data-driven approaches, for predicting materials behavior and calculate properties in various timescales, simple and complex geometries, under ambient or extreme conditions¹. More specifically, in the field of materials incorporated in structural and civil engineering, ML techniques have been employed to predict concrete properties that affect its strength and quality measures, such as the compressive strength [1]. In this work, purely experimental data from measurements of the compressive strength of fiber-reinforced polymer (FRP) concrete composites have been employed. Various structural and mechanical properties have been found to affect the compressive strength and each one is evaluated on the effect on the acquired compressive strength measurement. The process followed is summarized in Fig. 1. We conclude that data science and ML can be valuable tools towards the full exploitation of the vast amount of data coming from experiments and simulations [2], as they may pose as alternatives to expensive or extreme case experiments or computationally intensive simulations, complement their applicability, and extend our ability to argue on hidden data connections.

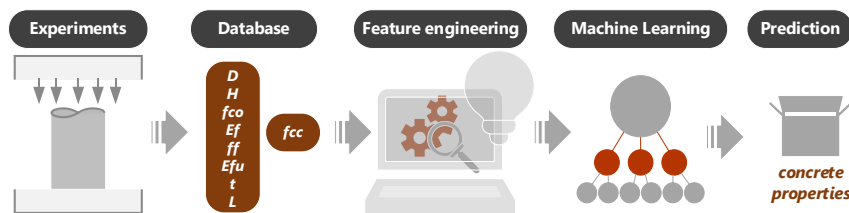


Figure 1: Machine Learning data flow for compressive strength prediction

Acknowledgment

F.S. acknowledges support by the Center of Research Innovation and Excellence of University of Thessaly, funded by the Special Account for Research Grants of University of Thessaly.

References

- [1] R. Cook, J. Lapeyre, H. Ma, and A. Kumar, Prediction of Compressive Strength of Concrete: Critical Comparison of Performance of a Hybrid Machine Learning Model with Standalone Models, *Journal of Materials in Civil Engineering* **31**, 04019255 (2019).
- [2] F. Sofos, A. Charakopoulos, K. Papastamatiou, and T. E. Karakasidis, A Combined Clustering/Symbolic Regression Framework for Fluid Property Prediction, *Physics of Fluids* **34**, 062004 (2022).

* fsofos@uth.gr

PLA nanocomposites with antimicrobial action, based on encapsulated natural extracts for food packaging applications

I.V. Tudose¹, C. Romanitan², C. Pachi², I. Rosca³, K. Petrotos⁴, S. Zaoutsos⁵, G. A. Fragkiadakis⁶, A. Bouranta¹, M.P. Suche^{a*1,2}, E. Koudoumas^{*1}

¹Center of Materials Technology and Photonics, School of Engineering, Hellenic Mediterranean University, 71410 Heraklion, Crete, Greece

²National Institute for Research and Development in Microtechnologies (IMT-Bucharest), Bucharest, 023573, Romania

³Petru Poni” Institute of Macromolecular Chemistry, 41A Grigore Ghica Voda Alley, 700487, Iasi, Romania

⁴Department of Agriculture-Agrotechnology, Laboratory of Food and Biosystems Engineering, University of Thessaly, Geopolis of Larissa, 41500, Greece

⁵Department of Energy Systems, School of Technology, University of Thessaly, Larissa, 41500, Greece

⁶Department of Nutrition & Dietetics Sciences, School of Health Sciences, Hellenic Mediterranean University, 72300 Sitia, Crete, Greece

Composite packaging can take many different forms, and its use is increasing the last years; a tendency largely due to the many cost and efficiency benefits that can be offered in the supply chain. The potential use of composites based on PLA in packaging applications exhibiting antimicrobial action, has been investigated in recent years, as presented by Tawakkal (2014) et al. and Becerril et al. (2020) in their reviews [1, 2]. Generally, polymeric composite materials can be fabricated with various techniques including printing and roll-milling techniques. In this work, a roll-mill system was employed, a technique allowing the easy and effective mixing of materials, in order to get composite materials. The composite materials were produced by mixing encapsulated natural extracts with polylactic acid (PLA) in a pellet form. The composite materials were characterized using SEM, XRD and Raman spectroscopy and their antimicrobial activity was evaluated using a modified Kirby-Bauer methodology. The antimicrobial efficiency of the composite materials was found quite effective; and depending on the type and the concentration of the active material.

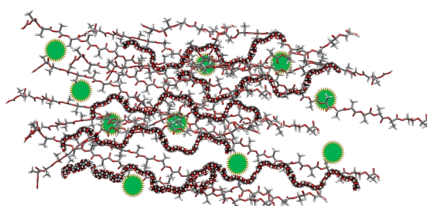


Figure 1: Schematic representation of PLA-encapsulated natural extracts composite material

Acknowledgments. This research was funded by the project NanoBioPack which is co-financed by the European Union and Greek national funds through the Operational Program Competitiveness, Entrepreneurship and Innovation, under the call 'Specific Actions, Open Innovation for Industrial Materials' (project code: T6YBII-00307).

References

[1] I. S. M. A. Tawakkal, M. J. Cran, J. Miltz, and S. W. Bigger, *Journal of Food Science*, **79** (8), R1477, 2014.// [2] R. Becerril, C. Nerín, F. Silva, *Molecules*, **25**(5), 1134, 2020.

* Email: mirasuchea@hmu.gr; mira.suchea@imt.ro; koudoumas@hmu.gr